THESIS FOR THE DEGREE OF DOCTOR OF PHILOSOPHY

Dynamics of open fermionic nano-systems – a fundamental symmetry and its application to electron transport in interacting quantum dots

JENS SCHULENBORG

Department of Microtechnology and Nanoscience (MC2)
Applied Quantum Physics Laboratory
CHALMERS UNIVERSITY OF TECHNOLOGY

Göteborg, Sweden 2018

Dynamics of open fermionic nano-systems – a fundamental symmetry and its application to electron transport in interacting quantum dots
JENS SCHULENBORG
Göteborg, Sweden 2018
ISBN 978-91-7597-781-2

Doktorsavhandlingar vid Chalmers tekniska högskola
Ny serie Nr 4462
ISSN 0346-718X

ISSN 1652-0769 Technical Report MC2-398
Applied Quantum Physics Laboratory
Department of Microtechnology and Nanoscience (MC2)
Chalmers University of Technology
SE-412 96 Göteborg, Sweden
Telephone: +46 (0)31-772 1000

Cover
Sketch of how fermionic duality crosslinks energies (red,blue bars) and electron occupations (yellow balls) in the system of interest (left) to its dual model (right).

Printed by Chalmers Reproservice
Göteborg, Sweden 2018

Dynamics of open fermionic nano-systems – a fundamental symmetry and its application to electron transport in interacting quantum dots

JENS SCHULENBORG
Applied Quantum Physics Laboratory
Department of Microtechnology and Nanoscience (MC2)
Chalmers University of Technology

Abstract

The study of electronic transport through strongly confined, interacting open quantum systems has regained considerable interest over the past years. One main motivation behind this concerns the possibility of *time-dependently* controlled operations on individual electrons, promising applications in, e.g., metrology and electron-based quantum computing. In particular, fundamental questions of quantum thermodynamics and the practical necessity to recover waste heat from nanocircuits have attracted attention towards *electronic energy currents*.

The research articles covered by this thesis contribute to this topic by deriving and exploring a fundamental symmetry relation – the *fermionic duality*. This duality applies to the quantum master equation of *any* locally interacting, fermionic open quantum system tunnel-coupled to non-interacting reservoirs. It yields a crosslink between modes and amplitudes corresponding to the evolution rates in the time-dependent decay of the open-system state. This crosslink involves a mapping between the system of interest and a *dual* system with inverted environment potentials, local energies, and thus especially inverted interactions. The duality thereby explains many, at first sight unintuitive, transport features and significantly improves their analytic accessability. In particular, we can understand why charge- and energy currents through quantum dots with strong local Coulomb repulsion in fact exhibit features of electron-electron *attraction*, both in the time-dependent decay after a sudden switch and in the stationary limit.

More fundamental insights are obtained by identifying the duality to be rooted in Pauli's exclusion principle and the parity superselection principle. Namely, this implies that the duality is independent of, and hence combinable with many other general symmetries, including particle-hole symmetry, time-reversal symmetry, detailed balance and Onsager reciprocity. Especially the combination with the latter offers a novel perspective on the thermoelectric response of open, locally interacting electronic nanosystems.

Keywords: open fermionic quantum system, master equation, fermionic duality, fermion parity, inverted energy, quantum dot, voltage switch, transient response, non-equilibrium transport, charging energy, energy-dependent coupling

Acknowledgements

First and foremost, I would like to thank my supervisor Janine Splettstößer for her truly exceptional moral and scientific support. I really could not have asked for a better supervisor throughout all these years. Thank you for bearing all my shortcomings for such a long time, and for kicking me back on track when needed.

Special thanks also go to my long-term collaborator and co-supervisor Maarten Wegewijs. You have been the perfect counterbalance to my routine with Janine, and without your work, none of all this would have been possible. In this respect, I also owe a great deal to the "father of duality", Roman Saptsov.

I furthermore thank *all* people I had the pleasure to work with, including Michele Governale, Uli Zülicke, Masaya Kataoka, Angelo Di Marco, Federica Haupt, Joren Vanherck and Hristo Barakov. I appreciate the fruitful discussions, valuable input, and your open minds. In particular, I thank Maarten, Michele and Masaya for their hospitality during my visits. Big thanks go to Maciej Misiorny, for being the "half-full" person, having a car, and for valuable feedback on "BibItNow!". I also thank Nastaran Dashti for her help with the cover figure.

Some words to those willing to spend more off-duty time with me: I know it can be tricky sometimes, so I sincerely appreciate making the effort anyhow. Thank you for bringing some joy to my life, Giovanni, Thomas, Jan, Ben, Markus, Freddi, Yevgeniy, and all my hometown gang, Michael, Sebastian, Georg, Ansgar, Daniel, Stefan and your associates. I will never forget you!

A salute to all current and former colleagues at AQP. I have enjoyed the many interesting conversations, the warmth, and the (mostly Iranian) goodies during the (too) many coffee breaks and gatherings at sometimes strange hours. My time with you has been a good lesson about life, science, and about becoming a grown-up person. I see the international perspective you have offered as invaluable.

The last lines belong to all my relatives, and especially to you, mother, father, brother and your lovely wife and kids. Thank you for the constant moral support during the roughest years I have ever had. Thank you, for being the proof that deep, unconditional love can be felt and shared even with me.

I devote this thesis to you, my aunt Moni. I promised to talk to you once more before Christmas, but I did not keep that promise. I am so sorry. I miss you. Life has not been fair with you.

List of publications

This thesis presents an introduction, summary and extension to the following appended papers:

[I] J. Schulenborg, J. Splettstoesser, M. Governale, and D. Contreras-Pulido, "Detection of the relaxation rates of an interacting quantum dot by a capacitively coupled sensor dot", Phys. Rev. B **89**, 195305 (2014).

[II] J. Schulenborg, R. Saptsov, F. Haupt, J. Splettstoesser, and M. Wegewijs, "Fermion-parity duality and energy relaxation in interacting open systems", Phys. Rev. B **93**, 081411 (2016).

[III] J. Vanherck, J. Schulenborg, R. Saptsov, J. Splettstoesser, and M. Wegewijs, "Relaxation of quantum dots in a magnetic field at finite bias – Charge, spin, and heat currents", Phys. Status solidi B **254**, 1600614 (2017).

[IV] J. Schulenborg, A. Di Marco, J. Vanherck, M. Wegewijs, and J. Splettstoesser, "Thermoelectrics of Interacting Nanosystems—Exploiting Superselection Instead of Time-Reversal Symmetry", Entropy **19**, 668 (2017).

[V] J. Schulenborg, J. Splettstoesser, and M. Wegewijs, "Duality for open fermion systems: energy-dependent weak coupling and quantum master equations", arXiv, 1808.10223 (2018).

We always refer to these publications as paper I, II, ..., according to the labeling in the list above.

Specification of my contributions to the appended papers

I The calculations for this paper are based on my master project. During the PhD, I have substantially improved these results and their physical explanation, I have created the final figures, and I have written most of the paper with feedback from my coauthors.

II The derivation of the duality was conceived and written mainly by Roman Saptsov and Maarten Wegewijs (supplement). I have contributed mostly to the understanding of the physical context of the duality and related concepts (e.g., dual system). For the concrete example of time-dependent energy current out of the quantum dot, I have done all the calculations and the plots. The paper has been written with equal contributions to content and formulation by all coauthors. As shared first author together with Roman Saptsov, I have been responsible for the final editing, implementing most of the comments and suggestions from my collaborators.

III Excluding the discussion of the Iche-duality from Roman Saptsov, the paper is based on Joren Vanherck's master project co-supervised by me. I have coordinated the initial writing phase with concrete instructions and feedback to Joren Vanherck and Roman Saptsov. I have conceived and written a major part of the more general introduction to the duality and of the part about decay at finite magnetic field; the other parts have been improved with my feedback and suggestions. Together, Joren Vanherck and I have done all the numerical calculations and the plots.

IV Based on previous work from Angelo Di Marco and Janine Splettstößer, I have done all analytical calculations that appear in the final paper. I have conceived and written the entire appendix, deriving all main analytical results and presenting a new duality-based way of constructing the master equation kernel of a single-level quantum dot. I have helped writing some parts of the main paper, and I have improved a few plots.

V I have conceived the original idea and I have done all analytical calculations, helped by improvements and additions from both coauthors. I have written the original version of the paper, followed by a rewrite by my coauthors and an extension by Maarten Wegewijs. I have created all except one plot. All authors have been equally involved in the final editing.

Contents

1 Introduction

1.1 General context and structure of the thesis

At their core, almost all realistic physical systems of interest in experiments or in applications share two fundamental properties. First, they are open, meaning that they couple in some form to their environment. This environment could, e.g., be any electrically, optically or mechanically coupled apparatus to control and read out the device of interest, wanted or unwanted electromagnetic fields, or simply the matter surrounding the system. Second, for the device to be useful, an external agent must typically modify or operate it in some time-dependent, periodic or aperiodic fashion, driving the system away from the stationary state it would otherwise maintain in the presence of its environment: an experimentalist sets up a sample to emit a signal and then measures the signal, or a transistor is switched on and off to control an electrical current. The overarching topic of this thesis and its appended papers I-V are two central questions guiding any such operations on open systems:

1. What is the time-dependent response of the system after the externally controlled operation, i.e., how long does it take the device to decay to a new stationary state, and what are the dissipative effects during this decay process?

2. Once the new stationary state is reached, how does the device behave under these new conditions, and does the device fulfill its designated purpose?

This work addresses these questions in the timely context of *fermionic*, and in fact mostly *electronic* open *nanosystem* – devices small and confining enough for their internal physics to be strongly governed by both quantum mechanics and particle-particle interaction.

As illustrated in Fig. 1.1, the appended papers focus mostly on studying electronic charge and energy transport between artificially designed *quantum dots* [1–5]. Introduced in section 1.2.1, these are quasi 0-dimensional structures with a pronounced, tunable level-splitting and a coupling to electronic contacts via electron tunneling [6]. As such, they represent an elementary ingredient of a possibly larger or more complex electronic nanodevice.

Concretely speaking, the covered articles investigate the transport of charge and energy flowing in between such quantum dots and the coupled contacts. We focus,

on the one hand, on the *time-dependent* emission after a sudden system-parameter change. The latter is important, since it represents a basic building block of more complex device operations. On the other hand, we also study stationary currents driven by voltage- and temperature gradients applied to the coupled contacts.

The main point of this work is, however, not the electronic transport itself. Instead, what we highlight here is the unconventional way and the general point of view from which we approach this problem. As the title of this thesis suggests, the research project summarized here has identified and applied a general symmetry relation – originally labeled fermion-parity duality in paper II and now simply called *fermionic duality* – that emerges in the theoretical description of dynamics open fermionic quantum systems. The purpose of this text is the following. First, we give the experimental context and theoretical background necessary to understand this duality relation. We then to introduce the relation itself, and finally to provide a review of the insights which the appended papers have gained, and possible future studies may gain from it.

Regarding the detailed structure of this thesis, the remainder of this first chapter 1 gives an introduction to both time-dependent and stationary charge- and energy transport through quantum dots. What do these topics entail, and why are they of interest both for the appended papers and from a more general point of view? Chapter 2 then reviews the quantum master equation approach which we employ to theoretically study stationary and time-dependent physics in open fermionic quantum systems. The focus is on explaining the key concepts necessary to motivate and understand the duality relation and its applications; detailed derivations can be found either in the appendix of this thesis, the appended papers, or in cited references.

The main part of this thesis is covered in chapter 3: the fermionic duality relation identified in paper II, and applied as well as extended in papers II - V. We explain in detail what precisely the duality is, which theoretical insights we gain from it, and why the duality emerges at all for the class of systems we consider. With the appended papers predominantly discussing concrete quantum dot setups, chapter 3 complements and connects the individual papers in a more general fashion. In some, later on clearly indicated aspects, the chapter also extends the analysis beyond what the papers have pointed out so far, mainly to provide a more satisfactory completion of the discussion. Chapter 4 then finally switches back to a more concrete context. It provides an outlook to the how duality can help studying systems of practical relevance for future applications.

The thesis finishes with chapter 5 giving a brief summary of the content of every paper, and with chapter 6 wrapping up with an overall conclusion and outlook to this work. Note that the appendix of this thesis also shows mostly technical, yet new results. This concerns possible microscopic interpretations of the duality [App. (E)], a systematic approach to *larger* fermionic systems [App. (D)], and a more detailed discussion of bosonic systems [App. (G)].

1.2 Quantum dots and their time-dependent operation

The time-dependent operation of a device becomes particularly interesting for modern day physics once the functionality of this device critically depends on, or even benefits from *quantum mechanical* and *interaction-related* effects between individual particles. With regards to the open *electronic* nanoscale system addressed in this work, this concerns so-called single-electron transistors (SETs) [7–13] and, most-importantly, nanoscale capacitors [14–16] realized by artificially created quantum dots [1–5, 17–25]. The first task is hence to describe such systems and their key properties.

1.2.1 Level quantization and charging energy in nanosystems

The lower panels of Fig. 1.1(a) and Fig. 1.1(b) illustrate and explain one of many ways to realize a tunable quantum dot: a semiconductor based, gate-defined *potential well* [1–5]. Also called "artificial atoms", these systems electrostatically confine particles to regions in space with diameters on the order of the quantum mechanical particle wave length or even less. As a result, both quantum coherence and the quantized, discrete spectrum of particle energies – characterized in Fig. 1.1(a) by a typical level-splitting Δ – start to play a role. Namely, only [1] electrons with these energies are allowed to tunnel between the contacts in the environment and the dot itself through the confining potential barrier. Quantum dots of this type are particularly interesting for this work: first, the experimentally demonstrated [5, 10–12] ability to externally control the applied gate potentials and the associated physical system-parameters enables a *time-dependent device operation*. Second, as already indicated in Fig. 1.1, such quantum dots can be integrated into electrical nanocircuits, thereby enabling electrical readout.

To account for the effect of quantized energy levels while still benefiting from intuitively accessible, classical electrical circuit models, Büttiker et al. have developed the theory of the *mesoscopic capacitor* [14–16]. The idea is to characterize even mesoscale and nanoscale [2] devices such as quantum dots as circuit elements with resistance R, capacitance C, and the (here less relevant) inductance L. More precisely, one introduces the effective *charge relaxation resistance* and *electrochemical capacitance* which, next to the already classically relevant device geometry and material parameters, furthermore account for the electronic density of states of the components in the circuit, possibly exhibiting level quantization. Without going into detail, we note that one general, intruiging, and experimentally verified consequence of this quantum effect is the violation of the classical Kirchhoff

[1] Within the level broadening due to higher order coupling effects.

[2] This typically corresponds to lateral dimensions $\lesssim 100$ nm, given that temperatures are low enough (at least below $T \lesssim 100$ K, see [27]) to expose quantum effects.

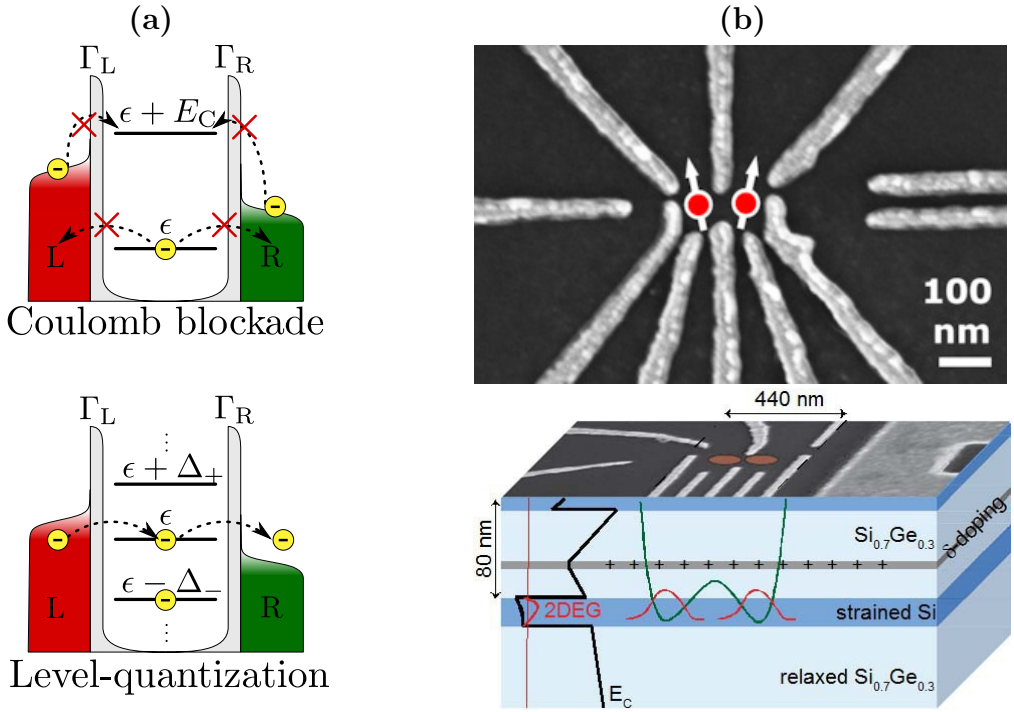

Figure 1.1: (a): *Sketch of Coulomb blockade (top panel) and level quantization (bottom panel) leading to discrete transition energies ϵ in an electronic open nanosystem. The example system couples via tunnel barriers Γ_L and Γ_R to a left (L) and right (R) electronic reservoir with biased chemical potentials $\mu_L > \mu_R$. Coulomb blockade means that the additional Coulomb interaction energy E_C (charging energy) which an electron entering the system needs to bring may completely block transport, given that both transition energies $\epsilon, \epsilon + E_C$ are outside the energetic bias window $\mu_R < E < \mu_L$. For large level splittings, $\Delta_\pm > \mu_L - \mu_R$, and a single level ϵ in the bias window $\mu_L > \epsilon > \mu_R$, it is mainly electrons with this specific energy ϵ that tunnel through.* **(b)**: *Illustration of semi-conductor based, gate-defined quantum dots. In the micrograph in the top panel, the white regions indicate gate electrodes that generate an electrostatic potential beneath the surface of the shown sample, the red circles mark two quantum dots confining electrons (here: spin-aligned) to small regions in space. The lower panel illustrates how the charge confining quantum dots are realized. Perpendicular to the sample surface, the electrochemical potential landscape of a SiGe/Si heterostructure traps electrons in a 2 dimensional electron gas (2DEG) within the thin Si layer. Movement within this layer is then further restricted to quasi 0-dimensional quantum dots using the electrostatic fields of gate electrodes on top of the sample.* ***Source***: *[26].*

laws [17].

As further highlighted in the next subsection 1.2.2, what is particular important for us is that time-dependent responses to device operations, i.e. typical charge and discharge times and the resulting limits on operation frequencies can often be

understood analogously to RC-times $\tau_{\mathrm{RC}} = R \cdot C$ of classical capacitors [1]. From this perspective, large parts of the appended papers are concerned with exactly these times – including their generalization to the emission of energy and spin – for the most elementary type of quantum capacitor: the single-level quantum dot [29], with a level-splitting Δ large enough that only a single orbital is accessible for electrons in the environment.

Importantly, the idea that RC-times are affected not only by an effective resistance, but also by a capacitance, immediately brings in the second key property of the systems of interest here: the presence of *Coulomb interaction* and the resulting charging energy $E_{\mathrm{C}} \sim e^2/C$ of each electron with charge e, which is inversely proportional to the capacitance C of the device [2]. The effect of this charging energy is illustrated in the upper panel of Fig. 1.1(a), displaying a system with a small level-splitting $\Delta \ll E_{\mathrm{C}}$ compared to the charging energy, as practically realized in metallic islands [7–13]. What here leads to the pronounced and relevant discretization of allowed energies for transported electrons is not quantum mechanics, but the simple fact that each electron which has entered the island increases the energy for the next electron to enter by roughly [3] the charging energy E_{C}, as a consequence of the increasing Coulomb energy. As shown in Fig. 1.1(a), and as first demonstrated for small metallic tunnel junctions by Fulton et al. [7], this can cause transport to and from the device to be completely blocked; the system exhibits what is known as *Coulomb blockade*. One key application of this effect is to build the above mentioned *single-electron transistors*: by lowering or raising the system energies compared to the environment potentials, one charges or discharges only in discrete steps of individual electrons, even when the quantum mechanically related level-splitting Δ is completely negligible. The point is rather that every electron addition or removal changes the possible *many-body* transition energies by E_{C}, thereby bringing the system immediately back into a blocked state again. Or put differently, the "levels" in the upper panel of Fig. 1.1(a) do not represent actual single-particle states occupied by individual electrons, but rather the excess energies required for one *among a possibly large number of accessible electrons* to enter or leave the system [4].

Coming back to the quantum dot systems of interest in this thesis and its papers, we emphasize that we consider a regime in which *both* quantum mechanical level-splitting and charging energy play a role, as detailed in Sec. 2.1 of the next chapter 2. More precisely, we start from the premise that the level-splitting Δ can be tuned to be as large, or even much larger than the Coulomb charging energy

[1] If one accounts for cotunneling and pair tunneling, this understanding needs to be revised [28].

[2] In fact, only the classical, geometric part of the capacitance defines the charging energy e^2/C, whereas the capacitance in the RC-time $\tau_{\mathrm{RC}} = R \cdot C$ is also affected by the density of states.

[3] This holds in the constant-interaction approximation.

[4] Note that this does not contradict the indistinguishableness of electrons. What matters is not which, but *how many* among all electrons can in principle take the interaction energy to enter or leave the system.

E_C, which in fact has been experimentally demonstrated in, e.g., Ref. [27]. If the charging energy E_C is in return still large compared to typical environment temperatures T and potential biases V between the contacts, and if by virtue of degeneracies in spin or orbital degrees of freedom, the single relevant energy level can be multiply occupied, the above mentioned physics implied by Coulomb interaction also play a role. In Sec. 2.1.1, we introduce the *interacting spin-degenerate single-level quantum dot* as the most elementary manifestation of this type of systems. Being the simplest nontrivial and experimentally relevant example of interplay between level-quantization and Coulomb interaction, it represents the "working horse" of all concrete, system-related studies in the appended papers. Most importantly, and as further highlighted in chapter 4, it clearly exposes the benefits of the fermionic duality relation: natively formulated in a quantum many-body context, the latter continues to hold and simplify the analysis even when simple, mean-field single-particle pictures are either completely inappropriate, or at least need to be nontrivially modified [30, 31] in order to capture the relevant many-body physics. To better understand what precisely these effects are in the context of time-dependent transport of charge and energy, let us now turn more specifically to this problem for few-level quantum dots.

1.2.2 Time-dependent control of individual electrons

Motivated by sheer scientific curiosity and by the soon-relevant fundamental limits in downsizing conventional semi-conductor technology [32], several key fields of research have attracted considerable attention to time-dependently operated quantum dots over the years. Potential applications include electron-based quantum computation [18, 33–37] and metrological purposes, with the latter including the long-standing [21, 23, 38–43] quest of providing a more reasonable *primary* current standard in accordance with the soon redefined Ampère [44]. Prompted by more recent technological advances, research interest in the field has also shifted towards measuring and even using the *energy* involved in time-dependent operations of nanosystems, apart from the mere consideration of electron charge and spin. Next to a fundamental relevance in the field of quantum thermodynamics [45–50], possible applications are, e.g., so-called nanoscale *heat engines* [51–59] or even time-dependently boosted thermoelectrics [60–62]. As such, time-dependence in quantum dots forms a timely and relevant context for this thesis and its papers, and is hence topic of this and the following subsection.

As a start, we note that the main purpose of quantum dot operations in the majority of the above cited works is to control the coherent and incoherent emission, absorption and detection of *individual* electrons or spins [18–21, 24, 25, 34, 37, 39, 42, 43, 63–74]. With this thesis mostly concerned with emission and absorption, let us illustrate the basic principle in Fig. 1.2, showing a quantum-dot based nanocapacitor of the type which has been studied by, e.g., Gabelli et al. [17], and

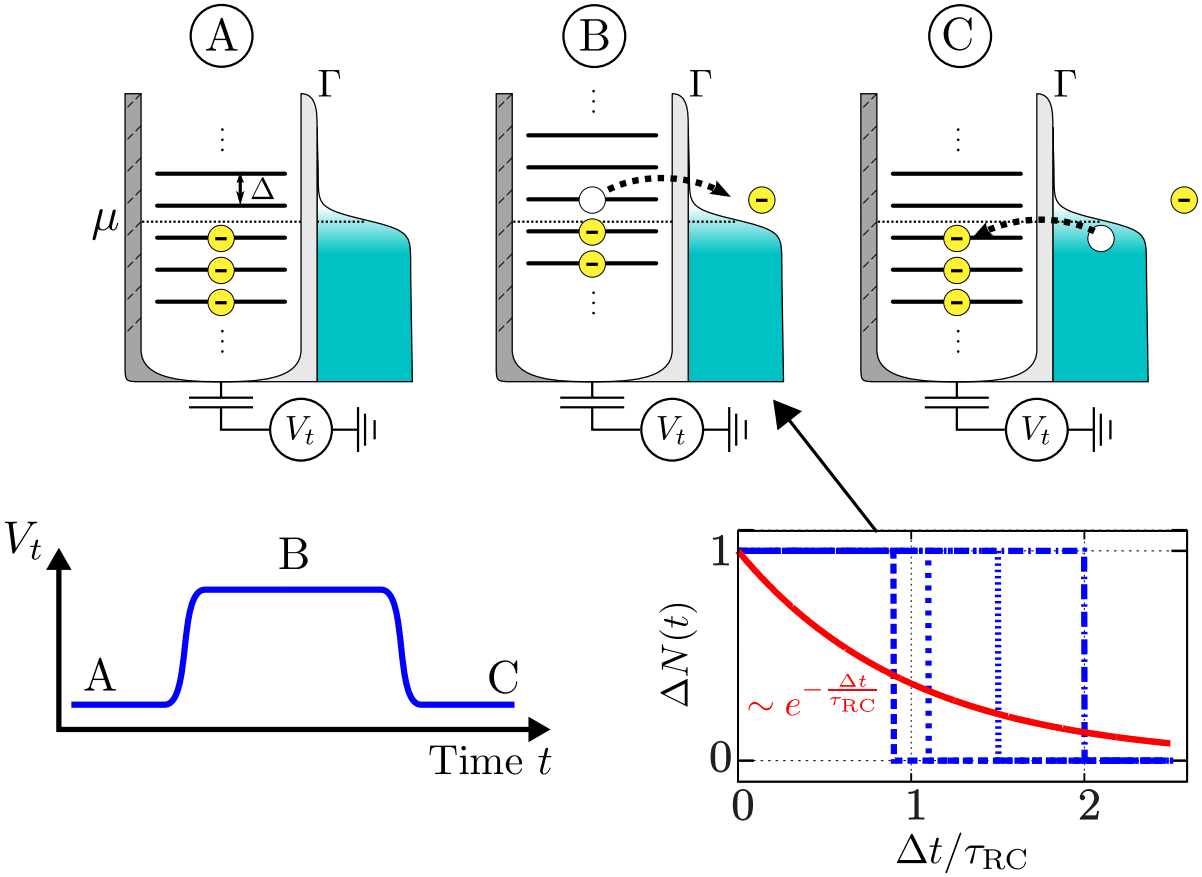

Figure 1.2: *The upper panel shows a quantum capacitor [17] with level-splitting* Δ *that is used as a single electron source [18]. A periodically time-dependent gate potential* V_t *is applied to the tunnel-coupled quantum dot in order to shift its discrete energy level spectrum, thereby emitting and reabsorbing individual electrons. The lower left panel shows the corresponding time-dependent gate potential, indicating the three stages A,B,C in the upper panel. The lower right panel describes the time-dependent decay of the quantum dot excess occupation* $\Delta N(t)$ *for times* Δt *after the first potential shift. The blue lines represent a thought experiment obtaining* individual *time traces of the charge – showing sharp steps at the time of emission. The red curve shows the* average *over all these time-dependent traces, yielding an exponential decay of* $\Delta N(t)$ *on the scale of the RC-time* τ_{RC} *of the dot [Sec. (1.2.1)].*

later used as a single-electron source by Fève et al. [18]. At some initial time at which the dot assumes some stationary occupation, the discrete spectrum of the quantum dot is rapidly shifted by an external gate potential, such that one singly-occupied [1] energy level is lifted above the Fermi edge of the tunnel-coupled reservoir. As a response to this shift, the system is brought out of equilibrium with its environment – or more generally, out of stationarity – causing one or several electrons to tunnel out. From the point of view of the quantum dot, this

[1] Note that one often applies a strong magnetic field to filter out one spin direction.

tunneling induces a *decay* of its (quantum) state, changing its excess occupation $\Delta N(t)$ on a typical time scale given by the above mentioned [Sec. (1.2.1)] RC-time τ_{RC} of the system. In the red curve of the lower right panel of Fig. 1.2, this RC-time is reflected in the exponential behavior of the time-dependent *average* of $\Delta N(t)$ over many emission processes. Finally, in order to operate the device periodically, the dot potential is shifted back at some later time and the dot is recharged, again inducing a decay process.

A simple property that is nevertheless highly relevant for successfully performing the above described time-dependent manipulation is the fact that the typical decay time is finite. If the circuit is, e.g., operated at a frequency that is too high compared to the decay times, the electrons do not have enough time on average to leave or enter the dot. A detailed understanding of these times is therefore crucial. Experimentally, the relevant times can be determined with detectors which are sensitive enough to detect single electrons, and which possess a bandwidth that is high enough to perform *time-resolved measurements* [34, 43, 63, 65–67, 69–71]. In Ref. [18], decay times on the order of a few nanoseconds have been obtained. A first theoretical understanding can be developed by describing the time-dependent response of the *average* occupation (red curve in Fig. 1.2) to an instantaneous level shift with a master equation and Fermi's Golden rule [28, 75, 76]. This requires that for the system of interest, the *tunnel coupling can be assumed to be weak*. As we clarify in the next chapter 2, weak here means that the typical tunneling rates are sufficiently small compared to the frequencies of thermal fluctuations in the coupled environment. Moreover, it requires the time between two subsequent operations on the device not to become as small as or even smaller than the typical decay time. For the majority of situations described in the appended papers, both requirements are assumed to be fulfilled.

However, we note that from a more general point of view, it can also be interesting to explicitly break weak-coupling conditions by, e.g., increasing the operation frequency or coupling, as the detailed *transient* behavior of the dot starts to play a role. While this may not anymore guarantee reliable emission and absorption of a precise number of particles, these transient dynamics can – if measurable – also be an additional source of extractable information, since they typically reflect properties which characterize the device of interest. Time-dependently driven open quantum systems are therefore also a topic of more fundamental research, on, e.g., non-Markovian dynamics [64, 77–85], qubit gate control [86–88], or the role of fluctuations [19, 72, 89, 90].

Another aspect next to the coupling and the operation frequency is how local Coulomb interactions in the quantum dot change the emission times. This problem is discussed in detail in Refs. [28, 76] for the above introduced *interacting single-level quantum dot*, and is precisely the starting point for this thesis, its appended papers, and the application of fermionic duality as the central topic of this work. Namely, after an extensive theoretical introduction to this duality in

chapters 2 and 3, chapter 4 returns to the question how the appended papers help in the theoretical understanding of decay times of the above described electron emitters, and their dependence on local interaction. In particular, our approach is not limited to time scales in particle currents, but also extends to spin- and electronic energy currents, with the latter differing nontrivially from the particle current due to the Coulomb interaction. Hence, let us adress such time-dependent electronic energy currents a bit more in detail.

1.2.3 Time-dependent electronic energy currents

The time-dependent flow of energy carried by electrons in nanosystems such as quantum dots involves several interesting aspects. One simple yet important thermodynamic fact is that any time-dependent operation typically requires work which is at least partly carried away be electrons and dissipated in form of heat. While the resulting increase of the environment temperature is already very relevant for the current, commercially available technology, this becomes all the more important for the nanoscale systems of interest here. Namely, in order to exploit the effects of level-quantization and Coulomb blockade [Sec. (1.2.1)], one needs to make sure that the temperature T around the device always remains small compared to the typical level-splitting Δ and charging energy E_{C}, meaning $E_{\mathrm{C}}, \Delta \gg T$. For the quantum dot devices of interest here, this corresponds to temperatures which are at least below $T \lesssim 100$ K, but in many cases rather on the order of $T \sim$ K or even less [27]. External cooling with modern cryostats is often capable of maintaining the necessary temperatures, but it requires a lot of resources.

A potential way to alleviate this problem has gained attention in the last decade. In fact, one could use more of the very, time-dependently driven nanodevices we try to cool: so-called *nanoscale heat engines* [51–59, 91] or driven thermoelectrics [60–62], both relying on, or at least benefiting from time-dependently controlled operation to convert thermal gradients into useful electrical power. As Fig. 1.3(a) shows, this can be used to, e.g., pump electrons against a voltage bias, thereby effectively charging a battery.

In fact, the concept might seem flawed, since an additional, time-dependently driven device is also expected to lead to additional heat dissipation. However, there are several advantages which might in the end still result in an overall benefit and efficiency increase. First, themselves being based on quantum dots or similar devices, nanoscale heat engines can be integrated directly into the same nanocircuits as those connecting the devices which dissipate the energy (on-chip). This allows to convert the heat back into usable energy right where the heat is generated, thereby reducing irrecoverable losses. Second, functionally relevant parts of the device might in any case be subject to time-dependently varied (electromagnetic) signals or fields to work properly. If the latter affect other, non-relevant

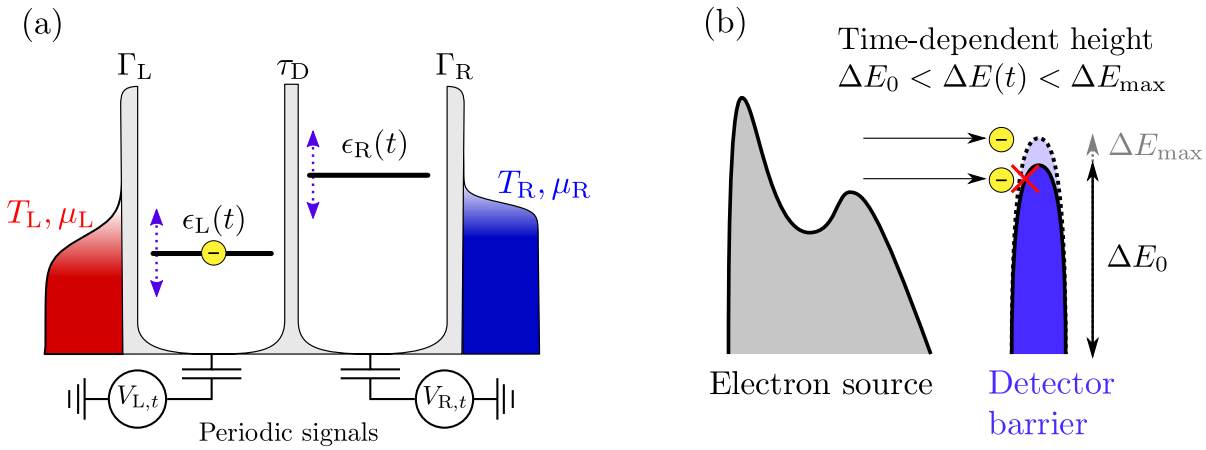

Figure 1.3: ***(a)*** *Model of the nanoscale heat engine as described in detail, e.g., in Refs. [54, 91]. The basic idea is that by applying time-dependent gate potentials to periodically shift the level positions $\epsilon_L(t)$ and $\epsilon_R(t)$ of two tunnel-coupled (τ_D) single-level quantum dots L and R, one can use the thermal gradient $\Delta T = T_L - T_R > 0$ between two tunnel-coupled reservoirs to pump against an oppositely directed potential bias $\mu_R - \mu_L > 0$.*
(b) *Simplified sketch of how the experiments described in Refs. [22, 74] measure a time- and energy-resolved distribution of individual electrons emitted from a quantum dot source. With the detailed technical procedure being rather sophisticated [22, 74], the basic idea is to periodically emit electrons towards a detector barrier which time-dependently resolves arriving electrons via a modulated barrier height $\Delta E(t)$, and filters them out completely if below a tunable threshold energy ΔE_0.*

parts of the device in a random way that leads to energy losses, it is thus always better to instead use such signals and fields in additional heat engines to regain some energy. Finally – and this is a main idea behind driven thermoelectrics – time-dependent operation also breaks microscopic time-translational invariance, and thus in particular, time-reversal symmetry. This may in return break Onsager's reciprocity relations [92, 93], which, as detailed below in Sec. 1.3.1 and Sec. 2.5, restrict the linear response of electrical currents to thermal gradients, and hence the efficiency of the heat-to-work conversion. Nevertheless, we emphasize that time-dependently driven systems are naturally not the only way to gain back some of the energy lost as heat, in particular since they lose passivity and the resulting minimal maintenance requirements as one of the biggest advantages of conventional thermoelectrics. In fact, the next section 1.3 further emphasizes that quantum dots and similar nanosystems are equally well suited under completely stationary conditions, acting as passive thermoelectrics, nanofridges, thermal current rectifiers or as so-called energy-harvesters [91, 94–108].

Solving the practical problem of converting between *time-dependent* electronic heat currents and electrical power is in fact intimately connected to more fundamental questions, arising especially in the context of the electronic nanosystems

of the type addressed here. First, in order to optimize periodic driving cycles of heat engines, it is essential to understand – both theoretically and experimentally – how the system and the time-dependent energy current behaves under elementary operations [51]. This includes in particular the step pulses studied in the appended papers, as shown in Fig. 1.2, or continuous sinusoidal driving, see chapter 4. Moreover, one might ask about the Coulomb interaction energy at the time of emission and its effect on the relevant decay time scales [Sec. (1.2.2)] in case more than one electron is emitted, see, e.g., Ref. [24]. This is precisely what papers II,III,V are concerned with theoretically. From the experimental point of view, this surmounts to the formidable challenge of *measuring* [22, 74, 109] time-dependent energy currents of individual electrons on the order of $\sim$ meV/ ns. The basic principle of one possible way of solving this using tunable energy barriers is illustrated in Fig. 1.3(b). While seemingly straightforward, the detailed technical realizations of such setups is still a technological challenge [74] and to a large extent work in progress.

A second, implicitly relevant question for this work is in fact even more fundamental than the question of *measuring* time-dependent single-electron heat currents: How can one *define* the energy current carried by single electrons in an open system with *quantum correlations*? At its core, this problem is related to an essential question of quantum thermodynamics: what is the time-dependent energetic contribution of a particle to a thermodynamic device if the particle exists, at least temporarily, in a *quantum superposition* [1] between being inside and outside of the device? For the work described in this thesis, we can assume that the energy current through *weakly coupled systems*, as precisely defined in the next chapter 2 and relevant in most parts of the appended papers, is not affected by such superpositions, see App. A and the author's Licentiate thesis [2] Ref. [110] (from here on referred to as Lic. Th. [110]). Or in simple terms, we always say that whatever energy "leaves" a reservoir immediately ends up in the quantum dot of interest. We stress, however, that deviations from this behavior are a topic of active current research [48, 111–116] in strongly coupled systems, touching upon the very limits of describing quantum mechanics in the framework and terminology of thermodynamics.

[1] To be clearly distinguished from a statistical mixture!

[2] Following the standards of the Swedish higher education system, the research summarized in this thesis represents an extension of the work published by the same author in his Licentiate thesis [110], which reflects this research only up to what is known in paper II. Naturally, since the general experimental and theoretical context of the research project has not changed, chapter 1 and chapter 2 are – in structure and content – based on Ref. [110]. However, new aspects have been added, and formulations have been improved where necessary and reasonable.

1.3 Stationary thermoelectric transport

Having covered the basics of time-dependent electronic charge- and energy transport, let us now turn to the second relevant aspect from the list given in Sec. 1.1: the electronic behavior under stationary conditions, i.e., without any further time-dependent, externally controlled device operation. Being mostly relevant for papers IV,V, we here focus on stationary thermoelectric transport in the above introduced few-level quantum dots weakly tunnel-coupled to electronic contacts [Sec. (1.2)]. The main interest is both the linear and nonlinear response of stationary particle- and heat currents I_N and I_Q through the quantum dot to potential biases V and temperature gradients ΔT between the different contacts [97, 103–105, 107, 117–126]. We start with a short overview of why this topic has originally attracted attention, and then turn towards modern studies and how they connect to the papers described in this thesis. Of special importance for us are some recent, well-known experimental realizations [104, 105, 107, 127, 128] that make explicit use of the energy structure in the coupling between the quantum dot and its environment – a central topic in paper V.

1.3.1 Thermoelectric effect in quantum dots

The classical stationary thermoelectric effect refers mostly to either the flow of charge in response to a temperature gradient – known as *Seebeck effect* – or the flow of heat due to electrochemical potential gradient – named *Peltier* effect. In modern, macroscopic thermoelectric materials, both effects are exploited for a variety of applications [129, 130]. This includes waste heat recovery in, e.g., power plants and automobiles, body-heat powered electronics [131–133], thermocouple or thermopile based thermometry [134], but also so-called Peltier cooling in a variety of scientific, industrial and consumer-oriented products [135], such as, e.g., air conditioners. One main benefit of thermoelectrics is their autonomous operation at relatively low maintenance costs and efforts. Another advantage is that they can typically be small enough to be placed close to where the actual heat is produced. However, on the downside, the efficiency of the heat-to-work conversion or cooling is rather low. This is quantified in terms, of e.g., a rather small maximum output power $P_{\max}$ or a low ratio $\eta = P/I_Q$ of electrical output power P and flowing heat I_Q compared to the Carnot efficiency $\eta_C = 1 - T_{\rm cold}/T_{\rm hot}$, in particular at maximum output power, $\eta_{\max} = P_{\max}/I_Q$.

As first argued by Refs. [120–122, 136], the above described quantization of charge and energy in quantum dots can improve this efficiency. The original discussion was focused mostly on the linear response regime – studied in papers IV,V for an interacting single-level quantum dot – in which the stationary particle and heat currents between the contacts I_N and I_Q depend linearly on the potential

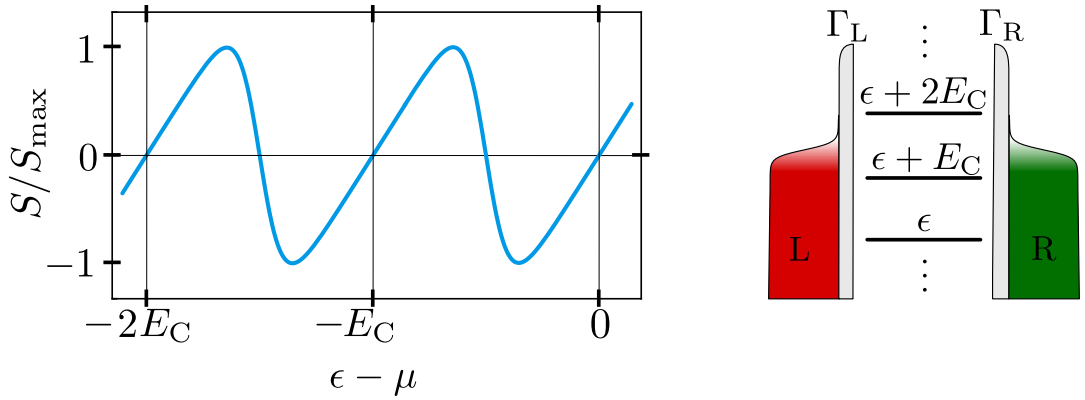

Figure 1.4: *Coulomb blockade oscillations in the linear thermopower* $S = V/\Delta T_{I_N,V,\Delta T\to 0}$ *as a function of a tunable base level-position* ϵ *of a nanosystem with small level-splitting* Δ *but large charging energy* $E_C \gg \Delta, T$*, such as a metallic island [Fig. 1.1]. Given a minimal energy* ϵ *required to add a particle to a base charge occupation and assuming a constant-interaction model, the n-th subsequent addition of a particle costs the addition energy* $\epsilon + n \cdot E_C$*. If any addition energy* $\epsilon + n \cdot E_C$ *is in resonance with the common environment potential* μ *at full equilibrium – known as Coulomb resonances* $\epsilon - \mu + n \cdot E_C = 0$ *– the linear thermopower* S *vanishes due to the particle-hole antisymmetric effect of any infinitesimal increase in* ΔT *on the energy-dependent environment occupation (Fermi function). The saw-tooth shape of* $S(\epsilon)$ *is typically understood as a crossover between the linear behavior around two subsequent resonances [118]. Alternatively, the sharp step in* S *can itself be interpreted as a* resonance *when employing the fermionic duality [Sec. (3.2.3)] .*

and temperature bias V and ΔT via the Onsager matrix [93]:

$$\begin{pmatrix} I_N \\ I_Q \end{pmatrix} = \begin{pmatrix} G & G \cdot S \\ G \cdot \Pi & G \cdot S \cdot \Pi + \kappa \end{pmatrix} \cdot \begin{pmatrix} V \\ \Delta T \end{pmatrix}. \tag{1.1}$$

The matrix contains the electrical conductance $G = I_N/V|_{\Delta T=0}$, the Peltier coefficient $\Pi = I_Q/I_N|_{\Delta T=0}$, the thermal conductance $\kappa = I_Q/\Delta T|_{I_Q=0}$, and the linear thermopower (Seebeck coefficient) $S = V/\Delta T|_{I_N=0}$. These quantities in return enter the efficiency η via the thermoelectric *figure of merit* $ZT = GS^2T/\kappa$, which can in principle be relatively high compared to macroscopic materials due to the discretized density of states in nanosystems [120–122, 136]. Of particular relevance for the appended papers are the well-known [118, 137] and experimentally observed [119, 138, 139] Coulomb blockade oscillations in the thermopower S, illustrated and explained in Fig. 1.4. Namely, apart from affecting ZT and η, the origin and shape of these oscillations can be understood from a completely different point of view when arguing from the *fermionic duality relation* discussed in this thesis: instead of considering the oscillations as a *crossover* between two transport regimes, we in fact identify them as a *resonant effect*, as Sec. 3.2.3 points out.

Next to these interesting fundamental aspects in linear response, more recent investigations [97, 102–106, 124, 125, 140–147] show that few-level systems of interest here can overcome fundamental limits imposed on the efficiency η in the *nonlinear* regime, i.e., accounting for terms in the currents I at least quadratic in $V, \Delta T$. This concerns for instance the above mentioned limit due to time-reversal symmetry and *Onsager reciprocity* [92, 148], which in fact bounds the maximum efficiency to $\eta_C/2$ in the linear regime by imposing $\Pi = S \cdot T$. The problem from a theoretical point of view is, however, that precisely due to the absence of such limiting symmetries, accessing nonlinear response analytically is significantly more difficult. This concerns both simple quantum dot models [146] and more complex systems with a larger amount of degrees of freedom [147]. In this respect, Paper IV exploits that the fermionic duality relation explored in this thesis relies mainly on fermions fulfilling fermionic statistics and what is known and explained below as parity superselection [Sec. (3.3)]; it hence also holds and simplifies the analytical treatment in the strongly nonlinear regime. More explicitly, this allows us to find insightful analytical expressions for both the nonlinear thermopower $S_{\mathrm{nl}} = V/\Delta T|_{I_N=0}$ and thermal conductance $\kappa_{\mathrm{nl}} = I_Q/\Delta T|_{I_Q=0}$. These expressions explicitly reveal the physics underlying previously observed [119, 143] deviations from the linear regime which could, in some cases, only be studied numerically or using more simplified, effective models.

Finally, as already announced above, some recent experiments [104, 105, 107] have shown, based on previous theoretical work [97], that the combination of local Coulomb interaction in discrete few-level systems and *a specifically tuned energy-dependent transparency* of the tunnel barriers can be used as so-called *energy harvesters*; such harvesters convert (thermal) charge fluctuations into directed usable electrical current. Given that this is one major motivation of paper V to formulate the fermionic duality for energy-dependent tunneling, let us describe this a bit more in detail.

1.3.2 Effect of energy-dependent tunneling

A well-known system that demonstrates the interplay between Coulomb interaction and energy-dependent coupling is the three-terminal *Coulomb blockade heat engine* that was theoretically proposed by Sanchèz and Büttiker [97], and experimentally realized by Thierschmann et al. [104]. Figure 1.5 explains the working principle: a single-level [1] quantum dot is tunnel coupled to one hot reservoir at temperature T_{h} – the heat source – and capacitively coupled to another single-level quantum dot which tunnel couples to two cold reservoirs at temperature $T_{\mathrm{c}} < T_{\mathrm{h}}$. Both level-positions are tuned such that the capacitive coupling locks the combined system to stable single occupation. Hence, if a thermally excited

[1] We stress again that a single-level dot is effectively realized by having a large level splitting Δ compared to the temperature(s) T in the environment.

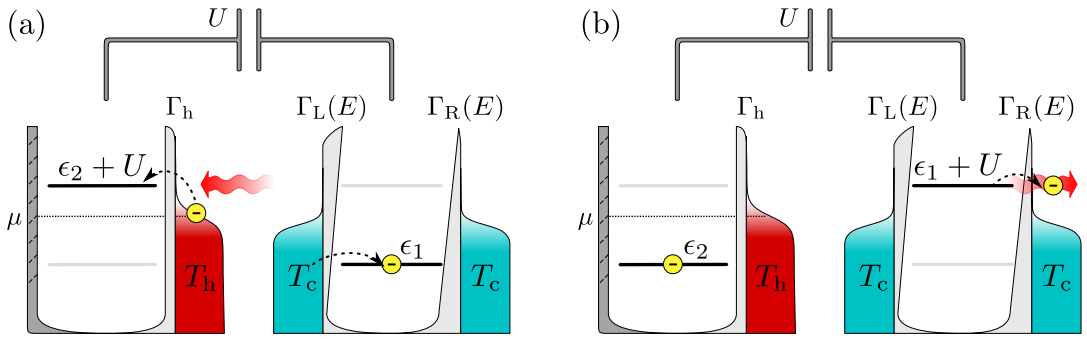

Figure 1.5: *Illustration of the Coulomb blockade heat engine studied in [97, 104]. Two (spinless) electronic levels ϵ_1 and ϵ_2 are capacitively coupled with coupling strength U, and tunnel coupled to reservoirs at different temperatures $T_h > T_c$. The tunnel barriers to the two cold reservoirs are asymmetrically energy-dependent with respect to the left and right contact, such that electrons at energy ϵ_1 preferably tunnel from the left reservoir, and electrons at energy $\epsilon_1 + U$ mostly tunnel to the right reservoir. The levels are tuned such that only one of the two dots can be stably occupied, due to the capacitive interaction. The working principle is as follows: given an electron that has preferably entered level 1 from the left, the hot reservoir might thermally excite electrons which have enough energy to pay the additional charging energy U required to tunnel to level 2* **(a)**. *This then causes the electron on level 1 to tunnel out, mostly to the right reservoir due to the asymmetric tunnel barriers* **(b)**. *Altogether, the charging energy is transfered from the hot to the cold reservoir, and a directed charge current is generated.*

electron tunnels from the hot reservoir to the coupled quantum dot, an electron that is already occupying the dot coupled to the cold reservoirs is pushed out, thereby taking away the charging energy. The crucial point is that if the left-right asymmetry of the couplings to the two cold baths depends on energy, this yields a *directed* current: in the setting of Fig. 1.5, an electron enters at a lower energy from the left and leaves with a higher energy taken from the electron in the other dot to the right.

Paper V also analyzes the consequences of such energy filtering via energy-dependent barriers, in the simpler setting of an interacting single-level quantum dot coupled to two reservoirs. For example, the level position (gate voltage) at which the linear thermopower S takes the steps in between two Coulomb resonances illustrated in Fig. 1.4 shifts due to the energy-asymmetry in the barriers, as the latter favors transport via either of the Coulomb resonances. Moreover, considering the transient behavior discussed in the previous Sec. 1.2, it may lead to decay via pronouncedly time-correlated, bunched sequential tunneling of two electrons, and to quasi-stationary occupations which are normally highly unfavorable in a non-equilibrium environment.

More generally, the analysis carried out in Ref. [97] again exemplifies that while analytically accessing nonlinear transport is in principle possible for quantum dot

systems, the large number of free parameters makes it difficult to derive concise results. In this respect, paper V demonstrates that, as always when making use of symmetry relations, the fermionic duality can effectively reduce the analytical complexity of the parameter-dependence, both in the stationary and in the transient regime, and in particular for systems with energy-dependent tunnel coupling. This in return is precisely what leads paper V to the above mentioned insights regarding the step in the thermopower, bunched tunneling and quasi-stationary states. Moreover, concerning the Coulomb-blockade heat engine described in Fig. 1.5, we note that this model is very generally used to describe a variety of problems in which capacitive interaction between modes plays a role, including realizations of Maxwell's demon [149, 150], the study of Coulomb drag [151, 152], measurement setups such as described below in Sec. 2.1.2 and studied in paper I, and, more recently, even as building blocks for effectively *attractive* quantum dots [153]. A better analytical understanding is thus desirable in many different contexts.

Chapter 4 shall pick up the discussion of the last paragraph again. At this point, we conclude that papers IV,V tie in with many currently studied aspects of stationary thermoelectric transport in open, interacting few-level systems, and turn to the next chapter 2, which introduces the theoretical description of precisely such systems.

2 Decay dynamics in open fermionic systems

Let us now introduce the theory necessary to understand the topic of this thesis and its appended papers I to V. As pointed out above, we analyze both stationary and time-resolved charge and energy transport through fermionic open nanoscale systems – and in particular few-level quantum dots – by making use of a novel duality relation. This relation has been found and published in paper II under the name "fermion-parity duality", and has been relabeled as "fermionic duality" in paper V. As a motivation and point of reference for this chapter, we start upfront by stating in a few words what this duality is, then devote this chapter to explaining concepts necessary to understand it, and finally, in the next chapter, precisely explain the duality and discuss what we can learn from it.

To start in summarizing terms: given a *fermionic open system* that exchanges particles via tunneling with a number of large fermionic reservoirs in the environment, we here describe the *dynamics* induced in the open subsystem by this particle exchange using a master equation for the system's *reduced density operator* $\rho(t)$. For *weak tunnel coupling* in the Markovian limit – which is precisely defined below – this equation assumes the simple linear form $\partial_t \rho(t) = W\rho(t)$ with the *evolution kernel* W. Unlike the Hamiltonian H entering Schrödinger's equation $\partial_t|\psi(t)\rangle = -\mathrm{i}H|\psi(t)\rangle$, this kernel is neither Hermitian nor anti-Hermitian, $W^\dagger \neq \pm W$. However, the *fermionic duality* still establishes the following, nontrivial relation to the Hermitian conjugate $W^\dagger$:

$$W^\dagger = -\Gamma - \mathcal{P}\overline{W}\mathcal{P}, \tag{2.1}$$

with Γ representing a shift, $\mathcal{P}$ denoting the *fermion parity* of the open system, and $\overline{W}$ being the evolution kernel of an *energy-inverted, dual system.*

Simply put, this chapter explains the basic concepts mentioned in the previous paragraph. Based on this knowledge, chapter 3 then reintroduces Eq. (2.1) in a precise way, and details how the appended papers use Eq. (2.1) to gain new insights. As a final introductory remark, we note that paper II actually presents the duality in a more general form that applies beyond the, here most relevant weak-coupling Markovian limit assumed in Eq. (2.1). The following treatment is therefore also extended beyond the weak coupling theory where reasonable.

Let us now turn to the model for both the general class of systems treated in this thesis, and for the quantum dot systems studied in the appended papers.

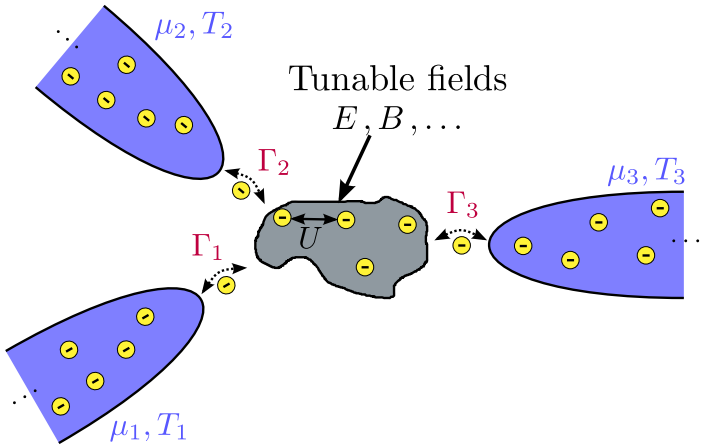

Figure 2.1: *Model sketch for the class of open fermionic quantum systems investigated in this work. The central open system can in general be subject to many-body interactions, such as Coulomb repulsion (indicated by strength U), and to external, controllable (classical) electromagnetic fields, $E, B, \ldots$. The system is coupled – via tunneling through barriers with typical tunneling frequencies Γ_α – to several fermionic reservoirs α at electrochemical potential μ_α and temperature T_α.*

2.1 General model and quantum dot systems

A simplified sketch of the type of systems we are interested in is shown in Fig. 2.1. The central region constitutes the open fermionic system, representing, e. g., some electronic device. This system may internally be subject to many-body interactions such as Coulomb repulsion, and may furthermore be externally tunable via electromagnetic fields. Most importantly, being an open system, the region can exchange particles via tunneling to and from contacting reservoirs. The latter are assumed to be effectively describable as non-interacting systems, i. e., systems for which a Fermi-gas or Fermi-liquid theory can be applied. The typical frequencies Γ_α of tunneling between open system and reservoirs are determined by tunnel barriers separating the open system locally from its environment. Typical experimental realizations of such situations are, e.g., two dimensional electron gases within GaAs or SiGe heterostructures that are electrostatically confined by the gate electrodes, see Fig. 1.1(b).

This work focuses on how the (quantum) state describing only the fermions occupying the open system, and how associated observables such as charge and energy evolve in time under particle-exchange with the environment. We do not account for any coupling between these fermions and other bosonic quantum excitations such as phonons or photons. The external fields enter our description implicitly via their effect on the potential landscape, and consequently, on the energy eigenstates of the system. Moreover, while the appended papers and thus the following description are limited to time-independent system parameters, Sec. 2.6.2

below briefly elaborates on how the theory extends to situations in which the explicit time-dependence is crucial. This is, e.g., the case for the charge, energy and spin pumps described in Refs. [21, 22, 24, 54, 154–157], see also chapter 4.

Given the above stated system and assumptions, the full-system Hamiltonian H_{tot} decomposes into the local open-system part H, the environment contribution H_{R}, and the tunnel coupling H_{tun}:

$$H_{\mathrm{tot}} = H + H_{\mathrm{R}} + H_{\mathrm{tun}}. \tag{2.2}$$

The local dynamics of the open subsystem is governed by H.

$$H = \sum_{l} \epsilon_l d_l^\dagger d_l + H_{\mathrm{int}}. \tag{2.3}$$

The first term introduces creation ($d_l^\dagger$) and annihilation operators (d_l) for fermions in the single-particle states $|l\rangle$ defining the open system. The latter are thus energy eigenstates of only the non-interacting, single-particle contribution to H, with the energies labeled ϵ_l. The multi-index $l = \phi_l, \sigma_l, \ldots$ fully characterizes the states in terms of an orbital quantum number ϕ, a spin $\sigma = \uparrow, \downarrow$ with respect to a fixed quantization axis, and any further *discrete* degree of freedom necessary.

The local interaction H_{int} can in principle include any type of fermionic multi-particle interaction that respects the parity superselection principle [158–160]. The latter prohibits any quantum superposition between states of an even and an odd number of fermions, and technically implies that the Hamiltonian H must commute with the local fermion-parity operator,

$$0 = [(-\mathbb{1})^N, H_{\mathrm{int}}] = [(-\mathbb{1})^N, H] \tag{2.4}$$

where

$$N = \sum_{l} d_l^\dagger d_l \quad , \quad (-\mathbb{1})^N = \exp\left(i\pi N\right) \tag{2.5}$$

are the local open-system particle number operator N and the parity operator $(-\mathbb{1})^N$, respectively. Most importantly, this includes the, for us crucial local two-particle Coulomb interaction between charged electrons.

The Hamiltonian H_{R} describes the reservoirs α in the environment for effectively non-interacting fermions:

$$H_{\mathrm{R}} = \sum_{\alpha} H_\alpha = \sum_{\mathbf{k}m} \epsilon_m(\mathbf{k}) c_{\mathbf{k}m}^\dagger c_{\mathbf{k}m}. \tag{2.6}$$

Equation (2.6) introduces creation ($c_{\mathbf{k}m}^\dagger$) and annihilation operators ($c_{\mathbf{k}m}$) for the single-particle states $|\mathbf{k}m\rangle$ defining the environment. Their energies are labeled $\epsilon_m(\mathbf{k})$, being a function of a continuous wave vector $\mathbf{k}$ and a discrete multi-index $m = \alpha_m, \nu_m, \sigma_m, \ldots$. The latter indicates fermions in reservoir α with

band/orbital index ν, spin projection σ, and any further degree of freedom necessary to distinguish the states.

Finally, open system and environment couple via the tunneling Hamiltonian

$$H_{\text{tun}} = \sum_{\mathbf{k}ml} \tau_{\mathbf{k}ml} c^\dagger_{\mathbf{k}m} d_l + \text{H.c.} \tag{2.7}$$

The tunneling amplitudes $\tau_{\mathbf{k}ml}$ quantify the coupling between the single-particle state $|l\rangle$ in the open system and the single-particle state $|\mathbf{k}m\rangle$ in the environment. Together with the density of states in the environment, these amplitudes define the characteristic tunneling frequency scales

$$\Gamma_{m,ll'}(E) = 2\pi \sum_{\mathbf{k}} \delta(E - \epsilon_m(\mathbf{k}))\, \tau_{\mathbf{k}ml} \tau^*_{\mathbf{k}ml'}. \tag{2.8}$$

Note that we have set $\hbar = 1$.

The concrete systems considered in the appended papers are studied in the *weak coupling regime*, which can now be defined as the limit in which the times $\sim 1/\Gamma_{m,ll'}(E)$ are much longer than the typical memory times of the non-interacting reservoirs. The latter are typically limited by thermal fluctuations, and hence given by the typical inverse temperatures $\sim 1/T_\alpha$. Formally, weak coupling thus means $|\Gamma_{m,ll'}|/T_\alpha \ll 1$.

Another important aspect of the couplings (2.8) is their dependence on the energy E carried by the tunneling particles. In the appended papers I to IV, this dependence is in fact neglected: in this so-called *wideband limit*, one assumes that the density of states in the environment changes on a much larger energy scale compared to the splittings between the energy levels in the open system which are relevant for the studied dynamics. However, this thesis also addresses the systems described in Sec. 1.3.2 of the introduction, i.e., for which energy-dependent tunnel barriers are essential [22, 74, 161, 162] to capture all relevant physics or even specifically *designed* to achieve a certain effect [97, 104, 105, 107, 127, 128]. Paper V hence explicitly takes their energy-dependence into account. Note in particular that this needs to be clearly distinguished from *effectively* energy-dependent Γ due to hybridizing orbitals in the open system, as for example considered in Refs. [156, 163]: whereas the latter refers only to local energies, and is thus never sensitive to *total* shifts of the open-system spectrum with respect to a fixed reference energy in the environment [1], a $\Gamma(E)$ due to energy-dependent tunnel barriers *does in general* depend on such shifts [2]. As such, these two types of energy-dependences also have different implications for the fermionic duality (2.1) presented in chapter 3, see Sec. 3.5.

Having set up the Hamiltonian for the most general type of systems considered in this thesis, we finish the model section by describing the specific open

[1] For example, the global band bottom, $E \equiv 0$.

[2] This is *not* to be confused with a *global* energy shift of both open system and environment, which, of course, has no effect due to the global phase invariance.

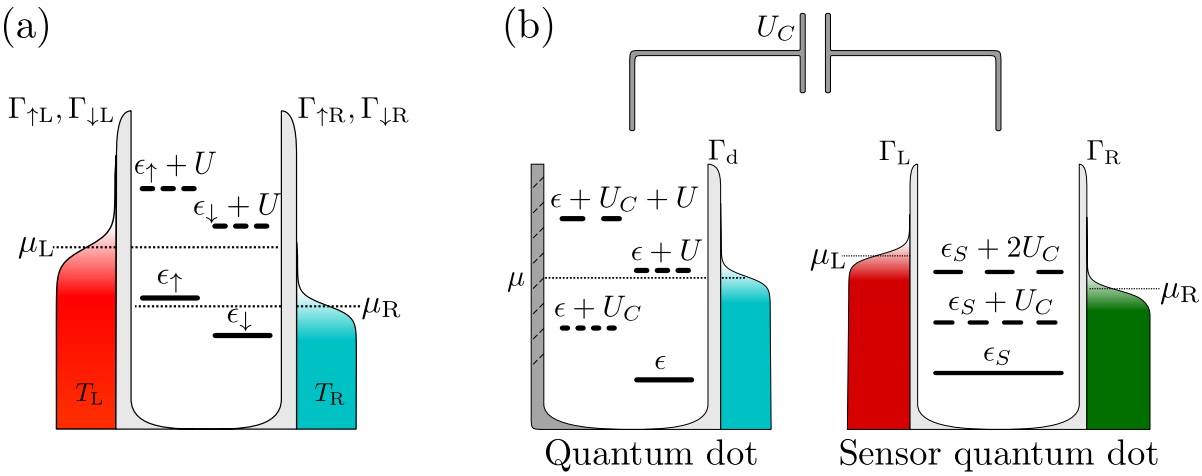

Figure 2.2: ***(a)*** *Quantum dot consisting of one spin-split orbital with single-particle energies $\epsilon_\uparrow, \epsilon_\downarrow$ and Coulomb interaction strength U [Eq. (2.9)]. The dot is spin-dependently tunnel coupled ($\Gamma_{\sigma\alpha}$ with $\sigma = \uparrow, \downarrow$ and $\alpha = L,R$) to a left (L) and right (R) reservoir. The latter are characterized by their potentials μ_L, μ_R and temperatures T_L, T_R.*
(b) *Spin-degenerate locally interacting single-level quantum dot [Eq. (2.11)] (level-position ϵ, interaction strength U) tunnel coupled to a single reservoir (potential μ, coupling strength Γ_d) and capacitively coupled (interaction energy U_C) to a sensor quantum dot (SQD). The latter is represented by a single fermionic mode (level-position ϵ_S) tunnel coupled to a left and right reservoir ($\mu_L \neq \mu_R, T_L = T_R = T_d = T$). The addition energies $\epsilon_S + U_C$ and $\epsilon_S + 2U_C$ correspond to the coupled quantum dot being occupied by one or two electrons, respectively.*

system Hamiltonians H studied in the appended papers – which is both the individual single-level quantum dot (papers II - V), and a spinless *sensor quantum dot* coupled to a spin-degenerate single-level dot (paper I).

2.1.1 Electronic single-level quantum dot

As figure 2.2(a) illustrates, we here regard an open electronic, interacting single-level quantum dot as a single, either spin-degenerate or spin-split orbital that tunnel-couples to the reservoirs in the environment. Given that this orbital can be simultaneously occupied by two electrons with a spin-up and spin-down with respect to a fixed quantization axis, we take into account the local Coulomb interaction between these electrons, as quantified by the interaction strength U. The open system Hamiltonian H is therefore specified by

$$H = \sum_{\sigma=\uparrow,\downarrow} \epsilon_\sigma N_\sigma + U N_\uparrow N_\downarrow, \tag{2.9}$$

where ϵ_σ is the single-particle energy and $N_{\sigma=\uparrow,\downarrow} = d_\sigma^\dagger d_\sigma$ are the occupation number operators for the individual spins σ. The energy ϵ_σ may depend on the spin via

a local magnetic field B giving rise to an effective Zeeman splitting, $\epsilon_\sigma = \epsilon + \sigma\frac{B}{2}$ with $\sigma = \uparrow, \downarrow \equiv +, -$. The many-body energy eigenstates of this Hamiltonian and the corresponding energies are hence

$$\begin{aligned} |E_0\rangle = |0\rangle \quad , \quad |E_\uparrow\rangle = |\uparrow\rangle \quad , \quad |E_\downarrow\rangle = |\downarrow\rangle \quad , \quad |E_2\rangle = |2\rangle \\ E_0 = 0 \quad , \quad E_\uparrow = \epsilon_\uparrow \quad , \quad E_\downarrow = \epsilon_\downarrow \quad , \quad E_2 = \epsilon_\uparrow + \epsilon_\downarrow + U, \end{aligned} \tag{2.10}$$

indicating an empty dot (0), occupation by a single spin ($\sigma = \uparrow, \downarrow$), and double occupation (2). Paper III investigates how the combination of such a Zeeman splitting and a large Coulomb interaction $U/T \gg 1$ with respect to the temperature T of a single reservoir in the environment affects the tunneling-induced dynamics of the occupations of the energy eigenstates (2.10). In particular, it is contrasted to the simpler case $B = 0$ with an absent spin-splitting:

$$H \overset{B=0}{\rightarrow} \epsilon(N_\uparrow + N_\downarrow) + UN_\uparrow N_\downarrow \overset{(2.5)}{=} \epsilon N + UN_\uparrow N_\downarrow, \tag{2.11}$$

implying the simpler, spin-degenerate spectrum

$$E_0 = 0 \quad , \quad E_\uparrow = E_\downarrow = \epsilon \quad , \quad E_2 = 2\epsilon + U. \tag{2.12}$$

We use this simpler, well-known *single-level Anderson model* [29] to capture and study the essential effect of strong local Coulomb interaction on both time-dependent (paper II,III,V) as well as stationary non-equilibrium (paper IV,V) electronic charge- and energy transport, flowing between the dot and either one or two possibly voltage- and temperature biased reservoirs. This effect is precisely what can be distilled very clearly by the fermionic duality, as discussed in the next chapter.

2.1.2 Sensor quantum dot

One way to experimentally observe the occupation dynamics of the single-level quantum dot without *interfering* too much with the dynamics of interest itself is to capacitively couple the dot to another sensor quantum dot (SQD); this sensor dot is then in return read out electronically via external circuits. The idea of paper I is precisely to investigate this situation, as displayed in Fig. 2.2(b). Starting from the spin-degenerate system (2.11), we account for the sensor dot by introducing another spinless [1] fermionic mode S with on-site energy ϵ_S and a coupling to the measured dot via the electrostatic Coulomb interaction, quantified by $U_C < U$:

$$H = \epsilon N + UN_\uparrow N_\downarrow + \epsilon_S N_S + U_C N N_S. \tag{2.13}$$

The 8 energy eigenstates $|d = 0, \uparrow, \downarrow, 2; S = 0, 1\rangle$ are products of the four single-level quantum dot states (2.10) and the two occupation number states of the

[1] This could experimentally be achieved by a large magnetic field localized to the sensor dot.

sensor dot, $|N_S = 0/1\rangle$. The many-body spectrum is accordingly given by

$$\begin{aligned} E_{00} = 0 \quad , \quad E_{\sigma 0} = \epsilon \quad , \quad E_{20} = 2\epsilon + U \\ E_{10} = \epsilon_S \quad , \quad E_{\sigma 1} = \epsilon + \epsilon_S + U_C \quad , \quad E_{21} = 2\epsilon + \epsilon_S + U + 2U_C. \end{aligned} \tag{2.14}$$

The model includes two important ingredients, as precisely argued in paper I. First, the extra energy due to the influence of the interdot coupling U_C does depend on the precise occupation number N in the dot to be measured, allowing the sensor dot to extract not just the *average* dot occupation, but in fact occurrence probability for each dot state. Second, the readout circuit of the sensor dot is completely separated from the reservoir coupled to the dot to be measured, as Fig. 2.2(b) shows. In the considered model, the only back-action effect of the readout on the dot occupation is hence through the capacitive coupling itself, and this effect is shown in paper I to be well controllable in theory.

2.2 Transient open-system dynamics

Our main interest is both the transient and long-time limit behavior of the *reduced density operator* $\rho(t)$ of the open subsystem, after being prepared in an initially non-stationary state ρ_0 by, e.g., a switch of some externally applied gate voltage *precisely before* a fixed time $t_0 \equiv 0$, see Fig. 2.3. Formally, this reduced density operator is obtained from the time-dependent density operator $\rho^{\mathrm{tot}}(t)$ of the full system by taking the partial *Fock-space* [1] trace over all environment states. Given that $\rho^{\mathrm{tot}}(t)$ represents the pure or mixed state of a *closed* quantum system with time-independent Hamiltonian, it is governed by the Liouville-von Neumann equation and hence evolves exponentially according to

$$\rho^{\mathrm{tot}}(t) = \exp\left(-\mathrm{i}L_{\mathrm{tot}}t\right)\rho_0^{\mathrm{tot}} \quad , \quad L_{\mathrm{tot}}\bullet = [H_{\mathrm{tot}}, \bullet]. \tag{2.15}$$

The total-system Liouvillian L_{tot} for $t \geq 0$ is defined as the commutator $[L_{\mathrm{tot}}, \bullet]$ of the total-system Hamiltonian (2.2) with some operator $\bullet$. The reduced density operator thereby formally reads

$$\rho(t) = \operatorname*{Tr}_{\mathrm{R}}\left[\rho^{\mathrm{tot}}(t)\right] = \operatorname*{Tr}_{\mathrm{R}}\left[\exp\left(-\mathrm{i}L_{\mathrm{tot}}t\right)\rho_0^{\mathrm{tot}}\right]. \tag{2.16}$$

The central task in obtaining an explicit form for $\rho(t)$ is to actually carry out the reservoir trace. This thesis and its appended papers follow the diagrammatic perturbative approach originally developed in [164, 165] and more recently refined [166, 167] to a form that has eventually allowed us to derive the duality (2.1) in paper II. The first step is to assume that the initial state ρ_0^{tot} from which the system evolves can statistically be treated as a product of the initial

[1] See Lic. Th. [110] for more details on this trace.

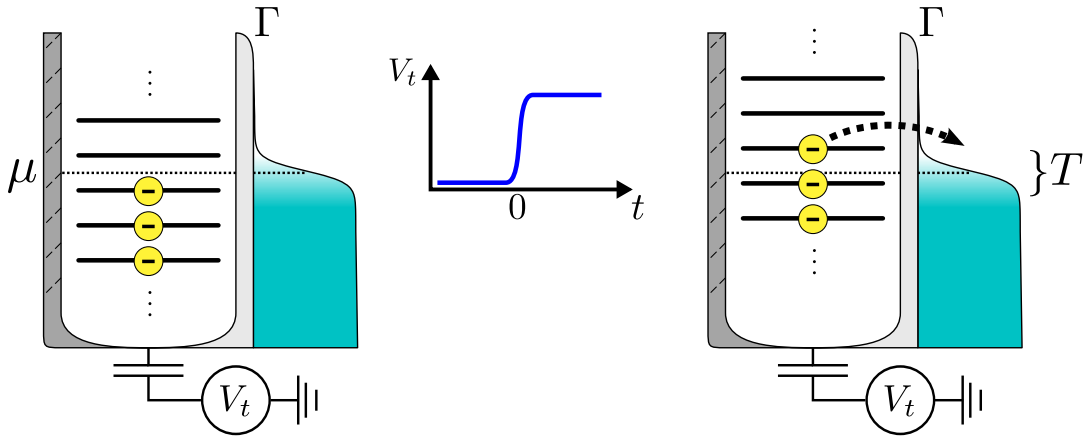

Figure 2.3: *Example of a voltage switch applied to an open quantum system with n discrete (many-particle) energies, tunnel-coupled with tunneling strength Γ to an electronic reservoir at chemical potential μ and temperature T. Initially, the system is filled up to the Fermi edge μ. The voltage switch described by $V(t)$ then leads to an approximately instantaneous shift of the open system energies, thereby driving the system out of stationarity. This induces tunneling process(es) which let the system relax to a new stationary state.*

open-system state $\rho_0 = \operatorname{Tr}_{\mathrm{R}}[\rho_0^{\mathrm{tot}}]$ and the environment state $\rho_0^{\mathrm{R}} = \operatorname{Tr}[\rho_0^{\mathrm{tot}}]$. More precisely, this means

$$\operatorname{Tr}_{\mathrm{R}}\left[A^{\mathrm{R}} B \rho_0^{\mathrm{tot}}\right] = \operatorname{Tr}_{\mathrm{R}}\left[A^{\mathrm{R}} \rho_0^{\mathrm{R}}\right] \cdot B\rho_0 \tag{2.17}$$

for any operation A^{R} that only depends on the occupations in the environment, and any operation B that only depends on the open-system occupations. Using this relation, we can simplify Eq. (2.16) to

$$\rho(t) = \operatorname{Tr}_{\mathrm{R}}\left[\rho^{\mathrm{tot}}(t)\right] = \operatorname{Tr}_{\mathrm{R}}\left[\exp\left(-\mathrm{i}L_{\mathrm{tot}}t\right)\rho_0^{\mathrm{tot}}\right] = \operatorname{Tr}_{\mathrm{R}}\left[\exp\left(-\mathrm{i}L_{\mathrm{tot}}t\right)\rho_0^{\mathrm{R}}\right]\rho_0 = \Pi(t)\rho_0, \tag{2.18}$$

for all $t > 0$, with the time propagator

$$\Pi(t) = \operatorname{Tr}_{\mathrm{R}}\left[\exp\left(-\mathrm{i}L_{\mathrm{tot}}t\right)\rho_0^{\mathrm{R}}\right] \tag{2.19}$$

being left to evaluate. Next, we use that the environment state ρ_0^{R} describes the occupation of not directly coupled reservoirs which are large compared to the open system. Namely, we thus assume that $\rho_0^{\mathrm{R}} = \operatorname{Tr}[\rho_0^{\mathrm{tot}}]$ is a product of grand-canonical ensembles for each reservoir α, characterized by the electrochemical potential μ_α and temperature T_α (we set $k_{\mathrm{B}} \equiv 1$):

$$\rho_0^{\mathrm{R}} = \exp\left(-\sum_\alpha \left(H_\alpha - \mu_\alpha N_\alpha\right)/T_\alpha\right) \Big/ \operatorname{Tr}_{\mathrm{R}}\left[\exp\left(-\sum_\alpha \left(H_\alpha - \mu_\alpha N_\alpha\right)/T_\alpha\right)\right]. \tag{2.20}$$

By $N_\alpha = \sum_m^{\alpha_m=\alpha} c_m^\dagger c_m$, we denote the particle number operator for reservoir α.

Using Eqs. (2.18) – (2.20) together with the fact that the reservoir Hamiltonians H_α are only quadratic in the fields, we may now apply the Liouville-space diagrammatic technique from Refs. [166, 167] to expand $\rho(t)$ in orders of the tunnel-coupling Liouvillian $L_{\text{tun}}\bullet = [H_{\text{tun}}, \bullet]$. This leads to what is known as the *generalized master equation*, or quantum kinetic equation, see Eq. (2.25) in Sec. 2.2.2. To discuss this equation and its solution in a way appropriate for the following chapters, we, however, first need to introduce a few key elements of this Liouvillian approach. Detailed derivations of the method are given in Refs. [166, 167] and in the supplementary to the appended paper II.

2.2.1 Liouville space notation

The time evolution propagator $\Pi(t)$ given in Eq. (2.19) is in fact a linear *superoperator*, since it acts on the set of linear operators x which in turn act on the Hilbert space of the reduced, open system. This set of operators x in itself forms a vector space which is called *Liouville space*, and it contains the reduced density operator $\rho(t)$ describing the open-system dynamics as the central object. Thus, to clarify that we consider operators x acting on the open-system Hilbert space as *vectors*, we introduce the superket and superbra notation Refs. [77, 166]:

$$|x) = x \quad , \quad (x|\bullet) = \text{Tr}[x^\dagger \bullet] = \sum_i \langle i|x^\dagger \bullet |i\rangle. \tag{2.21}$$

Operators x such as the reduced density operator $\rho(t)$ or its basis elements are expressed as rounded superkets. The rounded bra vectors $(x|$ are, as usual, defined via the scalar product $(x|\bullet)$ with another vector $|\bullet)$. The scalar product is chosen as the Hilbert-Schmidt product involving the trace of $x^\dagger\bullet$ over the reduced-system, which in Eq. (2.21) is explicitly formulated as the diagonal sum in any complete orthonormal *many-body* Hilbert-space basis $(|i\rangle)_i$. The notion of the Hermitian adjoint for superoperators $\mathcal{A}$ acting on the Liouville space is also defined in the usual way via this product [1]: $(x|\mathcal{A}^\dagger|y) = [(y|\mathcal{A}|x)]^*$. An example of a superhermitian superoperator fulfilling $A^\dagger = A$ is the left-action of the fermion parity, $\mathcal{P}\bullet = (-\mathbb{1})^N\bullet$, which is especially important for us as it appears directly in the fermionic duality (2.1).

More practically, superkets and superbras are on the one hand used to compactly write expectation values $\langle A\rangle_\rho$ of an observable $A = A^\dagger$ with respect to a state $|\rho)$, or to write individual matrix elements ρ_{ij} of such a state (or any other operator):

$$\langle A\rangle_\rho = (A|\rho) = \text{Tr}\,[A\rho] \quad , \quad \rho_{ij} = (P_{ij}|\rho) = \text{Tr}\left[(|i\rangle\langle j|)^\dagger \rho\right] = \langle i|\rho|j\rangle, \tag{2.22}$$

[1] Note the difference between bold-type daggers $\dagger$ for the superhermitian adjoint, and regular daggers $\dagger$ for the usual Hermitian adjoint.

where $P_{ij} = |i\rangle\langle j|$. On the other hand, it is equally important for us that since the Liouville space is also a vector (Hilbert) space, sets of superbras $\left((v'_n|\right)_n$ and superkets $\left(|v_n)\right)_n$ can form a complete, biorthogonal basis

$$(v'_n|v_m) = \mathrm{Tr}\left[(v'_n)^\dagger v_m\right] \propto \delta_{nm} \quad , \quad \mathcal{I}\bullet = \sum_n \frac{1}{(v'_n|v_n)}|v_n)(v'_n|\bullet = \bullet \tag{2.23}$$

that we can use to insert the Liouville space identity $\mathcal{I}$ and to basis-expand *superoperators* $\mathcal{A}$ such as the time evolution propagator $\Pi(t)$ [Eq. (2.19)]:

$$\mathcal{A} = \mathcal{I}\mathcal{A}\mathcal{I} = \sum_{nm} \alpha_{nm}|v_n)(v'_m| \quad , \quad \alpha_{nm} = \frac{(v'_n|\mathcal{A}|v_m)}{(v'_n|v_n)(v'_m|v_m)}. \tag{2.24}$$

If both the ket and bra basis is constructed by physical-state density operators $\{|v_n)\}$, the coefficients α_{nm} describe amplitudes for transitions from the state $|v_m)$ to $|v_n)$ due to the effect that is represented by the action of the superoperator $\mathcal{A}$. However, as the primed symbols indicate, a set of $(v'_n|$ that is suitable and physically insightful does not necessarily have to be formed by the adjoint of the kets $|v_n)$, since the superoperator $\Pi(t)$ is generally not unitary, and its generator thus generally not Hermitian. As we further argue below and in the next chapter, this observation is in fact at the heart of a central problem of open-system dynamics – a problem that we show is directly addressed by the fermionic duality (2.1).

2.2.2 Master equation and currents

With the suitable notation at hand, let us now obtain the time evolution of the reduced density operator $|\rho(t))$ by evaluating the propagator Eq. (2.19) perturbatively in the coupling L_{tun}. Referring the reader to, e.g., Refs. [165, 167] for the detailed calculation, its result is a Dyson series that can be expressed as the *generalized master equation* [164, 165, 168–170]:

$$\partial_t|\rho(t)) = -\mathrm{i}L|\rho(t)) + \int_0^t dt' \mathcal{W}(t-t')|\rho(t')). \tag{2.25}$$

This equation is the starting point for the following analysis of the reduced system dynamics. The Liouvillian $L\bullet = [H, \bullet]$ describes the local, coherent dynamics of the open system, whereas the integral and its kernel $\mathcal{W}(t-t')$ express the coupling to the environment. The latter hence depends on the local open-system Hamiltonian H as well as on the couplings $\Gamma(E)$ [Eq. (2.8)], and furthermore on the reservoir density of states as well as the temperatures T_α and chemical potentials μ_α of the initial reservoir state ρ_0^{R} [Eq. (2.20)]. The coupling established by $\mathcal{W}$ is generally non-Markovian, as it relates $\partial_t|\rho(t))$ to the state $|\rho(t'))$ at a possibly earlier time $t' \leq t$. Nevertheless, since no part of the full Hamiltonian (2.2) is explicitly time-dependent [1], time translation invariance causes $\mathcal{W}$ to only depend

[1] After some initial switch that is not explicit, but only accounted for by the non-stationary initial state ρ_0^{tot}.

on the difference $t - t'$. Moreover, the major part of the appended papers and of this thesis is concerned with the *Markovian* limit, in which all dependences on earlier times $t' < t$ are dropped, as explained in the next section 2.3.

Let us furthermore address two properties of $\mathcal{W}$ which turn out to be crucial in applying the fermionic duality (2.1). First, since the dynamics are required to conserve probability conservation to be physically reasonable, $(\mathbb{1}|\rho(t)) = 1$, the kernel must fulfill $\mathrm{Tr}\left[\mathcal{W}(t-t')\bullet\right] = (\mathbb{1}|\mathcal{W}(t-t') = 0$ for any operator $\bullet$ in the open-system Liouville space, and for any two times t, t' after the initial time $t_0 = 0$. Or formulated in the language of Liouville space vectors and superoperators, $(\mathbb{1}|$ is a nontrivial *left eigenvector* of $\mathcal{W}$ to the eigenvalue 0. The second, related property of the coupling $\mathcal{W}$ is that for dissipative open systems as considered in this work, it eventually causes $|\rho(t))$ to decay to a stationary state $|\rho_\infty) = \lim_{t\to\infty}|\rho(t))$. In the Markovian limit, this is formulated more precisely later in Sec. 2.4.2, stating a well-known, sufficient condition under which $|\rho(t))$ reaches a stationary state that is independent of the initial state $|\rho_0)$.

Note that the generalized master equation (2.25) in principle describes the *entire* reduced density operator $|\rho(t))$. Experiments, however, do not always have or reveal the full information about the complete (quantum) state. Instead, one aims to measure physical observables which expose the information of $|\rho(t))$ which one is most interested in, such as, e.g., the average occupation number $\langle N\rangle = (N|\rho(t))$. For the quantum dot systems analyzed in the appended papers, the experimentally most natural and relevant quantities to characterize how $|\rho(t))$ decays as a function of time are the average electronic particle- (I_N) and energy- (I_E) or heat current (I_Q) to or from the reservoirs[1]. This concerns both the transient domain for a non-stationarity initial state ρ_0 (papers I-III,V), and the stationary long-time limit, due to biased reservoirs (papers IV,V). For each reservoir α, these tunnel currents can be defined by the time derivative of the respective average particle number and energy:

$$I^\alpha_{\mathrm{N}}(t) = \partial_t \langle N_\alpha\rangle(t) = \partial_t \mathrm{Tr}\underset{\mathrm{R}}{\mathrm{Tr}}\left[N_\alpha \rho^{\mathrm{tot}}(t)\right] \tag{2.26a}$$

$$I^\alpha_{\mathrm{E}}(t) = \partial_t \langle H_\alpha\rangle(t) = \partial_t \mathrm{Tr}\underset{\mathrm{R}}{\mathrm{Tr}}\left[(H_\alpha)\,\rho^{\mathrm{tot}}(t)\right] \tag{2.26b}$$

$$I^\alpha_{\mathrm{Q}}(t) = \partial_t \langle H_\alpha - \mu_\alpha N_\alpha\rangle(t) = I^\alpha_{\mathrm{E}}(t) - \mu_\alpha I^\alpha_{\mathrm{N}}(t). \tag{2.26c}$$

Due to total particle number conservation, one can straightforwardly [166] express the particle current in terms of the *open-system* particle number operator N and only *a part* of the full coupling kernel $\mathcal{W}$:

$$I^\alpha_{\mathrm{N}}(t) = -\int_0^t dt' (N|\mathcal{W}^\alpha(t-t')|\rho(t')) \quad , \quad \mathcal{W}(t-t') = \sum_\alpha \mathcal{W}^\alpha(t-t'), \tag{2.27}$$

where $\mathcal{W}^\alpha(t-t')$ represents a coupling to the reservoir α that is renormalized

[1] For systems with Zeeman splitting, one can also consider spin-resolved currents.

by the presence of all other reservoirs $\alpha' \neq \alpha$ when accounting for higher than leading-order terms [171–173] in the perturbative expansion in H_{tun}.

More care needs to be taken for the definition (2.26c) of the heat current. Precisely formulated, Eq. (2.26c) constitutes the time-dependent *excess* energy of each tunneling particle with respect to the chemical potential of the respective reservoir. For a *weakly* coupled, Markovian system, the next section 2.3 shows that this energy is indeed the energy that for a particle tunneling *into* the reservoir is subsequently converted to heat due to bath-internal relaxation processes. However, as pointed out already at the end of Sec. 1.2.3, the definition (2.26c) leads to inconsistencies with the thermodynamic laws for strongly coupled systems in which quantum superpositions between open system and environment play a role. On the level of a Hamiltonian description, this refers to the problem that some energy may be stored in the coupling H_{tun} itself. Consequently, even if Eq. (2.26c) is a suitable definition for the time-dependent heat current, it cannot be as straightforwardly related to the open-system Hamiltonian H as the particle current (2.27) can be related to the particle number operator N. Instead, one introduces the energy current kernel $\mathcal{W}_E^\alpha$ to write

$$I_{\mathrm{Q}}^\alpha(t) = I_{\mathrm{E}}^\alpha(t) - \mu_\alpha I_{\mathrm{N}}^\alpha(t) \quad , \quad I_{\mathrm{E}}^\alpha(t) = \int_0^t (\mathbb{1}|\mathcal{W}_E^\alpha(t-t')|\rho(t')). \tag{2.28}$$

Technical details on this kernel can be found, e.g., in Refs. [174, 175]. Physically most important for us is that, unlike the average particle current $I_{\mathrm{N}}^\alpha(t)$, $I_{\mathrm{E}}^\alpha(t)$ and $I_{\mathrm{Q}}^\alpha(t)$ *directly contain* the energy due to particle-particle interactions in the open system. Similarly to the relation between particle current *noise* and average current, this means that the energy- and heat current reveal more information about the full quantum state evolution $|\rho(t))$ than the average particle current. In case of a single-level spin-degenerate quantum dot [Sec. (2.1.1)], the heat current together with the particle current even allow to determine *all* probabilities, i.e., diagonal elements of the density operator $|\rho(t))$ in the local energy-eigenbasis, see papers II,III.

2.3 Time evolution for weakly coupled, Markovian systems

Having established the generalized master equation (2.25) and the related transport quantities (2.26) in a general fermionic setting, let us now specify our treatment to weakly tunnel-coupled, Markovian systems [$\Gamma/T \ll 1$, see Eq. (2.8)]. As announced earlier, an approximation of the exact solution to Eq. (2.25) that captures the essence of time-dependent decay in this regime is commonly referred to as *Born-Markov approximation*. Let us first state this approximation and then explore in detail its physical implications for the time-dependent reduced density operator $|\rho(t))$.

2.3.1 Born-Markov approximation

The Born-Markov approximation involves in fact several approximations. First, it only accounts for terms in the kernel $\mathcal{W}(t-t')$ up to the leading, linear order in the coupling constants Γ [Eq. (2.8)], corresponding to the quadratic order in the tunneling Hamiltonian $H_{\rm tun}$: $\mathcal{W}(t-t') \to \mathcal{W}_1(t-t')$, where the 1 indicates the first order in the coupling. Second, all memory terms are neglected by setting $\rho(t') \to \rho(t)$ in the integral part of the generalized master equation (2.25), yielding the fully time-local equation

$$\partial_t |\rho(t)) \approx \left[-\mathrm{i}L + \int_0^t dt' \mathcal{W}_1(t-t')\right] |\rho(t)) \approx \left[-\mathrm{i}L + \int_{-\infty}^t dt' \mathcal{W}_1(t-t')\right] |\rho(t)). \tag{2.29}$$

This step can be justified if $\mathcal{W}(t-t')$ is peaked around $t'=t$ with a typical broadening given by the memory time of the environment. For the effectively non-interacting reservoirs studied in this thesis, and for fermions tunneling at energies far away from the band bottom of the environment (large Fermi energy), this memory time is set by the inverse temperatures [1] $1/T_\alpha$. Therefore, we can approximate the kernel as $\propto \delta(t'-t)$ if we assume that the memory time is much smaller than the typical tunneling times $1/\Gamma$, which is precisely the weak-coupling condition $1/T \ll 1/\Gamma$ or $\Gamma \ll T$. It thereby also justifies the expansion of $\mathcal{W}$ up to the linear order in the couplings Γ, since any higher-order effect is suppressed by the factor Γ/T.

Finally, exploiting that $\mathcal{W}$ is time-local, we have extended the lower bound of the integral in Eq. (2.29) to $-\infty$. The integral can thus be understood as a particular zero-frequency(ω) limit of the Fourier-Laplace transform, and yields the time-local *Born-Markov master equation*

$$\partial_t |\rho(t)) = [-\mathrm{i}L + W]\, |\rho(t)) \quad , \quad W = \lim_{\omega \to \mathrm{i}0} \int_0^\infty dt \mathcal{W}_1(t) e^{\mathrm{i}\omega t}. \tag{2.30}$$

Physically, the matrix elements of W with respect to some many-body basis states $|ij) = |i\rangle\langle j|$ of the open system,

$$W_{iji'j'} = (ij|W|i'j'), \tag{2.31}$$

constitute state transition rates ($i=j$,$i'=j'$) as well as couplings to coherences ($i \neq j$ and/or $i' \neq j'$). A general formula for W expressed using the fermionic superoperator framework from Refs. [166, 167] can be found in paper V and in the appendix of Lic. Th. [110]; papers I-IV moreover provide expressions of W for the specific quantum dot systems described in sections 2.1.1 and 2.1.2.

Defining the combined kernel $A = -\mathrm{i}L + W$, (2.30) dictates $|\rho(t))$ to evolve purely exponentially in time in the Born-Markov limit,

$$|\rho(t)) = \exp\left(A \cdot t\right) |\rho_0). \tag{2.32}$$

[1] Technically, this is because a larger temperature implies a flatter Fermi distribution in energy space, and thus a more delta-like Fourier transform back into the time-domain.

The master equation (2.30) and its solution (2.32) form the central starting point for the study of time evolution in the appended papers, and is hence also detailed in the following subsections. Before, let us finish this section with the Born-Markov limit formulae for the particle- and heat current into the reservoirs [Eq. (2.26c)]. By applying the scheme outlined from Eq. (2.29) to Eq. (2.32) to the general expressions for the currents, Eq. (2.27) and Eq. (2.28), one finds (see appendix of Lic. Th. [110])

$$I_{\mathrm{N}}^{\alpha}(t) \to -\big(N|W_\alpha|\rho(t)\big) \quad , \quad I_{\mathrm{E}}^{\alpha}(t) \to -\big(H|W_\alpha|\rho(t)\big) \quad , \quad I_{\mathrm{Q}}^{\alpha}(t) = I_{\mathrm{E}}^{\alpha}(t) - \mu_\alpha I_{\mathrm{N}}^{\alpha}(t). \tag{2.33}$$

The kernel W_α is the leading order Γ, zero-frequency Laplace transform of the reservoir-resolved kernels introduced in equations (2.27) and (2.28). Note that when assuming the tunnel coupling $H_{\mathrm{tun},\alpha}$ to each individual reservoir α to conserve the *total* energy H_{tot} – which Lic. Th. [110] shows to hold for the weakly-coupled quantum dots relevant in the appended papers – also the reservoir-resolved energy current is conserved in the sequential tunneling regime [App. (A)]. It can hence be expressed in terms of the *local* energies H. Moreover, it is crucial that unlike for corrections beyond the weak coupling limit, the W_α *do not* depend on the properties of any other reservoir $\alpha' \neq \alpha$. This enables us to meaningfully decompose the full kernel into *mutually independent* reservoir contributions:

$$W = \sum_\alpha W_\alpha. \tag{2.34}$$

This reservoir sum is exploited heavily in both paper IV and V.

The important conclusion at this point is that for all calculations in the appended papers, only the reservoir-resolved Born-Markov kernels W_α and the full kernel $W = \sum_\alpha W_\alpha$ are required next to the local Liouvillian L. They are enough to obtain both the exponential form of $|\rho(t)\big)$ according to Eq. (2.32), and the currents (2.33). In particular, the fermionic duality (2.1) detailed in the next chapter 3 holds separately for both W_α and W, and yields nontrivial insights mostly *in combination* with other general properties of these kernels. It is thus worthwhile to explore the latter more in detail. In fact, since the appended papers study mostly *incoherent* transport properties, the following discussion strictly focuses on the *coupling kernel* W only; a study of the full evolution kernel $-\mathrm{i}L + W$ can be found in Lic. Th. [110] and in the general discussion of paper V. In this thesis, it is, however, not necessary, since the local coherent part $-\mathrm{i}L$ either decouples, $[L, W] = 0$, or does not contribute at all (degenerate levels) to the time evolution for all concrete example systems considered.

2.3.2 Probability conservation, dissipativity and exponential decay

For efficiency, we now use explicitly that the reservoir-resolved kernel W_α for any reservoir α is independent from all other reservoirs $\alpha' \neq \alpha$. Namely, this

implies that both W and each W_α on its own must be a valid physical kernel to be meaningful. Except for properties relying on the sum rule Eq. (2.34), the following analysis of the *full kernel* W can thus be exactly carried over to the reservoir-resolved kernels W_α, and is therefore not repeated for each W_α.

As already stated, the first important requirement of the kernel W is to be physical. This implies *at least* [1] that it must keep probabilities valid for $t \geq 0$, i. e. $0 \leq P_i(t) = \langle i|\rho(t)|i\rangle \leq 1$ for any open-system many-body state $|i\rangle$ and $\sum_i P_i(t) = \mathrm{Tr}\,[\rho(t)] = 1$. Given that the exponential solution $|\rho(t)) = \exp(Wt)\,|\rho_0)$ [Eq. (2.32)] holds for arbitrary initial density operators ρ_0 and arbitrary times $t \geq 0$, it becomes clear that $\mathrm{Tr}\,[\exp(Wt)\,\rho_0] = \mathrm{Tr}\,[\rho_0]$ requires

$$0 \overset{!}{=} \mathrm{Tr}\,[W\bullet] \equiv (\mathbb{1}|W, \tag{2.35}$$

expressing conservation of probability. Or formulated more towards its use for the fermionic duality, the unit trace $(\mathbb{1}|\bullet = \sum_i \langle i|\bullet|i\rangle$ of $\bullet$ over the open-system states is always a *left eigenvector* of the kernel W to the eigenvalue 0.

Next, the probabilities can only all be bounded by 0 and 1 if $\exp(Wt)$ at least does not *grow* exponentially in time. This is what *dissipativity* expresses:

$$\mathrm{Re}\,[W] = \frac{W + W^\dagger}{2} \leq 0, \tag{2.36}$$

meaning in words that the Hermitian superoperator $\mathrm{Re}\,[W] \leq 0$ is negative semi-definite. This dictates non-negative *decay rates*, given by the negated real parts $\gamma_x = -\mathrm{Re}\,[\lambda_x]$ of the eigenvalues λ_x of W,

$$\gamma_x = -\mathrm{Re}\,[\lambda_x] = -\frac{\lambda_x + \lambda_x^*}{2} \overset{(2.36)}{\geq} 0, \tag{2.37}$$

and thus indeed guarantees that $\exp(Wt)$ governs constant or exponentially *decaying* time evolution. Even more interestingly, as we show in the next chapter 3, dissipativity (2.36) combined with the fermionic duality (2.1) even sets an *upper* bound on the rates γ_x.

Apart from the eigenvalues λ_x themselves, it is important for our purpose to physically understand their corresponding eigenvectors. To focus on the main picture, we assume for the moment that W is a non-Hermitian, yet *diagonalizable* superoperator, and refer to App. B for an overview of the, mostly technical, differences in case of a non-diagonalizable kernel. In this case, one may expand $|\rho(t)) = \exp(Wt)\,|\rho_0)$ as

$$|\rho(t)) = \sum_x (x'|\rho_0) e^{\lambda_x t} |x). \tag{2.38}$$

[1] For a more rigorous treatment, we refer the reader to Choi's seminal work [176] on complete positivity.

with the $|x)$ and $(x'|$ forming a biorthonormal basis set of right and left eigenvectors of the kernel W to the eigenvalues λ_x, where $(y'|x) = \delta_{xy}$.

In the following, we call the right eigenvectors $|x)$ the *decay modes*. Equation (2.38) stipulates that the basis elements of these modes specify how a certain probability (diagonal element with respect to local energy-eigenbasis) or coherence (off-diagonal element) in $|\rho(t))$ evolves in relation to all other probabilities and/or coherences *on the same specific time scale* determined by λ_x. The corresponding left eigenvectors $(x'|$ are called *amplitude covectors*. The overlap $(x'|\rho_0)$ of these vectors $(x'|$ with the initial state $|\rho_0)$ determines how strongly the given time scale influences the entire time evolution $|\rho(t))$ of the reduced system *in comparison to all other time scales*. In other words, to understand the physics represented by the evolution rates λ_x, one needs to understand the properties of modes and amplitudes. Let us therefore continue by addressing exactly those properties that are most important for the appended papers.

2.3.3 Stationary state

As indicated by Eq. (2.35), probability conservation dictates the kernel W to have the unit trace $(\mathbb{1}|$ as at least one nontrivial *amplitude* to the eigenvalue 0. This implies that there is also at least one *mode* $|z)$ to the eigenvalue 0 that can furthermore be trace-normalized to 1, i.e.,

$$W|z) = 0 \quad , \quad (\mathbb{1}|z) = 1. \tag{2.39}$$

Dissipativity (2.36) and the resulting, non-negative decay rates (2.37) then ensure, together with probability conservation (2.35), that the time-dependent density operator $|\rho(t))$ actually evolves to a normalized linear combination of all such trace-normalizable zero modes $|z)$. In other words, the latter are *stationary states*, possibly assumed by the open system in the long-time limit $\lim_{t\to\infty} |\rho(t))$, and therefore play an important physical role. In particular, while $|z)$ may be regarded trivially as zero modes in the context of a full time-dependent description, the majority of experiments on fermionic open system as introduced in Sec. 2.1 in fact happen in the stationary limit, and therefore only probe the properties of such stationary states $|z)$. In fact, as pointed out in Sec. 1.3, one main motivation of IV is to connect the fermionic duality (2.1) to the experimentally well-understood thermoelectric transport in a weakly coupled single-level quantum dot.

Given its general importance for our work, Sec. 2.4 shall explore the most relevant properties of $|z)$ – concerning, e.g., its independence of the initial state $|\rho_0)$ in the appended papers – more in detail. Following the logic of our current discussion, it is, however, more reasonable to first address the more general relation between evolution modes and their amplitudes.

2.3.4 Amplitude covectors and their relation to modes

The previous example of the unit trace covector $(\mathbb{1}|$ and the stationary mode $|z)$ already hints at a another crucial aspect. Namely, since the kernel is in general neither Hermitian nor anti-Hermitian, $W^\dagger \neq \pm W$, the amplitude covector corresponding to a rate λ_x is in general not the Hermitian adjoint of the respective mode, $(x'| \neq [|x)]^\dagger$. In the context of the appended papers and the fermionic duality, this is an important difference to closed-system unitary evolution $\sim \exp(-\mathrm{i}Lt)$ generated by the *Hermitian* Liouvillian $L^\dagger = L$. For the latter,

$$\exp(-\mathrm{i}Lt)\,|\rho_0) = \sum_{ij} \exp(-\mathrm{i}(E_i - E_j)t)\,(E_{ij}|\rho_0)\cdot|E_{ij}) \tag{2.40}$$

dictates that the energy eigenstates and coherences $|E_{ij}) = |E_i\rangle\langle E_j|$ contribute with amplitudes intuitively given by how the many-body wave functions $|E_i\rangle$ overlap with the initial state ρ_0. This interpretation, however, breaks down for open systems with left eigenvectors $(x'| \neq |x)$, making it desirable to develop an alternative understanding of how the amplitudes relate to modes. One way to tackle this systematically is in fact to use the fermionic duality (2.1), as illustrated in chapter 3 and the appended papers. However, we here first present an alternative approach that in some cases turns out to be particularly useful for experiments studying the exponential decay of open systems.

Starting from Eq. (2.38) and using the biorthonormality of the set of left and right eigenvectors, one finds

$$\langle x'\rangle(t) = (x'|\rho(t)) \overset{(2.38)}{=} (x'|\rho_0)e^{\lambda_x t}. \tag{2.41}$$

The average of the operator $(x')^\dagger$ over $\rho(t)$ thereby evolves exponentially at only a single time scale given by λ_x. In case $(x') = (x')^\dagger$ is an actual observable, the amplitude $(x'|$ and the rate λ_x attain a very concrete physical interpretation: $\lambda_x \to -\gamma_x = \mathrm{Re}[\lambda_x]$ becomes the real [1] positive relaxation rate γ_x governing the *exponential decay* of the expectation value of x'.

As stated above, Eq. (2.41) can in principle be very useful for experiments if $(x') = (x')^\dagger$, as it instructs how to study the time scales of the system by measuring well-understood observables, such as the total charge or spin of the open subsystem. For the quantum dot systems studied in the papers II,IV, one amplitude in the Born-Markov time evolution of the single-level quantum dot in the wideband limit is in fact always given by $(c'| = (N| - (N|z)(\mathbb{1}|$, see Refs. [28, 76]. It corresponds to the time-dependent deviation of the average particle number $N(t) = (N|\rho(t))$ from the stationary limit $n_z = (N|z)$:

$$(c'|\rho(t)) = N(t) - n_z = [N(t=0) - n_z]\cdot\exp(-\gamma_c t)\,. \tag{2.42}$$

[1] An imaginary part would contradict the fact that x' is an observable with real expectation value.

The rate γ_c is thus the "charge rate" governing the exponential decay of the dot charge. The physical properties of this rate are addressed in detail in Ref. [28] and paper I.

As appealing as it seems to associate rates with observables, the concept has its limits. First of all, we again note that due to $W^\dagger \neq \pm W$, the mode vector $|c)$ corresponding to the charge rate γ_c is *not* simply the same charge deviation, $(c'| \neq |c)$. Moreover, as papers III and V show, lifting either the spin-degeneracy of the quantum dot or the assumption of energy-independent bare couplings Γ is already enough for $(c'|$ to *not* be an exact left eigenvector anymore. Instead, the relevant observables become complicatedly parameter-dependent linear combinations of the base observables particle number N, total spin S, and fermion parity $(-\mathbb{1})^N$. When not studied in the proper framework, such linear combinations seem to have little meaning. As we show in the next chapter, the fermionic duality promises to provide exactly such a framework for the type of systems studied in this thesis.

2.4 Semi-classical Markovian limit: Rate matrix, recurrence and equilibrium

Everything we have discussed so far in Sec. 2.3 in principle applies to the full Born-Markov quantum master equation (2.30) under the condition that the purely local evolution governed by the open-system Liouvillian L decouples [1]. To gain more insights, this section exploits that this decoupling is often – and in particular for the concrete constellations in the appended papers – concomitant with the coherences $(E_{ij}|\rho(t))$ evolving *entirely* independently from the probabilities $P_i(t) = (E_i|\rho(t))$. If only the latter are important, one may reduce the quantum master equation (2.30) to a Markovian rate equation, which is semi-classical in the sense that while it does account for the quantization of states, it neglects quantum superpositions. The following analysis first formally introduces this rate equation, and then explores in detail its implications with regards to the appended papers.

2.4.1 Rate equation and its graphical representation

If the coherent evolution of the off-diagonals in $|\rho(t))$ decouples from the diagonals, the latter follow the rate equation

$$\partial_t \boldsymbol{P}(t) = \mathbf{W} \cdot \boldsymbol{P}(t) \quad , \quad \boldsymbol{P}(t=0) = \boldsymbol{P}_0 \tag{2.43}$$

with the column vector of the initial and time-dependent probabilities $\boldsymbol{P}_0$ and $\boldsymbol{P}(t)$, i.e., with the i-th component being $[\boldsymbol{P}]_i = P_i = (E_i|\rho)$. The elements of the rate matrix $\mathbf{W}$ are obtained from the Born-Markov kernel W via $W_{ij} :=$

[1] In fact, dissipativity as written in Eq. (2.36) even holds if the local term $-\mathrm{i}L$ is taken into account!

$[\mathbf{W}]_{ij} = (E_i|W|E_j)$; they represent rates for state transitions $|E_j) \to |E_i)$. Naturally, a dissipative kernel W which conserves probability also implies that the corresponding rate matrix fulfills these properties. This means

$$W_{i\neq j} \geq 0 \quad , \quad \sum_i W_{ij} = 0 \quad \forall j. \tag{2.44}$$

Explicitly, the rates W_{ij} for the general type of fermionic systems introduced in Sec. 2.1 can be obtained from Fermi's Golden rule [75]; in the notation used in this thesis, they can be found in the appendix to Lic. Th. [110]. For the simple example of only one reservoir with potential μ and temperature T, the rates assume the form $W_{ij} \sim \Gamma_{ij}(E_{ij})f(E_{ij})$ with $f(x) = \left[\exp\left(\frac{x-\mu}{T}\right)+1\right]^{-1}$ being the Fermi function. Modes and amplitudes of W as introduced in Sec. 2.3.4 are now represented by column vectors (mode) and row vectors (amplitude), respectively. For example, the appended papers introduce the row vector $\mathrm{e}^T = (1,1,\ldots,1)$ for the unit trace $(\mathbb{1}|$ and the column vector $\boldsymbol{P}_z = (P_{z,1}, P_{z,2}, \ldots, P_{z,N})^T$ for the stationary probabilities $P_{z,i} = (E_i|z)$.

Apart from the reduced complexity, the main advantage of the rate-equation description compared to the quantum master equation is that the transition rates W_{ij} in fact describe a *classical Markov process*. This enables us to benefit from the well-established mathematical and physical framework for such processes [177]. More specifically, we here employ a well-known graph representation [178] of classical Markovian random walks [179, 180] for a finite, discrete set of states. It is based on the states i forming nodes connected by arrows representing the rates $W_{i\neq j}$ for transitions from state j to state i; if $W_{ij} = 0$, the corresponding arrow is omitted, so that there is no *direct* connection from state j to state i. Figure 2.4 shows examples of such graphs for the quantum dot systems introduced in Sec. 2.1: the spinful single-level quantum dot [Fig. 2.4(a)], and the sensor quantum dot capacitively coupled to a spinful single-level dot [Fig. 2.4(b)].

With particular focus on the duality-based study of the non-equilibrium stationary thermoelectric transport in papers IV,V, we now make use of these graphs to address two questions related to the *stationary probabilities* $\boldsymbol{P}_z$: first, whether they are *unique* for a given rate matrix $\mathbf{W}$, i.e., whether there is only one solution to $\mathbf{W} \cdot \boldsymbol{P}_z = 0$ that the system inevitably evolves to irrespective of the initial probabilities $\boldsymbol{P}(t=0)$. And second, whether and *in what sense* $\boldsymbol{P}_z$ represents an *equilibrium* state.

2.4.2 Recurrence and the unique stationary state

Let us first look at the graph in Fig. 2.4(b), referring to the sensor dot system sketched in Fig. 2.2(b) and described in Sec. 2.1.2. We recall that according to Eq. (2.34), $\mathbf{W}$ is a sum of mutually independent terms governing the tunneling to and from the reservoir α. As such, the upper and lower panel of Fig. 2.4(b) show,

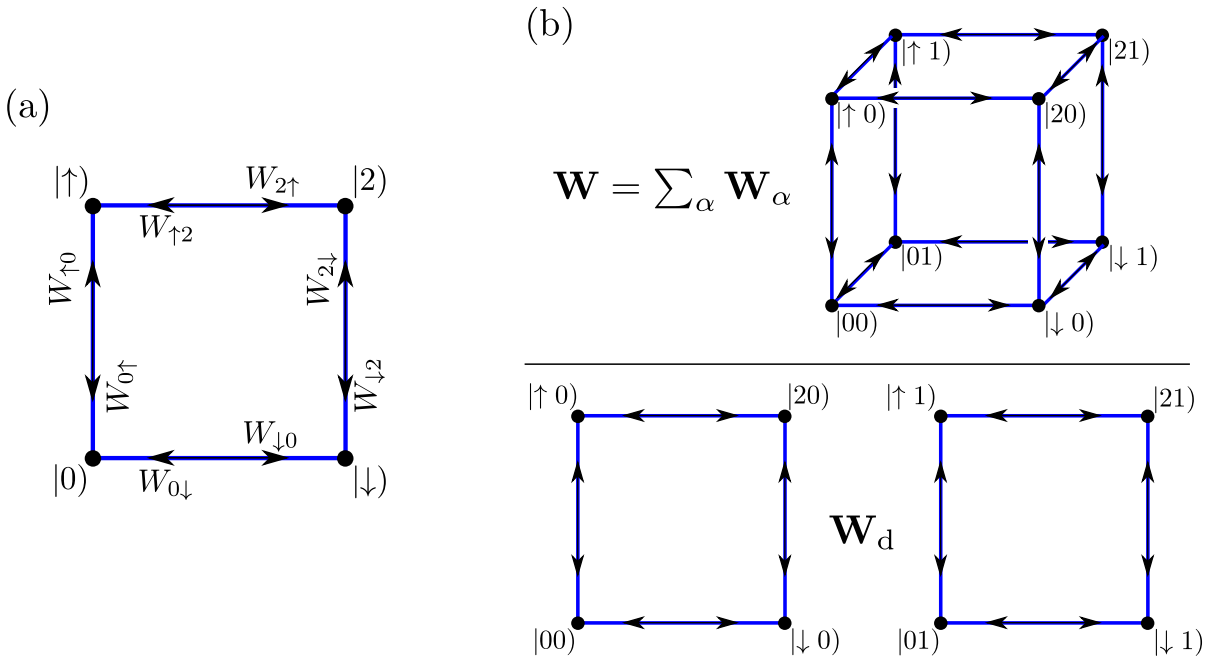

Figure 2.4: *Random walk graph-representation [178] of the rate matrices* $\mathbf{W}$ *describing the spin-degenerate interacting single-level quantum dot* ***(a)*** *[Sec. (2.1.1)] and the dot-sensor dot system* ***(b)*** *[Sec. (2.1.2)]. The upper panel in* ***(b)*** *shows the full rate matrix* $\mathbf{W}$ *including the coupling to all three reservoirs; the system is in fact equivalent to a random walk on a cube. The lower panel displays the rate matrix* $\mathbf{W}_d$*, representing exclusively the effect of the single reservoir coupled to the quantum dot to be measured by the sensor dot. The fact that the graph of* $\mathbf{W}_d$ *separates into two disconnected groups physically means that the stationary solution of* $\mathbf{W}_d|x) = 0$ *is not uniquely determined: since the corresponding reservoir is not coupled to the sensor dot, it cannot uniquely fix its occupation.*

respectively, the graph for the full rate matrix $\mathbf{W}$, and for the rate matrix $\mathbf{W}_\mathrm{d}$ describing exclusively the effect of the reservoir coupling to the spin-degenerate dot. The decisive difference is that $\mathbf{W}$ has a fully connected graph – known as recurrence- or communication class – in which each state i can be reached from each other state $j \neq i$ in a finite number of steps along the arrow directions; the graph for $\mathbf{W}_\mathrm{d}$ alone instead separates into two disconnected classes, physically representing either an empty (left square) or filled (right square) sensor quantum dot. The crucial point, and a central result from the theory of Markov processes, see, e.g., Refs. [177, 181] or the appendix of Lic. Th. [110], is that rate matrices $\mathbf{W}$ corresponding to only one fully connected graph always have a *unique* stationary solution $\boldsymbol{P}_z$ that is furthermore *strictly positive*, $P_{z,i} > 0$. The latter means physically that each possible state is *recurrent*, i. e., the system eventually comes back to each state i after a mean recurrence time that, according to Kac's lemma [182], is proportional to $1/P_{z,i}$ in the stationary limit. If the full graph,

however, splits into several such communication classes, the stationary state can be any normalized, real *non-negative* [1] linear combination of as many linearly independent base solutions as there are communication classes. For the example at hand in the lower panel of Fig. 2.4(b), there are thus two such base solutions.

Why is this relevant for us? First, it simply shows that the stationary state for *any* of the concrete weak-coupling, Markovian situations studied in the appended papers is always unique and positive, since the relevant rate matrices can be represented by a random walk on either a fully connected square [Fig. 2.4(a)] or a fully connected cube [Fig. 2.4(b)]. This is not only interesting in itself, but is in fact crucial in applying the fermionic duality (2.1) to relate the stationary zero mode $|z)$ of the kernel W to a nontrivial amplitude, see Sec. 3.4.1 of the next chapter 3 and papers IV,V. Moreover, the comparison between $\mathbf{W}$ and $\mathbf{W}_\mathrm{d}$ illustrates that the behavior of the system containing both quantum dot and sensor quantum dot [paper I] crucially depends on the *simultaneous* presence of all reservoir couplings: only the net effect of all three reservoirs uniquely determines the stationary state.

The second central property of a recurrent system with unique, *positive* stationary probabilities $P_{z,i} > 0$, is that it allows to precisely define a notion of *detailed balance* for the open system. It is thus directly related to our second question, about whether and how the system is *in equilibrium*.

2.4.3 Detailed balance: local vs. global equilibrium

Given several environment reservoirs in their own local equilibrium, but at *mutually different* potentials μ_α and temperatures T_α, it is clear by construction that the total system of reservoirs and the open subsystem is not in an equilibrium state, and that the open subsystem itself cannot be in equilibrium *with the whole environment* in the stationary limit. If the latter was true, such as for the case of only one reservoir at potential μ and temperature T (paper II), $|z) \sim \exp\left(-(H-\mu N)/T\right)$ would simply assume the grand-canonical ensemble with respect to μ and T under Markovian, weak-coupling conditions. However, we need to clearly distinguish such a global equilibrium from an open system in its own *local* equilibrium, as the latter does not necessarily imply the former. For a recurrent system governed by rates W_{ij} and with $P_{z,i} > 0$, the local equilibrium is instead characterized by the *detailed balance condition*

$$W_{ij} \cdot P_{z,j} = W_{ji} \cdot P_{z,i} \quad \forall i,j. \tag{2.45}$$

Note that Eq. (2.45) is stronger than the mere stationarity condition $\sum_j W_{ij} P_{z,j} = 0 \quad \forall i$. It physically implies that there is no net probability flow between any two open-system states i and j.

[1] This includes taking only one base solution which might have exactly vanishing probabilities $P_{z,i} = 0$ for some states i.

When precisely is equation (2.45) fulfilled, and what does it imply? Concerning the first question, we note that Eq. (2.45) in fact *defines* time-reversal symmetry on the level of Markov processes, in the sense that the process between state i and j happens with equal probability in both directions. Namely, the elements $W_{ij}^{\leftarrow}$ of the rate matrix for the *time reverse* of a recurrent Markov process with truly positive stationary probabilities $P_{z,j} = (E_j|z) > 0$ are

$$W_{ij}^{\leftarrow} = \frac{P_{z,i}}{P_{z,j}} W_{ji}. \tag{2.46}$$

Time-reversal symmetry in the sense of $W_{ij}^{\leftarrow} = W_{ij}$ is equivalent to Eq. (2.45) being valid.

The practical problem of naively checking whether Eq. (2.46) holds is that one first needs to calculate the stationary state $\boldsymbol{P}_z$. Kolmogorov, however, proved a sufficient and required criterion [183] that explicitly refers to the graph representing the rates W_{ij}, and whose power is that it *does not* need explicit knowledge of the stationary probabilities $P_{z,i}$. Its statement is also explained in paper V: when closing any possible loop in the graph in a specific direction, the *product* of all arrows, i.e., transition rates W_{ij} along this loop direction must be equal to the product of all rates when closing the loop in the opposite direction. For the random walk on the square in Fig. 2.4(a), this means

$$W_{0\uparrow} W_{\uparrow 2} W_{2\downarrow} W_{\downarrow 0} \stackrel{!}{=} W_{0\downarrow} W_{\downarrow 2} W_{2\uparrow} W_{\uparrow 0}. \tag{2.47}$$

It is straightforward to see that as long as the rates are spin-symmetric, $W_{\uparrow i} = W_{\downarrow i}, W_{i\uparrow} = W_{i\downarrow}$, this condition and hence detailed balance (2.45) is *always fulfilled*. Importantly, this is the case for the concrete studies of the single-level dot in papers II,IV and V. This includes *global* non-equilibrium conditions with several reservoirs at different potentials μ_α and temperatures T_α, leading to a flow *between open system and reservoir* and causing the stationary state $|z)$ to deviate from a simple Boltzmann factor $\sim \exp(-(H - \mu N)/T)$. In fact, only the combination of a non-equilibrium environment, local Coulomb interaction in the dot, *and* a locally broken spin-symmetry leads to a breaking of *local* equilibrium (2.47), see paper III. Altogether, this shows that, strictly speaking, time-reversal symmetry of the underlying Hamiltonian is not equivalent to time-reversal symmetry in Markov processes. In particular, the latter may hold even for a time-reversal symmetry-breaking Hamiltonian as long as the transitions rates W_{ij} are symmetric enough to fulfill Kolmogorov's criterion.

Within the current context of time evolution in the rate-equation limit, there are two main implications of the local detailed balance condition as formulated [1] in Eq. (2.45). First, it is sufficient to prove that the rate matrix $\mathbf{W}$ is diagonalizable and that all its eigenvalues λ_x are purely real [App. (C)]. This means that

[1] In transport literature, detailed balance often refers to Eq. (2.45) evaluated for the specific stationary state $|z) \sim \exp(-(H - \mu N)/T)$.

$\boldsymbol{P}(t)$ describes a pure exponential decay without any oscillations, and, in reference to the mode-amplitude discussion in Sec. 2.3.4, that each *amplitude* $(x'|$ in the probability sector of the kernel W can in principle be understood as a real observable of the open system. Second, as demonstrated in paper V and Sec. 3.4.1, detailed balance (2.45) can readily be combined with the fermionic duality (2.1) to yield new, independent insights. This is exploited implicitly, yet heavily in papers IV and V: it is used to derive unexpected results for both the transient decay and stationary thermoelectric response of the spin-degenerate single-level quantum dot.

2.5 Linear response in the Liouville space approach

With the previous subsection 2.4 having clarified the notion of *local* equilibrium in the open subsystem, let us complete the discussion of the Markovian, weak-coupling limit by turning to how the stationary state $|z)$ responds to small deviations from the *global* equilibrium condition. This well-known *linear response regime* is studied both in paper IV for energy-independent couplings Γ, and in paper V for any analytical energy-dependence $\Gamma(E)$. Let us hence explain how we tackle this problem in our open-system, density-operator centric Liouville space approach. We start by introducing the notation

$$q|_{\rm eq} = q|_{\mu_\alpha\to\mu, T_\alpha\to T} \quad , \quad |z)|_{\rm eq} = |z_{\rm eq}), \tag{2.48}$$

used in the papers to denote the *global equilibrium limit* of any quantity q, that is, for reservoirs at equal potential μ and temperature T.

To study linear response, the object of interest is the *first derivative* of the reservoir-resolved stationary current of observable O – most importantly the charge and heat currents (2.33) – with respect to any variable x, as for example the chemical potential μ_α of any given reservoir taken at equilibrium:

$$\delta_x I^\alpha_{O,{\rm eq}} = \partial_x I^\alpha_O|_{\rm eq}\cdot\delta x \quad , \quad I^\alpha_O = -(O|W_\alpha|z), \tag{2.49}$$

where W_α is the *reservoir-resolved* kernel defined below Eq. (2.33).

In principle, once $|z)$ is determined explicitly for arbitrary reservoir parameters, which is always possible in the Markovian, weak-coupling limit by solving $W|z) = 0$, the full nonlinear response can be obtained and the derivative can be calculated straightforwardly using the explicit expressions for $|z)$ and W_α. The problem is, however, that already for systems as small as the single-level quantum dot [Sec. (2.1.1)], this brute-force method typically involves dealing with unwieldy terms. These offer little analytical insight, and even less opportunity of being combined with the fermionic duality.

More systematic approaches have been developed [137, 147] for systems that can be described by a rate equation as given in Eq. (2.43). They are based on expanding $|z)$ in terms of (possible) stationary states $|z_\alpha)$ of the reservoir-resolved kernels

W_α: since the latter govern the coupling to only the single reservoir α, the $|z_\alpha)$ are typically given by a simple equilibrium Boltzmann factor $\sim \exp\left(-(H-\mu_\alpha N)/T_\alpha\right)$ of which the derivative with respect to any system parameter is straightforward to take. In particular, both Ref. [137] and Ref. [147] assume *energy-independent* bare couplings Γ [Eq. (2.8)], with the difference that Ref. [137] furthermore assumes local detailed balance (2.45) to always hold.

The crucial point is that the concrete systems of this thesis and the appended papers are not particularly well-suited for these approximations. Most importantly, paper V lifts the restriction to energy-independent couplings, and the most general situation considered in paper III furthermore explicitly breaks local detailed balance (2.45), as argued below Eq. (2.47). Moreover, the case of spin-polarized leads addressed in Ref. [184] and Sec. 3.4.2 cannot even be described in the rate-equation limit anymore.

With the details of the derivation given in the appendix to V, let us therefore simply state our alternative approach: under the conditions that

1. the full kernel W has a non-degenerate zero eigenvalue, such as it is the case for the recurrent Markov processes discussed in the previous section 2.4

2. the reservoir sum rule (2.34) holds,

$$W = \sum_\alpha W_\alpha, \tag{2.50}$$

3. each reservoir-resolved kernel W_α has a *possible* [1] stationary state $|z_\alpha)$ which behaves as

$$|z_\alpha)|_{\rm eq} = |z)|_{\rm eq} = |z_{\rm eq}), \tag{2.51}$$

one finds

$$\partial_x I_O^\alpha|_{\rm eq} = -(O|\, W_\alpha|_{\rm eq}\, \partial_x \left[|z) - |z_\alpha)\right]\Big|_{\rm eq}. \tag{2.52}$$

The $|z_\alpha)$ are exactly the reservoir-resolved stationary solutions which fulfill Eq. (2.51), and, most crucially,

$$\partial_x|z)|_{\rm eq} = \frac{1}{\tilde{W}_{\rm eq.}} \sum_\alpha W_\alpha|_{\rm eq} \cdot \partial_x|z_\alpha)|_{\rm eq}. \tag{2.53}$$

The term $\frac{1}{\tilde{W}_{\rm eq.}}$ represents the equilibrium limit of the *generalized reflexive inverse* [185, 186] of the kernel W. Since W has a non-degenerate eigenvalue 0 by assumption, this inverse is obtained by first projecting out the zero eigenspace of

[1] As pointed out in Sec. 2.4, a reservoir-resolved kernel often does not have only one unique stationary state.

W formed by $|z)$ and $(\mathbb{1}|$, and then by taking the inverse of the rest. This implies in particular that

$$\frac{1}{\tilde{W}_{\text{eq.}}}\, W|_{\text{eq}} = W|_{\text{eq}}\, \frac{1}{\tilde{W}_{\text{eq.}}} = \mathcal{I} - |z)(\mathbb{1}|, \tag{2.54}$$

where $\mathcal{I}$ is the open-system Liouville space identity introduced in Sec. 2.2.1.

Equations (2.52) and (2.53) allow to calculate the linear current response (2.49) in terms of simple equilibrium quantities. In particular, if the stationary state for each reservoir-resolved kernel is given by the grand-canonical ensemble with respect to μ_α, T_α,

$$|z_\alpha) = \exp\left(-(H-\mu_\alpha N)/T_\alpha\right) \Big/ \operatorname{Tr}\left[\exp\left(-(H-\mu_\alpha N)/T_\alpha\right)\right], \tag{2.55}$$

the derivatives $\partial_x |z_\alpha)$ at equilibrium are

$$\partial_x |z_\alpha)|_{\text{eq}} \overset{(2.55)}{\underset{(2.48)}{=}} -\left[\partial_x A_\alpha - (\partial_x A_\alpha |z_{\text{eq}}) \cdot \mathbb{1}\right]\Big|_{\text{eq}} \cdot |z_{\text{eq}}) \quad , \quad A_\alpha = \frac{H-\mu_\alpha N}{T_\alpha}. \tag{2.56}$$

The main benefit of the above approach for us is that it *does not* rely on neither the wideband limit $\Gamma(E) \to \Gamma$ nor detailed balance (2.45). In fact, it even holds beyond the rate-equation limit as long as the 3 above-listed conditions hold. The price to pay is that one needs to calculate the generalized inverse $1/\tilde{W}_{\text{eq.}}$. For the small, fully diagonalizable kernels of the systems considered in this thesis, this is, however, no complication and can be straightforwardly done analytically, see paper V. A particularly accessible result is found for the single-level quantum dot in the rate-equation limit, and for spin-symmetric and energy-independent bare couplings to the reservoirs α, $\Gamma_{\alpha\uparrow} = \Gamma_{\alpha\downarrow} = \Gamma_\alpha$. Namely, since one then has $W|_{\text{eq}} = (\Gamma/\Gamma_\alpha)\, W_\alpha|_{\text{eq}}$ with $\Gamma = \sum_\alpha \Gamma_\alpha$, equation (2.53) simplifies to the weighted sum

$$\partial_x |z)|_{\text{eq}} = \sum_\alpha \frac{\Gamma_\alpha}{\Gamma} \cdot \partial_x |z_\alpha)|_{\text{eq}}\,. \tag{2.57}$$

This is used extensively in paper IV to calculate thermoelectric transport using the fermionic duality instead of – as usual – referring to time reversal symmetry and its famous consequence, Onsager's *reciprocity relation*. The latter is known to hold for time-reversal symmetric open systems described by a rate equation [148], and for us explicitly implies a relation between the stationary linear responses of charge and heat current [Eq. (2.33)]:

$$\partial_{T_\alpha} I_N^\alpha|_{\text{eq}} = \frac{1}{T}\, \partial_{\mu_\alpha} I_Q^\alpha\Big|_{\text{eq}}\,. \tag{2.58}$$

Equation (2.58) expectedly holds for the time-reversal symmetric situation studied in paper IV. By contrast, an application of Eq. (2.57) to the spin-resolved system of paper III for spin-symmetrically approximated bare couplings $\Gamma_\uparrow = \Gamma_\downarrow$ should reveal precisely how and why Onsager reciprocity (2.58) is violated. This last question is, however, open to future studies and not addressed any further by the work described in this thesis.

2.6 Extension to non-Markovian corrections and explicit time-dependence

Before finally switching chapter and turning to the fermionic duality, we finish by briefly introducing two types of extensions to the so-far developed theory: *non-Markovian dynamics* and *time-dependent driving*. Both of these are relevant either for parts of the appended papers or for ongoing follow-up projects, and are hence worthwhile to be outlined here.

2.6.1 Non-Markovian dynamics

In its most general form, the validity of the wideband-limit fermionic duality relation presented in paper II extends to open fermionic systems which are strongly coupled to reservoirs at possibly low temperatures $T_\alpha \ll \Gamma_\alpha$, leading in general to *non-Markovian* dynamics according to the generalized master equation (2.25). To better understand how the duality works in this case, it is thus helpful to describe the most general solution to Eq. (2.25).

Formally speaking, the generalized master equation is an integro-differential equation with an integral convolution in time on finite support. It can hence in principle be converted into an easily solvable algebraic equation by applying the Fourier-Laplace transform, $|\rho(\omega)) = \int_0^\infty dt e^{\mathrm{i}\omega t}|\rho(t))$, with $\mathrm{Im}(\omega) > 0$. This gives

$$-\mathrm{i}\omega|\rho(\omega)) - |\rho_0) = [-\mathrm{i}L + W(\omega)]\,|\rho(\omega)) \quad , \quad W(\omega) = \int_0^\infty dt e^{\mathrm{i}\omega t}\mathcal{W}(t), \quad (2.59)$$

with the initial state $|\rho_0) = |\rho(t=0))$, and hence

$$|\rho(\omega)) = \Pi(\omega)|\rho_0) \quad , \quad \Pi(\omega) = \frac{\mathrm{i}}{\omega - \mathrm{i}A(\omega)} \quad , \quad A(\omega) = -\mathrm{i}L + W(\omega). \quad (2.60)$$

The inverse transform back into the time domain then yields for $t > 0$:

$$\begin{aligned} |\rho(t)) = \Pi(t)|\rho_0) \quad , \quad \Pi(t) &= \frac{1}{2\pi}\int_{-\infty}^{\infty} d\omega e^{-\mathrm{i}(\omega+\mathrm{i}\eta)t}\Pi(\omega+\mathrm{i}\eta) \\ &= \frac{-1}{2\pi\mathrm{i}}\int_{-\infty}^{\infty} d\omega e^{-\mathrm{i}(\omega+\mathrm{i}\eta)t}\frac{1}{\omega+\mathrm{i}\eta-\mathrm{i}A(\omega+\mathrm{i}\eta)} \quad , \quad \eta > 0, \end{aligned} \quad (2.61)$$

where $\eta > 0$ is a real positive convergence factor for the Fourier-Laplace transform of the density operator, $|\rho(\omega))$. In order to understand this, up to now, purely formal result (2.61), one may in principle pursue the same idea as laid out in Sec. 2.3.4 for the Markovian case: expand $A(\omega)$ in terms of the, now frequency-dependent, modes and amplitudes $(x'(\omega)|$ and $|x(\omega))$ corresponding to

the eigenvalues $-\lambda_x(\omega)$. Assuming for simplicity of the following argument that A is fully diagonalizable, this means ($\eta \to 0_+$)

$$|\rho(t)) = \frac{-1}{2\pi \mathrm{i}} \sum_x \int_{-\infty}^{\infty} d\omega \, (x'(\omega)|\rho_0) \cdot \frac{e^{-\mathrm{i}\omega t}}{\omega - \mathrm{i}\lambda_x(\omega) + \mathrm{i}0_+} \cdot |x(\omega)). \tag{2.62}$$

Compared to the Born-Markov expression (2.38), the frequency-dependence of the eigenvectors and eigenvalues $\lambda_x(\omega)$ introduces both new time scales in the exponential evolution as well as completely non-exponential behavior [64, 77–85]. Physically, both phenomena are related to memory effects in the environment to which the system becomes susceptible in the strong-coupling regime, see also the slightly extended discussion in Lic. Th. [110].

Yet, next to these intricate additions to the time-dependent behavior of $|\rho(t))$, a fundamental question that is in principle still the same as in the Born-Markov limit is how the modes $|x(\omega))$ in (2.62) are related to their amplitudes $(x'(\omega)|$. With the latter in particular depending on the generally complex Laplace frequency, an attempt to interpret amplitudes in terms of observables as in the Born-Markov limit [Eq. (2.41)] seems futile from the start. By contrast, we shall see in the next chapter that the fermionic duality can still establish a mode-amplitude relation, even for this frequency-dependent strong-coupling case.

2.6.2 Time-dependent driving

In this final subsection, let us remember that each part of the full Hamiltonian H_{tot} as given in Eq. (2.2) has so far been assumed to be time-independent. As such, it fails to capture situations in which certain system parameters are continuously driven in time, as further detailed below in Sec. 4.1.2. Let us therefore quickly show how one can modify our theory to account for this situation.

Starting from a time-dependent Hamiltonian, it is clear that $|\rho(t))$ can in general *not* evolve to a stationary state $|z)$, since the system parameters which define the stationary condition change continuously. However, given that the time-dependent driving is *periodic* in time, we can ask for a possible *attractor* of the $|\rho(t))$, i.e., the *geometrically* constant Liouville-space trajectory $|\rho(t))$ passes through as a function of time after possibly many driving periods. To find this attractor, we here follow Refs. [187, 188] by setting up the master equation

$$\partial_t |\rho(t)) = \int_{-\infty}^{t} dt' \mathcal{W}(t,t') |\rho(t')). \tag{2.63}$$

Apart from the fact that the time-local Liouvillian part $-iL(t)\delta(t-t')$ is now formally included into the integral kernel $\mathcal{W}(t,t')$, Eq. (2.63) differs from its counterpart (2.25) for time-independent Hamiltonians in two ways. First, we note that the lower bound of the integral is set to $-\infty$ instead of 0. This accounts for the fact that we are interested in the long-time limit attractor of $|\rho(t))$. Second, the

broken time-translational invariance causes the kernel $\mathcal{W}(t,t')$ to not only depend on the time difference $t-t'$, but also explicitly on t. With the full solution to this problem discussed, e.g., in Ref. [188], we are here only interested in its Markovian, weak-coupling limit, obtained after a further systematic expansion of $\mathcal{W}$ and ρ in both the tunnel couplings (2.8) and any *driving frequencies* Ω_i on which the system parameters are varied [54, 154, 188]. The final result is the Born-Markov master equation in the *instantaneous limit*,

$$\partial_t|\rho(t)) = (-\mathrm{i}L_t + W_t)|\rho(t)). \tag{2.64}$$

The index t indicates that the local open-system Liouvillian L_t and, most importantly, the dissipative kernel W_t are *exactly* the same as for time-independent parameters [Eq. (2.30)] *except* that all time-dependent system parameters are taken at time t. In the context of this thesis, this has two important implications. First, while the lower integral bound $-\infty$ in Eq. (2.63), from which the master equation (2.64) derives, in general restricts the validity of the latter to the long-time limit, we note that extending the lower integral bound from 0 to $-\infty$ is in fact always part of the Born-Markov approximation (2.29). As long as the latter is justified, it is thus consistent to use Eq. (2.64) both for attractor dynamics of periodically driven systems as well as for the here most relevant time-independent systems relaxing from a non-stationary initial state $|\rho_0) \neq |z)$.

The latter point directly connects to the second important property of the instantaneous kernel W_t, which is that it has *the same symmetries* as the time-independent Born-Markov kernel W. For example, the eigenvector property

$$(N|W_t = -\gamma_c\left[(N| - n_z(\mathbb{1}|\right] \tag{2.65}$$

illustrated in Sec. 2.3.4 for the interacting spin-degenerate single-level dot continues to hold for the *instantaneous* kernel W_t *at any time* t, with the instantaneous charge rate γ_c and stationary particle number $n_z = (N|z)$ depending parametrically on t. In fact, the validity of (2.65) is the crucial ingredient employed by Ref. [31] to extend time-dependent density functional theory [189, 190] to few-level open systems with strong on-site interaction. Yet, what matters most in our current context is that W_t *obeys the fermionic duality* (2.1), just as W does for a time-independent Hamiltonian. All insights and benefits which derive from this duality, as pointed out in the next chapter, can therefore in principle be exploited not only for the decay problems studied in the appended papers, but also for periodically driven systems [191]. As further discussed in Sec. 4.1.2, this ties in with the latest research on charge and energy pumping in quantum dots: it includes, e.g., a systematic classification of geometric effects [192], time-dependently driven temperatures [193], or the implementation and exploitation [194] in the more recently studied quantum dots with tunable or even attractive on-site interaction [153, 195].

3 The fermionic duality – implications and physical origin

With the necessary theoretical basis set up, we now come to the main result of this thesis – the fermionic duality. After its quick, ad-hoc introduction in Eq. (2.1) at the beginning of the previous chapter 2, we here provide its precise definition, origin and physical implication from a theoretical point of view. Chapter 4 then discusses more concretely the application of duality to experimentally relevant systems.

3.1 Mode-amplitude duality for open fermionic systems

One main problem pointed out by the previous chapter is that studying open-system dynamics requires knowledge and physical interpretations for the *modes and amplitudes* in the eigenvector expansion of the time propagator $\Pi(t)$, both in the general non-Markovian case (2.62) and, in particular, in the Born-Markov limit [Eq. (2.38)]. So far, we have concluded that while possible for models with particular symmetries [Sec. (2.3.4)], understanding the amplitudes $(x'|$ as projectors of simple physical observables is neither always possible nor reasonable.

Here, we show how the fermionic duality (2.1) helps in this matter. More precisely, this section starts by laying the foundation necessary to precisely understand the duality from a purely analytical point of view; section 3.2 then applies this knowledge to derive the systematic mode-amplitude relation which the appended papers mainly rely on to gain physical insights into time-dependent decay (papers II,III,V) and stationary transport (papers IV,V).

3.1.1 General form of fermionic duality

In and around equation (2.40) in Sec. 2.3.4, we have argued that the duality $(E_{ij}| = [|E_{ij})]^\dagger$ between modes and amplitudes in *closed systems* via the Hermitian adjoint is induced by the unitarity of the dynamics, and hence the hermiticity of the Liouvillian, $L^\dagger = L$. This suggests that in order to find a duality for open systems, one requires an analogous relation between the open-system evolution kernel $A(\omega) = -\mathrm{i}L + W(\omega)$ [Eq. (2.60)] and its Hermitian conjugate.

Paper II proves that such a relation does exist – even in the most general case of non-Markovian, strong-coupling, low-temperature dynamics – for *any* fermionic open system governed by the Hamiltonian set up in Sec. 2.1, given energy-independent tunneling constants (2.8), $\Gamma_{m,ll'}(E) \to \Gamma_{m,ll'}$ (wideband limit). This relation is the most general wideband-form of what we call the *fermionic duality*:

$$A(\omega; H, H_{\rm tun}, \{\mu_\alpha\}) = -\Gamma + \mathcal{P} A^\dagger(\overline{\omega}; \overline{H}, \overline{H}_{\rm tun}, \{\overline{\mu}_\alpha\})\mathcal{P}. \tag{3.1}$$

This duality generalizes the hermiticity for closed systems, $L^\dagger = L$, to *any* open system that belongs to the large class of systems defined by the general model set up in Sec. 2.1. Next to the (super)Hermitian conjugate, Eq. (3.1) involves the following extra ingredients:

1. A shift by the real non-negative constant Γ, defined as the lump sum over all couplings $\Gamma_{m,ll}$ [Eq. (2.8)] which are *diagonal* in the single-particle states $|l\rangle$ of the open system:

$$\Gamma = \sum_{ml} \Gamma_{m,ll} = 2\pi \sum_{\mathbf{k}ml} \delta\left(E - \epsilon_m(\mathbf{k})\right) \cdot |\tau_{\mathbf{k}ml}|^2 \geq 0. \tag{3.2}$$

2. Left action by the open-system fermion-parity operator, $\mathcal{P}\bullet = (-\mathbb{1})^N \bullet = e^{\mathrm{i}\pi N}\bullet$ as defined in Sec. 2.2.1. The occurrence of these operators originally led to the name "fermion-parity duality".

3. A transform to a *dual model*, defined in terms of

$$\begin{aligned} \text{inverted energy signs in the open system, } & \overline{H} = -H, \\ \text{inverted signs for the chemical potentials, } & \overline{\mu}_\alpha = -\mu_\alpha, \\ \text{"Wick rotated" couplings, } & \overline{H}_{\rm tun} = \mathrm{i}H_{\rm tun}, \\ \text{dual Laplace frequency, } & \overline{\omega} = \mathrm{i}\Gamma - \omega^* \end{aligned} \tag{3.3}$$

   with the complex-conjugated Laplace frequency ω^*. Note that the generator $A(\omega; H, H_{\rm tun}, \{\mu_\alpha\})$ denotes a functional dependence on the H and $H_{\rm tun}$: for a given ω, A generally depends on entire ranges of energies in the spectrum of these Hamiltonians.

Two central questions immediately suggest themselves: what is the physical origin of the duality (3.1), and what can we learn from it, in particular in terms of *physically* relating evolution modes $|x)$ with its amplitudes $(x'|$? It is especially the *transform to the dual model* which is essential to answer these questions, and which is therefore addressed in detail in Sec. 3.2.2. To stay close to the appended papers, and with Lic. Th. [110] already providing a discussion of Eq. (3.1) for the general, frequency-dependent case, we here continue by focussing on the duality in the Born-Markov limit [Sec. (2.3)]. Namely, while this simplification turns

out to keep the duality's main physical implications intact, it does make these implications substantially more transparent and applicable. The appended papers and the following sections in fact prove that the duality in the Markovian, weak-coupling limit offers even additional insights that cannot be generalized beyond the Born-Markov limit. Most importantly, it allows us to lift the restriction to energy-independent bare couplings, as paper V and Sec. 3.5 demonstrate. By contrast, what the most general, frequency-dependent form (3.1) offers in addition to the Born-Markov limit remains an interesting topic for future investigations.

3.1.2 Duality in the Born-Markov limit

Applying the Born-Markov approximation to the duality (3.1), we follow Eq. (2.29) by setting $\omega \to \mathrm{i}0_+$ and expanding the kernel $\mathcal{W}$ up to the leading order in all $\Gamma_{m,ll'}$. This eventually [1] leads to the fermionic duality for the Born-Markov kernel W [Eq. (2.30)]. As posted in a simpler form in Eq. (2.1), it reads

$$W(H,\{\mu_\alpha\}) = -\Gamma - \mathcal{P}W^\dagger(-H,\{-\mu_\alpha\})\mathcal{P}, \tag{3.4}$$

becoming identical to Eq. (2.1) when introducing the notation

$$\overline{W} = W(-H,\{-\mu_\alpha\}) \tag{3.5}$$

for the dual kernel. Unlike for the general form (3.1), the dual transform here only involves the inversion of the local energies $H \to -H$ and the reservoir potentials μ_α. The "Wick-rotation" $H_{\mathrm{tun}} \to \mathrm{i}H_{\mathrm{tun}}$ is instead explicitly accounted for by the additional minus sign in $-\mathcal{P}\overline{W}\mathcal{P}$ in the duality (3.4), using that the weak-coupling approximation involves only terms *quadratic* in the parameters of H_{tun}. Thus, given that all tunneling dynamics should in the end be determined by *differences* between the local energies and the environment potentials, it is reasonable to assume for the remainder of this thesis that the both the Born-Markov kernel W and its dual $\overline{W}$ are physically valid according to the criteria set in Sec. 2.3.2. As we see below, this *physical* input is a central aspect of why the duality (3.4) becomes useful.

As a first step, we explicitly write how Eq. (3.4) relates the modes and amplitudes of W, i.e., its left and right eigenvectors $(x'|$ and $|x)$ governing the Markovian time evolution $|\rho(t)) = \exp(Wt)\,|\rho_0)$ according to Sec. 2.3.2 and Sec. 2.3.4. Papers II,III and Lic. Th. [110] prove in more detail that Eq. (3.4) implies

$$\begin{aligned} (x'|W = \lambda_x(x'| \Rightarrow W|y) = \lambda_y|y) \quad &, \quad |y) = \mathcal{P}|\overline{x}'), \\ W|x) = \lambda_x|x) \Rightarrow (y'|W = \lambda_y(y'| \quad &, \quad (y'| = (\overline{x}|\mathcal{P} \\ \lambda_y = -\overline{\lambda}_x^* - \Gamma, & \end{aligned} \tag{3.6}$$

[1] Note that frequency-dependence of the *dual* kernel evaluated at the dual frequency $\overline{\omega} = \mathrm{i}\Gamma - \omega^*$ vanishes only because of the combined effect of setting $\omega \to \mathrm{i}0_+$ and expanding in Γ.

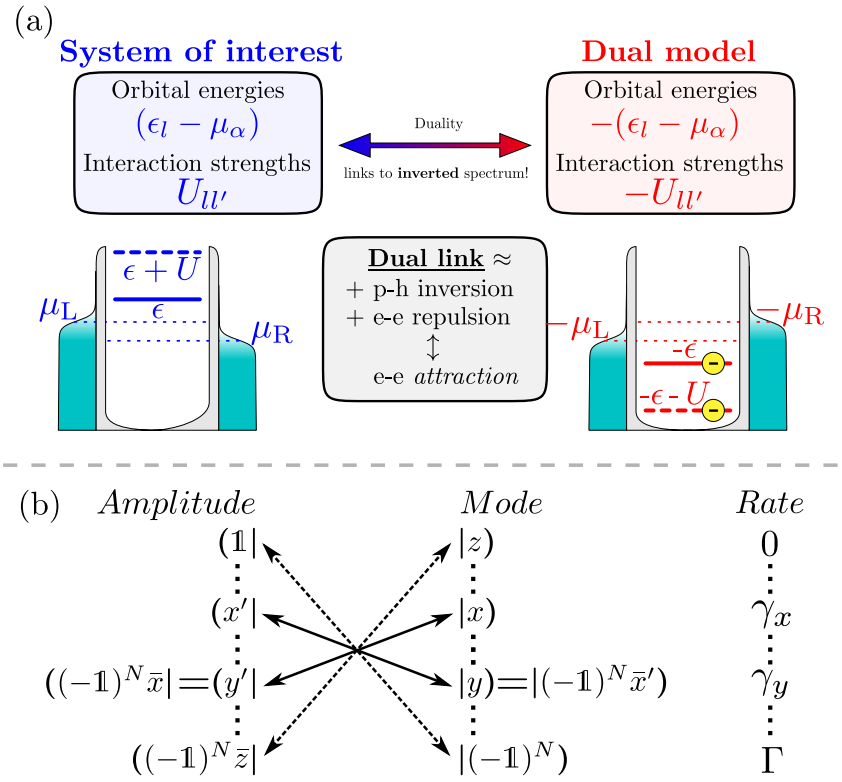

Figure 3.1: ***(a)*** *Mapping between the system of interest, characterized by reservoir potentials μ_α and a local Hamiltonian H with single-particle energies ϵ_l as well as interaction energies $U_{ll'}$ (here: two-particle interaction $\sim N_l N_{l'}$), and the* dual *system/model with inverted energies. From the point of view of the open system (here: single-level quantum dot governed by the Hamiltonian (2.11)), the energy inversion is established by a combination of a particle-hole transform and the inversion of all interaction strengths.*
(b) *Illustration of the dual crosslink (3.6) between modes and amplitudes of the dissipative Born-Markov kernel W [Eq. (2.30)].*
Source: *Modified version of a figure originally published by Wiley in paper III.*

Figure 3.1(b) illustrates that Eq. (3.6) *crosslinks* any mode $|x)$ corresponding to an evolution rate λ_x to an amplitude covector $(y'|$ corresponding to the *generally* different rate $\lambda_y = -\overline{\lambda}_x^* - \Gamma$ via the fermion parity $\mathcal{P}$ and the dual transform. Importantly, this dual transform $\overline{x}$ of any operator/quantity x can be performed by a *parameter transform* which realizes the energy inversion $H, \mu_\alpha \to -H, -\mu_\alpha$. In the analytical practice, having found a mode $|x)$ of W to the eigenvalue λ_x for *arbitrary* system parameter values, the dual transform of x and λ_x is achieved by adding a minus to all local energies and all chemical potentials in the parametric dependence of x and λ_x on these energies. Note also that the possible non-diagonalizability of W does not in any way impede the application of duality and its induced mode-amplitude crosslink: as detailed in App. B.2, the duality applies

exactly in the same form (3.6) if $|x)$, $(x'|$ are *generalized eigenvectors* corresponding to an eigenvalue λ_x in the Jordan normal form [196] of non-diagonalizable kernels.

Figure 3.1(a) illustrates how Eq. (3.4) and (3.6) map the dissipative dynamics of the system of interest – governed by W – to the dynamics in a *dual* system – governed by $\overline{W}$ – with inverted local energies and environment potentials. Importantly, the local energy inversion applies not only to the single-particle energies ϵ_l [Eq. (2.3)], but in particular to the *interaction energies*, such as e.g., the Coulomb interaction strength of the interacting single-level quantum dot [Sec. (2.1.1)], $U \to -U$. The dual model thereby represents a mapping between repulsive and attractive systems – a crucial ingredient in exploiting duality as shown in the appended papers.

Returning to the origin and implication of the duality, we are now in the position to give more concrete answers. The next section 3.2 starts by pointing out how Eqs. (3.4),(3.6), and the assumed physicality of the dual kernel $\overline{W}$ alone provide the above promised, systematic approach to understanding the relation between evolution amplitudes and modes. This gives further intuition into the, at first sight, unusual physics implied by the dual model, and thereby shows how the appended papers use duality – and in particular the interaction inversion – to better understand both time-dependent decay and stationary transport. By afterwards comparing and combining these insights with other symmetries and duality relations in open fermionic systems – such as time-reversal symmetry and detailed balance [Eq. (2.45)] – sections 3.3 to 3.4 then develop a more general perspective which also shows *why* the fermionic duality (3.4) holds for the systems of interest here.

In order to keep the discussion simple, we continue by focussing on the case most relevant for the appended papers, with the local dynamics generated by the Liouvillian L not entering the time-dependent probabilities $P_i(t) = (E_i|\rho(t))$, due to, e.g., $[L, W] = 0$ or special level-degeneracies. Thus, as in Sec. 2.3, we approximate $|\rho(t))$ to evolve only according to the dissipative kernel W,

$$|\rho(t)) \to \exp(Wt)\,|\rho_0). \tag{3.7}$$

We emphasize, however, that the results obtained in the following section 3.2 are likewise true for the full evolution kernel $A = -\mathrm{i}L + W$, as previously shown in Lic. Th. [110] and further detailed in paper V. In fact, the difference between A and W mostly concerns the possibility of a consistent, microscopic physical picture of the dual model, which for the interested reader is addressed in App. E. Finally, we note that while we discuss mostly the kernel W for the complete system *including all reservoir contributions* [Eq. (2.34)], it is crucial for the papers III-V that each reservoir-resolved kernel W_α itself represents a system of the type introduced in Sec. 2.1. The duality (3.4) and all its implications therefore also hold individually for each W_α.

3.2 Duality-based analysis of open-system dynamics

We now show how to systematically understand decay modes and their amplitudes using the duality (3.4) and its implied crosslink (3.6), and how this approach yields physical insights. More precisely, the first 3 following subsections are devoted to the two most important and most well-studied results that can be deduced from duality: the *fermion-parity mode* in Sec. 3.2.1, and the *dual stationary state* in sections 3.2.2 and 3.2.3. The final step in Sec. 3.2.4 is to merge these results into the promised, duality-based systematic description of modes and amplitudes.

3.2.1 The fermion-parity mode

Our discussion starts from the assumption of physicality for the dual kernel $\overline{W}$. Following section 2.3.2, this means that the dual kernel $\overline{W}$ must at least be dissipative [Eq. (2.36)] and conserve probability, with the latter implying the existence of the nontrivial zero amplitude given by the unit trace,

$$(\mathbb{1}|\overline{W} = 0. \tag{3.8}$$

Combining (3.8) with Eq. (3.6), paper II has proven for any fermionic open system described by the general Hamiltonian (2.2) and energy-independent couplings $\Gamma_{m,ll'}$ that the *fermion-parity operator* $(-\mathbb{1})^N$ [Eq. (2.5)] is a decay mode of the kernel [1] W corresponding to the eigenvalue $-\Gamma$:

$$W|(-\mathbb{1})^N) = -\Gamma|(-\mathbb{1})^N), \tag{3.9}$$

This is, in fact, what earlier works [76, 166, 167] have already noted using different methods, and have labeled as *fermion-parity mode*. The corresponding relaxation rate $\gamma_p = \mathrm{Re}\,[-\Gamma] = \Gamma$ [Eq. (2.37)] is accordingly called *fermion-parity rate*. Remarkably, being the lump sum of all bare wideband-limit couplings (3.2), this rate is independent of any other system parameter except for the couplings themselves. This excludes in particular any dependence on the environment temperatures T_α and the many-body interactions energies U in the open subsystem. To better understand this peculiar parameter dependence, let us further analyze both the mode $|(-\mathbb{1})^N)$ and, in the next subsection 3.2.2, its corresponding amplitude covector.

A first hint at why $\gamma_p = \Gamma$ is given by the sum of all diagonal couplings follows from the second requirement which physicality imposes on the dual kernel $\overline{W}$ next to probability conservation: its dissipativity, $\mathrm{Re}\left[\overline{W}\right] \leq 0$, see Eq. (2.36). As derived in detail in paper V, this property dictates $\gamma_p = \Gamma$ to be the *largest* decay

[1] It is also a mode of the full kernel $A = -\mathrm{i}L + W$ to the rate $\gamma_p = \Gamma$, since $L|(-\mathbb{1})^N) = 0$ by virtue of the fermion-parity superselection principle.

rate for the system of interest in the wideband limit, i.e., it forms a tight upper bound for the real parts (2.37) of all eigenvalues $-\lambda_x$ of $-W$:

$$0 \leq \mathrm{Re}\,[-\lambda_x] = \gamma_x \leq \gamma_p = \Gamma. \tag{3.10}$$

This suggests a close relation between the fermion-parity rate and a more fundamental principle – identified in Sec. 3.3 and paper III as Pauli's principle – which limits the possible ways, and thus the highest rate at which the time-dependent state $|\rho(t))$ may decay in the Markovian, weak coupling limit.

Let us continue by studying how exactly the mode $|(-\mathbb{1})^N)$ and the parity rate γ_p enter the time evolution of the state $|\rho(t))$ and any derived observable expectation value. By combining Eq. (3.9) with the exponential formal solution $|\rho(t)) = \exp(Wt)\,|\rho_0)$ [Eq. (3.7)], we infer that

$$|\rho(t)) = a_p \cdot e^{-\Gamma t}|(-\mathbb{1})^N) + |\rho^{\mathrm{rest}}(t)). \tag{3.11}$$

The amplitude a_p is discussed in more detail in the next subsection 3.2.2; $|\rho^{\mathrm{rest}}(t))$ represents the remaining part that is orthogonal to the parity, $(\rho^{\mathrm{rest}}|(-\mathbb{1})^N) = 0$. Most importantly, however, Eq. (3.11) shows that any expectation value or projection $\langle O\rangle(t) = (O^\dagger|\rho(t))$ of any operator O with respect to the time-dependent open-system state $\rho(t)$ can only be affected by the parity mode if $(O^\dagger|(-\mathbb{1})^N) \neq 0$. As proven in the appendix of Lic. Th. [110], this requires O to be an observable that *simultaneously* measures the occupation of each single-particle eigenstate $|l\rangle$, and hence contains the product of all occupation number operators N_l:

$$O \stackrel{!}{=} K \cdot \prod_l N_l + O^{\mathrm{rest}} \quad , \quad K \in \mathbb{R}^{\neq 0}, \tag{3.12}$$

with the remaining part O^{rest} defined to be orthogonal to $\prod_l N_l$.

What do equations (3.11) and (3.12) tell us about the parity rate γ_p and its parameter-dependence? Regarding the quantum dot systems of the appended papers, they explain two main observations. First, for the single-level quantum dot with the two single-particle states $|\uparrow\rangle, |\downarrow\rangle$ studied in paper II-V, the parity mode only affects the decay of two-particle correlations and expectation values. Thus, while time-dependent averages of the total occupation $N = N_\uparrow + N_\uparrow$ and spin $S = N_\uparrow - N_\downarrow$, both sums of single-particle quantities, are completely insensitive to the parity rate γ_p, the latter plays an *essential role* for the time-dependent dissipation of the two-particle Coulomb interaction energy $U \cdot N_\uparrow N_\downarrow$ [Eq. (2.11)]. Second, since any observable considered for the dot-sensor dot system in paper I can be expressed in terms of occupation numbers of only one of the two subsystems, the parity mode drops out completely in this study. With the complete kernel W of the two dots spanned by 8 modes and amplitudes in the probability sector, this allows us to immediately reduce W to the *relevant* 7-dimensional subblock of W that is biorthogonal to the parity mode $|(-\mathbb{1})^N)$ and its amplitude.

More generally, equations (3.11) and (3.12) further elucidate why the parity rate is given by the sum of all diagonal couplings $\Gamma_{m,ll}$ [Eq. (3.2)]. With M single-particle states, any M-particle observable whose expectation value depends on the parity rate is, by construction, susceptible to an occupation change in any of these M states. It is therefore consistent that the parity rate accounts for all these M possible ways – or *channels* – in which the system can decay via tunneling, as the maximal rate for any channel involving tunneling to/from open-system single-particle state $|l\rangle$ is given by $\sum_m \Gamma_{m,ll}$. This picture is further supported by the parameter-independent analytical form of the parity mode $|(-\mathbb{1})^N)$. According to Eq. (3.11), it dictates any decay governed by γ_p to time-dependently increase/decrease (depending on the sign of a_p) the probability of *every* even-parity state in the mixture $|\rho(t))$ by precisely the same amount as it decreases/increases the probability of every odd-parity state. Such a highly (anti-)symmetric effect on each probability must be the result of an, on average, equally destabilized occupation in every single-particle state. As we shall see in Sec. 3.2.3, this is also reflected by the parameter-dependence of the parity excitation amplitude a_p.

3.2.2 Parity amplitude covector

Following Sec. 2.3.3, the dissipativity and the existence of the zero amplitude $(\mathbb{1}|$ for the dual kernel $\overline{W}$ implies that the latter has at least one physically valid, trace-normalizable stationary state $|\overline{z}) = |z(-H, \{-\mu_\alpha\}))$, i.e.,

$$\overline{W}|\overline{z}) = 0 \text{ and } (\mathbb{1}|\overline{z}) = 1. \tag{3.13}$$

Introducing the notation $z_\mathrm{i} = \overline{z}$ used in the appended papers to indicate the energy **i**nversion, we continue by applying the mode-amplitude duality (3.6) to $|z)$. This yields $(z_\mathrm{i}(-\mathbb{1})^N|$ as the amplitude covector corresponding to the parity mode $|(-\mathbb{1})^N)$ for the kernel of interest W:

$$(z_\mathrm{i}(-\mathbb{1})^N|W = -\Gamma(z_\mathrm{i}(-\mathbb{1})^N|. \tag{3.14}$$

As outlined in Sec. 3.2.4 and detailed in Sec. D, the kernel W can always be expanded in a basis in which $(z_\mathrm{i}(-\mathbb{1})^N|$ is orthogonal to each right basis vector $|x)$ apart from the parity mode $|(-\mathbb{1})^N)$, for which we have $(z_\mathrm{i}(-\mathbb{1})^N|(-\mathbb{1})^N) = (\mathbb{1}|z_\mathrm{i}) = 1$. This implies, on the one hand, the orthogonality to the stationary state $|z)$,

$$(z_\mathrm{i}(-\mathbb{1})^N|z) = 0, \tag{3.15}$$

which would in fact be a highly nontrivial relation if one was not aware of $(z_\mathrm{i}(-\mathbb{1})^N|$ being an eigenvector. On the other hand, by applying $(z_\mathrm{i}(-\mathbb{1})^N|$ from the left to the two expressions of $|\rho(t))$ given in Eq. (3.7) and (3.11), and using the above stated biorthonormality of $(z_\mathrm{i}(-\mathbb{1})^N|$, we obtain the parity amplitude

a_p:

$$(z_{\rm i}(-\mathbb{1})^N|\rho(t)) \overset{(3.14)}{\underset{(3.7)}{=}} a_p \cdot \exp(-\gamma_p t) \quad , \quad a_p = (z_{\rm i}(-\mathbb{1})^N|\rho_0). \tag{3.16}$$

This means that analyzing the parity amplitude in the time-dependent decay does not only require knowledge about the initial state $|\rho_0)$, but in fact also an understanding of the *stationary state* $|z_{\rm i})$ in the *dual* model. This insight is precisely what papers II,III,V employ to analyze the time-dependent decay of the single-level quantum dot. In the following, we show how this analysis works.

The most crucial aspect is that we benefit from $|z_{\rm i})$ being *physically valid*, just as $|\rho_0)$. From a purely technical point of view, this implies $z_{\rm i} = z_{\rm i}^\dagger$ and $0 \leq \mathrm{Tr}\left[z_{\rm i}^2\right] = (z_{\rm i}|z_{\rm i}) \leq 1$, which together with the Cauchy-Schwarz inequality and $(-\mathbb{1})^N(-\mathbb{1})^N = \mathbb{1}$ sets the bound

$$-1 \leq a_p = (z_{\rm i}(-\mathbb{1})^N|\rho_0) \leq 1 \tag{3.17}$$

on the parity amplitude. But more importantly, in order to describe a_p as a function of the system parameters, we may not only rely on detailed calculations, but also on our *physical intuition* about $|z_{\rm i})$, given that we accept the unusual dynamics generated by the inverted dual Hamiltonian $\overline{H} = -H$. Let us illustrate this idea in more detail.

3.2.3 The physics of the dual stationary state

The most important physical intuition about the dual state $|z_{\rm i})$ is related to the above highlighted [Sec. (3.1.2)] mapping between repulsive and attractive many-body interactions. As well-known from, e.g., superconducting systems, attractive interactions between fermions typically lead to a pairing effect. If the open system of interest has strong repulsive interaction $\sim U$ compared to all other relevant energy scales, the *dual* stationary state $|z_{\rm i})$ is governed by strong attraction, and hence not expected to be a mixture of states with even and odd fermion parity, $|(-\mathbb{1})^N z_{\rm i}) \to \pm|z_{\rm i})$. The amplitude a_p [Eq. (3.16)] can thereby be understood to a very good approximation as the simple state overlap

$$a_p \overset{(3.16)}{=} (z_{\rm i}(-\mathbb{1})^N|\rho_0) \approx \pm(z_{\rm i}|\rho_0). \tag{3.18}$$

As long as the pairing is dominant in the dual system, the parity mode is therefore excited proportionally to how much the initially prepared state resembles the *dual* stationary state. The following examples demonstrate why this is relevant both for the concrete studies in the appended papers as well as for a general understanding of the parity rate, mode and amplitude.

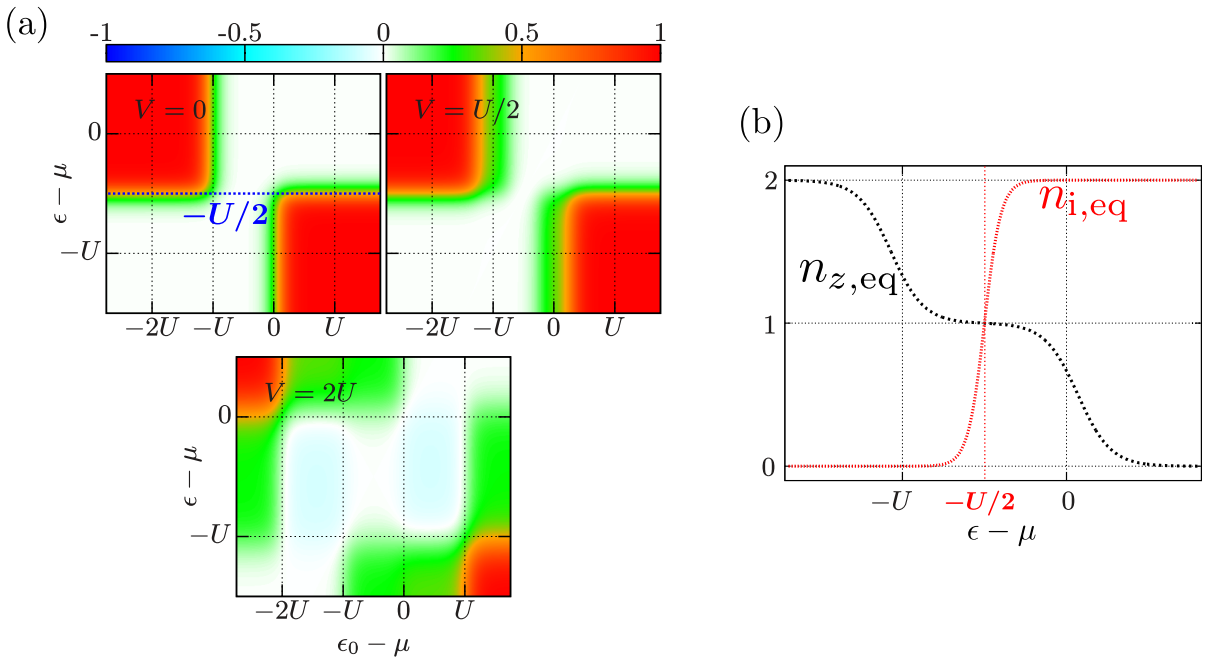

Figure 3.2: ***(a)*** *Parity amplitude* $a_p = (z_i(-\mathbb{1})^N|\rho_0)$ *[Eq. (3.16)] of a spin-degenerate single-level quantum dot [Eq. (2.11)] subject to a sudden shift of the level-position* $\epsilon_0 \to \epsilon$*. The initial quantum dot state* $|\rho_0)$ *is the stationary state with respect to the initial level-position,* $|\rho_0) = |z(\epsilon_0))$*. The three panels correspond to three different biases* $V = \mu_L - \mu_R$ *between the two weakly coupled reservoirs L,R, where* $\mu = (\mu_L + \mu_R)/2$*.* ***(b)*** *Average dot occupation* $n_{z,eq} = (N|z_{eq})$ *and dual dot occupation* $n_{i,eq} = (N|z_{i,eq}) = (N|z_i)|_{eq}$ *as a function of the level-position* ϵ *at global equilibrium (2.48), i.e., for* $V = 0$*.*
In all figures, we assume equal temperatures $T_L = T_R = T$ *in both reservoirs, strong local Coulomb interaction* $U = 10T$*, as well as spin- and reservoir symmetric tunnel coupling,* $\Gamma_{\uparrow L} = \Gamma_{\uparrow R} = \Gamma_{\downarrow L} = \Gamma_{\downarrow R}$*.*
Source: *Figure (a) has been adapted from paper III, originally published by Wiley.*

Time-dependent decay

In papers II,III, Eq. (3.18) explains how the parity amplitude a_p – next to a single-particle contribution $a_N \cdot I_N(t)$ proportional to the particle current I_N – affects the time-dependent electronic *heat current*

$$I_Q(t) = a_N \cdot I_N(t) + U\Gamma \cdot a_p \exp(-\Gamma t) \tag{3.19}$$

out of the single-level quantum dot [Eq. (2.11)] in response to a sudden level-position shift $\epsilon_0 \to \epsilon$. With the initial state prepared as the stationary state with respect to the initial level-position, $|\rho_0) = |z(\epsilon_0))$, the amplitude $a_p = (z_{\mathrm{i}}(-\mathbb{1})^N|\rho_0)$ shows steps as a function of ϵ_0 at the points displayed in Fig. 3.2(a). These steps are expectedly located at the Coulomb resonances $\epsilon_0 - \mu = 0, -U$ at which the stationary occupation number $n_z = (N|z)$ of a *repulsive quantum*

dot system changes between two stable plateaus, see black curve in Fig. 3.2(b). By contrast, the dependence on the *final* level ϵ after the switch is determined by the *dual* average occupation $n_{\rm i} = (N|z_{\rm i})$, governed by attractive interaction. The amplitude a_p thus exhibits the much sharper step of only a one two-particle transition $0 \leftrightarrow 2$ around $\epsilon - \mu = -U/2$. This well-known feature [197, 198] of attractive quantum dots is displayed by the red curve in Fig. 3.2(b). Moreover, the different panels in Fig. 3.2(a) illustrate the higher robustness of this ϵ-step – compared to those in the ϵ_0-dependence – to external bias, showing the case of two coupled reservoirs L,R, average potential $\mu = (\mu_{\rm L}+\mu_{\rm R})/2$, and a bias $V = \mu_{\rm L}-\mu_{\rm R}$ studied in paper III. Only a $|V| > U$ large enough to break the pairing invalidates the approximation (3.18), and substantially changes the ϵ-dependence of a_p. Note that paper III shows the same argument to apply to magnetic fields B lifting the spin-degeneracy of the quantum dot: a sizable effect on $|z_{\rm i})$ only occurs for pair-breaking field strengths $|B| > U$. Altogether, this shows how to use duality instead of cumbersome calculations to elucidate measurable analytical features in the parameter-dependence of the time-dependent decay of a quantum dot – features that otherwise seem very counter-intuitive and difficult to explain.

Next, let us consider a case in which the approximation (3.18) for the amplitude a_p is justified for a more general system. If this is the case, we can further clarify the general role of the parity mode and the dual state in the time-dependence $|\rho(t))$ as stated in Eq. (3.16) by combining the latter equation with $(z_{\rm i}(-\mathbb{1})^N| \approx \pm(z_{\rm i}|$. Namely, we deduce

$$(z_{\rm i}|\rho(t)) \approx (z_{\rm i}(-\mathbb{1})^N|\rho(t)) \overset{(3.16)}{\approx} (z_{\rm i}|\rho_0) \cdot \exp\left(-\gamma_p t\right). \tag{3.20}$$

The *time-dependent* overlap of $|z_{\rm i})$ and $|\rho(t))$ thus always decays monotonously as long as $|(-\mathbb{1})^N z_{\rm i}) \approx |z_{\rm i})$ is valid, irrespective of the initial state $|\rho_0)$. This suggests – or rather defines – $|z_{\rm i})$ to be a *state of maximal instability*, i.e., to which $|\rho(t))$ returns, on average, with least probability. One way of understanding this has already been suggested in the previous section 3.2.1: if the system is initially prepared in the dual stationary state, $|\rho_0) = |z_{\rm i})$, the occupation of every open-system single-particle state is unstable, and in principle subject to change with the first tunneling event in the full, Markovian sequence of tunneling events dictating $|\rho(t))$. This is also consistent with the parity rate $\gamma_p = \Gamma$ being the sum over all diagonal couplings, (3.2). Moreover, Eq. (3.20) reflects this explanation by the fact that whenever $|\rho_0)$ and $|z_{\rm i})$ have fixed parity and sizable overlap $(z_{\rm i}|\rho_0)$ leading to a sizable a_p, $(z_{\rm i}|\rho(t))$ vanishes as soon as $|\rho(t))$ leaves the initial parity sector, which is precisely what the first tunneling event causes.

Alternatively, we may understand maximal instability as $|z_{\rm i})$ having the least probability to recur in the long-time limit. Indeed, analytically combining the duality (3.4) with the concepts of recurrence and and detailed balance [Eq. (2.45)] introduced in Sec. 2.4, section 3.4.1 and paper V rigorously relate $|z_{\rm i})$ to the *mean recurrence times* of the stationary state $|z)$.

However, what happens if $(z_\mathrm{i}(-\mathbb{1})^N| \neq \pm(z_\mathrm{i}|$, as for example for the single-level dot with a large bias voltage $|V| > U$ between different coupled reservoirs? As paper III shows, such situations *far* away from equilibrium essentially allow each open-system many-body energy eigenstate to recur with a sizable probability at any time; the notion of maximal instability thereby loses its meaning. For the special case of a single-level dot with two reservoirs at temperature T, interaction energy $U \gg T$, and both ϵ and $\epsilon + U$ in the bias window, the completely uniform probability distribution for all quantum dot eigenstates causes the dual state to even be equal to the actual stationary state: $|z_\mathrm{i}) \to |z)$. A suitable physical understanding of the dual state $|z_\mathrm{i})$ in such cases is an interesting, yet still open question.

Linear and nonlinear response

Apart from its importance for time-dependent decay, the dual state $|z_\mathrm{i})$ also exhibits a feature that is practically useful in analyzing *stationary thermoelectric transport*, and as such, *has in fact already been measured* more than two decades ago [119, 138, 139]. Namely, paper IV proves that the stationary heat current out of a single-level quantum dot into one of several weakly coupled reservoirs α can be written as

$$I_\mathrm{Q}^\alpha = \left(\epsilon - \mu_\alpha + \frac{2 - n_{\mathrm{i}\alpha}}{2} U\right) I_\mathrm{N}^\alpha + U\Gamma_\alpha (z_{\mathrm{i}\alpha}(-\mathbb{1})^N|z). \tag{3.21}$$

The symbol I_N^α denotes the corresponding particle current, and $n_{\mathrm{i}\alpha} = (N|z_{\mathrm{i}\alpha})$ is the average occupation of the *dual* stationary state $|z_{\mathrm{i}\alpha})$ with respect to only the reservoir α, i.e., fulfilling $\overline{W}_\alpha |z_{\mathrm{i}\alpha}) = 0$ for the reservoir-resolved dual kernel $\overline{W}_\alpha$.

According to paper IV, equation (3.21) reveals several important properties of the thermoelectric behavior that can readily be understood by duality. First, the factor in front of I_N^α, which we denote as the "tightly coupled" average energy per particle, surprisingly contains an interaction term following the *dual* average hole number $(2 - n_{\mathrm{i}\alpha})/2$ instead of the average (reservoir-resolved) particle number [1] $n_{z\alpha}/2 = (N|z_\alpha)/2$. Using Onsager reciprocity [Eq. (2.58)] and Matveev's argument [199], this means that the equilibrium limit (2.48) of precisely this tight-coupling term determines the linear response of the *particle current* I_N to a temperature gradient ΔT between different leads. As such, it also enters the experimentally well-studied [119, 138, 139] *Seebeck coefficient* $S = V|_{I_N=0}/\Delta T$, introduced in Sec. 1.3.1 as the voltage V necessary to cancel the stationary current induced by ΔT:

$$S = \frac{1}{T}\left[\epsilon - \mu + \frac{2 - n_{\mathrm{i,eq}}}{2} U\right] \quad , \quad n_{\mathrm{i,eq}} = n_{\mathrm{i}\alpha}|_\mathrm{eq} = (N|z_{\mathrm{i}\alpha})|_\mathrm{eq}\,, \tag{3.22}$$

[1] The latter would typically occur as the effective interaction-related contribution in a mean-field approximation.

where μ and T are the equilibrium potential and temperature introduced in Eq. (2.48). In Fig. 1.4, we have shown that the Seebeck coefficient S of small systems with strong Coulomb interaction exhibits well-known [118] jumps in between two Coulomb resonances. As Fig. 3.2(b) illustrates for the single-level quantum dot, the $n_{\mathrm{i,eq}}$-dependence in Eq. (3.22) identifies precisely such a jump at $\epsilon - \mu = -U/2$ as a *resonant effect*: it corresponds to the sharp transition in the charge stability of a quantum dot with strong attractive interaction, given that $|U| \gg T$. Paper IV uses this insight to derive helpful approximations for the analytical features of S, such as the slope around the symmetry point and local extreme points.

The second, purely interaction-related term in Eq. (3.21) is associated with the (nonlinear) thermal conductance. Introduced as Fourier heat in Sec. 1.3.1 – and having been studied using Fermi's Golden rule in, e.g., Refs. [147, 200] – it refers to the heat transferred from one reservoir to another in the absence of an average particle current, $I^{\alpha}_{\mathrm{Q}}\big|_{I^{\alpha}_{\mathrm{N}}=0}$. Given by $U\Gamma_{\alpha}(z_{\mathrm{i}\alpha}(-\mathbb{1})^N|z)$, we can again use that $(z_{\mathrm{i}\alpha}|(-\mathbb{1})^N \approx (z_{\mathrm{i}\alpha}|$ to intuitively explain, in terms of a state overlap, why this thermal conductance is typically very small on the scale $U\Gamma_{\alpha}$ as long as $|V| < |U|$. Namely, using that the total energy inversion in the dual model is achieved by a combination of a particle-hole transform and an interaction inversion [Fig. 3.1], papers IV,V argue that $|z_{\mathrm{i}\alpha})$ and $|z)$ are never in the same occupation sector, and hence orthogonal. The only exception are level-positions ϵ in the effectively $T_{\alpha}/2$ broadened window around $\epsilon - \mu_{\alpha} = -U/2$ in which $n_{\mathrm{i}\alpha}$ jumps. Alternatively, one may argue that the reservoir-resolved dual state $|z_{\mathrm{i}\alpha})$ is approximately equal to the full dual state $|z_{\mathrm{i}})$ for most parameter values if $|V| < U$, so that $(z_{\mathrm{i}\alpha}(-\mathbb{1})^N|z) \approx (z_{\mathrm{i}}(-\mathbb{1})^N|z) = 0$ according to Eq. (3.15). By contrast, a large pair-breaking bias $|V| > U$ invalidates this argument for level-positions in which both ϵ and $\epsilon+U$ are in the bias window, showing that the thermal conductance can become sizable.

3.2.4 Duality-induced basis expansion

This final part of Sec. 3.2 refocuses on the section's main goal: developing a *systematic* approach to understanding decay modes and amplitudes in the Markovian, weak-coupling decay dynamics of fermionic open systems. The reader should note from the start that the following, extended analysis in Sec. 3.2.4 goes beyond the appended papers, and is therefore mostly carried out in App. D. The final result nevertheless represents a valuable conclusion to Sec. 3.2, as it completes the discussion by *merging* the insights from sections 3.2.1-3.2.3 into the above promised, systematic recipe.

Up to this point, one may argue that the duality (3.4) has provided analytical expressions and physical understanding for only a single pair of eigenvectors of the kernel W next to $(\mathbb{1}|$ and $|z)$: the parity mode $|(-\mathbb{1})^N)$ and its amplitude covector $(z_{\mathrm{i}}(-\mathbb{1})^N|$, both corresponding to the parity rate $\gamma_p = \Gamma$. Given that

already the probability subspace of the kernel W for a system with M fermionic single-particle states is spanned by 2^M of such pairs, characterizing one additional pair seems far away from a "systematic approach".

This first impression, however, turns out to be incorrect. Starting from the example of an open system consisting only of one fermionic single-particle state $|l\rangle$ (see paper V), the eigenvectors $|z)$ and $(z_{\rm i}(-\mathbb{1})^N|$ both refer to the reduced density operators $z, z_{\rm i}$ and fermion parity $(-\mathbb{1})^N \to 1-2N_l$ of only this one single-particle state $|l\rangle$. When coupling this state to a second state, and calling the two states the $|\uparrow\rangle$ and $|\downarrow\rangle$ states of a single-level quantum dot [Sec. (2.1.1)], $|z)$ and $(z_{\rm i}(-\mathbb{1})^N|$ are again eigenvectors, but with the density operators and parity now referring to both single-particle states, meaning, e.g., $(-\mathbb{1})^N \to (1-2N_\uparrow)(1-2N_\downarrow)$. In the latter case, one may therefore ask how the kernel acts on the corresponding vectors containing the *even further reduced* density operators of only one of the two single-particle states,

$$|z_\uparrow \otimes \mathbb{1}_\downarrow) \quad , \quad (z_{{\rm i},\uparrow}(-\mathbb{1})^{N_\uparrow} \otimes \mathbb{1}_\downarrow|, \tag{3.23}$$

with the reduced density operators $z_\uparrow = {\rm Tr}_\downarrow[z]$ as well as $z_{{\rm i},\uparrow} = {\rm Tr}_\downarrow[z_{\rm i}]$ for the spin-up state, and with $\mathbb{1}_\downarrow$ being the identity in the subsystem containing only the spin-down state.

More generally, given a set $\mathcal{S}$ of M single-particle states, it is clear that one can ask the same question about any possible bipartition $\{\mathcal{A}, \mathcal{S}\setminus\mathcal{A}\}$ of these M states, i.e., with the reduced system describing all states in $\mathcal{A}$, and with all other states traced out. The key advantage of the dual link between the zero eigenvectors $(\mathbb{1}|, |z)$ and the parity mode/amplitude $|(-\mathbb{1})^N), (z_{\rm i}(-\mathbb{1})^N|$ is now that for any number M, it guides us how to *systematically* construct 2^M pairs of bra and ket vectors using the same idea as in Eq. (3.23): through tracing out single-particle states from $|z)$ and $(z_{\rm i}|$, and by multiplying with parity operators related to these states. With the detailed procedure given in App. D, let us here simply write down its final result – the sequences of left ($\mathcal{L}$) and right ($\mathcal{R}$) vectors which we can use to construct left and right basis vectors for W:

$$\begin{aligned} \mathcal{L} = ((p'_\mathcal{A}|)_\mathcal{A} \quad &, \quad \mathcal{R} = (|p_\mathcal{A}))_\mathcal{A} \\ (p'_\mathcal{A}| = (z_{{\rm i},\mathcal{A}}(-\mathbb{1})^{N_\mathcal{A}} \otimes \mathbb{1}_{\mathcal{S}\setminus\mathcal{A}}| \quad &, \quad |p_\mathcal{A}) = |(-\mathbb{1})^{N_\mathcal{A}} \otimes z_{\mathcal{S}\setminus\mathcal{A}}), \end{aligned} \tag{3.24}$$

where the sequence runs over all 2^M bipartitions $\{\mathcal{A}, \mathcal{S}\setminus\mathcal{A}\}$ of the set $\mathcal{S}$ of M single-particle states. In analogy to the example (3.23), the symbols $z_\mathcal{A} = {\rm Tr}_{\mathcal{S}\setminus\mathcal{A}}[z]$ as well as $z_{{\rm i},\mathcal{A}} = {\rm Tr}_{\mathcal{S}\setminus\mathcal{A}}[z_{\rm i}]$ denote the reduced density operators for all single-particle states in $\mathcal{A}$, defined in terms of the partial *Fock space trace* over all occupations of the single-particle states in $\mathcal{S}\setminus\mathcal{A}$. The operators $N_\mathcal{A}$ are the corresponding occupation number operators. For $\mathcal{A}$ being the empty set $\mathbb{0}$, we define $(-\mathbb{1})^{N_\mathcal{A}} \to 1$, and furthermore infer from probability conservation that also $z_\mathcal{A}, z_{{\rm i},\mathcal{A}} \to 1$.

As detailed in App. D, future applications of the duality-induced basis expansion of W using the vectors Eq. (3.24) offer [1] several advantages over taking the usual eigenvectors $|E_{ij})$ [Sec. (2.3.4)] of the Liouvillian L as basis vectors.

- First, any off-diagonal element of W in a basis constructed by the vectors (3.24) must be due to a coupling of single-particle eigenstates in the open system, via many-body interactions or via the coupling to the reservoirs. This allows to directly identify and analyze nontrivial physical effects stemming from precisely these many-body interactions and coherent couplings. Or in other words, the vectors (3.24) solve the weak-coupling eigenvalue problem for a completely non-interacting fermionic open system.

- Second, the idea of the parity mode $|(-\mathbb{1})^N)$ affecting only N-particle observables according to Eq. (3.12) extends to the subparity mode $|p_{\mathcal{A}})$ affecting only $N_{\mathcal{A}}$-particle observables. Knowing which observable one is interested in, this allows to neglect many terms in the calculation from the start.

- Finally, the reduced dual states $z_{\mathrm{i},\mathcal{A}}$ in the subparity covectors $(p'_{\mathcal{A}}|$ may often be understood as the *most unstable subsystem* states with fixed parity. This in return may cause at least one or several $(p'_{\mathcal{A}}|$ to become approximate left eigenvectors of the kernel W to the *subparity rates* $\Gamma_{\mathcal{A}}$, i.e., with the lump sum (3.2) reduced only to the single-particle states $|l\rangle \in \mathcal{A}$. In fact, the sensor-dot setup discussed in paper I is an example of such behavior, since the subparity covector $(p'_{\{\uparrow,\downarrow\}}|$ referring only to the spin-up and spin-down state of the dot to be measured is indeed found to be an approximate eigenvector to the subparity rate $\Gamma_{\{\uparrow,\downarrow\}} = \Gamma_\uparrow + \Gamma_\downarrow$.

3.3 The importance of fermionic statistics and superselection

With the previous section 3.2 providing an extensive overview of how the appended papers have made, and future studies can still make use of the fermionic duality in the "theoretical practice", let us now turn towards understanding *why* duality holds and what it means from a more general point of view.

More concretely, this section addresses the central and name-giving aspect of the *fermionic* duality, which is its fermionic nature itself. Summarizing and complementing paper II and paper V, we further elucidate why the duality emerges in the first place, which problem can arise for bosonic systems, and finally explain how the duality can be extended to energy-dependent bare couplings $\Gamma_{m,ll'}(E)$ in the Born-Markov limit. With the latter being addressed in Sec. 3.5, this section focuses on energy-independent couplings for clarity and efficiency. Furthermore,

[1] After an orthogonalization procedure.

we consider a simplified treatment in the *rate-equation limit* [Sec. (2.4.1)], reduced to many-body energy eigenstate probabilities $P_i(t) = (E_i|\rho(t))$.

3.3.1 Duality, Pauli's principle and Fermi-Dirac statistics

First, we note that in the subspace of probabilities, the fermionic duality (3.4) assumes a remarkably simple form when studying off-diagonal elements $W_{ji} = (E_j|W|E_{i\neq j})$ with respect to the energy eigenstates $|E_i)$ of the open-system Hamiltonian H:

$$W_{ji} = \overline{W}_{ij} = W_{ij}(-H, \{-\mu_\alpha\}) \quad \forall i \neq j. \tag{3.25}$$

This follows from $(E_j|E_{i\neq j}) = 0$ and the fact that for $i \neq j$, the only non-vanishing rates $W_{ij} \neq 0$ in the sequential-tunneling regime are those representing transitions due to exchange of exactly one particle. Consequently, a transition involves a change in the local fermion parity, $(E_i|\mathcal{P}|E_i) = -(E_j|\mathcal{P}|E_j)$.

For simplicity, let us look at the case of only a single reservoir with potential $\mu \equiv 0$ and temperature T. The typical "Fermi's Golden rule" form of the rates then reads $W_{i\neq j} \sim \Gamma \cdot f(E_{ij})$ with the Fermi function $f(x) = \left[\exp\left(\frac{x}{T}\right) + 1\right]^{-1}$ and $E_{ij} = E_i - E_j$. Consequently, Eq. (3.25) boils down to a simple, commonly made observation in fermionic rate equations: if a particle carrying the energy $E_{ij} = E_i - E_j$ tunnels into the open system and causes the state transition $i \leftarrow j$ at a rate $W_{ij} \sim f(E_{ij})$, the inverted transition $j \leftarrow i$ with a particle tunneling out happens at the rate

$$W_{ji} = \overline{W}_{ij} \sim f(E_{ji}) = f(-E_{ij}) = 1 - f(E_{ij}). \tag{3.26}$$

From the point of view of the *non-interacting* reservoir, this is explained straightforwardly: the chance of a particle at any energy E tunneling away from the reservoir is obviously proportional to the chance of a particle occupying an orbital at precisely this energy; for fermionic, *effectively* [1] non-interacting reservoirs in their own local equilibrium, this is ultimately dictated by Pauli's principle to be given by the Fermi-Dirac distribution $f(E)$. Conversely, the chance of a particle tunneling back (a hole tunneling away) is proportional to the chance of having an empty reservoir orbital, again determined by Pauli's principle to be $1 - f(E) = f(-E)$.

The crucial observation in the above argument is that the environment occupations of particles and holes are related either by a particle-hole transform of the reservoir state, or equivalently, by an energy inversion. We clarify in Sec. 3.3.2, and derive in App. F, that together with probability conservation (2.44) and the parity superselection principle [Sec. (2.1)], this is enough to *derive* the fermionic

[1] What is important is that the Hamiltonian H_R is quadratic in the fields. One may consider quasi-particles as in Fermi liquids, describing interaction effects in a single-particle picture.

duality in the rate-equation limit. Fermionic duality is thus to a large extent the insight that the simple relation between particle- and hole occupations in the non-interacting reservoirs can also be established from the point of view of the open system; not by a particle-hole transform as in the reservoirs, since this does not generally invert interaction energies in the open system. Instead, one employs an explicit energy inversion (3.5), thereby mapping to the dual open system [Fig. 3.2]. As further detailed below in Sec. 3.5.2, this also clarifies how paper V extends the duality to energy-dependent bare couplings $\Gamma_{m,ll'}(E)$.

Finally, a connected argument from paper III makes it plausible why Pauli's principle yields the parity rate Γ as an upper bound on the Born-Markov limit decay rates (2.37) according to Eq. (3.10): since Pauli exclusion restricts each open-system single-particle state $|l\rangle$ to be occupied by maximally one particle, and since the rate of one particle tunneling into/out of this state is at max $\Gamma_l = \sum_m \Gamma_{m,ll}$, the sum $\Gamma = \sum_l \Gamma_l$ is the maximum rate of *any* particle tunneling into/out of any state $|l\rangle$.

3.3.2 The role of fermion-parity superselection

The main statement of the previous section 3.3.1, which is that duality is mostly the exploitation of Pauli's principle and the resulting Fermi-Dirac statistics in the non-interacting reservoirs, seems to be somewhat at odds with papers II-IV. The latter instead highlight *fermion-parity superselection* [158–160] – dictating $[H, (-\mathbb{1})^N] = 0$ and thereby forbidding any *pure* physical state to be a quantum superposition of states with different fermion parity – as the central principle behind the fermionic duality. The truth is in fact, as paper V emphasizes, that duality is a combination of both principles.

Details of where exactly the superselection principle plays a role can be deduced from paper II and App. F. To understand this on a simple level, let us go back to the off-diagonal rate equation (3.25). We have previously argued that the correct sign on the right-hand side of this equation is established by the parity superoperators $\mathcal{P}\bullet = (-\mathbb{1})^N\bullet$ in the duality relation (3.4): the fermion parity flips for any energy eigenstate transition $|E_i) \leftarrow |E_j)$ with a finite rate $W_{ij} > 0$ in the sequential tunneling regime. For this statement and Eq. (3.25) to have any meaning, it is implied that the fermion parity is a good quantum number for the pure [1] energy eigenstates, so that $\mathcal{P}|E_i) = \pm|E_i)$ for any i. This is precisely what fermion-parity superselection $[(-\mathbb{1})^N, H] = 0 \Rightarrow [\mathcal{P}, L] = 0$ guarantees, not just in the here presented rate-equation limit. In fact, as papers II,V show, this likewise holds for quantum master equations including coherences, and even beyond the weak-coupling limit. An interesting aspect for future applications of duality is that this expressly allows for open-system Hamiltonians H that *break* (quasi-)particle number conservation, as long as the fermion parity is still conserved. The duality

[1] Note that this does not apply to mixed states such as, e.g., the stationary state $|z)$.

therefore in principle applies to *superconducting* devices similar to those studied in recent works on topological quantum computing [201–203].

3.3.3 Mode-amplitude duality for bosonic systems

Apart from dictating the reservoir occupations to be Fermi-Dirac distributed, Pauli's principle plays in fact another critical role for the duality to become a reasonable and useful statement. This can be seen when attempting to establish a similar duality relation for bosonic systems. With a more general treatment left open for future studies, let us here consider the well-known example of a single bosonic mode (harmonic oscillator) with frequency ω, bilinearly coupled with strength g to a thermal bath of bosonic modes excited according to the Bose-Einstein distribution.

The Born-Markov master equation for the reduced density operator $|\rho(t))$ describing the occupation of the single mode in the zero-temperature limit can be obtained from any standard textbook on open quantum systems [81, 82], or by adjusting the superoperator formalism used in Ref. [167] to bosonic systems, see Refs. [204, 205] and in particular App. G. Formally, the result again reads $\partial_t|\rho(t)) = [-\mathrm{i}L + W]\,|\rho(t))$. It contains the local Liouvillian $L\bullet = [H, \bullet]$, i.e., the commutator with the Hamiltonian [1] $H = \omega b^\dagger b$ of the single bosonic mode created (annihilated) by the bosonic field operator $b^\dagger$ (b). As such, the latter fulfill the commutation relations $[b, b] = [b^\dagger, b^\dagger] = 0$ as well as $[b, b^\dagger] = 1$. Considering for simplicity the low-temperature limit, the dissipative kernel W is given by the well-known Lindblad dissipator [206, 207]

$$W\bullet = -\Gamma\left[\frac{1}{2}L_N^+ - \zeta\right]\bullet, \tag{3.27}$$

with the coupling frequency $\Gamma \sim |g|^2 > 0$, the anti-commutator $L_N^+\bullet = N\bullet + \bullet N$ of the occupation number $N = b^\dagger b$ with any other operator $\bullet$, and $\zeta\bullet = b\bullet b^\dagger$.

By repeating the derivation for the dual system as defined in Eq. (3.5), i.e., *without* considering any chemical potentials μ_α, one formally obtains the duality relation

$$W + \overline{W}^\dagger = +\Gamma \tag{3.28}$$

involving the dual kernel $\overline{W} = W(-H)$. Comparing this to the fermionic duality $W + \mathcal{P}\overline{W}^\dagger\mathcal{P} = -\Gamma$ [Eq. (3.4)], it is not at all surprising that Eq. (3.28) does not contain any parities $\mathcal{P}$: there is no parity superselection principle for bosonic systems, and parity is often not even a good quantum number, such as for the well-known Glauber coherent states [208]. The tricky part is, however, the

[1] Note that since we are dealing with the commutator $[H, \bullet]$, the constant vacuum energy $\omega/2$ in the Hamiltonian $H = \omega\,[b^\dagger b + 1/2]$ can be neglected, as it commutes with any operator $\bullet$.

+-sign on the right-hand side of Eq. (3.28). On an elementary level, this difference to the fermionic duality (3.4) stems from the difference between Fermi-Dirac statistics $f(E)$ obeying $-\Gamma[f(E)+f(-E)] = -\Gamma$, and Bose-Einstein statistics $\mathrm{b}(E) = [\exp(E/T)-1]^{-1}$ obeying $-\Gamma[\mathrm{b}(E)+\mathrm{b}(-E)] = +\Gamma$. Since both W and $\overline{W}$ can be shown to conserve probability, $(\mathbb{1}|W = (\mathbb{1}|\overline{W} = 0$, the consequence of this additional sign becomes visible when naively applying $|\mathbb{1})$ from the right to Eq. (3.28):

$$+\Gamma|\mathbb{1}) \overset{(3.28)}{=} \left[W+\overline{W}^{\dagger}\right]|\mathbb{1}) = W|\mathbb{1}) + \left[(\mathbb{1}|\overline{W}\right]^{\dagger} = W|\mathbb{1}), \tag{3.29}$$

which can be confirmed explicitly by applying (3.27) to the identity $\mathbb{1}$ and using $[b, b^{\dagger}] = 1$.

It is, at first sight, rather alarming that Eq. (3.29) shows the unit vector $|\mathbb{1})$ to be a right eigenvector of W to a *positive* eigenvalue Γ. This, however, *does not* mean that W is not dissipative, and hence unphysical. Due to the unconstrained particle/excitation number N of the bosonic open-system mode, it is rather a consequence of $|\mathbb{1})$ being unconstrained, and hence not part of the *physical* Liouville space of right vectors of W, which are either traceless or trace-normalizable. As a related consequence, it is in particular not anymore possible – unlike for fermions – to infer an upper bound on the decay rates of W from the duality (3.28) and the physicality of $\overline{W}$: since the transition rates are not restricted by the number of particles or excitations occupying the mode, the argument given at the end of Sec. 3.3.1 for an upper bound on the decay rates does not apply any longer.

To conclude, while we cannot completely rule out any useful future application of the duality (3.28) at this time, it is much less obvious whether the latter can yield any valuable insight, since it is a mapping between to the *unphysical* sector of the kernel's Liouville space. This also makes clear that the decisive difference to the fermionic duality (3.4) is indeed Pauli's principle. Given a finite number of single-particle states defining the open system, it ensures that the corresponding many-body Liouville space is also finite. Exactly this property is a *basic* requirement for the existence and meaningfulness of the mode-amplitude crosslink Eq. (3.6); it is what in principle allows us to map the space of amplitude covectors $(x'|$ of the kernel W to the space of *physical* modes $|x)$. For unconstrained bosonic systems, this is never possible, since the many-body space is infinitely large even for only a single mode. What remains to be investigated is thus whether a duality exists for bosonic systems with a fixed particle number.

3.4 Combining duality with time reversal

One main prerequisite for paper V is that $\overline{W}$ does not simply represent the *time-reversed* counterpart of the actual kernel of interest W, despite the energy inversion in the dual model suggesting the opposite [App. (E)]. This in return means that, being inequivalent to the fermionic duality, time-reversal symmetry or its breaking can in principle be *combined* with duality to yield independent, new insights. Papers III-V demonstrate this explicitly, and this section intends to give an overview over these findings.

3.4.1 Duality and detailed balance

In the introductory section 2.4.3, we have defined time-reversal symmetry in the context of Markovian rate equations as the validity of *detailed balance* (2.45). Here, we illustrate how paper V *combines* detailed balance with the fermionic duality (3.4) in the rate-equation limit. This implies that we assume the energy inversion $(H, \{\mu_\alpha\}) \to (-H, \{-\mu_\alpha\})$ to the dual model not to break positive recurrence and detailed balance:

$$W_{jk}P_{z,k} = W_{kj}P_{z,j} \quad , \quad \overline{W}_{ij}\overline{P}_{z,j} = \overline{W}_{ji}\overline{P}_{z,i}, \tag{3.30}$$

where $\overline{P}_{z,j} = (E_j|z_\mathrm{i}) > 0$ are the *positive* probabilities of the dual stationary state. A simple, yet important observation from relation (3.25) is that the dual kernel $\overline{W}$ is generally not equal to the time-reversed counterpart $W^{\leftarrow}$ [Eq. (2.46)] of the kernel of interest W,

$$\overline{W}_{i\neq j} \overset{(3.25)}{=} W_{ji} \neq \frac{P_{z,j}}{P_{z,i}} W_{ji} \overset{(2.46)}{=} W^{\leftarrow}_{ij}, \tag{3.31}$$

except at the special point at which $P_{z,i} = P_{z,j}$. Thus, fermionic duality is indeed inequivalent to time *reversal*, and can therefore be combined with detailed balance. To achieve the latter, one uses

$$P_{z,i}\overline{P}_{z,i} \overset{(3.30)}{=} \frac{W_{ij}}{W_{ji}} \cdot \frac{\overline{W}_{ij}}{\overline{W}_{ji}} P_{z,j}\overline{P}_{z,j} \overset{(3.25)}{=} P_{z,j}\overline{P}_{z,j} \tag{3.32}$$

for any two states $i \neq j$ connected by finite transition rates $W_{ij}, \overline{W}_{ij}$. As paper V argues in detail, this eventually leads to

$$z_\mathrm{i} = \frac{1}{C} \cdot z^{-1} \quad , \quad \overline{P}_{z,j} = \frac{1}{C} \cdot \frac{1}{P_{z,j}} \quad , \quad C = \sum_j \frac{1}{P_{z,j}}, \tag{3.33}$$

i.e., the dual stationary density operator z_i is proportional to the *operator inverse* [1] of the stationary operator z.

[1] This inverse is guaranteed to exist by positive recurrence and the resulting positivity of all probabilities $P_{z,j} > 0$, see Sec. 2.4.2.

Relation (3.33) has both fundamental and practically relevant consequences. First, we note that it implies the orthogonality relation

$$(z_{\mathrm{i}}(-\mathbb{1})^N|A\cdot z) \overset{(3.33)}{=} \frac{1}{C}((-\mathbb{1})^N|A) = 0 \tag{3.34}$$

for any operator A that is orthogonal to the parity operator, $(A|(-\mathbb{1})^N) = 0$. As such, Eq. (3.34) is a very compact form of expressing the consequences of both the fermionic duality and detailed balance. For the quantum dot systems of interest in the appended papers, (3.34) applies to the important case of A being the total particle number operator N. This enables paper IV to heavily exploit equation (3.34) in order to calculate linear-response coefficients for the single-level quantum dot [Sec. (2.1.1)]. Section 3.5 furthermore shows that (3.34) simplifies the application of duality in the case of energy-dependent bare couplings $\Gamma(E)$ in paper V, as it guarantees the orthogonality of duality-induced basis vectors constructed according to Sec. 3.2.4.

Another consequence of Eq. (3.33) that is derived in paper V is that for a rate matrix describing transitions in a system of d local energy eigenstates $|E_j)$, the overlap of the stationary state $|z)$ and its dual $|z_{\mathrm{i}})$ is bounded by

$$0 < (z_{\mathrm{i}}|z) = \sum_j^d \overline{P}_{z,j}P_{z,j} \leq \frac{1}{d}. \tag{3.35}$$

For the weakly-coupled single-level quantum dot with $d = 4$ many-body states [Sec. (2.1.2)], paper IV uses the orthogonality (3.34) to show that the *linear* thermal conductance [Sec. (2.5)] – introduced in Sec. 1.3.1 and Sec. 3.2.3 as the heat current in the absence of a net particle current – is proportional to $(z_{\mathrm{i}}|z)$ at global equilibrium conditions [Eq. (2.48)]. This thermal conductance is thus also bounded from above by Eq. (3.35) yielding $1/d \to 1/4$.

To conclude this subsection from a more fundamental point of view, we note that $\overline{P}_{z,j} \sim 1/P_{z,j}$ rigorously confirms our statement from Sec. 3.2.3 that if detailed balance (3.30) holds, $|z_{\mathrm{i}})$ is the most unstable or, rather, rarest state. Namely, as pointed out in Sec. 2.4.2 for a recurrent Markov process, Kac's lemma [182] dictates that the inverse probability $1/P_{z,j}$ quantifies the mean stationary *recurrence time* of the energy eigenstate $|E_j)$ in the mixture $|z)$. The state with the least chance of recurring has the largest $1/P_j$, and hence the highest probability in the mixed *dual* stationary state $|z_{\mathrm{i}})$ according to Eq. (3.33). Finally, we stress that while we here only consider the rate-equation limit, extensions to the quantum coherent regime have been developed both for detailed balance [209, 210] and for Kac's lemma [211]. Future studies may thus potentially be able to combine these extensions with fermionic duality to derive relations analogous to (3.33) for density operators z with non-vanishing off-diagonals in the energy eigenbasis.

3.4.2 Duality and magnetic fields

Let us use this last subsection to address two examples in which the appended papers and related works exploit duality in the explicit absence of time-reversal symmetry and detailed balance.

Local magnetic field in quantum dot

Paper III uses the fermionic duality to study the decay behavior of the single-level quantum dot with a local spin-splitting magnetic field B, breaking the time-reversal symmetry of the underlying Hamiltonian (2.9). As argued in Sec. 2.4.3, this system also explicitly breaks detailed balance (3.30) in the presence of a finite Coulomb interaction strength $U > 0$ and several coupled reservoirs at different potentials μ_α. Nevertheless, given the experimentally most relevant case of two reservoirs L,R, paper III proves that the system exhibits an additional symmetry relation that follows by combining the fermionic duality (3.4) with another duality due to Iche, see Refs. [198, 212, 213]. It states that the Born-Markov limit decay rates (2.37) are symmetric under *swapping* the magnetic $B/2$ with the centered level-position $\tilde{\epsilon} = \epsilon - \mu + U/2$ in the parameter dependence, where $\mu = (\mu_\mathrm{L} + \mu_\mathrm{R})/2$ is the average potential:

$$\gamma_{1/2}(\tilde{\epsilon}, B/2) = \gamma_{1/2}(B/2, \tilde{\epsilon}) \tag{3.36}$$

for the two charge- and spin-related rates $\gamma_{1/2}$ next to the energy-independent parity rate $\gamma_p = \Gamma$ [Eq. (3.9)]. There are two main implications of Eq. (3.36). On the one hand, assuming that applying local magnetic fields on the order $B \sim U$ is experimentally possible, testing the validity of (3.36) would also be a test of the fermionic duality, since the latter is essential for Eq. (3.36) to hold. On the other hand, assuming that duality *does* hold, it allows to infer the behavior of the decay rates at large, potentially difficult to control magnetic fields B and small $\tilde{\epsilon}$ from the behavior at small B and large $\tilde{\epsilon}$. Crucially, the latter situation might be more straightforward to technically realize.

Non-collinear environment fields

Apart from the case of a *local* magnetic field inducing a spin-splitting in the quantum dot, Ref. [184] applies the fermionic duality (3.4) to investigate spin-precession in a locally spin-degenerate level, but with non-collinear magnetic fields in weakly tunnel-coupled *reservoirs* [214–221]. Importantly, the dissipative kernel W of this system couples probabilities to coherences – quantifying the spin-precession – even though the local coherent dynamics generated by the Liouvillian $L\bullet = [H, \bullet]$ are irrelevant due to the local spin-degeneracy in H.

As one simple yet important result, reference [184] explicitly verifies the fermionic duality (3.4) to hold in case the dynamics cannot be fully described in the rate-equation limit [Sec. (2.4.1)].

More precisely, as previously pointed out in Refs. [215, 218], the stationary state $|z)$ is equal to the case without magnetic fields in the leads, and hence fully incoherent, i.e., it has no off-diagonal elements in the energy eigenbasis. The additional insight provided by duality and, in particular, Eq. (3.14) is that this also dictates $(z_{\mathrm{i}}(-\mathbb{1})^N|$ to be a fully incoherent left eigenvector. The dynamics of probabilities and coherences – the latter representing the x and y direction of the average dot spin if z is the chosen quantization axis – are therefore only coupled via the single amplitude $(c'| = (N| - (N|z)(\mathbb{1}|$, given by the charge deviation from the stationary limit, and the corresponding mode $|c) = (-\mathbb{1})^N \left[|N) - (N|z_{\mathrm{i}})|\mathbb{1})\right]/2$; in the absence of non-collinear reservoir fields, these vectors are exact eigenvectors of W, see Eq. (2.42). In the same way as pointed out in Sec. 3.2.1, the duality thereby immediately – and without any explicit calculations – reduces the complexity of the problem in case one is interested in the coherent dynamics. In future investigations, this can be relevant when, e.g., extending the Liouville-space linear response formalism introduced in Sec. 2.5 to study the effect of coherences on the thermoelectric response.

3.5 Duality for energy-dependent couplings

This final part of chapter 3 summarizes how paper V extends the fermionic duality formalism developed and explored in papers II-IV to weakly-coupled, Markovian systems with explicitly energy-dependent bare couplings $\Gamma_{m,ll'}(E)$. This energy-dependence is precisely defined below Eq. (2.8) in Sec. 2.1, and illustrated for the single-level quantum dot [Sec. (2.1.1)] in Fig. 3.3. With the main message being that most insights of duality presented in the previous sections remain valid on a physically intuitive level, we here give a quick quantitative overview over the main similarities and differences to the wideband limit which paper V points out in detail. The central idea is again to eventually establish a duality-based analysis of the kernel W which makes it easier to expose the physical effects introduced by energy-dependent tunnel barriers.

3.5.1 Extended duality

Let us start right away by writing down the extension of the fermionic duality (3.4) to energy-dependent bare couplings. Following paper V and its appendix, we find that

$$W + \mathcal{P}\overline{W}^{\dagger}\mathcal{P} = -\mathbb{\Gamma} \quad , \quad \overline{W} = W(-H, -H_{\mathrm{R}}, \rho_0^{\mathrm{R}}(-H_{\mathrm{R}}, \{-\mu_\alpha\})). \tag{3.37}$$

and analogously,

$$W_\alpha + \mathcal{P}\overline{W}_\alpha^{\dagger}\mathcal{P} = -\mathbb{\Gamma}_\alpha \quad , \quad \overline{W}_\alpha = W(-H, -H_\alpha, \rho_{0,\alpha}^{\mathrm{R}}(-H_\alpha, -\mu_\alpha)) \tag{3.38}$$

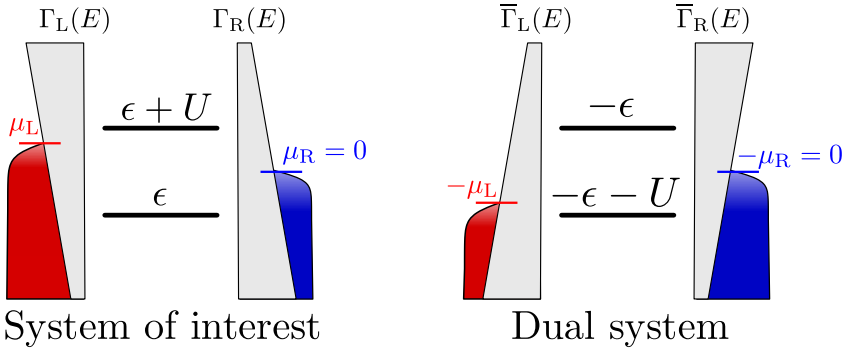

Figure 3.3: *Illustration of energy-dependent tunnel coupling for the simple example of the interacting spin-degenerate single-level quantum dot discussed in Sec. 2.1.1 with two attached reservoirs. The barrier thickness represents the transparency quantified by the energy-profiles* $\Gamma_{\alpha=L,R}(E)$*. The left panel shows the system of interest, the right panel the corresponding energy-inverted dual model. Note that since the* $\Gamma_{\alpha=L,R}(E)$ *are evaluated at the original transition energies* $+\epsilon, +\epsilon + U$ *in the dual kernel* $\overline{W}$ *[Eq. (3.37)], the dual barrier profiles* $\overline{\Gamma}_{\alpha=L,R}(E)$ *are effectively inverted as well.*

for the reservoir-resolved kernel W_α [Eq. (2.34)], where $\mathbb{\Gamma} = \sum_\alpha \mathbb{\Gamma}_\alpha$.

There are two important differences to the wideband limit duality (3.4) that we need to address in the following. First, we note that the right-hand side of Eq. (3.37) is not simply a shift by the lump sum of diagonal couplings (3.2), but instead by the *coupling superoperator* $\mathbb{\Gamma}$ of which the explicit expression can be found in paper V. This superoperator generally depends on all parameters in the *total* Hamiltonian $H_{\rm tot}$, but it is independent of the *reservoir state* $\rho^{\rm R}$, and thus, in particular, of the environment potentials μ_α and temperatures T_α. In fact, $\mathbb{\Gamma}$ has a number of both insightful and convenient properties, as pointed out in subsection 3.5.3. This indicates that the duality (3.37) is not just a trivial rewriting of the superoperator W in terms of two other superoperators $\overline{W}$ and $\mathbb{\Gamma}$, but indeed a symmetry relation that is similarly useful as in the wideband limit. Namely, apart from $\mathbb{\Gamma}$ being an operator, the duality (3.37) has the same *form* as in the wideband limit. This means that many insights following from duality according to sections 3.2.1 to 3.4 generalize by simply substituting $\Gamma \to \mathbb{\Gamma}$.

However, before we turn to this, we note the second difference to the wideband limit, which is that the dual kernel $\overline{W}$ as defined above [1] now explicitly involves the energy inversion of the environment Hamiltonian $H_{\rm R}$, both in the dynamics and in the initial reservoir state $\rho_0^{\rm R}$. Since this point is crucial for understanding how exactly the duality extends to energy-dependent bare couplings, let us address this first in the now following subsection 3.5.2. Details of this full energy inversion are also given in App. E.

[1] In paper V, the energy inversion in the bath is kept mostly implicit, and only briefly discussed in the appendix.

3.5.2 Including energy-dependent tunnel barriers

Section 3.3.1 has related duality to the simple property $-\Gamma\left[f(E_{ij})+f(-E_{ij})\right]=-\Gamma$ of the Fermi function evaluated at some difference $E_{ij}=E_i-E_j$ between many-body energies E_i of the open-system Hamiltonian H. Clearly, when introducing an energy-dependence to $\Gamma\to\Gamma(E)$, the same energy inversion does not work anymore, since $-\Gamma(E_{ij})f(E_{ij})-\Gamma(-E_{ij})f(-E_{ij})\neq-\Gamma(\pm E_{ij})$. It obviously would work, however, if the energy was not inverted inside the bare coupling $\Gamma(E)$. Paper V discusses how to fix this in the dual kernel $\overline{W}$. Namely, one takes the definition (2.8) of the bare couplings $\Gamma(E)$ and realizes that any sign inversion $E\to-E$ can be compensated by an additional sign inversion of all reservoir energies ϵ_m, and thus by $H_{\rm R}\to-H_{\rm R}$, using the symmetry of the delta function $\delta(x)=\delta(-x)$. The inversion in the initial reservoir state $\rho_0^{\rm R}(-H_{\rm R},\{-\mu_\alpha\})$ then ensures that the sign of E in the Fermi function $f(E)$ is not affected by the opposite sign in $H_{\rm R}$. Thus, in practice, all this boils down to the simple rule that $\overline{W}$ is constructed as for energy-independent couplings, except that all $\Gamma_{m,ll'}(E)$ are evaluated at the *original* many-body open-system transition energies $+E_{ij}=E_i-E_j$ in the final expression. Or in other words, one effectively inverts the energy-profile of the tunnel barrier, as illustrated in Fig. 3.3.

What remains as a complication is, nevertheless, that the couplings $\Gamma_{m,ll'}(E_{ij})$ between *single-particle states* $|\mathbf{k}m\rangle$ in the reservoirs, and $|l\rangle,|l'\rangle$ in the open system, do not only depend on the energy of these single-particle states. For instance considering the rate equation of the spin-degenerate single-level quantum dot with one, weakly-coupled reservoir at $\mu\equiv0$, the sum

$$W_{i\neq j}+\overline{W}_{i\neq j}=-\Gamma(E_{ij}) \tag{3.39}$$

still differs for the two different many-body state transitions $2\leftarrow1\neq1\leftarrow0$, even if the associated tunneling process involves the same single-particle states (e.g., tunneling into the spin-up orbital of the dot) in both cases. This is the essential difference to the wideband limit, and ultimately the reason why the lump sum of couplings Γ [Eq. (3.2)] in the wideband duality (3.4) becomes the coupling superoperator $\mathbb{\Gamma}$ in the duality (3.37) for energy-dependent couplings. Understanding the latter case thus means understanding the operator $\mathbb{\Gamma}$, which is precisely what we go about now.

3.5.3 Properties of the coupling superoperator

Paper V provides an explicit expression and a detailed analysis of the coupling superoperator $\mathbb{\Gamma}$ for the general class of fermionic open systems defined in Sec. 2.1. Here, we focus on highlighting its main properties and their physical implications, for which the only relevant technical ingredients are that $\mathbb{\Gamma}$ commutes with the parity due to fermion-parity superselection [Sec. (3.3.2)], $[\mathbb{\Gamma},\mathcal{P}]=0$, and that the real part $\mathrm{Re}\left[\mathbb{\Gamma}\right]=(\mathbb{\Gamma}+\mathbb{\Gamma}^\dagger)/2$ is positive semidefinite, $\mathrm{Re}\left[\mathbb{\Gamma}\right]\geq0$.

Upper bound on decay rates

Given that for energy-independent couplings, Eq. (3.10) sets Γ as an upper bound on the decay rates γ_x [Eq. (2.37)] of the system, one expects $\mathbb{\Gamma}$ to play an analogous role. Indeed, assuming dissipativity (2.36) to hold for both for W and $\overline{W}$, paper V derives in analogy to Eq. (3.10) that the rates are bounded from above by the largest eigenvalue of the positive semidefinite operator $\mathrm{Re}\,[\mathbb{\Gamma}]$:

$$0 \leq \gamma_x \leq \max\left\{\mathrm{spec}\left(\mathrm{Re}\,[\mathbb{\Gamma}]\right)\right\}. \tag{3.40}$$

Crucially, paper V shows that $\mathrm{Re}\,[\mathbb{\Gamma}]$ can be evaluated analytically without explicit knowledge of the precise energy-dependence $\Gamma_{m,ll'}(E)$, since the typically appearing integrals over the energy E cancel out when taking the Hermitian real part $\mathrm{Re}\,[x] = (x + x^\dagger)/2$. Together with the very fact that $\mathrm{Re}\,[\mathbb{\Gamma}]$ is Hermitian, this makes it much easier to determine the eigenvalues of the latter compared to finding the eigenvalues of the full kernel W. However, unlike in the wideband limit, the obtained bound (3.40) is not necessarily tight. This will become clearer in Sec. 3.5.4, once we discuss what happens to the parity mode $|(-\mathbb{1})^N)$ [Eq. (3.9)] and its amplitude covector $(z_\mathrm{i}(-\mathbb{1})^N|$ [Eq. (3.14)].

Rate equation limit

In the rate-equation limit [Sec. (2.4.1)], which is the relevant regime for the application of duality (3.37) to the single-level quantum dot in paper V, the coupling superoperator $\mathbb{\Gamma}$ assumes a particularly convenient form. As the paper derives in more detail, the duality (3.37) in combination with $\mathbb{\Gamma} = \mathcal{P}\mathbb{\Gamma}\mathcal{P}$ dictates $\mathbb{\Gamma}$ to be Hermitian ($\mathbb{\Gamma} = \mathrm{Re}\,[\mathbb{\Gamma}]$) and *diagonal* in the energy eigenbasis:

$$(E_i|\mathbb{\Gamma}|E_j) = \delta_{ij}(E_i|\mathrm{Re}\,[\mathbb{\Gamma}]\,|E_i). \tag{3.41}$$

This implies that for all *off-diagonal* elements W_{ij}, the duality can still formally be translated to wideband limit result (3.25) when accounting for the adjustments to the dual transform pointed out in Sec. 3.5.2. The key consequence is that all relations and insights obtained in Sec. 3.4.1 by combining the wideband duality with *detailed balance* are still perfectly valid. This includes in particular the interpretation of the dual stationary state $|z_\mathrm{i}) = |\overline{z})$ as the least recurring state, and the nontrivial orthogonality relation (3.34) – both essential for the duality-based analysis in paper V. To understand this in more detail, the now following subsections return to the question how the duality (3.37) helps in analyzing the effect of energy-dependent bare couplings on the modes and amplitudes of the kernel W.

3.5.4 Link between modes and amplitudes

In analogy to Sec. 3.1.2, we can apply the duality (3.37) to any left eigenvector $(x'|$ or right eigenvector $|x')$ of W to the eigenvalue λ_x, and obtain the generalized

dual link

$$\begin{aligned}(x'|W = \lambda_x(x'| \Rightarrow W|y) = [-\lambda_y - \mathbb{\Gamma}]\,|y) \quad &, \quad |y) = \mathcal{P}|\overline{x}'),\\ W|x) = \lambda_x|x) \Rightarrow (y'|W = (y'|\,[-\lambda_y - \mathbb{\Gamma}] \quad &, \quad (y'| = (\overline{x}|\mathcal{P}\\ \lambda_y = \overline{\lambda}_x^*.&\end{aligned} \tag{3.42}$$

Unlike in the wideband limit (3.6), this is not a direct relation between left and right eigenvectors. However, given that $\mathbb{\Gamma}$ is, according to Sec. 3.5.3, easier to deal with analytically compared to W, Eq. (3.42) still maps each eigenvector to another vector that behaves "simpler" under application of the kernel W.

To better illustrate the usefulness of (3.42), let us proceed as in sections 3.2.1 and 3.2.2, and apply the duality to the zero eigenvectors $(\mathbb{1}|$ and $|z)$ of the kernel W. This gives

$$W|(-\mathbb{1})^N) = -\mathbb{\Gamma}|(-\mathbb{1})^N) \quad , \quad (z_{\rm i}(-\mathbb{1})^N|W = -(z_{\rm i}(-\mathbb{1})^N|\mathbb{\Gamma}, \tag{3.43}$$

and the orthogonalities

$$\begin{aligned}0 = (\mathbb{1}|W|(-\mathbb{1})^N) &\overset{(3.43)}{=} (\mathbb{1}|\mathbb{\Gamma}|(-\mathbb{1})^N)\\ 0 = (z_{\rm i}(-\mathbb{1})^N|W|z) &\overset{(3.43)}{=} (z_{\rm i}(-\mathbb{1})^N|\mathbb{\Gamma}|z).\end{aligned} \tag{3.44}$$

Thus, while not immediately yielding new eigenvectors for W, these relations still help in evaluating any matrix element

$$(x'|W|(-\mathbb{1})^N) = -(x'|\mathbb{\Gamma}|(-\mathbb{1})^N) \text{ and } (z_{\rm i}(-\mathbb{1})^N|W|x) = -(z_{\rm i}(-\mathbb{1})^N|\mathbb{\Gamma}|x), \tag{3.45}$$

that is, involving either the fermion parity $|(-\mathbb{1})^N)$ or the covector $(z_{\rm i}(-\mathbb{1})^N|$ including the dual stationary state. The crucial point is that we may use all simplifying properties of $\mathbb{\Gamma}$ pointed out in the previous Sec. 3.5.3, including its diagonal form (3.41) in the rate-equation limit. This suggests that it is still advantageous – if possible – to expand W in a left and right basis containing $(\mathbb{1}|, (z_{\rm i}(-\mathbb{1})^N|$ as well as $|z), |(-\mathbb{1})^N)$. Let us detail this in several steps.

3.5.5 Dual stationary state and generalized parity rate

One benefit of expanding W in a basis including the covector $(z_{\rm i}(-\mathbb{1})^N|$ is that we may again rely on our physical intuition about the dual stationary state $|z_{\rm i})$, as illustrated in Sec. 3.2.3. Given a system with strong repulsive Coulomb interaction $|U| \gg T, B, V, \ldots$ – such as the quantum dot system in paper V – the resulting strong attraction and pairing in the dual system may often cause the probability distribution in the mixed state $|z_{\rm i})$ to be peaked around a pure energy eigenstate $|E_i)$. If this holds in the rate-equation limit, plugging the diagonal form (3.41)

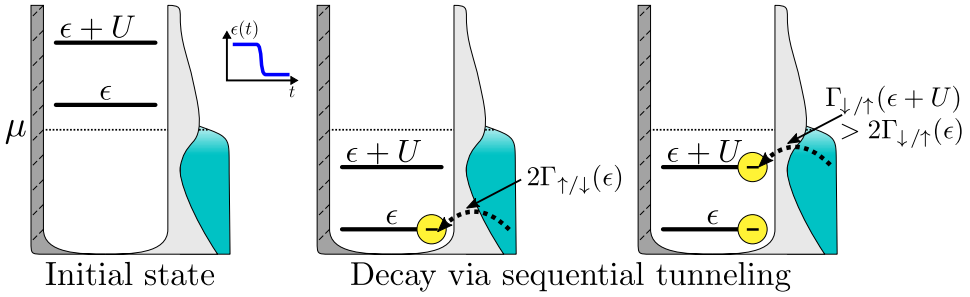

Figure 3.4: *Time-dependent decay of a spin-degenerate single-level quantum dot [Sec. (2.1.1)], subject to a sudden shift of its level-position ϵ which induces electron tunneling from a single, weakly coupled electronic reservoir. The energy-dependence of the tunnel barrier – visually indicated by its thickness – causes the first of two sequential tunneling processes, either by a spin up or down, to take place at the slower rate $\Gamma_\uparrow(\epsilon) + \Gamma_\downarrow(\epsilon) = 2\Gamma_{\uparrow/\downarrow}(\epsilon)$ compared to the rate $\Gamma_{\uparrow/\downarrow}(\epsilon + U) > 2\Gamma_{\uparrow/\downarrow}(\epsilon)$ of the second process by a fixed spin down or up. This is in contrast to energy-independent tunneling rates, in which the degeneracy factor 2 due to the fact that either a spin up or spin down can enter always makes the first rate larger than the second.*

of $\mathbb{\Gamma}$ into Eq. (3.43) enables us to infer that $(z_\mathrm{i}(-\mathbb{1})^N|$ is still an approximate left eigenvector of W:

$$(z_\mathrm{i}(-\mathbb{1})^N|W \overset{(3.43)}{=} -(z_\mathrm{i}(-\mathbb{1})^N|\mathbb{\Gamma} \overset{(3.41)}{\approx} -(E_i|\mathbb{\Gamma}|E_i) \cdot (z_\mathrm{i}(-\mathbb{1})^N|. \tag{3.46}$$

If this is true, at least one of the diagonal elements of $\mathbb{\Gamma}$ also yields an approximate decay rate $\tilde{\gamma}_p$ of the system. According to Sec. 3.5.2, this rate is independent of all μ_α and T_α, and only *implicitly* depends on the system parameters via the couplings $\Gamma_{m,ll'}(E)$. If the open-system dynamics H conserve the occupation N_l of each open-system single-particle state $|l\rangle$, $[H, N_l] = 0$ as true for the systems in the appended papers, the explicit expressions of these diagonal elements read

$$(E_i|\mathbb{\Gamma}|E_i) \to \sum_{ml,j} \Gamma_{m,ll}(E_{ij}) \left|(E_i|E_j^{+l})\right|^2 + \Gamma_{m,ll}(E_{ji}) \left|(E_i|E_j^{-l})\right|^2, \tag{3.47}$$

with $|E_i^{+l}) = d_l^\dagger|E_i\rangle\langle E_i|d_l$ and $|E_i^{-l}) = d_l|E_i\rangle\langle E_i|d_l^\dagger$. Assuming furthermore that $(z_\mathrm{i}(-\mathbb{1})^N|$ is indeed part of a biorthogonal basis including the stationary state $|z)$ and the parity vector $|(-\mathbb{1})^N)$ as right vectors – which may not be possible due to a technical, yet important subtlety discussed in Sec. 3.5.6 – we can again separate

$$|\rho(t)) \overset{(2.32)}{=} \exp(Wt)\,|\rho_0) \approx (z_\mathrm{i}(-\mathbb{1})^N|\rho_0) \cdot e^{-\tilde{\gamma}_p t}|(-\mathbb{1})^N) + |\rho^\mathrm{rest}(t)). \tag{3.48}$$

as in Eq. (3.11), with $|\rho^\mathrm{rest})$ being orthogonal to $|(-\mathbb{1})^N)$. This results in

$$(z_\mathrm{i}(-\mathbb{1})^N|\rho(t)) \approx (z_\mathrm{i}|\rho(t)) \overset{(3.48)}{\approx} (z_\mathrm{i}|\rho_0) \cdot e^{-\tilde{\gamma}_p t}, \tag{3.49}$$

as in Eq. (3.20). This together with Eq. (3.47) indicates that $\tilde{\gamma}_p$ represents a straightforward generalization of the parity rate γ_p [Eq. (3.9)] as the lump sum (3.2) of diagonal wideband couplings $\Gamma_{m,ll}$: each coupling in (3.47) is evaluated at precisely the energy which the particle carries during a tunneling process after which the system ends up in the many-body state $|E_i)$.

In particular, for the reasons previously pointed out in Sec. 3.2.3, the monotonous decay behavior expressed in Eqs. (3.48) and (3.49) again suggest that $\tilde{\gamma}_p$ governs the decay of a *most unstable* initial configuration $|\rho_0) = |z_\mathrm{i})$ in which every single-particle state occupation is destabilized with respect to the stationary limit. And indeed, this is exactly what paper V finds for the concrete case of the single-level quantum dot [Sec. (2.1.1)].

Finally coming back to the generalized upper bound (3.40) on the decay rates, the above findings prompt the question whether $\tilde{\gamma}_p$ is in fact equal to this upper bound, just as the wideband parity rate $\gamma_p = \Gamma$ yields the upper bound (3.10) in the wideband limit. The answer to this question is, however, a clear "no". Figure 3.4 illustrates this with the simple example of two particles sequentially tunneling into an initially empty single-level quantum dot that in the stationary limit assumes double occupation, $|z) = |2)$. The initial, most unstable configuration $|\rho_0) = |z_\mathrm{i}) = |0)$ decays at a rate $\tilde{\gamma}_p \to \Gamma_\uparrow(\epsilon)+\Gamma_\downarrow(\epsilon) = 2\Gamma_\uparrow(\epsilon) = 2\Gamma_\downarrow(\epsilon) \equiv 2\Gamma_{\uparrow/\downarrow}(\epsilon)$, with the factor 2 expressing that either a spin-up or spin-down particle can tunnel in. However, despite the fact that with one spin-state filled, the second process happens at a rate $1 \cdot \Gamma_{\uparrow/\downarrow}(\epsilon + U)$, this rate could in principle still be higher than $2\Gamma_{\uparrow/\downarrow}(\epsilon)$ if the transparency of the tunnel barrier increases accordingly between ϵ and $\epsilon + U$. In other words, a main effect of energy-dependent couplings in *combination* with many-body interactions is that they may interfere with the direct increase of the decay rates with the amount of destabilized single-particle state occupations in the decaying open-system configuration $|\rho)$. Interestingly, this combined effect of energy-dependent tunneling and interaction is in essence also what Refs. [97, 104, 105, 107, 108] exploit under stationary conditions to conceive and/or realize energy harvesters and refrigerators, as pointed out in Sec. 1.3.2.

3.5.6 Basis expansion guided by duality

Equipped with the insights from the previous section 3.5.5, it seems logical to again try to *systematically* benefit from the duality (3.37) by establishing a basis expansion for the kernel W according to Sec. 3.2.4. However, one problem is that even if the eigenvector property (3.46) of $(z_\mathrm{i}(-\mathbb{1})^N|$ is a good approximation, $(z_\mathrm{i}(-\mathbb{1})^N|$ is neither an *exact* eigenvector of W, nor has it the same *explicit* expression as a function of the system parameters as in the wideband limit, since both $|z)$ and $|z_\mathrm{i})$ depend on the $\Gamma(E)$ if the coupled reservoirs are voltage- or temperature biased. As a result, $(z_\mathrm{i}(-\mathbb{1})^N|$ alone is not strictly guaranteed to be orthogonal to $|z)$, and as such, cannot be part of a *biorthogonal* basis including

$|z)$ as a right vector [1].

To fix this issue, one must in principle enforce orthogonality by redefining $(z_\mathrm{i}(-\mathbb{1})^N| \to (z_\mathrm{i}(-\mathbb{1})^N| - (z_\mathrm{i}(-\mathbb{1})^N|z)(\mathbb{1}|$. In paper V, this is, however, not necessary, since the studied single-level quantum dot always – even for energy-dependent bare couplings and in a global non-equilibrium – fulfills local detailed balance (2.45), as argued in Sec. 2.4.3. We can therefore simply use the orthogonality relation (3.34) for the operator $A = \mathbb{1}$ to infer $(z_\mathrm{i}(-\mathbb{1})^N|z) = 0$. More generally, we note that the correction term $(z_\mathrm{i}(-\mathbb{1})^N|z)(\mathbb{1}|$ is irrelevant whenever one is interested in matrix elements $(z_\mathrm{i}(-\mathbb{1})^N|W|x)$ of the kernel, since $(\mathbb{1}|W = 0$. For other superoperators, one may still try to simply approximate $(z_\mathrm{i}(-\mathbb{1})^N|z) \approx 0$ if Eq. (3.46) holds well enough, but the quality of this approximation has not been investigated yet.

Nevertheless, once the basis including $(z_\mathrm{i}(-\mathbb{1})^N|$ is established, we do not only profit from everything we have learned about the wideband and non-wideband duality in sections 3.2,3.4 and 3.5.5. In fact, one can also straightforwardly isolate nontrivial differences between wideband and non-wideband couplings, thereby highlighting the physical effects of the latter. Namely, any non-zero off-diagonal kernel matrix elements of the type (3.45) must originate from energy-dependent bare couplings $\Gamma(E)$. This insight is heavily exploited in paper V, and follows by the fact that $|(-\mathbb{1})^N), (z_\mathrm{i}(-\mathbb{1})^N|$ are continuously connected to their wideband limit in which they become exact eigenvectors. It allows us to concisely parameterize the full dissipative kernel W of the single-level quantum dot [Sec. (2.1.1)], including several arbitrarily bias reservoirs, in terms of only the two bare couplings $\Gamma(\epsilon), \Gamma(\epsilon + U)$, and the two intuitively understandable average occupation numbers $n_z = (N|z), n_\mathrm{i} = (N|z_\mathrm{i})$. Such a drastic simplification improves the analytical accessibility of both the time-dependent decay and the stationary transport considerably compared to a traditional "Fermi's Golden rule" approach; it thereby allows paper V to readily identify nontrivial effects of energy-dependent tunnel barriers.

3.6 Summary

Chapter 3 has provided an extensive overview, background and additional information about the fermionic duality and how the appended papers make use of it. In summarizing terms, Sec. 3.1 has defined the duality as a symmetry relation for the kernel W generating the dissipative, tunneling induced dynamics in the master equation for the reduced density operator $\rho(t)$ of open fermionic quantum systems as defined in Sec. 2.1. In the Markovian, weak-coupling limit [Sec. (2.3)] and for energy-independent tunneling constants $\Gamma_{m,ll'}$ [Eq. (2.8)], this symmetry assumes

[1] Note by contrast that even though $|(-\mathbb{1})^N)$ is always far from being an exact eigenvector for energy-dependent couplings [Eq. (3.43)], there is no issue with orthogonality due to the tracelessness of $(-\mathbb{1})^N$ or any subparity, see appendix to Lic. Th. [110].

the particularly useful form (3.4), representing the generalized hermiticity relation $W + \mathcal{P}\overline{W}^{\dagger}\mathcal{P} = -\Gamma$. It thereby links – both mathematically and physically – right and left eigenvectors of the non-Hermitian kernel W, denoted as modes and amplitude covectors.

Section 3.2 has explored the main results which can be derived from duality. These are, first and foremost, the existence of the fermion-parity mode $|(-\mathbb{1})^N)$ corresponding to the parity decay rate $\gamma_p = \Gamma$ given by the lump sum of diagonal couplings (3.2), and the associated amplitude covector $(z_\mathrm{i}(-\mathbb{1})^N|$. The latter contains the stationary state $|z_\mathrm{i})$ of the *dual* kernel $\overline{W}$. This kernel represents a system in which all reservoir potentials μ_α, and the local open-system Hamiltonian H including all many-body interaction energies come with opposite sign. We have argued why the dual state $|z_\mathrm{i})$ can – in particular under local detailed balance (2.45) – be understood as the most unstable for a given kernel W. From a more practical point of view, we have moreover shown how especially the effect of inverted interactions in $|z_\mathrm{i})$ explains otherwise surprising features in the decay- and transport behavior of the quantum dot systems considered in the appended papers. Section 3.2 has then closed by proposing how to systematically extend this duality-based analysis to open systems larger than those quantum dot setups.

The symmetries underlying the fermionic duality (3.4) have been elucidated in section 3.3. In essence, we have traced its origin back to the interplay between two fundamental principles of fermionic (open) systems: first, *fermion-parity superselection*, forbidding any pure energy eigenstates which are superpositions of states with even and odd fermion parity $(-\mathbb{1})^N$. Second, *Pauli's principle*, leading both to Fermi Dirac statistics in the environment as well as to a finite Liouville space for a finite set of single-particle states defining the open system.

The implications of duality in conjunction with (non-)symmetric behavior under time-*reversal* have been explored in Sec. 3.4. We have shown how detailed balance (2.45) rigorously identifies the dual stationary state $|z_\mathrm{i})$ as the *least recurrent* state, and furthermore dictates the orthogonality relation (3.34) which is the key for papers IV,V to combine time-reversal symmetry with the fermionic duality. Moreover, we have pointed out that even in the presence of time-reversal symmetry breaking magnetic fields, as, e.g., considered in paper III, duality remains valid, useful, and can still be combined with other symmetries and dualities such as Iche's duality [198, 212, 213] to gain further insights into the decay dynamics.

Finally, Sec. 3.5 has extended the fermionic duality to the case of energy-dependent bare couplings $\Gamma_{m,ll'}(E)$ in the Markovian, weak-coupling limit. We have found the actual relation (3.37) to formally differ only by the fact that the lump sum of wideband couplings Γ is replaced by the *coupling superoperator* $\mathbb{\Gamma}$. Unlike Γ, this superoperator does depend on local open-system energy differences, but it is still independent of the environment potentials μ_α and temperatures T_α. As intuitively expected, $\mathbb{\Gamma}$ takes over the role which Γ plays in the wideband limit, and as such, prohibits a direct link between left and right eigenvectors of

the kernel W. Nevertheless, with the central concept of the dual model and its stationary state $|z_\mathrm{i})$ still in tact, we have found most insights gained from duality in the wideband limit to still remain valid.

As a concluding remark, we note that this chapter 3 essentially finishes our effort to provide the background necessary to understand and appreciate the appended papers as such. What follows in the next chapter 4 can instead be seen as a continuation of the introductory chapter 1, tailored more towards potential future studies on and with the fermionic duality.

4 Applications of fermionic duality to experimentally relevant models

This chapter intends to demonstrate more concretely how the duality helps analyzing transport through the type of experimentally relevant quantum dots and few-level systems addressed in this thesis. The following sections refer mostly to the examples discussed in the introductory chapter 1, and points out insights we have gained from duality which can be useful in an experimental context.

4.1 Time-dependent currents and interaction

Owing to their use as high-fidelity single-electron sources, the quantum dots sketched in Fig. 1.2 and experimentally studied in, e.g., Refs. [18, 20, 68] only emit a single electron at a time, in the sense that the emitted electron is not correlated with the previous one. However, in an effort to provide on-demand sources of more complex electronic quantum states including two-particle entanglement, more recent studies have explored simultaneous *multi*-electron emission [22, 24, 222]. Such processes are thus also expected to be more susceptible to many-body interaction effects such as Coulomb repulsion, as studied by the appended articles using fermionic duality. This section highlights precisely this aspect.

4.1.1 Emission induced by gate-voltage switches

Let us start with the type of on-demand electron sources illustrated in Fig. 1.2 in Sec. 1.2.2. For simplicity, we consider a spin-degenerate single-level quantum dot that is affected by the local Coulomb repulsion in case it is occupied by two electrons [Sec. (2.1.1)]. This quantum dot is then assumed to be brought out of equilibrium with its environment by a sudden shift of the dot level ϵ, causing it to emit the occupying electrons via tunneling.

The concrete situation is sketched in Fig. 4.1. Earlier investigations in, for instance, Refs. [28, 76, 223], have shown that for weak coupling and tunnel-barrier transparencies idealized as energy-independent ($\Gamma(E) = \Gamma \ll T$), the time-dependent charge emission $I(t) \sim e^{-t/\tau_{\rm RC}}$ after the level-shift can still be understood by a single, effective RC-time $\tau_{\rm RC}$. Introduced in Eq. (2.42) of Sec. 2.3.4 as charge rate $1/\tau_{\rm RC} = \gamma_c$, this rate accounts for the fact that strong Coulomb

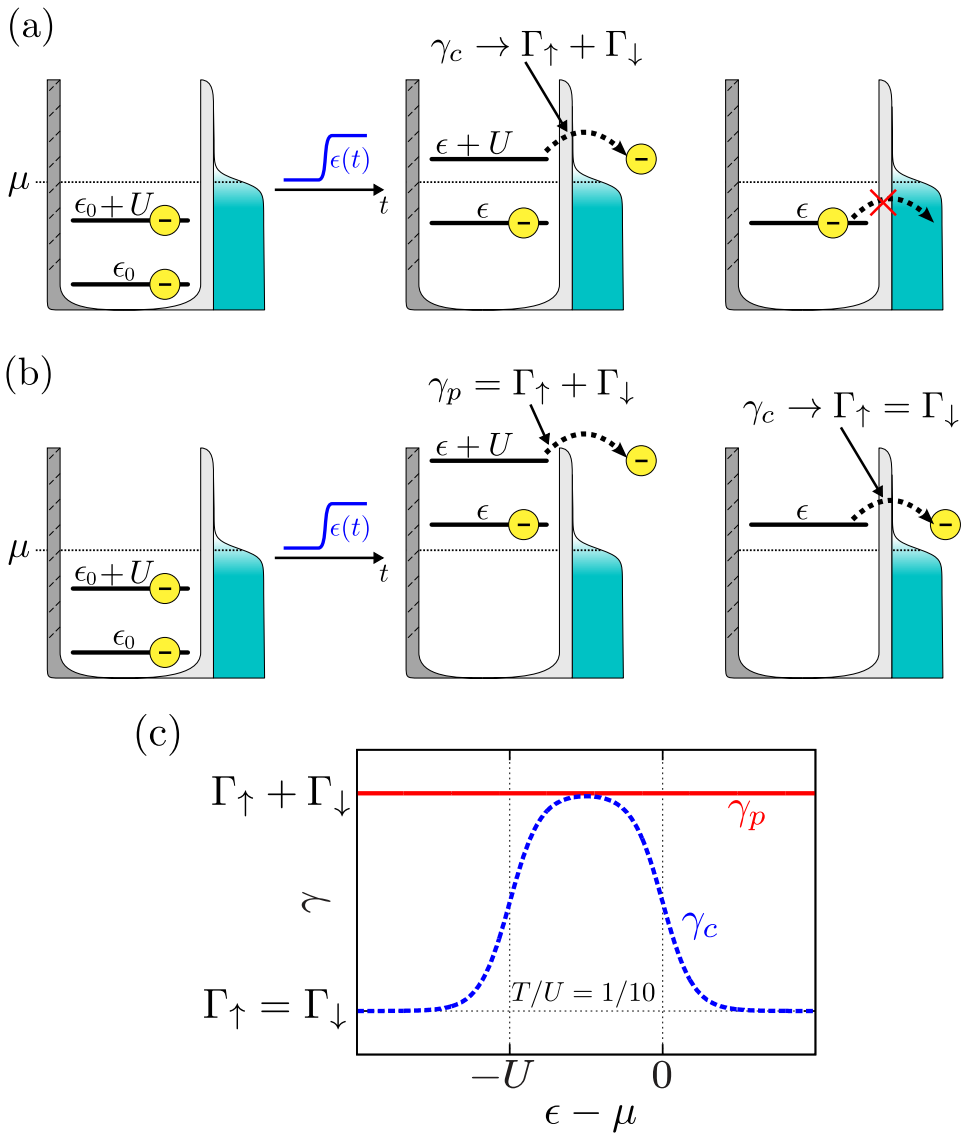

Figure 4.1: *Level-shift induced, time-dependent emission of one* ***(a)*** *or two* ***(b)*** *electrons from a spin-degenerate single-level quantum dot [Sec. (2.1.1)] (level-position ϵ) with strong local Coulomb repulsion strength U compared to the temperature T in the tunnel-coupled contact reservoir. The involved decay rates γ_c and γ_p are plotted as a function of ϵ in* ***(c)*** *and energy-independent bare couplings $\Gamma_\uparrow = \Gamma_\downarrow$ for the two possible spins (wideband limit). Following paper V, these rates represent the average effect of the last (γ_c) and first (γ_p in case of two emitted particles) tunneling transition.*

interaction in the dot leads to correlated emission. The effect can be seen by comparing Fig. 4.1(a) with Fig. 4.1(b), considering level-shifts leading to the emission of one vs. two electrons from the dot. In the first case, one electron cannot anymore be emitted when the other electron of opposite spin has previously left the dot. Since both spins are nevertheless initially unstable, the total decay rate be-

comes approximately $\gamma_c \to \Gamma_\uparrow + \Gamma_\downarrow = 2\Gamma_{\uparrow/\downarrow}$. By contrast, if the final level position ϵ allows both spins to leave the dot, their occupations $N_{\uparrow,\downarrow}$ decay independently at $\gamma_c = \Gamma_\uparrow = \Gamma_\downarrow$, and thus $N = N_\uparrow + N_\downarrow \to N_0 e^{-\Gamma_{\uparrow/\downarrow} t}$. This level-dependent behavior of γ_c is displayed by the blue curve in Fig. 4.1(c).

There are, however, two experimentally relevant aspects not captured by the above explanation. First, Sec. 1.3.2 has pointed out that the transparency of the tunnel barriers is in practice never completely independent of energy, and second, the above picture only applies to the time-dependent *charge current*, but not to the electronic *energy current*. The latter differs nontrivially from the charge current by the energy that is stored in the interaction between the emitted electrons. As such, it contains important information about, e.g., the Coulomb correlation of the emitted pair of electrons, and how to energy-selectively partition [24] this pair with the help of experimentally feasible detector barriers, see Fig. 1.3(b).

The duality-based analysis from paper II and paper V shows that while the simple picture of a single, effective RC-time in general breaks down, both energy-dependent couplings and energy currents can be accounted for in an intuitive way. Namely, one associates each involved decay rate with the average effect of a *specific emission process* in the full temporal sequence of particle emissions. Figure 4.1 illustrates that the rate γ_c more generally represents the decay due to the *last* electron emission after the voltage switch, while an additional rate describes the *first* emission whenever two particles are emitted. This additional rate is precisely the *fermion-parity* rate γ_p first found in Refs. [28, 76, 166], properly derived in paper II, and generalized to energy-dependent tunneling in paper V.

The above *temporal* association of decay rates may be guessed intuitively. However, since both our theory and typical experimental data in the end describes ensemble averages over many individual emission experiments (see lower right panel in Fig. 1.2, it is far from clear that such an intuitive connection between decay rates and tunneling transitions emerges analytically from this average picture. Duality as used in paper V not only exposes and confirms this connection; it furthermore shows it to be insensitive to the energy-dependence of the barrier transparency [1], potentially generalizable to n-particle emission processes [Sec. (3.2.4)], and, most importantly, of concrete help regarding measurements of time-dependently emitted charge and energy currents. Namely, as worked out in paper I, measuring the parity rate γ_p – and thereby confirming duality – is possible by emitting two particles and observing the dot occupation with a real-time charge detector that is only sensitive to the *first* emission. Such a detection scheme can be realized by, e.g., measuring the time-dependent charge current through a capacitively coupled radio-frequency single-electron transistor (RF-SET) [34, 65–67, 224] or a sensor quantum dot (SQD) [70, 225], with the latter considered in paper I and Sec. 2.1.2. In particular, paper I shows that the *capacitive backaction* of the SQD detector on the measured quantum dot source hardly influences the properties of the parity

[1] As long as the coupling is weak.

rate γ_p. This is because the first emitted electron is mostly affected by correlations due to *local* Coulomb interaction in the dot itself, as this interaction is expected to be stronger than the capacitive coupling between the dot and the locally separated sensor. In relative terms, the backaction effect on the rate γ_c of the final emission, during which there is no more local Coulomb interaction in the dot, is therefore stronger.

A second aspect that emerges from our understanding of the involved decay rates concerns the effect of Coulomb interaction on the time-dependently emitted *energy current*. Simply put, paper II argues that since the two emitted electrons in the situation shown in Fig. 4.1(b) obviously have the same charge, their only relevant difference in a spin-symmetric setup is the different energy due to the interaction. As such, only measuring the average time-dependent charge current $I_N(t)$ emitted from the dot is not enough to properly resolve the two emission processes. The energy current $I_E(t)$, however, can resolve these processes, as a result of the additional Coulomb charging energy. Consequently, it is not only governed by a single effective RC-time, but by the two involved decay rates, even in the idealized case of energy-independent barrier transparencies. Or in other words, *directly* exposing the properties of the parity rate γ_p – as a main manifestation of duality – without any external charge detector as in paper I requires experimentally challenging [22, 74, 109], time-resolved measurements of the energy carried by each of the two emitted particles.

4.1.2 Continuous driving

Our discussion has so far neglected that in practice, continuous modulation of the system parameters – such as the level-position $\epsilon(t)$ – at some driving frequency Ω is another useful way of operating a device next to the sudden potential *switches* considered in the previous subsection 4.1.1. This concerns, for instance, quantum dot charge pumps aimed at fast, high-accuracy emission of "hot"-electrons [20, 25, 68] – with energies far away from the Fermi Sea on the scale of the bath temperature, and with driving frequencies on the order of the typical decay rates or higher. By contrast, *adiabatic pumping* [41, 226, 227] achieves accurately quantized transfer – for, e.g., metrological purposes [43] – precisely by driving the system *slowly* compared to the decay rates. The system thereby operates in a regime in which the pumped charge per driving period becomes a *geometric/topological* quantity [64, 187, 192, 228], ensuring robustness to the precise driving frequency Ω/detailed time-dependence of the system parameters. Aware that continuous driving is not explicitly addressed by the appended papers, let us nevertheless honor its relevance for experiments and applications by emphasizing the main implications of fermionic duality for ongoing and future studies on this topic.

The first and most crucial prerequisite is that the duality still holds for continuously driven systems. In this respect, Sec. 2.6.2 emphasizes that we find this to

be true as long as the driving can be captured by a Born-Markov master equation (2.64) with a parametric time-dependence in the kernel W_t. As studied in, e.g., Ref. [188], this is a valid assumption in the adiabatic regime. For non-adiabatic hot-electron pumping [20, 25, 68], master equations have been applied, among in our own preliminary work and in, e.g., Refs. [68, 229], and have yielded reasonable agreement with the measured data. Second, we note that especially for "hot"-electron emitters [20, 25] – operating energetically far away from the Fermi Sea on the scale of the bath temperature – the tunneling times are little influenced by the environment occupation, but mostly by the energy structure of the barrier transparencies. The extension of fermionic duality to energy-dependent couplings in paper V is thus in general crucial.

Concerning more concrete applications of duality, research on the above cited, fast "hot"-electron pumps is still work in progress. However, Ref. [191] has employed fermionic duality to derive an experimentally interesting result in the *adiabatic-response* regime. Namely, one of the main practical questions of such pumps is how quickly they can be operated without losing their robustness to the driving frequency or the details of the driving protocol due to non-adiabatic corrections. Answering this question from a theoretical point of view requires to calculate such corrections, which is in principle possible. It, however, quickly becomes cumbersome and often yields unwieldy, uninformative expressions if many-body interactions are important, even for the simple, single-level quantum dot [Sec. (2.1.1)]. For such an interacting quantum dot, Ref. [191] has exploited duality, and in particular properties of the parity mode described in Sec. 3.2.1, to derive a concise and insightful expansion in non-adiabatic corrections up to any order in the driving frequency Ω. Importantly, this expansion puts no constraint on which system parameter is driven in what way (apart from being periodic), and it separately applies to *all* time-dependent probabilities $P_i(t)$ entering the quantum dot density operator $\rho(t)$. This means that the result from Ref. [191] is not only applicable to even more exotic forms of charge pumping, including driven Coulomb interaction strength $U(t)$ with a crossover to attractive interaction [194], but also to *energy pumping* [193]. The latter can be understood as a basic operation of the type of heat engines referred to in Sec. 1.2.3, and differs nontrivially from charge pumping for strong Coulomb interaction. Moreover, unlike for hot-electron emitters, the very purpose and working principle of energy pumping often demands operations which are energetically close to the bath Fermi level on the scale of the temperature. As pointed out in chapter 3, this is precisely the regime in which the fermionic duality – as a consequence of fermionic statistics of the environment occupation [Sec. (3.3.1)] – becomes most useful.

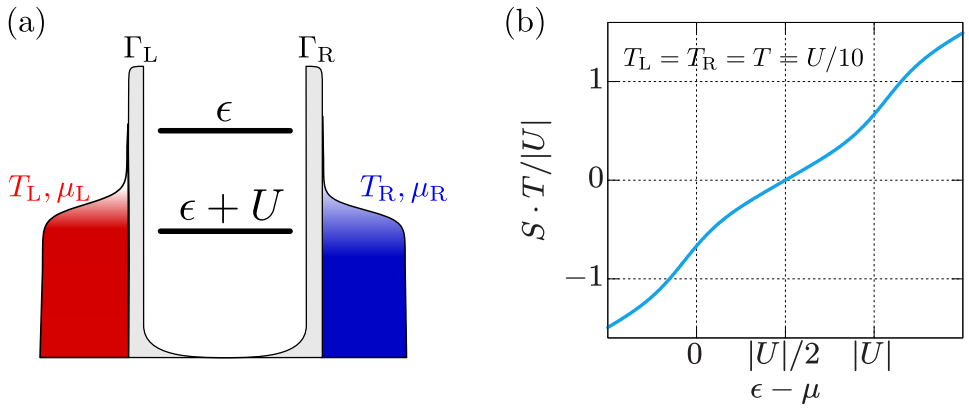

Figure 4.2: ***(a)*** *Sketch of a spin-degenerate single-level quantum dot [Sec. (2.1.1)] (level-position ϵ) with strong* attractive *interaction $U < 0$, weakly tunnel-coupled to two reservoirs L,R at possibly different potentials μ_L, μ_R and temperatures T_L, T_R.* ***(b)*** *Linear thermopower (3.22) as a function of the level-position ϵ for the system described in* ***(a)****, assuming energy-independent as well as spin- and reservoir-symmetric couplings $\Gamma_{L\uparrow} = \Gamma_{L\downarrow} = \Gamma_{R\uparrow} = \Gamma_{R\downarrow}$ and equilibrium potential $\mu_L = \mu_R = \mu$.*

4.2 Stationary transport

Let us finish this chapter by addressing how fermionic duality can help in future research on stationary transport in quantum dots.

4.2.1 Quantum dots with attractive interaction

As the first example, let us reconsider the linear thermopower $S = V/\Delta T|_{I_N=0}$ in quantum dots. For repulsive interaction, Fig. 1.4 in Sec. 1.3.1 has illustrated the well-known, experimentally verified [118, 119, 137–139] sawtooth shape of S as a function of an applied gate potential. In Sec. 3.2.3 and paper IV, we have shown that fermionic duality relates this sawtooth shape to a *resonant effect*, but in the *attractive dual* model.

However, apart from better understanding long-known, experimentally verified physics in terms of a new many-body theory, fermionic duality can also achieve the opposite. Namely, systems which have only recently become experimentally feasible [153, 195] are quantum dots with an *actual attractive* interaction. As an example, Fig. 4.2(a) shows the spin-degenerate single-level quantum dot [Sec. (2.1.1)] with an on-site *attraction* strength $U = -|U| < 0$. The main point for us is that unlike for the repulsive single-level dot whose many-body transition energies $\epsilon, \epsilon + U$ can often be approximately viewed as effective single-particle energy levels, the attractive system seems difficult to capture within such an intuitive single-particle picture: as clarified in Sec. 3.2.3 and shown theoretically as well as experimentally in Refs. [153, 195, 197, 198], the attractive dot is governed by

electron pairing, leading to a single transition energy $\epsilon + U/2$ associated with the tunneling of two particles. Nevertheless, fermionic duality does map such an attractive system to an energy-inverted, and thus *repulsive* dual model: new experiments governed by inherently complicated many-body effects of attractive interaction can thereby indeed be explained in terms of the long-known [29], often more intuitive effective single-particle physics of repulsive quantum dots.

As a concrete example, Fig. 4.2(b) plots the linear thermopower S of the single-level quantum dot as given by Eq. (3.22) in Sec. 3.2.3, but now evaluated at negative U. Consistent with the fact that the system has one 2-particle resonance at $\epsilon - \mu = -U/2 = |U|/2$, the Seebeck coefficient S grows linearly in ϵ close to this resonance on the temperature scale T. However, the slope in fact increases around the resonances $\epsilon - \mu = 0, -U \geq 0$ of the *dual repulsive* system, at which the dual equilibrium occupation $n_{\mathrm{i,eq}}$ [Eq. (3.22)] makes the transition from $0 \to 1$ and $1 \to 2$, respectively. These additional wiggles in S in fact coincide with the two steps of $n_{z,\mathrm{eq}}$ shown for a repulsive system in Fig. 3.2. In particular, the resonances at which the slope maximizes do not lie exactly *at* $\epsilon - \mu = 0, -U \geq 0$, but are shifted away by $\pm T \ln(2)$. This resonance shift is also well-known for the *repulsive* spin-degenerate single-level dot [54]. It can be interpreted in terms of the spin-degeneracy of the singly occupied state as well as Landauer's principle relating thermodynamic entropy and information [230, 231].

4.2.2 Nonlinear response and energy-dependent couplings

We close with a few more general remarks on possible future uses of duality, by recontemplating the three-terminal double-dot described by Fig. 1.5 in Sec. 1.3.2 of the introductory chapter 1. A problem for the theoretical description [97, 149] of this system in terms of a rate equation is the added complexity due to energy-dependent couplings and the breaking of detailed balance (2.45) for biased reservoirs. Accessing experimentally relevant quantities analytically can therefore quickly become cumbersome and uninformative. For instance, the operation of the system as a heat engine is described by Ref. [97] for the simpler case that no potential gradient is applied to the system. While this clearly exposes the charge current rectification, it may, depending on the type of experiment or application, be more interesting to assess how the device performs against an already present, and possibly large potential bias. Reference [149] does include such potential biases, but instead simplifies the equations by assuming a much faster tunneling in the dot coupled to only one reservoir. This is appropriate to describe the experimentally realized Maxwell daemon [150], but it is in general not true for a heat engine. In fact, it is even the opposite of a situation in which the dot coupled to two reservoirs acts as a charge detector as in paper I: the latter should ideally work much faster than the dot to be measured.

The general point is that in regimes in which stationary electronic transport

becomes relevant for current experiments and applications, most of the symmetries that simplify the life of a theoretician may ultimately be broken. This includes detailed balance and the commonly assumed wideband limit. Fermionic duality in the general form (3.37) for energy-dependent couplings is, however, hard to break, as long as only fermionic physics and the tunnel coupling to the environment matter. A duality-based analysis of stationary transport as in papers IV and V is therefore often still possible, and even advisable if the described experiment leaves nothing else that can simplify otherwise unwieldy theoretical expressions. This includes the description of effects due to energy-dependent couplings and of the nonlinear thermoelectric response, which Sec. 1.3.1 has identified as particularly interesting for quantum dots. But it is even useful in the linear response regime, when combining the linearization (2.53) and duality to describe devices for which the traditional approaches [118, 137, 147] fail. This applies precisely to systems with broken detailed balance and energy-dependent couplings, which is already true for the above mentioned, experimentally relevant [104, 105, 107, 150] three-terminal double-dot.

5 Overview of the papers

In this final chapter, we give a brief summary of each paper, stating the main motivations and results.

5.1 Paper I

Following previous publications [28, 76, 166] on the *fermion-parity rate* [Eq. (3.9)], paper I theoretically investigates whether it is feasible to measure the decay rates, and in particular the fermion-parity rate, of a weakly tunnel-coupled, spin-degenerate interacting single-level quantum dot [Sec. (2.1.1)] by a capacitively coupled *sensor quantum dot* (SQD), see Sec. 2.1.2. To fully account for capacitive backaction effects between the dot to be measured and the sensor dot, we set up a Markovian rate equation [Sec. (2.4.1)] for the combined dot-SQD system. This allows us to compute the time-dependent current through the SQD in response to a sudden level-shift $\epsilon_0 \to \epsilon$ applied to the dot.

The result is that the time-dependent decay of the SQD-current can indeed expose both the charge relaxation rate and the fermion-parity rate of the dot. Furthermore, we explain why the fermion-parity rate is, in contrast to the charge rate, only very weakly affected by capacitive back-action, see also Sec. 4.1 and App. D.

5.2 Paper II

A combination of the results of paper I and Refs. [166, 167] has ultimately led to the derivation of the most general, wideband-limit form of the fermionic duality [2] (3.1) in paper II. Using its Born-Markov limit $W + \mathcal{P}\overline{W}^{\dagger}\mathcal{P} = -\Gamma$ [Eq. (3.4)], the paper applies the duality to study time-dependent energy emission from a single-level quantum dot [Sec. (3.2.3)] via electron tunneling into a weakly coupled reservoir, induced by a sudden level-shift $\epsilon_0 \to \epsilon$.

The study shows that the parameter-independent fermion parity rate [Eq. (3.9)] is the typical time-scale for the emission of the many-body Coulomb interaction energy, thereby offering a more direct way to experimentally expose this rate and its properties. As also shown in Eq. (3.18), the corresponding decay amplitude is

[2] At that time called "fermion-parity duality".

demonstrated to exhibit the resonant behavior of the *attractive* dual system, despite the quantum dot being governed by strongly repulsive Coulomb interaction.

5.3 Paper III

Based on Ref. [191], the general part of this paper provides a less technical, more illustrative and physically oriented introduction to the fermionic duality (3.4) in the Born-Markov limit. It focuses on the mode-amplitude crossrelation (3.6) in the rate-equation limit [Sec. (2.4.1)].

In its application part, the paper extends paper II by applying duality to analyze the quantum dot decay rates for two arbitrarily biased reservoirs and a local Zeeman splitting due to a magnetic field on the dot, thereby explicitly breaking detailed balance (2.45). The paper shows that the properties of the parity rate are robust up to biases $|V|$ and magnetic fields B on the order of the Coulomb interaction strength U. This is explained by the fact that U is precisely the energy needed to break the electron pairing and resulting Coulomb blockade in the *attractive dual system*. Moreover, the paper combines the fermionic duality (3.4) with Iche's duality [198, 212, 213] to show that the decay rates must behave symmetrically under swapping the values of magnetic field B with level-position ϵ, see Eq. (3.36).

5.4 Paper IV

In an effort to apply duality to more experimentally accessible situations, paper IV studies stationary thermoelectric transport through an interacting single-level quantum dot weakly coupled to several reservoirs. The paper discusses both linear and nonlinear response of the stationary charge and heat current [Eq. (2.33)] to gradients between the chemical potentials and temperatures in the environment.

In the linear regime, the paper combines the fermionic duality with Onsager reciprocity [Eq. (2.58)]. The main results of this approach have partly been addressed in Sec. 3.2.3: first, we find that the well-known [118, 119, 138, 139] Coulomb oscillations in the linear thermopower (Seebeck coefficient) [Fig. 1.4] can be more efficiently analyzed in terms of the *pair resonance* in the dual attractive model [Fig. 3.2]. Second, whereas the electrical conductance G of the quantum dot is proportional to the equilibrium charge fluctuations $\delta n^2_{z,\mathrm{eq}} = \left\langle N^2 \right\rangle_{z_{\mathrm{eq}}} - \langle N \rangle^2_{z_{\mathrm{eq}}}$ on the dot – by virtue of the fluctuation-dissipation theorem – the parameter-dependence of the *thermal conductance* κ in absence of a charge current (Fourier heat) is in fact found to be governed by the *dual* equilibrium fluctuations $\delta n^2_{\mathrm{i,eq}} = \left\langle N^2 \right\rangle_{z_{\mathrm{i,eq}}} - \langle N \rangle^2_{z_{\mathrm{i,eq}}}$.

Finally, a key observation *beyond linear response* is that whereas the nonlinear charge conductance is proportional to *equilibrium* differences $n_{z\alpha} - n_{z\alpha'\neq\alpha}$ between reservoir-resolved charges $n_{z\alpha} = \langle N \rangle_{z_\alpha}$ [Eq. (2.55)], the nonlinear *thermal* conductance is proportional to the corresponding equilibrium *parity* difference $p_{z\alpha} - p_{z\alpha'\neq\alpha}$, where $p_{z\alpha} = \left\langle (-\mathbb{1})^N \right\rangle_{z_\alpha}$. This highlights that thermal conductance in absence of a net charge current in a weakly coupled quantum dot is due to many-body correlations, stemming from the local Coulomb interaction.

5.5 Paper V

Up to paper IV, the formulation of the fermionic duality has been limited to possibly strong, yet energy-independent tunnel couplings (wideband limit), and the concrete analysis has focussed on the rate-equation limit [Sec. (2.4.1)] in papers III,IV. In view of experiments [22, 74, 104, 105, 107] with specifically tuned energy-dependent tunnel barriers $\Gamma(E)$, paper V extends the fermionic duality to such energy-dependent couplings in the weak-coupling limit. Furthermore, it provides a more careful study of the fermionic duality for a quantum master equation, i.e., when the local coherent dynamics in the reduced density operator $\rho(t)$ play a role.

The general result, as detailed in Sec. 3.5, is that the duality remains similarly useful even for such cases. The main difference of energy-dependent couplings is that the duality $W + \mathcal{P}\overline{W}^\dagger\mathcal{P} = -\mathbb{\Gamma}$ contains the *coupling superoperator* $\mathbb{\Gamma}$ instead of the scalar sum of couplings $\Gamma > 0$ [Eq. (3.2)]. This superoperator is independent of the reservoir statistics and plays an analogous role as Γ in the wideband limit. The properties of $\mathbb{\Gamma}$ and their implications are summarized in Sec. 3.5. We highlight in particular the possibility to combine duality with detailed balance as shown in Sec. 3.4.1, and the substantial simplifications of the calculation of matrix elements for the kernel W [Eq. (3.45)].

The application part of paper V exploits precisely the latter simplifications to treat both the decay dynamics and linear thermoelectric transport for the most general case of a spin-degenerate, strongly-interacting single-level quantum dot with weak, yet arbitrarily energy-dependent tunnel coupling to several reservoirs. This offers a revised understanding of the decay rates under arbitrarily biased reservoirs in comparison to the wideband limit studied in paper III. Moreover, it shows that the properties of the *dual* equilibrium charge $n_{\mathrm{i,eq}}$ continue to govern the parameter dependence of both the linear thermopower and the Fourier heat, in the same way as shown by paper IV for energy-independent couplings.

6 Conclusion

6.1 Summary

This thesis and its appended papers have introduced and discussed a fundamental symmetry relation – the *fermionic duality*. This duality governs both the transient and stationary transport behavior of interacting fermionic open quantum systems tunnel-coupled to multiple reservoirs in the environment at arbitrary bias voltages and temperatures. Formulated in the framework of quantum master equations, the duality establishes a crosslink between modes and amplitudes in the time-dependent decay of the system of interest due to some external perturbation. Most importantly, this crosslink involves a mapping to *dual* system with inverted energy, and hence in particular inverted *interaction*. Several examples in our articles show that the duality thereby readily explains many analytical features in system observables which otherwise seem very unintuitive and difficult to interpret. Moreover, the duality significantly enhances the analytical accessibility of more complex problems. This includes not only the locally interacting, possibly energy-dependently coupled quantum dot setups studied in the appended papers, but in principle also large fermionic n-level systems. Given that such systems represent basic building blocks for many electronic nanodevices of experimental interest, the duality applies in a currently relevant context.

The more general point this thesis aims to make is that while the duality is fundamentally restricted to fermionic systems, its value is in many ways comparable to more general symmetry and fluctuation relations, such as, e.g., detailed balance. Solving a Markovian master equation for which detailed balance is known beforehand to hold, it would not be wise to solve this equation without making explicit use of detailed balance, as the latter drastically simplifies the analytical treatment. Fermionic duality should likewise be used, as it leads to similar simplifications, and – relying essentially only on fundamental properties of fermions – in fact extends straightforwardly to situations in which classical detailed balance is explicitly broken. This includes in particular systems which are far away from equilibrium, which depend on quantum coherences, and which are possibly coupled strongly to the environment, leading to non-Markovian effects. In this respect, this thesis and its appended papers offer an explicit template how to make use of these benefits in future studies. Let us therefore, in our final act, concretely name some of the interesting open questions which could be addressed in such studies.

6.2 Open questions and problems

Summarizing chapter 4, experimental verifications of the implications of fermionic duality would be possible in several ways: first, the parity rate may be exposed by measurements of the time-dependent energy current emitted from an interacting quantum dot close to the Fermi energy of the environment. Second, measurements of the Seebeck coefficient in a – nowadays technically feasible – *attractive* quantum dot is expected to clearly expose its duality to a repulsive system, given that the latter indeed holds. Furthermore, chapter 4 has emphasized that the duality also applies to continuously driven systems if the evolution kernel W_t may be approximated by its Markovian, instantaneous limit [Sec. (2.6.2)]; it should thus be useful in currently relevant research on charge-, spin- and energy pumping with quantum dots and similar nanodevices.

Regarding the interacting quantum dot system of paper V, our preliminary studies indicate that energy-dependent couplings can lead to a *qualitative* difference in *nonlinear* stationary transport. Unlike in the wideband limit shown in paper IV, there seem to be parameter regimes in which the condition of vanishing charge current $I_N = 0$ can have either no solution or multiple solutions for the potential bias V and otherwise fixed parameters. This needs to be confirmed and explained physically, requiring especially a revised understanding of the nonlinear thermopower $S_{\rm nl} = V/\Delta T|_{I_N=0}$ and thermal conductance $\kappa_{\rm nl} = I_Q/\Delta T|_{I_N=0}$.

More generally, duality should now be more concretely explored in larger, more complex interacting quantum systems out of equilibrium, in which many other symmetries and in particular detailed balance break down. For example, Paper V has identified the case in which both quantum coherences and energy-dependent couplings play a role as a particularly interesting regime, but it has not further explored this case. One question would be how to extend the Liouville-space linear response formalism outlined Sec. 2.5, and how this can be combined with the non-wideband duality relation (3.37). Another example is to explicitly test and explore the usefulness of the duality-guided basis expansion introduced in Sec. 3.2.4 on a larger n-level system.

Let us also address a few more *fundamental* aspects. First, it is still almost completely unanswered how *precisely* the most general, frequency-dependent wideband-limit duality (3.1) can help to describe non-Markovian dynamics in strongly coupled systems. Moreover, given that duality can be combined with detailed balance in the semi-classical rate-equation limit, it is interesting whether this can be generalized to the quantum regime and quantum detailed balance. Finally, it still stands to reason whether there is any generalization of the fermionic duality to bosonic systems with *constrained* particle numbers.

Appendices

Appendix A

Conserved energy current in weakly coupled systems

In this first appendix, we argue under which condition the time-dependent energy current *into* reservoir α, defined in Eq. (2.26c) through the heat current as

$$I_{\mathrm{E}}^{\alpha}(t) = \partial_t \langle H_\alpha \rangle (t) = \partial_t \mathrm{Tr} \underset{\mathrm{R}}{\mathrm{Tr}} \left[H_\alpha \rho^{\mathrm{tot}}(t) \right], \tag{A.1}$$

with reservoir Hamiltonian H_α is conserved in the Markovian, weak-coupling limit, and can hence be written in terms of the *open-system* Hamiltonian H:

$$I_{\mathrm{E}}^{\alpha}(t) \to -(H|W_\alpha|\rho(t)), \tag{A.2}$$

where W_α is the reservoir-resolved Born-Markov kernel [Eq. (2.34)] and $|\rho(t))$ the reduced density operator of the open subsystem.

Let us start from Eq. (A.1) by pulling in the time derivative (time-independent Hamiltonian H_α) towards $\rho^{\mathrm{tot}}(t)$ in order to use the Liouville-von Neumann equation [Eq. (2.15)]:

$$I_{\mathrm{E}}^{\alpha}(t) \underset{(2.15)}{\overset{(A.1)}{=}} -\mathrm{i}\mathrm{Tr} \underset{\mathrm{R}}{\mathrm{Tr}} \left[H_\alpha \left[H_{\mathrm{tot}}, \rho^{\mathrm{tot}}(t) \right] \right] = -\mathrm{i}\mathrm{Tr} \underset{\mathrm{R}}{\mathrm{Tr}} \left[\left[H_\alpha, H_{\mathrm{tot}} \right] \rho^{\mathrm{tot}}(t) \right], \tag{A.3}$$

where we have used the cyclicity of the total-system trace. Next, we substitute the total Hamiltonian H_{tot} by the expression given in Eq. (2.2), and use that the fermionic anti-commutation relations – together with the parity-superselection principle forcing each Hamiltonian to consist only of terms with an even number of field operators – imply

$$[H_\alpha, H_{\alpha'}] = [H_\alpha, H] = [H_\alpha, H_{\mathrm{tun},\alpha' \neq \alpha}] = 0, \tag{A.4}$$

with the reservoir-resolved tunneling Hamiltonian

$$H_{\mathrm{tun},\alpha} = \sum_{\mathbf{k}ml} \delta_{\alpha_m \alpha} \tau_{\mathbf{k}ml} c_{\mathbf{k}m}^\dagger d_l + \mathrm{H.c.} \quad , \quad H_{\mathrm{tun}} = \sum_\alpha H_{\mathrm{tun},\alpha}. \tag{A.5}$$

This leads to

$$I_{\mathrm{E}}^{\alpha}(t) \underset{(A.4)}{\overset{(A.3)}{=}} -\mathrm{i}\mathrm{Tr} \underset{\mathrm{R}}{\mathrm{Tr}} \left[\left[H_\alpha, H_{\mathrm{tun},\alpha} \right] \rho^{\mathrm{tot}}(t) \right]. \tag{A.6}$$

The most important step is now to *assume* that each reservoir-resolved tunneling Hamiltonian conserves, on its own, the *total system* energy,

$$\left[H_\alpha + H + \sum_{\alpha'\neq\alpha} H_{\mathrm{tun},\alpha'}, H_{\mathrm{tun},\alpha}\right] \overset{\substack{[H_{\mathrm{tun},\alpha},H_{\mathrm{tun},\alpha}]=0\\ [H_{\alpha'\neq\alpha},H_{\mathrm{tun},\alpha}]=0}}{=} \left[\sum_\alpha H_\alpha + H + \sum_{\alpha'} H_{\mathrm{tun},\alpha'}, H_{\mathrm{tun},\alpha}\right] \overset{(2.2)}{=} [H_{\mathrm{tot}}, H_{\mathrm{tun},\alpha}] = 0. \tag{A.7}$$

While not explicitly demanded by global phase symmetry, plugging this back into Eq. (A.6) allows us to rewrite

$$\begin{aligned} I^\alpha_{\mathrm{E}}(t) &\overset{\substack{(\mathrm{A.3})\\(\mathrm{A.4})}}{=} +\mathrm{i}\mathrm{Tr}\underset{\mathrm{R}}{\mathrm{Tr}}\left[[H, H_{\mathrm{tun},\alpha}]\,\rho^{\mathrm{tot}}(t)\right] + \mathrm{i}\mathrm{Tr}\underset{\mathrm{R}}{\mathrm{Tr}}\left[\left[\sum_{\alpha'\neq\alpha} H_{\mathrm{tun},\alpha'}, H_{\mathrm{tun},\alpha}\right]\rho^{\mathrm{tot}}(t)\right] \\ &= \mathrm{i}\mathrm{Tr}\left[H\cdot\underset{\mathrm{R}}{\mathrm{Tr}}\left[H_{\mathrm{tun},\alpha}, \rho^{\mathrm{tot}}(t)\right]\right] + \mathrm{i}\mathrm{Tr}\underset{\mathrm{R}}{\mathrm{Tr}}\left[\left[\sum_{\alpha'\neq\alpha} H_{\mathrm{tun},\alpha'}, H_{\mathrm{tun},\alpha}\right]\rho^{\mathrm{tot}}(t)\right]. \end{aligned} \tag{A.8}$$

Following the diagrammatic perturbation theory as shown in Refs. [164–167], we see that the first term in (A.8) is at least quadratic in the tunneling constants τ [Eq. (A.5)], whereas the second term must be at least of the order τ^4. In lowest order in the tunneling, we may therefore simply neglect the second, reservoir-reservoir correlation term, and approximate

$$I^\alpha_{\mathrm{E}}(t) \approx \mathrm{i}\mathrm{Tr}\left[H\cdot\underset{\mathrm{R}}{\mathrm{Tr}}\left[H_{\mathrm{tun},\alpha}, \rho^{\mathrm{tot}}(t)\right]\right] = -(H|W_\alpha|\rho(t)). \tag{A.9}$$

The last step reintroduces the Liouville space notation from Sec. 2.2.1 and identifies the definition of the reservoir-resolved kernel $W_\alpha\rho(t) = -\mathrm{i}\underset{\mathrm{R}}{\mathrm{Tr}}\,[H_{\mathrm{tun},\alpha}, \rho^{\mathrm{tot}}(t)]$ in the Born-Markov limit, as, e.g., shown in the appendix of Lic. Th. [110].

Appendix B

Generalized eigendecomposition of Born-Markov time evolution

In this appendix, we briefly show how to explicitly express the Born-Markov time evolution [Eq. (2.30)]

$$|\rho(t)) = \exp(At)\,|\rho_0). \tag{B.1}$$

for an initial state $|\rho_0)$ and a *non-diagonalizable* [2] Born-Markov evolution kernel $A = -\mathrm{i}L + W$, and how duality still helps to systematically construct particularly suitable and insightful basis vectors for this kernel.

B.1 Explicit expression of time evolution for non-diagonlizable kernels

Crucially, any Born-Markov kernel A for the finite fermionic open systems of interest in this thesis can be expressed by a complex $N \times N$ matrix which can be put into the blockdiagonal Jordan normal form [196]. Each block has all degenerate eigenvalues on the diagonal, and more non-vanishing matrix elements on the upper diagonal. This particular form for A can be used to derive the following generalized eigendecomposition of the matrix exponential:

$$\exp(At) = \sum_{m=1}^{M} \sum_{n,n'=1}^{M_m} e^{\lambda_m t} \cdot (e^{F_m t})_{nn'} \cdot |v_{m,n})(v'_{m,n'}|. \tag{B.2}$$

Let us explain the ingredients of Eq. (B.2). The index m goes over all M *mutually different* eigenvalues λ_m of A; the indices n, n' go from 1 to the multiplicity M_m of each eigenvalue λ_m. The ket $|v_{m,n})$ is a *generalized right eigenvector*. For any such generalized right eigenvector, there exists a minimal integer $M_{m,n} \in \mathbb{N}^{\leq M_m}$ – the so-called *rank* – such that

$$[A - \lambda_m \mathcal{I}]^{M_{m,n}} \cdot |v_{m,n}) = 0. \tag{B.3}$$

[2] Since $A^\dagger \neq \pm A$, the kernel is not guaranteed to be diagonalizable.

Analogously, the bras $(v'_{m,n'}|$ are *generalized left eigenvectors* with rank $M_{m,n'} \in \mathbb{N}^{\leq M_m}$,

$$(v_{m,n'}| \left[A - \lambda_k \mathcal{I}\right]^{M_{m,n'}} = 0. \tag{B.4}$$

The left and right generalized eigenvectors form a biorthonormal basis:

$$(v'_{m,n}|v_{m',n'}) = \delta_{mm'}\delta_{nn'} \quad , \quad \mathcal{I} = \sum_{m=1}^{M}\sum_{n=1}^{M_m} |v_{m,n})(v'_{m,n}|. \tag{B.5}$$

Importantly, there exists at least one left and one right generalized eigenvector for every eigenvalue λ_m that is a true eigenvector, meaning for which $M_{n,m} = 1$.

Finally, the important difference between Eq. (B.2) and the case of a diagonalizable kernel [Eq. (2.38)] are the subkernels F_m. These subkernels are nilpotent, meaning there exists an $p_m \in \mathbb{N}$ such that $(F_m)^{p_m} = 0$. As an important consequence, the matrix exponential $e^{F_m t}$ becomes a *finite* power series in t, and can therefore be expressed in a closed form. Physically, Eq. (B.2) expresses that whereas the long-time limit is still governed by the decaying $\exp(\lambda_m t)$ with $\mathrm{Re}\,[\lambda_m] \leq 0$, there is some additional polynomial behavior in earlier phases of the transient time evolution.

B.2 Mode-amplitude duality for generalized eigenvectors

In the main text, we have argued in the Born-Markov limit that the mode-amplitude dualities (3.6) and (3.42) likewise hold for generalized modes (B.3) and amplitudes (B.4). Here, we prove this statement.

Let $|x)$ be a generalized right eigenvector of the kernel W, corresponding to the eigenvalue λ_x and rank p:

$$\left[W - \lambda_x \mathcal{I}\right]^p |x) = 0. \tag{B.6}$$

Applying the energy inversion to the dual model, multiplying from the left with the parity $\mathcal{P}\bullet = (-\mathbb{1})^N \bullet$, and inserting the identity $\mathcal{I} = \mathcal{P}\mathcal{P}$, this gives

$$\mathcal{P}\left[\overline{W} - \overline{\lambda}_x \mathcal{I}\right]^p \mathcal{P}\mathcal{P}|\overline{x}) = \left[\mathcal{P}\overline{W}\mathcal{P} - \overline{\lambda}_x \mathcal{I}\right]^p \mathcal{P}|\overline{x}) = 0. \tag{B.7}$$

Now using the non-wideband duality (3.37) from the main text, we can rewrite Eq. (B.7) as

$$\begin{aligned}
0 &\overset{(B.7)}{=} \left[-\mathcal{P}\overline{W}\mathcal{P} + \overline{\lambda}_x \mathcal{I}\right]^p \mathcal{P}|\overline{x}) \\
&\overset{(3.37)}{=} \left[W^\dagger - (-\mathbb{\Gamma}^\dagger - \overline{\lambda}_x \mathcal{I})\right]^p \mathcal{P}|\overline{x}) = \left\{\left[W - (-\mathbb{\Gamma} - \overline{\lambda}_x^* \mathcal{I})\right]^p\right\}^\dagger \mathcal{P}|\overline{x}) \\
&\overset{\mathcal{P}=\mathcal{P}^\dagger}{=} \left\{(\overline{x}|\mathcal{P}\left[W - (-\mathbb{\Gamma} - \overline{\lambda}_x^* \mathcal{I})\right]^p\right\}^\dagger \\
\Rightarrow &(\overline{x}|\mathcal{P}\left[W - (-\mathbb{\Gamma} - \overline{\lambda}_x^* \mathcal{I})\right]^p = 0.
\end{aligned} \tag{B.8}$$

For any generalized mode $|x)$ of W corresponding to eigenvalue λ and rank p, there exists a generalized covector $(y'| = (\overline{x}|\mathcal{P}$ that most generally behaves as in Eq. (B.8), representing an extension to how Eq. (3.42) from the main text yields left covectors $(y'|$ from modes $|x)$. In the wideband limit $\mathbb{\Gamma} \to \Gamma$ [Eq. (3.2)], $(y'|$ then indeed becomes a generalized amplitude in the sense of Eq. (B.4), corresponding to the eigenvalue $\lambda_y = -\Gamma - \overline{\lambda}_x^*$ and *equal* rank p as $|x)$. Note in particular that p is indeed the rank of $(y'|$, i.e., the minimal power for which $(y'|$ fulfills Eq. (B.4): if the opposite was true, i.e., there was a $p' < p$ such that

$$\left[W - (-\mathbb{\Gamma} - \overline{\lambda}_x^* \mathcal{I})\right]^{p'} = 0, \tag{B.9}$$

one could revert the construction from Eq. (B.8) to Eq. (B.6) with $p \to p'$ and conclude that

$$[W - \lambda_x \mathcal{I}]^{p' < p} \, |x) = 0. \tag{B.10}$$

This would contradict the initial assumption (B.6) that $|x)$ is a generalized mode to eigenvalue λ_x and rank $p > p'$.

Repeating an analogous procedure of constructing generalized modes from generalized amplitudes, this proves that the wideband mode-amplitude duality (3.6) from the main text works exactly in the same way if $|x)$ or $(x'|$ are not true eigenvectors, but generalized eigenvectors to eigenvalue λ_x and rank p. The duality in this case establishes a crosslink between generalized modes and amplitudes of equal rank $p \geq 1$. For energy-dependent bare couplings, the relations (3.42) generalize in the sense of Eq. (B.8).

Appendix C

Diagonalizability and real eigenvalues under detailed balance

This short appendix shows the claim from Sec. 2.4.3 that if a real, positively recurrent rate matrix $\mathbf{W}$ as defined in Sec. 2.4.2 fulfills detailed balance (2.45), $\mathbf{W}$ is diagonalizable and its eigenvalues λ must be purely real, so that the Markovian time evolution governed by $\mathbf{W}$ is a pure exponential decay without oscillations.

To prove this, we use that for such positively recurrent rate matrices, all stationary probabilities are finite according to Sec. 2.4.2: $0 < P_{z,i} < 1$ for all many-body energy eigenstates $|E_i)$ of the local open-system Hamiltonian H. We may therefore define the following renormalization matrix:

$$(\mathbf{R})_{ij} = \delta_{ij} \frac{1}{\sqrt{P_{z,i}}} \Rightarrow (\mathbf{R}^{-1})_{ij} = \delta_{ij} \sqrt{P_{z,i}}. \tag{C.1}$$

We now use this matrix to perform the similarity transform

$$\mathbf{V} = \mathbf{R} \cdot \mathbf{W} \cdot \mathbf{R}^{-1}, \tag{C.2}$$

meaning $\mathbf{V}$ is also a real matrix and has the same eigenvalue spectrum as $\mathbf{W}$. The main point is now that due to detailed balance (2.45) applying to $\mathbf{W}$, the matrix $\mathbf{V}$ is real-symmetric, and hence Hermitian:

$$(\mathbf{V})_{ij} \overset{\text{(C.1)}}{\underset{\text{(C.2)}}{=}} \frac{\sqrt{P_{z,j}}}{\sqrt{P_{z,i}}} (\mathbf{W})_{ij} = \frac{\sqrt{P_{z,i}}}{\sqrt{P_{z,j}}} (\mathbf{W})_{ij} \frac{P_{z,j}}{P_{z,i}} \overset{(2.45)}{=} \frac{\sqrt{P_{z,i}}}{\sqrt{P_{z,j}}} (\mathbf{W})_{ji} \overset{\text{(C.1)}}{\underset{\text{(C.2)}}{=}} (\mathbf{V})_{ji}. \tag{C.3}$$

This implies that the similarity-transformed kernel $\mathbf{V}$ has real eigenvalues and is diagonalizable by another similarity transform. By Eq. (C.2), this in return means that also $\mathbf{W}$ is diagonalizable, and has the same real eigenvalues as $\mathbf{V}$.

Appendix D

Construction of duality-induced basis

In this appendix, we show how to properly understand, biorthogonalize and apply the duality-induced subsystem parity vectors

$$\begin{aligned} \mathcal{L} = ((p'_{\mathcal{A}}|)_{\mathcal{A}} \quad &, \quad \mathcal{R} = (|p_{\mathcal{A}}))_{\mathcal{A}} \\ (p'_{\mathcal{A}}| = (z_{\mathrm{i},\mathcal{A}}(-\mathbb{1})^{N_{\mathcal{A}}} \otimes \mathbb{1}_{\mathcal{S}\setminus\mathcal{A}}| \quad &, \quad |p_{\mathcal{A}}) = |(-\mathbb{1})^{N_{\mathcal{A}}} \otimes z_{\mathcal{S}\setminus\mathcal{A}}), \end{aligned} \tag{D.1}$$

introduced in Eq. (3.24) of Sec. 3.2.4. Section D.1 gives an overview over the general procedure, followed by more detailed technical considerations in sections D.2 and D.3. In this appendix, we assume the wideband limit, $\Gamma_{m,ll'}(E) \to \Gamma_{m,ll'}$.

D.1 General properties of duality-induced basis

The definitions (D.1) of the basis vectors $|p_{\mathcal{A}})$ and $(p'_{\mathcal{A}}|$ raise two central questions: how exactly can they be used to construct a basis for the kernel W, and – even more importantly – what is the advantage and additional insight of doing so? Answering these questions in more detail is the aim of this section D.1. As a start, let us look at the most important analytical properties of the vectors (D.1):

1. By construction, the sets $\mathcal{L}$ and $\mathcal{R}$ defined in Eq. (D.1) contain the four already known eigenvectors corresponding to the bounding eigenvalues $0, -\Gamma$ [Eq. (3.10)]:

$$\begin{aligned} (p'_{\mathbb{0}}| = (\mathbb{1}| \quad &, \quad |p_{\mathbb{0}}) = |z) \\ (p'_{\mathcal{S}}| = (z_{\mathrm{i}}(-\mathbb{1})^{N}| \quad &, \quad |p_{\mathcal{S}}) = |(-\mathbb{1})^{N}). \end{aligned} \tag{D.2}$$

   Moreover, we notice that the left and right vectors are crosslinked in the way prescribed by duality in Eq. (3.6):

$$(p'_{\mathcal{A}}| = \left[\mathcal{P}|\overline{p}_{\mathcal{S}\setminus\mathcal{A}})\right]^{\dagger} \quad \forall \mathcal{A} \subseteq \mathcal{S}, \tag{D.3}$$

   where $\mathcal{P}|\bullet) = |(-\mathbb{1})^{N}\bullet)$ and $\overline{x} = x(-H, \{-\mu_\alpha\})$. Using the vector sets $\mathcal{L}$ and $\mathcal{R}$ to expand W, we therefore benefit from all general insights pointed out in sections 3.1.2 and 3.2.1-3.2.3.

2. While the left vectors in $\mathcal{L}$ are in general not yet biorthonormal to *all* right vectors in $\mathcal{R}$, one finds

$$(p'_{\mathcal{A}}|p_{\mathcal{A}}) \overset{(\mathrm{D}.1)}{=} (z_{\mathrm{i},\mathcal{A}} \otimes \mathbb{1}_{\mathcal{S}\setminus\mathcal{A}}|\mathbb{1}_{\mathcal{A}} \otimes z_{\mathcal{S}\setminus\mathcal{A}}) = (z_{\mathrm{i},\mathcal{A}}|\mathbb{1}_{\mathcal{A}}) \cdot (\mathbb{1}_{\mathcal{S}\setminus\mathcal{A}}|z_{\mathcal{S}\setminus\mathcal{A}}) = 1 \quad \text{(D.4)}$$

and, for all $\mathcal{B} \setminus \mathcal{A} \neq \mathbb{0}$, i.e., $\mathcal{B}$ includes single-particle states which are not included in $\mathcal{A}$,

$$\begin{aligned}
(p'_{\mathcal{A}}|p_{\mathcal{B}}) &\underset{\mathcal{B}\setminus\mathcal{A}\neq\mathbb{0}}{\overset{(D.1)}{=}} (z_{\mathrm{i},\mathcal{A}}\,(-\mathbb{1})^{N_{\mathcal{A}\setminus\mathcal{B}}} \otimes \mathbb{1}_{\mathcal{S}\setminus\mathcal{A}}|\mathbb{1}_{\mathcal{A}\cap\mathcal{B}} \otimes (-\mathbb{1})^{N_{\mathcal{B}\setminus\mathcal{A}}} \otimes z_{\mathcal{S}\setminus\mathcal{B}}) \\
&\overset{\mathcal{B}\setminus\mathcal{A}\subseteq\mathcal{S}\setminus\mathcal{A}}{=} (z_{\mathrm{i},\mathcal{A}}\,(-\mathbb{1})^{N_{\mathcal{A}\setminus\mathcal{B}}} \otimes \mathbb{1}_{\mathcal{B}\setminus\mathcal{A}} \otimes \mathbb{1}_{(\mathcal{S}\setminus\mathcal{A})\setminus(\mathcal{B}\setminus\mathcal{A})}|\mathbb{1}_{\mathcal{A}\cap\mathcal{B}} \otimes (-\mathbb{1})^{N_{\mathcal{B}\setminus\mathcal{A}}} \otimes z_{\mathcal{S}\setminus\mathcal{B}}) \\
&= \underbrace{(z_{\mathrm{i},\mathcal{A}}\,(-\mathbb{1})^{N_{\mathcal{A}\setminus\mathcal{B}}} \otimes \mathbb{1}_{(\mathcal{S}\setminus\mathcal{A})\setminus(\mathcal{B}\setminus\mathcal{A})}|\mathbb{1}_{\mathcal{A}\cap\mathcal{B}} \otimes z_{\mathcal{S}\setminus\mathcal{B}})}_{K:=} \cdot (\mathbb{1}_{\mathcal{B}\setminus\mathcal{A}}|(-\mathbb{1})^{N_{\mathcal{B}\setminus\mathcal{A}}}) \\
&= K \cdot (\mathbb{1}_{\mathcal{B}\setminus\mathcal{A}}|(-\mathbb{1})^{N_{\mathcal{B}\setminus\mathcal{A}}}) = 0 \quad \forall \mathcal{B}\setminus\mathcal{A} \neq \mathbb{0}. \qquad \text{(D.5)}
\end{aligned}$$

The last line in Eq. (D.5) follows from the tracelessness of any parity or subparity operator $(-\mathbb{1})^{N_{\mathcal{A}}}$. Equations (D.4) and (D.5) indicate that in order for the left and right vectors (D.1) to form biorthonormal basis sets, one needs to orthogonalize [1] the $(p'_{\mathcal{A}}|$ only to the vectors $|p_{\mathcal{B}})$ with $\mathcal{B} \setminus \mathcal{A} = \mathbb{0}$, i.e., including the stationary state $|z)$. In the next section D.2, we provide the general technical scheme how to carry out this procedure; Sec. D.3 then shows how to apply this to the concrete cases of the single-level quantum dot and the dot-sensor studied in the appended papers.

3. If there exists a bipartition $\{\mathcal{A}, \mathcal{S}\setminus\mathcal{A}\}$ for which none of the states in $\mathcal{A}$ couple [2] to any of the states in $\mathcal{S}\setminus\mathcal{A}$ and vice versa, one can use the general weak-coupling expression of the kernel W as, e.g., given in paper V to show that

$$W = W_{\mathcal{A}} \otimes \mathcal{I}_{\mathcal{S}\setminus\mathcal{A}} + \mathcal{I}_{\mathcal{A}} \otimes W_{\mathcal{S}\setminus\mathcal{A}}, \qquad \text{(D.6)}$$

where $W_{\mathcal{A}}$ denotes the Born-Markov kernel for the open system comprised of only the single-particle states in $\mathcal{A}$, and $\mathcal{I}_{\mathcal{A}}$ is the corresponding Liouville space identity [Sec. (2.2.1)] for this subsystem.

With $W_{\mathcal{A}}$ in its own right representing the dynamics of an open fermion system of the type introduced in Sec. 2.1, it also obeys the duality relation (3.4) in its subsystem, and thus possesses the left and right eigenvectors $(\mathbb{1}_{\mathcal{A}}|, (z_{\mathrm{i},\mathcal{A}}(-\mathbb{1})^{N_{\mathcal{A}}}|$ and $|z_{\mathcal{A}}), |(-\mathbb{1})^{N_{\mathcal{A}}})$ according to Eqs. (3.9) and (3.14). In

[1] Using, e.g., the Gram-Schmidt procedure.

[2] Via many-body interactions $U_{jj'}$ or off-diagonal tunnel couplings $\Gamma_{m,ll'}$ [Eq. (2.8)]!

combination with Eq. (D.6), this means

$$\begin{aligned}
(p'_{\mathcal{A}}|W &\overset{\substack{(D.1)\\(D.6)}}{=} (z_{\mathrm{i},\mathcal{A}}(-\mathbb{1})^{N_{\mathcal{A}}}|W_{\mathcal{A}} \otimes (\mathbb{1}_{\mathcal{S}\setminus\mathcal{A}}| + (z_{\mathrm{i},\mathcal{A}}(-\mathbb{1})^{N_{\mathcal{A}}}| \otimes (\mathbb{1}_{\mathcal{S}\setminus\mathcal{A}}|W_{\mathcal{S}\setminus\mathcal{A}} \\
&\overset{\substack{(3.14)\\(2.35)}}{=} -\Gamma_{\mathcal{A}}(z_{\mathrm{i},\mathcal{A}}(-\mathbb{1})^{N_{\mathcal{A}}}| \otimes (\mathbb{1}_{\mathcal{S}\setminus\mathcal{A}}| \overset{(D.1)}{=} -\Gamma_{\mathcal{A}}(p'_{\mathcal{A}}| \\
W|p_{\mathcal{A}}) &\overset{\substack{(D.1)\\(D.6)}}{=} W_{\mathcal{A}}|(-\mathbb{1})^{N_{\mathcal{A}}}) \otimes |z_{\mathcal{S}\setminus\mathcal{A}}) + |(-\mathbb{1})^{N_{\mathcal{A}}}) \otimes W_{\mathcal{S}\setminus\mathcal{A}}|z_{\mathcal{S}\setminus\mathcal{A}}) \\
&\overset{\substack{(3.9)\\(2.39)}}{=} -\Gamma_{\mathcal{A}}|(-\mathbb{1})^{N_{\mathcal{A}}}) \otimes |z_{\mathcal{S}\setminus\mathcal{A}}) \overset{(D.1)}{=} -\Gamma_{\mathcal{A}}|p_{\mathcal{A}}).
\end{aligned} \tag{D.7}$$

with the *subparity rate*

$$\Gamma_{\mathcal{A}} = \sum_{\substack{m \\ l\in\mathcal{A}}} \Gamma_{m,ll}. \tag{D.8}$$

Since equations (D.7) and (D.8) likewise follow from the duality and Eq. (D.6) for the complementary set $\mathcal{S}\setminus\mathcal{A}$, we conclude that any $\mathcal{A}$ for which (D.6) holds identifies two vectors $(p'_{\mathcal{A}}|, (p'_{\mathcal{S}\setminus\mathcal{A}}|$ from the set $\mathcal{L}$ [Eq. (D.1)] as left eigenvectors, called *subparity amplitude covectors*, and two vectors $|p_{\mathcal{A}}), |p_{\mathcal{S}\setminus\mathcal{A}})$ from the set $\mathcal{R}$ as right eigenvectors, called *subparity modes*. In the simplest case that each single-particle state completely decouples from all others, Eq. (D.6) holds for all 2^M possible bipartitions $\{\mathcal{A}, \mathcal{S}\setminus\mathcal{A}\}$ of the M single-particle states. This implies that every left and right vector $(p'_{\mathcal{A}}|$ and $|p_{\mathcal{A}})$ defined in Eq. (D.1) becomes an eigenvector of the full kernel W corresponding to the eigenvalue $-\Gamma_{\mathcal{A}}$, given by the, possibly degenerate, subparity rates (D.8). Realizing furthermore that both z and z_{i} become tensor products of the stationary reduced density operators of each single-particle state $|l\rangle$, Eq. (3.15) then also guarantees [1] $(p'_{\mathcal{A}}|p_{\mathcal{B}}) \to \delta_{\mathcal{A}\mathcal{B}}$.

One main consequence from the above listed properties is that when taking the vectors (3.23) and orthogonalizing them to form basis vectors for the kernel W, any off-diagonal element

$$(\tilde{p}'_{\mathcal{A}}|W|\tilde{p}_{\mathcal{B}\neq\mathcal{A}}) \tag{D.9}$$

with respect to these orthogonalized basis vectors $(\tilde{p}'_{\mathcal{A}}|, |\tilde{p}'_{\mathcal{A}})$ defined in the next section D.2 must be due to a coupling of single-particle eigenstates in the open system, via many-body interactions or via the coupling to the reservoirs. Expanding W in terms of these vectors instead of the many-body energy eigenstates $|E_i) = |E_{ii})$ and coherences $|E_{ij})$ [Sec. (2.3.4)], we can thus directly identify and analyze nontrivial physical effects stemming from precisely these many-body interactions and coherent couplings. In fact, given that the relevant dynamics can be described in the rate-equation limit [Sec. (2.4.1)], the 2^M left and right basis

[1] Note that since the subparity rates (D.8) could be degenerate, the eigenvector property is not enough to guarantee biorthogonality.

vectors even form a *complete* basis in the probability sector, thereby fully characterizing the kernel of interest. This is particularly useful for the sensor dot system studied in paper I: since the duality had not been established when the paper was published, the choice of suitable basis vectors was to a considerable extent educated guessing. The above illustrated scheme makes this guessing obsolete, as detailed in Sec. D.3.

Apart from exposing interaction effects, another advantage of picking the vectors (D.1) to expand W is that we can generalize what we know about the fermion-parity mode $|(-\mathbb{1})^N)$ and the dual stationary state $|z_\mathrm{i})$. First, we may readily extend the idea of Eq. (3.12) to the orthogonalized subparity vectors $|\tilde{p}_\mathcal{A})$: since the tracelessness of (sub)parity operators dictates

$$(O|p_\mathcal{A}) = (O|(-1)^{N_\mathcal{A}} \otimes z_{\mathcal{S}\setminus\mathcal{A}}) = 0 \tag{D.10}$$

for any observable O which is orthogonal to all relevant subparities, $(O|(-\mathbb{1})^{N_\mathcal{B}}) = 0$ with $A \subseteq B$, Eq. (D.5) guarantees that (D.10) also holds for the vectors $|\tilde{p}_\mathcal{A})$. Physically, this means that in order for $O(t) = (O|\rho(t))$ to be affected by any contribution to $|\rho(t))$ which is proportional to $|\tilde{p}_\mathcal{A})$, the observable O needs to be at least an "$N_\mathcal{A}$-particle" observable. Knowing which observable expectation we are interested in, this may simplify the calculation considerably, as it allows us to neglect many terms in $|\rho(t))$ from the start.

Finally, considering that the dual state $|z_\mathrm{i})$ represents in many cases a maximally unstable state of fixed fermion parity for the entire open system [Sec. (3.2.3)], the reduced dual state $|z_{\mathrm{i},\mathcal{A}})$ describes how this maximal instability manifests itself in the subsystem containing the single-particle states $l \in \mathcal{A}$ – in the presence of the coupling to the remaining states. As long as this coupling has only a small effect on $|z_{\mathrm{i},\mathcal{A}})$, it is reasonable to assume that $|z_{\mathrm{i},\mathcal{A}})$ represents a most unstable configuration of the subsystem $\mathcal{A}$ relatively independently of how the other single-particle states are occupied; it should thus also have a fixed fermion parity whenever $|z_\mathrm{i})$ has fixed parity. Applying this in the same way as in Sec. 3.2.3, Eq. (3.20), one might *intuitively expect* that the time-dependent probability for the subsystem state $|\rho_\mathcal{A}(t)) = \mathrm{Tr}_{\mathcal{S}\setminus\mathcal{A}}[\rho(t)]$ to assume $|z_{\mathrm{i},\mathcal{A}})$ should also evolve monotonously according to a single exponential decay rate. This means that $(p'_\mathcal{A}|$ should be an *approximate* left eigenvector of W to this rate.

As Eqs. (D.7) and (D.8) confirm, the above intuition is exactly true if the subsystem $\mathcal{A}$ completely decouples: in this case, the decay rate is known to be the subparity rate $\Gamma_\mathcal{A}$. However, paper I also indicates that this *expected* behavior can in fact be observed for capacitively coupled systems such as the sensor dot setup described in Sec. 2.1.2. Specifically, we find that for a subsystem $\mathcal{A}$ comprising the spin-up and spin-down state of the spin-degenerate dot to be measured, the vector $(p'_\mathcal{A}|$ actually remains, to a very good approximation, a left eigenvector of W to the subparity rate $\Gamma_\mathcal{A} = \Gamma_\uparrow + \Gamma_\downarrow$; apart from small temperatures compared to the interaction strengths, the only condition for this to hold is that the local Coulomb

interaction U in the dot is stronger than the capacitive coupling U_C to the sensor, which, however, is obviously true for the considered system geometry. And indeed, while not referring to duality, the paper does explain the robustness of the rate in terms of the most unstable dot configuration being hardly influenced by the occupation of the sensor dot. With duality at hand, we can interpret this effect in the same way as in Sec. 3.2.3: the sensor dot is unable to break the attraction between two electrons in the dual dot system, as this requires a pair-breaking coupling strength $|U_C| > |U|$. A more rigorous evaluation of this argument for a more general class of open systems is, however, still open to future studies.

D.2 Biorthogonal basis vectors

This section derives the orthogonalization procedure referred to in the previous section D.1. We start by dealing with the case that several pairs of vectors $(p'_{\mathcal{A}}|, |p_{\mathcal{A}})$ with $\mathcal{A} \neq \mathcal{S}, \mathbb{0}$ are already eigenvectors of W. Since our orthogonalization procedure intends to leave eigenvectors of W untouched, the first step is to define the sets of vectors $\{(p'_{\mathcal{A},0}|\}, \{|p_{\mathcal{A},0})\}$ which differ from $\{(p'_{\mathcal{A}}|\}, \{|p_{\mathcal{A}})\}$ by the fact that *all* vectors $|p_{\mathcal{A},0})$ are already biorthonormal to all left *eigen*vectors $(p'_{\mathcal{A},0}| \neq (p'_{\mathcal{S}}|, (p'_{\mathbb{0}}|$, and that *all* vectors $(p'_{\mathcal{A},0}|$ are biorthonormal to all right *eigen*vectors $|p_{\mathcal{A},0}) \neq |p_{\mathcal{S}}), |p_{\mathbb{0}})$. The necessary orthogonalization can be carried using any convenient method of choice, such as Gram-Schmidt orthogonalization. Importantly, this procedure is simplified by equations (D.4) and (D.5), guaranteeing that $(p'_{\mathcal{A}}|p_{\mathcal{B}}) = \delta_{\mathcal{A}\mathcal{B}}$ if $\mathcal{B} \setminus \mathcal{A} \neq 0$ or $\mathcal{B} = \mathcal{A}$. Or formulated inversely, this means that any $(p'_{\mathcal{A}}|$ only needs to be orthogonalized to $|p_{\mathcal{B}})$ with $\mathcal{B} \setminus \mathcal{A}) = 0$. Consequently, this first orthogonalization preserves

$$(p'_{\mathcal{A},0}|p_{\mathcal{B},0}) = \begin{cases} 0 & \mathcal{B} \setminus \mathcal{A} \neq \mathbb{0} \\ 1 & \mathcal{B} = \mathcal{A} \\ K \in \mathbb{C} & \mathcal{B} \setminus \mathcal{A} = 0 \end{cases} . \tag{D.11}$$

Next, we introduce $\{\mathcal{S}_m\}$ as the set of all sets containing exactly m out of the M open-system single-particle states, where $\{\mathcal{S}_0\} = \{\mathbb{0}\}$ and $\{\mathcal{S}_M\} = \{\mathcal{S}\}$. With this notation, we can define the vectors

$$\begin{aligned} (p'_{\mathcal{A},1}| &= \begin{cases} (p'_{\mathcal{A},0}| & (p'_{\mathcal{A},0}|W = \lambda(p'_{\mathcal{A},0}| \\ (p'_{\mathcal{A},0}| & \mathcal{A} \notin \cup_{m=1}^{M}\{\mathcal{S}_m\} \\ (p'_{\mathcal{A},0}| - \sum_{\mathcal{B}\in\{\mathcal{S}_0\}} (p'_{\mathcal{A},0}|p_{\mathcal{B},0}) \cdot (p'_{\mathcal{B},0}| & \text{otherwise} \end{cases} \\ |p_{\mathcal{A},1}) &= \begin{cases} |p_{\mathcal{A},0}) & W|p_{\mathcal{A},0}) = \lambda|p_{\mathcal{A},0}) \\ |p_{\mathcal{A},0}) & \mathcal{A} \notin \cup_{m=1}^{M}\{\mathcal{S}_{M-m}\} \\ |p_{\mathcal{A},0}) - \sum_{\mathcal{B}\in\{\mathcal{S}_M\}} (p'_{\mathcal{B},0}|p_{\mathcal{A},0}) \cdot |p_{\mathcal{B},0}) & \text{otherwise} \end{cases} \end{aligned} . \tag{D.12}$$

It is straightforward to verify from Eq. (D.4) and Eq. (D.5) that $(p'_{\mathcal{A},1}|p_{\mathcal{B},1}) = \delta_{\mathcal{A}\mathcal{B}}$ is guaranteed for $\mathcal{B}\setminus\mathcal{A} \neq \mathbb{0}$, or $\mathcal{B} = \mathcal{A}$, *or* if $\mathcal{A} \in \{\mathcal{S}_M\}$ or $\mathcal{B} \in \{\mathcal{S}_0\}$. As moreover pointed out in the previous paragraph, if $(p'_{\mathcal{A},0}|$ and $|p_{\mathcal{A},0})$ form a pair of exact eigenvectors of W according to Eq. (D.7), $(p'_{\mathcal{A},1}| = (p'_{\mathcal{A},0}|$ and $|p_{\mathcal{A},1}) = |p_{\mathcal{A},0})$ form the same pair of eigenvectors by construction. Thus, compared to $(p'_{\mathcal{A},0}|$ and $|p_{\mathcal{A},0})$, the only difference of the vectors $(p'_{\mathcal{A},1}|$ and $|p_{\mathcal{A},1})$ is that they are furthermore guaranteed to be biorthogonal to the "outer most" eigenvectors, given by the parity amplitude covector $(p'_{\mathcal{S},1}| = (p'_{\mathcal{S},0}| = (z_{\mathrm{i}}(-\mathbb{1})^N|$ and the stationary state $|p_{\mathbb{0},1}) = |p_{\mathbb{0},0}) = |z)$ [Eq. (D.2)].

Continuing the orthogonalization process, the above observation suggests the following recursive definition for all $1 \leq n \leq \left\lceil \frac{M}{2} \right\rceil$:

$$
(p'_{\mathcal{A},n}| = \begin{cases} (p'_{\mathcal{A},n-1}| & (p'_{\mathcal{A},n-1}|W = \lambda(p'_{\mathcal{A},n-1}| \\ (p'_{\mathcal{A},n-1}| & \mathcal{A} \notin \bigcup_{m=n}^{M-n}\{\mathcal{S}_m\} \\ & \text{or } n > M-n \\ (p'_{\mathcal{A},n-1}| - \sum_{\mathcal{B}\in\{\mathcal{S}_{n-1}\}} (p'_{\mathcal{A},n-1}|p_{\mathcal{B},n-1}) \cdot (p'_{\mathcal{B},n-1}| & \text{otherwise} \end{cases}
$$

$$
|p_{\mathcal{A},n}) = \begin{cases} |p_{\mathcal{A},n-1}) & W|p_{\mathcal{A},n-1}) = \lambda|p_{\mathcal{A},n-1}) \\ |p_{\mathcal{A},n-1}) & \mathcal{A} \notin \bigcup_{m=n}^{M+1-n}\{\mathcal{S}_{M-m}\} \\ |p_{\mathcal{A},n-1}) - \sum_{\mathcal{B}\in\{\mathcal{S}_{M+1-n}\}} (p'_{\mathcal{B},n-1}|p_{\mathcal{A},n-1}) \cdot |p_{\mathcal{B},n-1}) & \text{otherwise} \end{cases} ,
\tag{D.13}
$$

where $(p'_{\mathcal{A},0}| \equiv (p'_{\mathcal{A}}|$ and $|p_{\mathcal{A},0}) \equiv |p_{\mathcal{A}})$. Note that the condition $n > M - n$ is important in order not to "over-orthogonalize" for an odd number M of single-particle states, as we will see in the next section D.3.

Let us now use induction to prove that for $1 \leq n \leq \left\lceil \frac{M}{2} \right\rceil$, the orthonormality $(p'_{\mathcal{A},n}|p_{\mathcal{B},n}) = \delta_{\mathcal{A}\mathcal{B}}$ holds for $\mathcal{B}\setminus\mathcal{A} \neq \mathbb{0}$, or $\mathcal{A} = \mathcal{B}$ *or* if $\mathcal{A} \in \bigcup_{m=0}^{n-1}\{\mathcal{S}_{M-m}\}$ or $\mathcal{B} \in \bigcup_{m=0}^{n-1}\{\mathcal{S}_m\}$. The start for $n = 1$ is already given in Eq. (D.12). So assuming that the hypothesis holds for any $\left\lceil \frac{M}{2} \right\rceil - 1 \geq n > 1$, we show that it holds for $n+1$. Let us therefore explicitly verify

$$
(p'_{\mathcal{A},n+1}|p_{\mathcal{B},n+1}) = \delta_{\mathcal{A}\mathcal{B}} \quad \forall \mathcal{B}\setminus\mathcal{A} \neq \mathbb{0} \text{ or } \mathcal{A} = \mathcal{B} \text{ or } \mathcal{A} \in \bigcup_{m=0}^{n}\{\mathcal{S}_{M-m}\} \text{ or } \mathcal{B} \in \bigcup_{m=0}^{n}\{\mathcal{S}_m\}
\tag{D.14}
$$

by going through the relevant cases.

1. Let us first choose $\mathcal{A}, \mathcal{B}$ such that (D.13) dictates $(p'_{\mathcal{A},n+1}| = (p'_{\mathcal{A},n}|$ and $|p_{\mathcal{B},n+1}) = |p_{\mathcal{B},n})$, meaning that $|p_{\mathcal{B},n+1})$ is an eigenvector or $\mathcal{B} \in \bigcup_{m=0}^{n-1}\{\mathcal{S}_m\} \cup \bigcup_{m=M-n}^{M}\{\mathcal{S}_m\}$, and either that $(p'_{\mathcal{A},n+1}|$ is an eigenvector or $\mathcal{A} \in \bigcup_{m=0}^{n}\{\mathcal{S}_m\} \cup \bigcup_{m=M-n}^{M}\{\mathcal{S}_m\}$, In all these cases, the scalar product (D.14) simply equals $(p'_{\mathcal{A},n}|p_{\mathcal{B},n})$. By the inductive assumption, it is then clear that the orthonormality $(p'_{\mathcal{A},n+1}|p_{\mathcal{B},n+1}) = \delta_{\mathcal{A}\mathcal{B}}$ holds for $\mathcal{B}\setminus\mathcal{A} \neq \mathbb{0}$, or $\mathcal{B} = \mathcal{A}$ *or* if $\mathcal{A} \in$

$\bigcup_{m=0}^{n-1}\{\mathcal{S}_{M-m}\}$ or $\mathcal{B} \in \bigcup_{m=0}^{n-1}\{\mathcal{S}_m\}$. For $\mathcal{A} \in \{\mathcal{S}_{M-n}\}$, the above stated conditions for $\mathcal{A}, \mathcal{B}$ imply several possibilities: first, $(p'_{\mathcal{A},n+1}| = (p'_{\mathcal{A},0}|$ is an eigenvector of W, and hence already properly biorthonormalized by the above construction of $(p'_{\mathcal{A},0}|$. Second, $|p_{\mathcal{B},n+1}) = |p_{\mathcal{B},n})$ means either that $|p_{\mathcal{B},n+1})$ is a biorthonormalized eigenvector, or that $\mathcal{B} \in \bigcup_{m=0}^{n-1}\{\mathcal{S}_m\} \cup \bigcup_{m=M-n}^{M}\{\mathcal{S}_m\}$, with the latter in any case guaranteeing the orthonormality $(p'_{\mathcal{A},n+1}|p_{\mathcal{B},n+1}) = \delta_{\mathcal{A}\mathcal{B}}$ to hold by the inductive assumption if $\mathcal{A} \in \{\mathcal{S}_{M-n}\}$. Finally, if $\mathcal{B} \in \{S_n\}$, the above condition for $\mathcal{B}$ also dictates $|p_{\mathcal{B},n+1})$ to be an orthonormalized eigenvector.

2. For $\mathcal{A}, \mathcal{B}$ chosen such that the "otherwise" case from Eq. (D.13) holds only for the left vector, we have $\mathcal{A} \in \bigcup_{m=n+1}^{M-1-n}\{\mathcal{S}_m\}$ and either $|p_{\mathcal{B},n+1}) = |p_{\mathcal{B},n})$ being a biorthonormalized eigenvector or $\mathcal{B} \in \bigcup_{m=0}^{n-1}\{\mathcal{S}_m\} \cup \bigcup_{m=M-n}^{M}\{\mathcal{S}_m\}$. If $|p_{\mathcal{B},n+1}) = |p_{\mathcal{B},n})$ is an eigenvector, the biorthonormality is clear. In the other case, we have $\mathcal{A} \neq \mathcal{B}$ and need to verify that the following expression vanishes under the relevant conditions:

$$(p'_{\mathcal{A},n+1}|p_{\mathcal{B},n+1}) \overset{(D.13)}{=} (p'_{\mathcal{A},n}|p_{\mathcal{B},n}) - \sum_{\mathcal{C}\in\{\mathcal{S}_n\}} (p'_{\mathcal{A},n}|p_{\mathcal{C},n}) \cdot (p'_{\mathcal{C},n}|p_{\mathcal{B},n}). \quad \text{(D.15)}$$

If $\mathcal{B} \setminus \mathcal{A} \neq \mathbb{0}$, the first term $(p'_{\mathcal{A},n}|p_{\mathcal{B},n})$ gives 0 by assumption, whereas the second term in (D.15) given by the sum over $\mathcal{C}$ vanishes because we then have either $\mathcal{B} \setminus \mathcal{C} \neq \mathbb{0}$ for which $(p'_{\mathcal{C},n}|p_{\mathcal{B},n}) = 0$ by Eqs. (D.4),(D.5), or $\mathcal{B} \subseteq \mathcal{C}$ and thus $\mathcal{C} \setminus \mathcal{A} \neq \mathbb{0}$ for which $(p'_{\mathcal{A},n}|p_{\mathcal{C},n}) = 0$. If $\mathcal{A} \in \bigcup_{m=0}^{n-1}\{\mathcal{S}_{M-m}\}$ or $\mathcal{B} \in \bigcup_{m=0}^{n-1}\{\mathcal{S}_m\}$, one scalar product in each of the two terms in Eq. (D.15) equals 0 again by assumption.

The extension to the condition $\mathcal{B} \in \{\mathcal{S}_n\}$ is straightforward, since this again means that $|p_{\mathcal{B},n+1}) = |p_{\mathcal{B},n})$ is an eigenvector. The case $\mathcal{A} \in \{\mathcal{S}_{M-n}\}$ is excluded already by the condition $\mathcal{A} \in \bigcup_{m=n+1}^{M-1-n}\{\mathcal{S}_m\}$.

3. If $\mathcal{A}$ and $\mathcal{B}$ are given such that the "otherwise" case from Eq. (D.13) instead holds only for the *right* vector, $(p'_{\mathcal{A},n+1}|$ is an eigenvector or $\mathcal{A} \in \bigcup_{m=0}^{n}\{\mathcal{S}_m\} \cup \bigcup_{m=M-n}^{M}\{\mathcal{S}_m\}$, whereas $\mathcal{B} \in \bigcup_{m=n}^{M-n-1}\{\mathcal{S}_m\}$. Apart from the clear case that $(p'_{\mathcal{A},n+1}|$ is a biorthonormal eigenvector, we find either $\mathcal{A}, \mathcal{B} \in \{S_n\}$ or $\mathcal{A} \neq \mathcal{B}$ and now need to confirm

$$(p'_{\mathcal{A},n+1}|p_{\mathcal{B},n+1}) \overset{(D.13)}{=} (p'_{\mathcal{A},n}|p_{\mathcal{B},n}) - \sum_{\mathcal{C}\in\{\mathcal{S}_{M-n}\}} (p'_{\mathcal{A},n}|p_{\mathcal{C},n}) \cdot (p'_{\mathcal{C},n}|p_{\mathcal{B},n}) = \delta_{\mathcal{A}\mathcal{B}} \quad \text{(D.16)}$$

for the relevant regimes. For $\mathcal{B}\setminus\mathcal{A} \neq \mathbb{0}$, $\mathcal{A} \in \bigcup_{m=0}^{n-1}\{\mathcal{S}_{M-m}\}$ or $\mathcal{B} \in \bigcup_{m=0}^{n-1}\{\mathcal{S}_m\}$, we can argue by the inductive assumption as for case 2. For $\mathcal{A} \in \{\mathcal{S}_{M-n}\}$, Eq. (D.16) vanishes for all $\mathcal{B}$ because $\mathcal{C} \in \{S_{M-n}\}$ and therefore $(p'_{\mathcal{A},n}|p_{\mathcal{C},n}) = \delta_{\mathcal{A}\mathcal{C}}$. For $\mathcal{A}, \mathcal{B} \in \{S_n\}$, we have either $\mathcal{B} \setminus \mathcal{A} \neq \mathbb{0}$ or $\mathcal{B} = \mathcal{A}$ and $\mathcal{C} \setminus \mathcal{A} \neq \mathbb{0}$ for

$\mathcal{C} \in \{S_{M-n}\}$, guaranteeing Eq. (D.16) to hold. For all other $\mathcal{A}, \mathcal{B}$ which are not excluded, we again have $\mathcal{B} \setminus \mathcal{A} \neq \mathbb{0}$ and $\mathcal{C} \setminus \mathcal{A} \neq \mathbb{0}$.

4. Finally assuming $\mathcal{A}$ and $\mathcal{B}$ for which the "otherwise" case from Eq. (D.13) holds for the left and right vector, we have $\mathcal{A} \in \bigcup_{m=n+1}^{M-n-1}\{\mathcal{S}_m\}$ and $\mathcal{B} \in \bigcup_{m=n}^{M-n-1}\{\mathcal{S}_m\}$. Moreover, we can use the restriction to $\left\lceil \frac{M}{2} \right\rceil - 1 \geq n > 1$ and hence $\mathcal{S}_{M-n} \setminus \mathcal{S}_n \neq \mathbb{0}$ to immediately simplify

$$\begin{aligned}(p'_{\mathcal{A},n+1}|p_{\mathcal{B},n+1}) \overset{\text{(D.13)}}{=} (p'_{\mathcal{A},n}|p_{\mathcal{B},n}) &- \sum_{\mathcal{C}\in\{\mathcal{S}_{M-n}\}} (p'_{\mathcal{A},n}|p_{\mathcal{C},n}) \cdot (p'_{\mathcal{C},n}|p_{\mathcal{B},n}) \\ &- \sum_{\mathcal{C}\in\{\mathcal{S}_n\}} (p'_{\mathcal{A},n}|p_{\mathcal{C},n}) \cdot (p'_{\mathcal{C},n}|p_{\mathcal{B},n}) \\ &+ \sum_{\substack{\mathcal{C}\in\{\mathcal{S}_n\} \\ \mathcal{D}\in\{\mathcal{S}_{M-n}\}}} (p'_{\mathcal{A},n}|p_{\mathcal{C},n}) \cdot \underbrace{(p'_{\mathcal{C},n}|p_{\mathcal{D},n})}_{=0} \cdot (p'_{\mathcal{D},n}|p_{\mathcal{B},n}) \\ = (p'_{\mathcal{A},n}|p_{\mathcal{B},n}) &- \sum_{\mathcal{C}\in\{\mathcal{S}_{M-n}\}\cup\{\mathcal{S}_n\}} (p'_{\mathcal{A},n}|p_{\mathcal{C},n}) \cdot (p'_{\mathcal{C},n}|p_{\mathcal{B},n}).\end{aligned} \tag{D.17}$$

The restriction to $\mathcal{A} \in \bigcup_{m=n+1}^{M-n-1}\{\mathcal{S}_m\}$ furthermore implies that the sum over $\mathcal{C} \in \{S_{M-n}\}$ vanishes due to $\mathcal{C} \setminus \mathcal{A} \neq \mathbb{0}$ and hence $(p'_{\mathcal{A},n}|p_{\mathcal{C},n}) = 0$:

$$(p'_{\mathcal{A},n+1}|p_{\mathcal{B},n+1}) = (p'_{\mathcal{A},n}|p_{\mathcal{B},n}) - \sum_{\mathcal{C}\in\{\mathcal{S}_n\}} (p'_{\mathcal{A},n}|p_{\mathcal{C},n}) \cdot (p'_{\mathcal{C},n}|p_{\mathcal{B},n}). \tag{D.18}$$

The vanishing of Eq. (D.18) is clear for $\mathcal{B} \setminus \mathcal{A} \neq \mathbb{0}$ by the same argument as given below Eq. (D.15); the cases $\mathcal{A} \in \bigcup_{m=0}^{n}\{\mathcal{S}_{M-m}\}$ or $\mathcal{B} \in \bigcup_{m=0}^{n-1}\{\mathcal{S}_m\}$ are already excluded by the "otherwise" case in Eq. (D.13). This holds in particular for $\mathcal{A} \in \{\mathcal{S}_{M-n}\}$. For $\mathcal{B} \in \{\mathcal{S}_n\}$, we can use $(p'_{\mathcal{C},n}|p_{\mathcal{B},n}) = \delta_{\mathcal{B}\mathcal{C}}$ to infer

$$\begin{aligned}(p'_{\mathcal{A},n+1}|p_{\mathcal{B},n+1}) \overset{\text{(D.18)}}{=} &(p'_{\mathcal{A},n}|p_{\mathcal{B},n}) - \sum_{\mathcal{C}\in\{\mathcal{S}_n\}} (p'_{\mathcal{A},n}|p_{\mathcal{C},n}) \cdot (p'_{\mathcal{C},n}|p_{\mathcal{B},n}) \\ \underset{(p'_{\mathcal{C},n}|p_{\mathcal{B},n})=\delta_{\mathcal{C}\mathcal{B}}}{\overset{\mathcal{B}\in\{\mathcal{S}_n\}}{=}} &(p'_{\mathcal{A},n}|p_{\mathcal{B},n}) - (p'_{\mathcal{A},n}|p_{\mathcal{B},n}) = 0.\end{aligned} \tag{D.19}$$

Cases 1 to 4 together complete the proof by induction that for $1 \leq n \leq \left\lceil \frac{M}{2} \right\rceil$, the orthonormality $(p'_{\mathcal{A},n}|p_{\mathcal{B},n}) = \delta_{\mathcal{A}\mathcal{B}}$ holds for $\mathcal{B} \setminus \mathcal{A} \neq \mathbb{0}$, or $\mathcal{A} = \mathcal{B}$ *or* if $\mathcal{A} \in \bigcup_{m=0}^{n-1}\{\mathcal{S}_{M-m}\}$ or $\mathcal{B} \in \bigcup_{m=0}^{n-1}\{\mathcal{S}_m\}$. The final point is to realize that for picking $n = \left\lceil \frac{M}{2} \right\rceil$, this means that $(p'_{\mathcal{A},n}|p_{\mathcal{B},n}) = \delta_{\mathcal{A}\mathcal{B}}$ holds for *any* $\mathcal{A}, \mathcal{B}$. The orthogonalized vectors introduced in Eq. (D.9) are therefore recursively defined through Eqs. (D.12),(D.13) as

$$(\tilde{p}'_{\mathcal{A}}| = (p'_{\mathcal{A},\lceil \frac{M}{2} \rceil}| \quad , \quad |\tilde{p}_{\mathcal{A}}) = |p_{\mathcal{A},\lceil \frac{M}{2} \rceil}). \tag{D.20}$$

D.3 Basis for quantum dot systems

As examples of applying the scheme outlined in the previous section D.2, let us choose the two quantum-dot systems described in Sec. 2.1.1 and Sec. 2.1.2 of the main text. We start with the possibly spin-resolved interacting single-level quantum dot.

D.3.1 Single-level quantum dot

There are $M = 2$ single-particle states: $\mathcal{S} = \{\uparrow, \downarrow\}$. Assuming for simplicity that $(p'_{\mathbb{0}}|, (p'_{\mathcal{S}}|, |p_{\mathbb{0}}), |p_{\mathcal{S}})$ are the only eigenvectors of the rate-equation limit kernel W in the (sub-)parity basis,

$$\begin{aligned}
(p'_{\mathbb{0},0}| = (\mathbb{1}| \quad &, \quad |z) = |p_{\mathbb{0},0}) \\
(p'_{\{\uparrow\},0}| = (z_{\mathrm{i},\{\uparrow\}}(-\mathbb{1})^{N_\uparrow} \otimes \mathbb{1}_{\{\downarrow\}}| \quad &, \quad |(-\mathbb{1})^{N_\uparrow} \otimes z_{\{\downarrow\}}) = |p_{\{\uparrow\},0}) \\
(p'_{\{\downarrow\},0}| = (z_{\mathrm{i},\{\downarrow\}}(-\mathbb{1})^{N_\downarrow} \otimes \mathbb{1}_{\{\uparrow\}}| \quad &, \quad |(-\mathbb{1})^{N_\downarrow} \otimes z_{\{\uparrow\}}) = |p_{\{\downarrow\},0}) \\
(p'_{\mathcal{S},0}| = (z_{\mathrm{i}}(-\mathbb{1})^{N}| \quad &, \quad = |(-\mathbb{1})^{N}) = |p_{\mathcal{S},0}),
\end{aligned} \tag{D.21}$$

we need only $\left\lceil \frac{M}{2} \right\rceil = \lceil 1 \rceil = 1$ orthogonalization step:

$$\begin{aligned}
(p'_{\mathbb{0},1}| &= (p'_{\mathbb{0},0}| = (\mathbb{1}| \ , \ |z) = |p_{\mathbb{0},0}) = |p_{\mathbb{0},1}) \\
(p'_{\{\uparrow\},1}| &= (p'_{\{\uparrow\},0}| - (p'_{\{\uparrow\},0}|z)(\mathbb{1}| \ , \ |p_{\{\uparrow\},0}) - (p'_{\mathcal{S},0}|p_{\{\uparrow\},0})|(-\mathbb{1})^{N}) = |p_{\{\uparrow\},1}) \\
(p'_{\{\downarrow\},1}| &= (p'_{\{\downarrow\},0}| - (p'_{\{\downarrow\},0}|z)(\mathbb{1}| \ , \ |p_{\{\downarrow\},0}) - (p'_{\mathcal{S},0}|p_{\{\downarrow\},0})|(-\mathbb{1})^{N}) = |p_{\{\downarrow\},1}) \\
(p'_{\mathcal{S},1}| &= (p'_{\mathcal{S},0}| = (z_{\mathrm{i}}(-\mathbb{1})^{N}| \ , \ |(-\mathbb{1})^{N}) = |p_{\mathcal{S},0}) = |p_{\mathcal{S},1}).
\end{aligned} \tag{D.22}$$

D.3.2 Single-level quantum dot coupled to sensor dot

Now, the $M = 3$ single-particle states are $\mathcal{S} = \{\uparrow, \downarrow, S\}$, and we again assume that $(p'_{\mathbb{0}}|, (p'_{\mathcal{S}}|, |p_{\mathbb{0}}), |p_{\mathcal{S}})$ are the only eigenvectors of the rate-equation limit kernel W in the (sub-)parity basis. We need $\left\lceil \frac{M}{2} \right\rceil = \left\lceil \frac{3}{2} \right\rceil = 2$ orthogonalization steps. The 8 left and right vectors to start from are

$$\begin{aligned}
(p'_{\mathbb{0},0}| = (\mathbb{1}| \quad &, \quad |z) = |p_{\mathbb{0},0}) \\
(p'_{\{\uparrow\},0}| = (z_{\mathrm{i},\{\uparrow\}}(-\mathbb{1})^{N_\uparrow} \otimes \mathbb{1}_{\{\downarrow,S\}}| \quad &, \quad |(-\mathbb{1})^{N_\uparrow} \otimes z_{\{\downarrow,S\}}) = |p_{\{\uparrow\},0}) \\
(p'_{\{\downarrow\},0}| = (z_{\mathrm{i},\{\downarrow\}}(-\mathbb{1})^{N_\downarrow} \otimes \mathbb{1}_{\{\uparrow,S\}}| \quad &, \quad |(-\mathbb{1})^{N_\downarrow} \otimes z_{\{\uparrow,S\}}) = |p_{\{\downarrow\},0}) \\
(p'_{\{S\},0}| = (z_{\mathrm{i},\{S\}}(-\mathbb{1})^{N_S} \otimes \mathbb{1}_{\{\uparrow,\downarrow\}}| \quad &, \quad |(-\mathbb{1})^{N_S} \otimes z_{\{\uparrow,\downarrow\}}) = |p_{\{S\},0}) \\
(p'_{\{\uparrow,\downarrow\},0}| = (z_{\mathrm{i},\{\uparrow,\downarrow\}}(-\mathbb{1})^{N_\uparrow+N_\downarrow} \otimes \mathbb{1}_{\{S\}}| \quad &, \quad |(-\mathbb{1})^{N_\uparrow+N_\downarrow} \otimes z_{\{S\}}) = |p_{\{\uparrow,\downarrow\},0}) \\
(p'_{\{\uparrow,S\},0}| = (z_{\mathrm{i},\{\uparrow,S\}}(-\mathbb{1})^{N_\uparrow+N_S} \otimes \mathbb{1}_{\{\downarrow\}}| \quad &, \quad |(-\mathbb{1})^{N_\uparrow+N_S} \otimes z_{\{\downarrow\}}) = |p_{\{\uparrow,S\},0}) \\
(p'_{\{\downarrow,S\},0}| = (z_{\mathrm{i},\{\downarrow,S\}}(-\mathbb{1})^{N_\downarrow+N_S} \otimes \mathbb{1}_{\{\uparrow\}}| \quad &, \quad |(-\mathbb{1})^{N_\downarrow+N_S} \otimes z_{\{\uparrow\}}) = |p_{\{\downarrow,S\},0}) \\
(p'_{\mathcal{S},0}| = (z_{\mathrm{i}}(-\mathbb{1})^{N}| \quad &, \quad = |(-\mathbb{1})^{N}) = |p_{\mathcal{S},0}).
\end{aligned} \tag{D.23}$$

Applying Eq. (D.13) as the first orthogonalization step, we obtain

$$
\begin{aligned}
(p'_{\mathbb{0},1}| = (p'_{\mathbb{0},0}| = (\mathbb{1}|\ ,\ |z) = |p_{\mathbb{0},0}) = |p_{\mathbb{0},1}) \\
(p'_{\{\uparrow\},1}| = (p'_{\{\uparrow\},0}| - (p'_{\{\uparrow\},0}|z)(\mathbb{1}|\ ,\ |p_{\{\uparrow\},0}) - (p'_{\mathcal{S},0}|p_{\{\uparrow\},0})|(-\mathbb{1})^N) = |p_{\{\uparrow\},1}) \\
(p'_{\{\downarrow\},1}| = (p'_{\{\downarrow\},0}| - (p'_{\{\downarrow\},0}|z)(\mathbb{1}|\ ,\ |p_{\{\downarrow\},0}) - (p'_{\mathcal{S},0}|p_{\{\downarrow\},0})|(-\mathbb{1})^N) = |p_{\{\downarrow\},1}) \\
(p'_{\{S\},1}| = (p'_{\{S\},0}| - (p'_{\{S\},0}|z)(\mathbb{1}|\ ,\ |p_{\{S\},0}) - (p'_{\mathcal{S},0}|p_{\{S\},0})|(-\mathbb{1})^N) = |p_{\{S\},1}) \\
(p'_{\{\uparrow,\downarrow\},1}| = (p'_{\{\uparrow,\downarrow\},0}| - (p'_{\{\uparrow,\downarrow\},0}|z)(\mathbb{1}|\ ,\ |p_{\{\uparrow,\downarrow\},0}) - (p'_{\mathcal{S},0}|p_{\{\uparrow,\downarrow\},0})|(-\mathbb{1})^N) = |p_{\{\uparrow,\downarrow\},1}) \\
(p'_{\{\uparrow,S\},1}| = (p'_{\{\uparrow,S\},0}| - (p'_{\{\uparrow,S\},0}|z)(\mathbb{1}|\ ,\ |p_{\{\uparrow,S\},0}) - (p'_{\mathcal{S},0}|p_{\{\uparrow,S\},0})|(-\mathbb{1})^N) = |p_{\{\uparrow,S\},1}) \\
(p'_{\{\downarrow,S\},1}| = (p'_{\{\downarrow,S\},0}| - (p'_{\{\downarrow,S\},0}|z)(\mathbb{1}|\ ,\ |p_{\{\downarrow,S\},0}) - (p'_{\mathcal{S},0}|p_{\{\downarrow,S\},0})|(-\mathbb{1})^N) = |p_{\{\downarrow,S\},1}) \\
(p'_{\mathcal{S},1}| = (p'_{\mathcal{S},0}| = (z_{\mathrm{i}}(-\mathbb{1})^N|\ ,\ |(-\mathbb{1})^N) = |p_{\mathcal{S},0}) = |p_{\mathcal{S},1}).
\end{aligned}
\tag{D.24}
$$

In the final orthogonalization process, this becomes

$$
\begin{aligned}
(\tilde{p}'_{\mathbb{0}}| = (\mathbb{1}| \quad &, \quad |z) = |\tilde{p}_{\mathbb{0}}) \\
(\tilde{p}'_{\{\uparrow\}}| = (p'_{\{\uparrow\},1}| \quad &, \quad |p_{\{\uparrow\},1}) - \sum_{s=\downarrow,S} (p'_{\{\uparrow,s\},1}|p_{\{\uparrow\},1})|p_{\{\uparrow,s\},1}) = |\tilde{p}_{\{\uparrow\}}) \\
(\tilde{p}'_{\{\downarrow\}}| = (p'_{\{\downarrow\},1}| \quad &, \quad |p_{\{\downarrow\},1}) - \sum_{s=\uparrow,S} (p'_{\{\downarrow,s\},1}|p_{\{\downarrow\},1})|p_{\{\uparrow,s\},1}) = |\tilde{p}_{\{\downarrow\}}) \\
(\tilde{p}'_{\{S\}}| = (p'_{\{S\},1}| \quad &, \quad |p_{\{S\},1}) - \sum_{s=\uparrow,\downarrow} (p'_{\{S,s\},1}|p_{\{S\},0})|p_{\{S,s\},1}) = |\tilde{p}_{\{S\}}) \\
(\tilde{p}'_{\{\uparrow,\downarrow\}}| = (p'_{\{\uparrow,\downarrow\},1}| \quad &, \quad |p_{\{\uparrow,\downarrow\},1}) = |\tilde{p}_{\{\uparrow,\downarrow\}}) \\
(\tilde{p}'_{\{\uparrow,S\}}| = (p'_{\{\uparrow,S\},1}| \quad &, \quad |p_{\{\uparrow,S\},1}) = |\tilde{p}_{\{\uparrow,S\}}) \\
(\tilde{p}'_{\{\downarrow,S\}}| = (p'_{\{\downarrow,S\},1}| \quad &, \quad |p_{\{\downarrow,S\},1}) = |\tilde{p}_{\{\downarrow,S\}}) \\
(\tilde{p}'_{\mathcal{S}}| = (z_{\mathrm{i}}(-\mathbb{1})^N| \quad &, \quad |(-\mathbb{1})^N) = |\tilde{p}_{\mathcal{S}}).
\end{aligned}
\tag{D.25}
$$

Note that since $n = 2 > M - n = 1$, the left vectors have not been modified anymore, see Eq. (D.13). This is in fact important: if we had applied the scheme also to $(p'_{\{\uparrow,\downarrow\},1}|$, $(p'_{\{\uparrow,S\},1}|$ and $(p'_{\{\downarrow,S\},1}|$, we would have overcompensated the effect of orthogonalizing the right vectors $|p_{\{\uparrow\},1})$, $|p_{\{\downarrow\},1})$ and $|p_{\{S\},1})$. This specialty occurs due to the odd number of $M = 3$ single-particle states.

Appendix E

Microscopic picture of the dual system

When confronted with the notion of the dual model and its involved energy inversion illustrated in Fig. 3.1(b), one question typically suggests itself immediately: is the dual system just a useful, yet ultimately effective notion that *happens* to enter the fermionic master equation, or does it correspond to a more fundamental, underlying microscopic picture of the system dynamics? Or put differently, does it have a deeper meaning if the dual kernel $\overline{W}$ is physical according to the criteria set in Sec. 2.3.2, or is this nothing more than a consequence of how the dual model is constructed? To answer these questions, it turns out to be very important to distinguish between the dissipative kernel W on the one hand, and the full evolution kernel $-\mathrm{i}L + W$ including the local coherent dynamics on the other hand, see Eq. (2.30). Let us develop this argument in this appendix.

A striking inconsistency in the definition (3.5) of the dual dissipative Born-Markov kernel $\overline{W} = W(-H, \{-\mu_\alpha\})$ is that the energy inversion applies only to the local energies H and the chemical potentials μ_α, whereas the reservoir energies H_R are kept as they are. The appendix to paper V demonstrates that in the Markovian, weak-coupling limit, one may alternatively obtain the dual kernel by first implementing a *total energy inversion* [2]

$$(\overline{H}_\mathrm{tot}, \{\overline{\mu}_\alpha\}) = (-H_\mathrm{tot}, \{-\mu_\alpha\}) \tag{E.1}$$

including the dual, energy-inverted reservoir Hamiltonian $\overline{H}_\mathrm{R} = \sum_\alpha \overline{H}_\alpha = -\sum_\alpha H_\alpha$. Subsequently, one repeats the derivation of the master equation outlined in sections 2.2 and 2.3 for the dual total Hamiltonian $\overline{H}_\mathrm{tot}$ and, importantly, for a *completely energy-inverted* initial reservoir state

$$\begin{aligned}\overline{\rho}_0^\mathrm{R} &= \exp\left(-\sum_\alpha \left(\overline{H}_\alpha - \overline{\mu}_\alpha N_\alpha\right)/T_\alpha\right) \Big/ \operatorname*{Tr}_\mathrm{R}\left[\exp\left(-\sum_\alpha \left(\overline{H}_\alpha - \overline{\mu}_\alpha N_\alpha\right)/T_\alpha\right)\right] \\ &\overset{\text{(E.1)}}{=} \exp\left(+\sum_\alpha \left(H_\alpha - \mu_\alpha N_\alpha\right)/T_\alpha\right) \Big/ \operatorname*{Tr}_\mathrm{R}\left[\exp\left(+\sum_\alpha \left(H_\alpha - \mu_\alpha N_\alpha\right)/T_\alpha\right)\right].\end{aligned} \tag{E.2}$$

[2] Note that the inversion of the tunneling Hamiltonian $H_\mathrm{tun} \to \overline{H}_\mathrm{tun} = -H_\mathrm{tun}$ is irrelevant, since W is quadratic in H_tun.

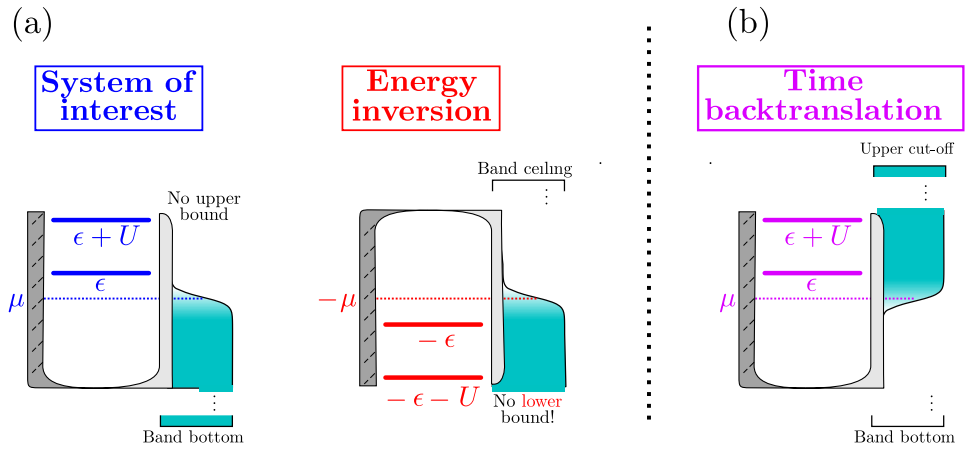

Figure E.1: ***(a)*** *Sketch of dual mapping through sign-inversion of the* total *system Hamiltonian – as specified in Eqs. (E.1) and (E.2) – applied to the example of a single-level quantum dot [Sec. (2.1.1)] weakly coupled to a non-interacting reservoir. The dual system can be understood as an energy-inverted open subsystem embedded into a Dirac sea occupied by particles of negative mass.*
(b) *Reinterpretation of the energy-inverted dual model in terms of a time-backtranslated, positive-energy system in which the environment assumes an anti-equilibrated, negative temperature state.*

The obtained dual dissipative kernel $\overline{W}$ is then given by

$$\overline{W} = W(\overline{H}_{\rm tot}; \overline{\rho}_0^{\rm R}) = W\left(-H_{\rm tot}; \rho_0^{\rm R}(-H_{\rm R}, \{-\mu_\alpha\})\right). \tag{E.3}$$

Figure E.1(a) illustrates that the dual system can be represented by an absolutely energy-inverted, possibly interacting open system embedded into non-interacting, absolutely energy-inverted reservoirs. The latter are ultimately nothing else but a manifestation of the *Dirac sea*. In particular, the inverted reservoirs suffer from the usual problem of hosting an infinite amount of particles at absolutely negative energies, and thus a pseudo-density $\overline{\rho}_0^{\rm R}$ which cannot be properly normalized, as a quick inspection of Eq. (E.2) confirms.

To avoid the typical problems of the Dirac sea interpretation, we apply the well-known trick of interpreting a forward time translation of the total, closed system according to an inverted Liouvillian $-L_{\rm tot}$ by a *time backtranslation* – not to be confused with time reversal [1] – according to the original Liouvillian $L_{\rm tot}$:

$$\overline{\rho}^{\rm tot}(t) = \exp\left(-i\overline{L}_{\rm tot}t\right)\overline{\rho}_0^{\rm tot} \underset{(2.17)}{\overset{(E.1)}{=}} \exp\left(-iL_{\rm tot}(-t)\right)\left[\overline{\rho}_0^{\rm R} \times \rho_0\right] \tag{E.4}$$

In the positive-energy picture, the dual reservoir state $\overline{\rho}_0^{\rm R}$ represents an inversion of all reservoir occupations, i.e., effectively an anti-equilibrated negative temperature

[1] Note that the antiunitary time reversal operator is a discrete member of the Lorentz group, as opposed to the continuous time backtranslation in the Poincaré group.

ensemble in which single-particle states with higher instead of lower energies are more likely occupied, see Fig. E.1(b). While formally still not normalizable, it is clear that since ρ_0^{R} as a function of energy has a cut-off at the global band bottom in the environment, and thus a finite total particle number, the inverted state $\overline{\rho}_0^{\mathrm{R}}$ must in principle be modified by an additional *high-energy* cut-off [1] to exactly match this total particle number and ensure normalizability.

Aside from these technical considerations, the important physical point is that the dual initial condition $\overline{\rho}_0^{\mathrm{R}} \times \rho_0$ is in fact a *final* condition for the dual evolution in the positive-energy picture. Together with the assumption of purely Liouvillian evolution, it fixes how $\overline{\rho}^{\mathrm{tot}}(t) = \rho^{\mathrm{tot}}(-t)$ has looked like for times $-t$ even *prior* to the final time $t = 0$, at which the environment is *demanded* to assume $\overline{\rho}_0^{\mathrm{R}}$ with statistical independence from the open system state ρ_0. While certainly an unusual concept, such a backtranslation from a final state is theoretically as valid as forward translation from an initial state, i.e., $\overline{\rho}^{\mathrm{tot}}(t) = \rho^{\mathrm{tot}}(-t)$ remains a valid density operator at any t. Focussing especially on the dual *reduced* density operator $\overline{\rho}(t) = \underset{\mathrm{R}}{\mathrm{Tr}}\,[\overline{\rho}^{\mathrm{tot}}(t)]$ in the Markovian, weak-coupling limit, the virtually impossible-to-realize statistical independence at the *final* time of the continuous total-system evolution is practically irrelevant for the long-time limit, or rather, the "distant past" limit of $\overline{\rho}(t)$ according to Sec. 2.3.1. More explicitly, applying the approximation scheme outlined in Sec. 2.3.1 to Eq. (E.4), $\overline{\rho}(t)$ obeys the usual Born-Markov master equation (2.30) with an energy-inverted kernel:

$$\partial_t |\overline{\rho}(t)) = \overline{A} |\overline{\rho}(t)) \quad , \quad \overline{A} = -\mathrm{i}\overline{L} + \overline{W}, \tag{E.5}$$

where $\overline{W}$ is defined in Eq. (E.3), and $\overline{L} = -L$.

Tracing back everything from Eq. (E.5) to Eq. (E.1), there indeed seems to be a microscopic picture behind duality. Namely, the dual open-system evolution $\overline{\rho}(t)$ answers the following question: given a *time-independent* Hamiltonian H_{tot}, i.e., no external interference, and assuming weak, Markovian coupling between open system and environment, where did the open system come from at times $-t$ if at some *final* time $-t \equiv 0$, the total system assumes $\overline{\rho}_0^{\mathrm{R}} \times \rho_0$ [Eq. (E.2)]?

In the above picture, the dual reservoir state $\overline{\rho}_0^{\mathrm{R}}$ can be seen as one possible past origin from where the locally equilibrated reservoirs ρ_0^{R} have come from. The state z_{i} [Sec. (3.2.2)] represents the *stationary*, infinite-past limit of the dual open-system state in the presence of these excited reservoirs. Interestingly, this makes it plausible that according to Sec. 3.2.3, z_{i} can often be interpreted as a maximally unstable state: a tunnel coupling to an anti-equilibrated environment is expected to also anti-equilibrate the open system. And indeed, as papers II-V explicitly show and use for the single-level quantum, the dual stationary state is given by

[1] Crucially, while this extra cut-off solves the formal problem of normalizability, it has no other consequences for the dual kernel $\overline{W}$ in the Born-Markov limit: since it is energetically equally far away from the dual potentials $\overline{\mu}_\alpha$ as the band bottom from the potentials μ_α, it is consitent to neglect the high-energy cut-off in evaluating $\overline{W}$ whenever the band bottom is neglected.

the temperature-inverted distribution $|z_\mathrm{i})\sim\exp\left(+(H-\mu N)/T\right)$ whenever $|z)$ is the equilibrium grand-canonical ensemble with respect to a common potential μ and temperature T in the reservoirs.

As intruiging as the above microscopic picture for duality may seem, there is one major inconsistency between Eq. (E.5) and the duality relation (3.4). Namely, the latter *does not* hold in the same form for the full evolution kernel $A=-\mathrm{i}L+W$, as one can easily check explicitly when using local parity-superselection, $\mathcal{P}L\mathcal{P}=L$:

$$A+\mathcal{P}\overline{A}^\dagger\mathcal{P}\underset{\mathcal{P}L\mathcal{P}=L}{\overset{(E.5)}{=}}W+\mathcal{P}\overline{W}^\dagger\mathcal{P}-\mathrm{i}L+\left[-\mathrm{i}\overline{L}\right]^\dagger\overset{(3.4)}{=}-\Gamma-2\mathrm{i}L\neq-\Gamma. \tag{E.6}$$

The original fix of this problem from paper II is to introduce the "Wick-rotated" coupling Hamiltonian $H_\mathrm{tun}\to\mathrm{i}H_\mathrm{tun}$, which chapter 3 has introduced at the very beginning in Sec. 3.1.1: since W is quadratic in H_tun in the sequential tunneling limit, the *only* effect is an additional sign in $\overline{W}$, which can be interpreted as an additional sign in the tunnel couplings (2.8), $\overline{\Gamma}_{m,ll'}=-\Gamma_{m,ll'}$. The duality relation then reads $A-\mathcal{P}\overline{A}^\dagger\mathcal{P}=-\Gamma$, see paper II and Lic. Th. [110]. The price of this additional sign is that $\overline{A}$ is not anymore dissipative, and thus, not physical, thereby prohibiting any microscopic interpretation of duality. In practice, we can, however, still derive the same general conclusions as in Sec. 3.2, with $|z)$ and $|z_\mathrm{i})$ now being the zero modes of A and $\overline{A}$ instead of W and $\overline{W}$. The crucial point is that $-\overline{A}$ *is* physical under the same assumptions made in Sec. 3.1.2, and has exactly the same (generalized) eigenvectors as $\overline{A}$. This means in particular that $|z_\mathrm{i})$ is a physically valid, dual stationary density operator, and has the same properties as described in sections 3.2.2 and 3.2.3 of the main text, apart from the minus sign in its $\Gamma_{m,ll'}$-dependence.

Alternatively, we may either consciously neglect the energy inversion $L\to-L$ in the purely local part $-\mathrm{i}L$ of the full kernel $A=-\mathrm{i}L+W$, as explained in paper V, or simply keep the definition (E.3) of the dual dissipative kernel as well as its microscopic interpretation. Following the latter variant, we consider Eq. (E.6) instead of Eq. (3.4) as the *actual* duality relation in the Markovian, weak-coupling limit. The term $-2\mathrm{i}L$ on the right-hand side of Eq. (E.6) then generally prevents us from establishing a direct link between modes and amplitude covectors of the type given in (3.6). Yet, everything developed in Sec. 3.2 is perfectly valid as long as there exists at least one stationary solution $|z)$ with vanishing coherences, i.e., $L|z)=0$ and hence $0=L|z_\mathrm{i})=(z_\mathrm{i}(-\mathbb{1})^N|L$. In this case, the duality-induced basis vectors from Sec. 3.2.4 would reside entirely in the probability sector of A.

As a final remark, we note that the quantum correction $-2\mathrm{i}L$ in Eq. (E.6) appears, in a very similar form, when generalizing detailed balance (2.45) beyond the rate-equation limit [Sec. (2.4.1)] to what is known as *quantum detailed balance* [209]. It is thus an interesting future question whether there is a deeper link between duality and quantum detailed balance, and whether this speaks in favor of one of the above ways to understand duality in case the local Liouvillian dynamics matter.

Appendix F

Derivation of the fermionic duality in the rate-equation limit

This appendix gives a straightforward proof of the fermionic duality (3.4) in the rate-equation limit [Sec. (2.4.1)] and for energy-independent diagonal couplings $\Gamma_{m,ll}$ [Eq. (2.8)]. We start with the lead sum Eq. (2.34) of the full kernel W :

$$W \overset{(2.34)}{=} \sum_{\alpha} W_{\alpha}. \tag{F.1}$$

If we prove the duality for the reservoir-resolved kernel W_α, i.e.,

$$W_\alpha + \mathcal{P}\overline{W}_\alpha^\dagger \mathcal{P} = -\Gamma_\alpha \quad , \quad \Gamma_\alpha = \sum_{ml} \delta_{\alpha_m \alpha} \Gamma_{m,ll}, \tag{F.2}$$

equation (F.1) immediately implies Eq. (3.4) for the full kernel W. The advantage of this approach is that for only a single reservoir, we can immediately write down the "Golden rule" rates $W_{\alpha,ij}$ for tunneling induced transitions $|E_i) \leftarrow |E_j) \neq |E_i)$ between many-body energy eigenstates $|E_i) = |E_i\rangle\langle E_i|$ of the open subsystem:

$$\begin{aligned} W_{\alpha,ij} &= (E_i|W_\alpha|E_j) \\ &= \sum_{mll'} \delta_{\alpha_m \alpha} \Gamma_{m,ll'} \left[f\left(\frac{E_{ij}-\mu_\alpha}{T_\alpha}\right) \langle E_i|d_l^\dagger|E_j\rangle\langle E_j|d_{l'}|E_i\rangle \right. \\ &\qquad \left. + \left[1 - f\left(\frac{E_{ji}-\mu_\alpha}{T_\alpha}\right)\right] \langle E_i|d_{l'}|E_j\rangle\langle E_j|d_l^\dagger|E_i\rangle \right], \end{aligned} \tag{F.3}$$

where $f(x) = [\exp(x)+1]^{-1}$ is the Fermi function, $E_{ij} = E_i - E_j$, and the state overlaps impose selection rules for possible transitions in the sequential tunneling regime. Using the key property $f(-x) = 1 - f(x)$ of this function, one finds

$$\begin{aligned} W_{\alpha,ji} \overset{(F.3)}{=} \sum_{mll'} \delta_{\alpha_m \alpha} \Gamma_{m,ll'} &\left[f\left(\frac{E_{ji}-\mu_\alpha}{T_\alpha}\right) \langle E_j|d_l^\dagger|E_i\rangle\langle E_i|d_{l'}|E_j\rangle \right. \\ &\left. + \left[1 - f\left(\frac{E_{ij}-\mu_\alpha}{T_\alpha}\right)\right] \langle E_j|d_{l'}|E_i\rangle\langle E_i|d_l^\dagger|E_j\rangle \right] \end{aligned}$$

$$= \sum_{mll'} \delta_{\alpha_m \alpha} \Gamma_{m,ll'} \left[\left[1 - f\left(-\frac{E_{ji} - \mu_\alpha}{T_\alpha} \right) \right] \langle E_i | d_{l'} | E_j \rangle \langle E_j | d_l^\dagger | E_i \rangle \right.$$
$$\left. + f\left(-\frac{E_{ij} - \mu_\alpha}{T_\alpha} \right) \langle E_i | d_l^\dagger | E_j \rangle \langle E_j | d_{l'} | E_i \rangle \right]$$
$$\overset{(F.3)}{=} W_{\alpha,ij}(-E_{ij}, -\mu_\alpha) = \overline{W}_{\alpha,ij}. \tag{F.4}$$

This already proves the duality (3.25) for the off-diagonal elements of the kernel W_α in the probability sector (rate matrix). For the diagonal elements, we now use that probability conservation (2.44) dictates

$$W_{\alpha,ii} = -\sum_{j \neq i} W_{\alpha,ji}. \tag{F.5}$$

Namely, using again $f(x) + f(-x) = 1$, this implies

$$W_{\alpha,ii} + \overline{W}_{\alpha,ii} \overset{(F.5)}{=} -\sum_{j \neq i} \left[W_{ji} + \overline{W}_{ji} \right]$$
$$\underset{(F.4)}{\overset{(F.3)}{=}} \sum_{\substack{mll' \\ j \neq i}} \delta_{\alpha_m \alpha} \Gamma_{m,ll'} \left[\langle E_j | d_l^\dagger | E_i \rangle \langle E_i | d_{l'} | E_j \rangle + \langle E_j | d_{l'} | E_i \rangle \langle E_i | d_l^\dagger | E_j \rangle \right]. \tag{F.6}$$

We now realize that since parity superselection [158–160] dictates $|E_j\rangle$ to be of fixed fermion-parity, $(-\mathbb{1})^N |E_j\rangle = \pm |E_j\rangle$, we have

$$\langle E_i | d_l^\dagger | E_i \rangle = \langle E_i | (-\mathbb{1})^N (-\mathbb{1})^N d_l^\dagger | E_i \rangle = -\langle E_i | (-\mathbb{1})^N d_l^\dagger (-\mathbb{1})^N | E_i \rangle$$
$$= -\langle E_i | d_l^\dagger | E_i \rangle = 0, \tag{F.7}$$

and, analogously, $\langle E_i | d_j | E_i \rangle = 0$. This allows us to extend the sum over j in Eq. (F.6) to all states including i, thereby simplifying the whole expression to a trace:

$$W_{\alpha,ii} + \overline{W}_{\alpha,ii} \underset{(F.7)}{\overset{(F.6)}{=}} -\sum_{mll'} \delta_{\alpha_m \alpha} \Gamma_{m,ll'} \mathrm{Tr} \left[d_l^\dagger | E_i \rangle \langle E_i | d_{l'} + d_{l'} | E_i \rangle \langle E_i | d_l^\dagger \right]$$
$$= -\sum_{mll'} \delta_{\alpha_m \alpha} \Gamma_{m,ll'} \mathrm{Tr} \left[\left\{ d_{l'}, d_l^\dagger \right\} | E_i \rangle \langle E_i | \right]$$
$$= -\sum_{mll'} \delta_{\alpha_m \alpha} \delta_{ll'} \Gamma_{m,ll'} \mathrm{Tr} \left[| E_i \rangle \langle E_i | \right] = -\sum_{ml} \delta_{\alpha_m \alpha} \Gamma_{m,ll} \overset{(F.2)}{=} -\Gamma_\alpha. \tag{F.8}$$

As the main text of the thesis argues, the relations (F.4) and (F.8) can be combined to the duality (F.2) for the kernel W_α (in the probability subspace) when using that the parity superoperators $\mathcal{P}$ applied from the left and right to $\overline{W}_\alpha$ only flip the sign of the off-diagonal elements, again as a consequence of fermion-parity superselection. This completes our proof for W_α, and thus, by virtue of Eq. (F.1), also for the full kernel W.

Appendix G

Bosonic superoperators for a harmonic oscillator coupled to a bath

Similarly to Ref. [205], this appendix shows how the fermionic superoperator formalism from Refs. [166, 167] can be adjusted to bosonic systems, and how this can be used to derive the dissipative, Born-Markov master equation kernel W for the example of a single bosonic mode discussed in Sec. 3.3.3. The application of superoperators to solve the latter problem can be found in, e.g., Ref. [204].

G.1 Prerequisites

Let us first introduce the index $\eta = \pm 1$ (particle-hole index in case of fermions) to differentiate between bosonic creation and annihilation operators, both for the mode of interest $(b^\dagger, b)$ and for the environment modes $(a^\dagger_{\mathbf{k}m}, a_{\mathbf{k}m})$ characterized by some continuous wave number $\mathbf{k}$ and any further necessary, discrete quantum numbers (e.g. photon polarization) included into the multi-index m:

$$b_\eta = \begin{cases} b^\dagger & \eta = +1 \\ b & \eta = -1 \end{cases} \quad , \quad a_{\eta \mathbf{k} m} = \begin{cases} a^\dagger_{\mathbf{k}m} & \eta = +1 \\ a_{\mathbf{k}m} & \eta = -1 \end{cases} . \tag{G.1}$$

The negation of the index η shall be denoted by $\bar{\eta} = -\eta$ Furthermore, the multi-index $i = \eta_i \mathbf{k}_i m_i$ and its negation $\bar{i} = \bar{\eta}_i \mathbf{k}_i m_i$ will appear. In particular, the Hamiltonians for the mode of interest (H), the environment (H_R) and the coupling (H_cpl) can be written as $(\hbar \equiv 1)$

$$H = \omega \left(b^\dagger b + \frac{1}{2} \right) = \sum_\eta \omega \delta_{\eta +} \cdot b_\eta b_{\bar{\eta}} + \frac{\omega}{2} = \omega \left(N + \frac{1}{2} \right) \quad , \quad N = b_+ b_- \tag{G.2}$$

$$H_\mathrm{R} = \sum_i \omega_i \delta_{\eta_i +} \cdot \left(a_i a_{\bar{i}} + \frac{1}{2} \right) \tag{G.3}$$

$$H_\mathrm{cpl} = \sum_{i,\eta} \left(K_i \cdot \delta_{\eta_i \bar{\eta}} \right) a_i b_\eta \quad , \quad K_i = \mathrm{Re}\left[g_{m_i}(\mathbf{k}_i) \right] + \eta_i \cdot \mathrm{i} \cdot \mathrm{Im}\left[g_{m_i}(\boldsymbol{k}_i) \right] , \tag{G.4}$$

where $g_{m_i}(\boldsymbol{k}_i)$ quantifies the coupling between the mode of interest in the open subsystem and the environment mode $\boldsymbol{k}_i, m_i$, and $N = b^\dagger b$ is the occupation/excitation number operator for the open subsystem. Note that in order to simplify the expression for H_{cpl}, we have used the bosonic commutation relations for the field operators (G.1):

$$[b_\eta, b_{\eta'}] = \eta' \delta_{\eta' \bar{\eta}} \quad , \quad [a_i, a_j] = \eta_j \delta_{j\bar{i}} \quad , \quad [b, a_i] = 0. \tag{G.5}$$

Next, we establish the Liouville space notation that will be used for the equations describing the transition matrices acting on the reduced density operator. We express the Liouvillians corresponding to the Hamiltonians in terms of the following superoperators with bosonic statistics, i.e., obeying commutation rules analogous to Eq. (G.5):

$$\begin{aligned} B_\eta^q \bullet &= \frac{1}{\sqrt{2}} \left[b_\eta \bullet + q \cdot \bullet b_\eta \right] \\ A_i^{q_i} \bullet &= \frac{1}{\sqrt{2}} \left[a_i \bullet + q_i \cdot \bullet a_i \right], \end{aligned} \tag{G.6}$$

with $i = \eta_i \boldsymbol{k}_i m_i$ and as defined above. The index $q = \pm 1$ is called the Keldysh index. As usual, its negation will be denoted by $\bar{q} = -q$.

Let us summarize important properties of these superoperators that we will use in the following:

- The commutation relations follow from the commutation relations for field operators (G.5):

$$\begin{aligned} \left[B_{\eta_1}^{q_1}, B_{\eta_2}^{q_2} \right] \bullet &= B_{\eta_1}^{q_1} B_{\eta_2}^{q_2} \bullet - B_{\eta_2}^{q_2} B_{\eta_1}^{q_1} \bullet \overset{\substack{(G.6)\\(G.5)}}{=} \eta_2 \delta_{\eta_2 \bar{\eta}_1} \delta_{q_1 \bar{q}_2} \bullet \\ \left[A_1^{q_1}, A_2^{q_2} \right] \bullet &= A_1^{q_1} A_2^{q_2} \bullet - A_2^{q_2} A_1^{q_1} \bullet \overset{\substack{(G.6)\\(G.5)}}{=} \eta_2 \delta_{2\bar{1}} \delta_{q_1 \bar{q}_2} \bullet \\ \left[B_{\eta_1}^{q_1}, A_2^{q_2} \right] &= 0. \end{aligned} \tag{G.7}$$

  Note that these superoperators are *not* associative. The product is *defined* as the subsequent mapping of the operator $\bullet$ to another one, with the leftmost superoperator in the product acting the last.

- The superhermitian conjugate is defined as in Sec. 2.2.1, via $\mathrm{Tr}\left[O_1^\dagger (\left(B_\eta^q \right)^\dagger O_2) \right] := \mathrm{Tr}\left[O_2^\dagger (B_\eta^q O_1) \right]^*$ and analogously for $A_i^{q_i}$. One finds

$$\left(B_{\eta_1}^{q_1} \right)^\dagger \bullet = B_{\bar{\eta}_1}^{q_1} \bullet \quad , \quad (A_1^{q_1})^\dagger \bullet = A_{\bar{1}}^{q_1} \bullet . \tag{G.8}$$

Unfortunately – and unlike for the fermionic superoperators from Refs. [166, 167] – Eq. (G.8) prevents us from interpreting the superoperators $A_i^{q_i}, B_\eta^q$ as

bosonic creation and annihilation operators. Namely, starting from the commutation relations (G.7), a fully consistent picture would instead require that the superhermitian conjugate of an annihilation superoperator gives a creation superoperator, $\left(B^q_\eta\right)^\dagger = B^{\bar{q}}_{\bar{\eta}}$ and $(A^{q_i}_i)^\dagger = A^{\bar{q}_i}_{\bar{i}}$. There is, to our current knowledge, no *obvious* way to fix the behavior under superhermitian conjugation without also affecting the commutation relations (G.7). A possible explanation could be that in the fermionic case, the additional introduction of parity operators is tied to a physical symmetry – the fermion-parity superselection – whereas in the bosonic case, no such symmetry exists.

G.2 Liouvillians

Having established the commutation rules (G.7), we can now write the system Liouvillians $L_x\bullet = [H_x, \bullet]$ in terms of the superoperators (G.6). As a first step, we expand left and right action of the field operators (G.1):

$$\begin{aligned} b_\eta\bullet &\overset{(G.6)}{=} \frac{1}{\sqrt{2}}\sum_{q=\pm} B^q_\eta\bullet \quad , \quad \bullet b_\eta = \frac{1}{\sqrt{2}}\sum_{q=\pm} qB^q_\eta\bullet \\ a_i\bullet &\overset{(G.6)}{=} \frac{1}{\sqrt{2}}\sum_{q_i=\pm} A^{q_i}_i\bullet \quad , \quad \bullet a_i = \frac{1}{\sqrt{2}}\sum_{q_i=\pm} q_i A^{q_i}_i\bullet\,. \end{aligned} \tag{G.9}$$

This can be used to find

$$\begin{aligned} L\bullet &\overset{(G.2)}{=} \omega\sum_\eta \delta_{\eta+}\left[b_\eta b_{\bar\eta}\bullet - \bullet\, b_\eta b_{\bar\eta}\right] \overset{(G.9)}{=} \frac{\omega}{2}\sum_{\eta_1\eta_2,q_1,q_2}\delta_{\eta_1+}\delta_{\eta_2\bar\eta_1}\left(B^{q_1}_{\eta_1}B^{q_2}_{\eta_2} - q_1q_2B^{q_2}_{\eta_2}B^{q_1}_{\eta_1}\right)\bullet \\ &\overset{(G.7)}{=} \frac{\omega}{2}\sum_{\eta_1\eta_2,q_1,q_2}\delta_{\eta_1+}\delta_{\eta_2\bar\eta_1}\left[(1-q_1q_2)\,B^{q_1}_{\eta_1}B^{q_2}_{\eta_2} + \eta_1\delta_{q_2\bar q_1}\right]\bullet \\ &= \omega\sum_{\eta_1\eta_2,q_1,q_2}\delta_{\eta_1+}\delta_{\eta_2\bar\eta_1}\delta_{q_2\bar q_1}\left(B^{q_1}_{\eta_1}B^{q_2}_{\eta_2} + \frac{1}{2}\right)\bullet \\ &= \omega\sum_{\eta,q}\delta_{\eta+}\left(B^q_\eta B^{\bar q}_{\bar\eta} + \frac{1}{2}\right)\bullet = \omega\sum_q\left(B^q_+B^{\bar q}_- + \frac{1}{2}\right)\bullet \end{aligned} \tag{G.10}$$

$$L_{\mathrm{R}}\bullet \overset{\text{analogous to } Eq.\ (G.10)}{\cdots} = \sum_{i,q_i}\omega_i\delta_{\eta_i+}\cdot\left(A^{q_i}_iA^{\bar q_i}_{\bar\imath} + \frac{1}{2}\right)\bullet \tag{G.11}$$

$$L_{\mathrm{cpl}}\bullet \overset{\text{analogous to } Eq.\ (G.10)}{\cdots} = \sum_{i,\eta,q_i,q}\left(K_i\cdot\delta_{\eta_i\bar\eta}\delta_{q_i\bar q}\right)A^{q_i}_iB^q_\eta = \sum_{i,q_i}K_iA^{q_i}_iB^{\bar q_i}_{\bar\eta_i}. \tag{G.12}$$

Let us collect some properties of these Liouvillians. It follows from the commutation rules (G.7) that

$$[L, L_{\mathrm{R}}]\bullet = [L, A^{q_i}_i]\bullet = [L_{\mathrm{R}}, B^q_\eta]\bullet = 0 \tag{G.13}$$

$$[L, B^q_\eta]\bullet \overset{(G.10)}{=} \omega\sum_{q'}[B^{q'}_+B^{\bar q'}_-, B^q_\eta]\bullet \overset{(G.7)}{=} \omega\sum_{q'}\left[\delta_{q'q}\delta_{\eta+}B^q_+ - \delta_{q'\bar q}\delta_{\eta-}B^q_-\right]\bullet = \eta\cdot\omega\cdot B^q_\eta\bullet \tag{G.14}$$

$$[L_{\mathrm{R}}, A_i^{q_i}] = \overset{\text{analogous to } Eq.\ (G.14)}{\vdots} = \eta_i \cdot \omega_i \cdot A_i^{q_i} \bullet . \tag{G.15}$$

Using the Campbell-Baker-Hausdorff formula, this yields

$$\begin{aligned} B_\eta^q(t)\bullet &= \exp\left(\mathrm{i}\cdot t\cdot (L+L_{\mathrm{R}})\right) B_\eta^q \exp\left(-\mathrm{i}\cdot t\cdot (L+L_{\mathrm{R}})\right)\bullet = \exp\left(i\cdot\eta\cdot\omega t\right)\cdot B_\eta^q\bullet \\ A_i^{q_i}(t)\bullet &= \exp\left(\mathrm{i}\cdot t\cdot (L+L_{\mathrm{R}})\right) A_i^{q_i} \exp\left(-\mathrm{i}\cdot t\cdot (L+L_{\mathrm{R}})\right)\bullet = \exp\left(i\cdot\eta_i\cdot\omega_i t\right)\cdot A_i^{q_i}\bullet . \end{aligned} \tag{G.16}$$

Finally, any Liouvillian L_x involving a Hermitian Hamiltonian H_x is *superhermitian*

$$\begin{aligned} (A|L_x^\dagger|B) &= \mathrm{Tr}\left[A^\dagger (L_x)^\dagger B\right] = \mathrm{Tr}\left[B^\dagger L_x A\right]^* = \mathrm{Tr}\left[[H_x, A]^\dagger B\right] = \mathrm{Tr}\left[\left[A^\dagger, H_x\right] B\right] \\ &= \mathrm{Tr}\left[A^\dagger\,[H_x, B]\right] = \mathrm{Tr}\left[A^\dagger L_x B\right] = (A|L_x|B). \end{aligned} \tag{G.17}$$

G.3 Equilibrium pair correlation function

In applying diagrammatic perturbation theory, one traces over the bath degrees of freedom in thermal equilibrium. Using Wick's theorem, we will hence need the pair correlation function

$$\begin{aligned} \langle A_1^{q_1}(t_1) A_2^{q_2}(t_2)\rangle_{\mathrm{R}} &= \underset{\mathrm{R}}{\mathrm{Tr}}\left[A_1^{q_1}(t_1) A_2^{q_2}(t_2) \frac{e^{-\beta H_{\mathrm{R}}}}{\underset{\mathrm{R}}{\mathrm{Tr}}\left[e^{-\beta H_{\mathrm{R}}}\right]}\right] \\ &\overset{(G.16)}{=} \exp\left(i\cdot(\eta_1\omega_1 t_1 + \eta_2\omega_2 t_2)\right)\cdot \frac{\underset{\mathrm{R}}{\mathrm{Tr}}\left[A_1^{q_1} A_2^{q_2} e^{-\beta H_{\mathrm{R}}}\right]}{\underset{\mathrm{R}}{\mathrm{Tr}}\left[e^{-\beta H_{\mathrm{R}}}\right]}, \end{aligned} \tag{G.18}$$

where $\beta = 1/T$ is the inverse bath photon temperature. Using the cyclicity of the trace operation, the trace in the numerator can more explicitly be written as

$$\begin{aligned} \underset{\mathrm{R}}{\mathrm{Tr}}\left[A_1^{q_1} A_2^{q_2} e^{-\beta H_{\mathrm{R}}}\right] &\overset{(G.6)}{=} \frac{1}{\sqrt{2}} \underset{\mathrm{R}}{\mathrm{Tr}}\left[A_1^{q_1}\left(a_2\cdot e^{-\beta H_{\mathrm{R}}} + q_2\cdot e^{-\beta H_{\mathrm{R}}} a_2\right)\right] \\ &\overset{(G.6)}{=} \frac{1+q_1}{2}\cdot\left(\underset{\mathrm{R}}{\mathrm{Tr}}\left[a_1 a_2\cdot e^{-\beta H_{\mathrm{R}}}\right] + q_2 \underset{\mathrm{R}}{\mathrm{Tr}}\left[a_2 a_1\cdot e^{-\beta H_{\mathrm{R}}}\right]\right). \end{aligned} \tag{G.19}$$

To further evaluate these traces, we use

$$\begin{aligned} L_{\mathrm{R}}(a_i) &\overset{(G.11)}{=} [H_{\mathrm{R}}, a_i] \\ &\overset{(G.3)}{=} \sum_j \omega_j \delta_{\eta_j +}\cdot [a_j a_{\bar{j}}, a_i] \overset{(G.5)}{=} \sum_j \eta_i\cdot\omega_j\delta_{\eta_j+}\cdot\left(a_j\delta_{ji} + a_{\bar{j}}\delta_{j\bar{i}}\right) \\ &= \eta_i\cdot\omega_i\left(\delta_{\eta_i+} + \delta_{\eta_i-}\right) a_i = \eta_i\cdot\omega_i\cdot a_i, \end{aligned} \tag{G.20}$$

and the Baker-Campbell-Hausdorff formula to write

$$e^{\beta H_{\mathrm{R}}} a_i e^{-\beta H_{\mathrm{R}}} = e^{\beta L_{\mathrm{R}}}(a_i) \overset{(G.20)}{=} e^{\eta_i\cdot\beta\omega_i} a_i \quad \Leftrightarrow \quad a_i\cdot e^{-\beta H_{\mathrm{R}}} = e^{\eta_i\cdot\beta\omega_i}\cdot e^{-\beta H_{\mathrm{R}}} a_i. \tag{G.21}$$

From this follows

$$\begin{aligned}\operatorname*{Tr}_{\mathrm{R}}\left[a_1a_2\cdot e^{-\beta H_{\mathrm{R}}}\right] &\overset{(\mathrm{G}.21)}{=} e^{\eta_2\cdot\beta\omega_2}\cdot\operatorname*{Tr}_{\mathrm{R}}\left[a_2a_1\cdot e^{-\beta H_{\mathrm{R}}}\right]\\ &\overset{(\mathrm{G}.5)}{=} e^{\eta_2\cdot\beta\omega_2}\cdot\left(\eta_1\cdot\delta_{2\bar{1}}\operatorname*{Tr}_{\mathrm{R}}\left[e^{-\beta H_{\mathrm{R}}}\right]+\operatorname*{Tr}_{\mathrm{R}}\left[a_1a_2\cdot e^{-\beta H_{\mathrm{R}}}\right]\right)\\ \Rightarrow \operatorname*{Tr}_{\mathrm{R}}\left[a_1a_2\cdot e^{-\beta H_{\mathrm{R}}}\right] &= \delta_{2\bar{1}}\cdot\eta_1\cdot\mathrm{b}^{\eta_1}(\omega_1)\cdot\operatorname*{Tr}_{\mathrm{R}}\left[e^{-\beta H_{\mathrm{R}}}\right]\end{aligned}\tag{G.22}$$

with the Bose-Einstein distribution of the bath,

$$\mathrm{b}^{\eta}(x)=\frac{1}{\exp\left(\eta\beta x\right)-1}=\frac{1}{\exp\left(\eta\frac{x}{T}\right)-1}\quad,\quad\eta=\pm1.\tag{G.23}$$

Plugging Eq. (G.22) back into Eq. (G.19) and using

$$\mathrm{b}^{\eta}(x)+\mathrm{b}^{-\eta}(x)=-1\quad,\quad\mathrm{b}^{\eta}(-x)=\mathrm{b}^{-\eta}(x),\tag{G.24}$$

we find

$$\begin{aligned}\frac{\operatorname*{Tr}_{\mathrm{R}}\left[A_1^{q_1}A_2^{q_2}e^{-\beta H_{\mathrm{R}}}\right]}{\operatorname*{Tr}_{\mathrm{R}}\left[e^{-\beta H_{\mathrm{R}}}\right]} &\underset{(\mathrm{G}.22)}{\overset{(\mathrm{G}.19)}{=}}\delta_{q_1+}\delta_{2\bar{1}}\cdot\left[\eta_1\cdot\mathrm{b}^{\eta_1}(\omega_1)+q_2\cdot\eta_2\cdot\mathrm{b}^{\eta_2}(\omega_2)\right]\\ &\overset{(\mathrm{G}.24)}{=}\delta_{q_1+}\delta_{2\bar{1}}\cdot\eta_1\cdot\left[\mathrm{b}^{\eta_1}(\omega_1)+q_2\cdot(\mathrm{b}^{\eta_1}(\omega_1)+1)\right]\\ &=\delta_{q_1+}\delta_{2\bar{1}}\cdot\eta_1\cdot\left[q_2+2\delta_{q_2+}\mathrm{b}^{\eta_1}(\omega_1)\right].\end{aligned}\tag{G.25}$$

Combining this equation with Eq. (G.18) yields the final result

$$\left\langle A_1^{q_1}(t_1)A_2^{q_2}(t_2)\right\rangle_{\mathrm{R}}=\delta_{q_1+}\delta_{2\bar{1}}\cdot\eta_1\cdot\left[q_2+2\delta_{q_2+}\mathrm{b}^{\eta_1}(\omega_1)\right]\cdot\exp\left(i\eta_1\omega_1(t_1-t_2)\right).\tag{G.26}$$

Importantly, when now continuing by applying diagrammatic perturbation theory as in Refs. [166, 167], the ω-independent part in the square brackets will, for a $\boldsymbol{k}$-independent coupling, merely lead to a quadratic, and hence exactly treatable contribution to the effective Liouvillian for the harmonic oscillator forming the open-system, just as in the fermionic case in the wideband limit discussed in Refs. [166, 167]. In the zero-temperature limit $T\to0$, i.e., an empty boson bath (as opposed to the infinite temperature limit for fermions, where the particle number is conserved and the Fermi sea always exists), this is then also the only effect of the bath on the oscillator. It physically represents the decay of the open-system state exclusively due to boson leakage; thermal excitation of the oscillator is impossible at zero temperature.

G.4 Born-Markov kernel and its dual

To derive the bosonic duality relation (3.29) from the main text, let us now evaluate the Born-Markov kernel W and its dual $\overline{W}$ using what we have defined in the

previous sections. Following the diagrammatic approach from Refs. [166, 167], we define the multi-indices $1 = \eta_1 \mathbf{k}_1 m_1$, $2 = \eta_2 \mathbf{k}_2 m_2$ and find

$$\begin{aligned}
\mathcal{W}(t-t') &\overset{(G.12)}{=} -\sum_{\substack{1,2\\ q_1,q_2}} K_1 K_2 \cdot \langle A_1^{q_1}(t) A_2^{q_2}(t')\rangle_{\mathrm{R}} \cdot B^{\bar{q}_1}_{\bar{\eta}_1} e^{-\mathrm{i}(t-t')L} B^{\bar{q}_2}_{\bar{\eta}_2} \\
&\overset{(G.26)}{=} -\sum_{\substack{1,2\\ q_1,q_2}} K_1 K_2 e^{i\eta_1\omega_1(t-t')} \delta_{q_1+}\delta_{2\bar{1}}\eta_1 \left[q_2 + 2\delta_{q_2+}\mathrm{b}^{\eta_1}(\omega_1)\right] B^{\bar{q}_1}_{\bar{\eta}_1} e^{-\mathrm{i}(t-t')L} B^{\bar{q}_2}_{\bar{\eta}_2} \\
&\underset{q_2\to\bar{q}}{\overset{(G.12)}{=}} \sum_{1,q} |K_1|^2 \cdot e^{i\eta_1\omega_1(t-t')} \cdot \eta_1 \cdot [q - 2\delta_{q-}\mathrm{b}^{\eta_1}(\omega_1)] \cdot B^{-}_{\bar{\eta}_1} e^{-\mathrm{i}(t-t')L} B^{q}_{\eta_1} \\
&\overset{(G.12)}{=} \int_{-\infty}^{\infty} d\omega \sum_{\eta,q}\sum_{\boldsymbol{k},m} |K_{\boldsymbol{k},m}|^2 \delta(\omega(\boldsymbol{k},m)-\omega) e^{\mathrm{i}\eta\omega(t-t')} \cdot \eta \cdot [q - 2\delta_{q-}\mathrm{b}^{\eta}(\omega)] \\
&\qquad\qquad \times B^{-}_{\bar{\eta}} e^{-\mathrm{i}(t-t')L} B^{q}_{\eta} \\
&= \frac{1}{2\pi}\int_{-\infty}^{\infty} d\omega\ \Gamma(\omega) \sum_{\eta,q} e^{\mathrm{i}\eta\omega(t-t')} \cdot \eta \cdot [q - 2\delta_{q-}\mathrm{b}^{\eta}(\omega)] \cdot B^{-}_{\bar{\eta}} e^{-\mathrm{i}(t-t')L} B^{q}_{\eta},
\end{aligned} \tag{G.27}$$

where we have introduced the leakage strength

$$\Gamma(\omega) = 2\pi \sum_{\boldsymbol{k},m} |K_{\boldsymbol{k},m}|^2 \delta(\omega(\boldsymbol{k},m)-\omega). \tag{G.28}$$

In the Markovian limit [Sec. (2.3)], we obtain

$$W = \lim_{\epsilon\to 0} \int_0^{\infty} d\Delta t\, \mathcal{W}(\Delta t) e^{-\epsilon\Delta t}. \tag{G.29}$$

In our specific case, the kernel W is explicitly given by (the limit $\epsilon \to 0$ is carried out before integrating over ω)

$$\begin{aligned}
W &= \int_0^{\infty} d\Delta t\, \mathcal{W}(\Delta t) e^{-\epsilon\Delta t} \\
&\overset{(G.27)}{=} \frac{1}{2\pi}\int_{-\infty}^{\infty} d\omega\ \Gamma(\omega) \sum_{\eta,q} \eta \cdot [q - 2\delta_{q-}\mathrm{b}^{\eta}(\omega)] \cdot B^{-}_{\bar{\eta}} \int_0^{\infty} d\Delta t\, e^{-\mathrm{i}\Delta t(L - \eta\omega - \mathrm{i}\epsilon)} B^{q}_{\eta} \\
&= \frac{i}{2\pi}\int_{-\infty}^{\infty} d\omega\ \Gamma(\omega) \sum_{\eta,q} \eta \cdot [q - 2\delta_{q-}\mathrm{b}^{\eta}(\omega)] \cdot B^{-}_{\bar{\eta}} \frac{1}{\eta\cdot\omega - L + \mathrm{i}\epsilon} B^{q}_{\eta} \\
&= \frac{i}{2\pi}\int_{-\infty}^{\infty} d\omega\ \Gamma(\omega) \sum_{\eta,q} [q - 2\delta_{q-}\mathrm{b}^{\eta}(\omega)] \cdot B^{-}_{\bar{\eta}} \frac{1}{\omega - \eta L + \mathrm{i}\eta\epsilon} B^{q}_{\eta}.
\end{aligned} \tag{G.30}$$

Let us now focus on energy-independent coupling $\Gamma(\omega) \to \Gamma$. To prove duality in this case, we need the superhermitian conjugate of the dual kernel $\overline{W} = W(-H)$ (no chemical potential involved). Effectively, we take Eq. (G.30) and replace

$L \to -L$, $\omega \to -\omega$, and use $\mathrm{b}^\eta(-\omega) = b^{\bar\eta}(\omega)$ [Eq. (G.24)]. After superhermitian conjugation, we arrive at

$$\begin{aligned}\overline{W}^\dagger &\underset{(G.8),(G.17)}{\overset{(G.30)}{=}} \int_{-\infty}^{\infty} d\omega\ \frac{\Gamma}{2\pi} \sum_{\eta,q} \eta \cdot \left[q - 2\delta_{q-}\mathrm{b}^{\bar\eta}(\omega)\right] \cdot B^q_{\bar\eta} \int_0^\infty d\Delta t\, e^{-\mathrm{i}\Delta t(L-\eta\omega-\mathrm{i}\epsilon)} B^-_\eta \\ &\overset{(G.24)}{=} \frac{1}{2\pi} \int_{-\infty}^{\infty} d\omega\ \Gamma \sum_{\eta,q} \eta \cdot [1 + 2\delta_{q-}\mathrm{b}^{\eta}(\omega)] \cdot B^q_{\bar\eta} \int_0^\infty d\Delta t\, e^{-\mathrm{i}\Delta t(L-\eta\omega-\mathrm{i}\epsilon)} B^-_\eta \\ &= \frac{i}{2\pi} \int_{-\infty}^{\infty} d\omega\ \Gamma \sum_{\eta,q} [1 + 2\delta_{q-}\mathrm{b}^{\eta}(\omega)] \cdot B^q_{\bar\eta} \frac{1}{\omega - \eta L + \mathrm{i}\eta\epsilon} B^-_\eta . \end{aligned} \tag{G.31}$$

We see that when adding this to W as given in Eq. (G.30), the $q = -1$ part cancels. The remaining terms read

$$\begin{aligned} W + \overline{W}^\dagger &\underset{(G.31)}{\overset{(G.30)}{=}} \frac{1}{2\pi} \int_{-\infty}^{\infty} d\omega\ \Gamma \sum_{\eta,q} \eta \cdot B^q_{\bar\eta} \int_0^\infty d\Delta t\, e^{-\mathrm{i}\Delta t(L-\eta\omega-\mathrm{i}\epsilon)} B^{\bar q}_\eta \\ &\overset{\eta\to-\eta}{=} -\Gamma \int_0^\infty d\Delta t \delta(\Delta t) \sum_{\eta,q} \eta \cdot B^q_\eta B^{\bar q}_{\bar\eta} = -\Gamma \int_0^\infty d\Delta t \delta(\Delta t) \sum_q [B^q_+, B^{\bar q}_-] \\ &\overset{(G.7)}{=} 2\Gamma \int_0^\infty d\Delta t \delta(\Delta t) = \Gamma. \end{aligned} \tag{G.32}$$

Note that the factor 2 cancels since the delta distribution is integrated from 0 to ∞ and not from $-\infty$ to ∞. Equation (G.32) is precisely the duality relation (3.28) discussed in Sec. 3.3.3.

The final step is to obtain the zero-temperature limit of W given in Eq. (3.27) of the main text. For $T \to 0$, we approximate $\mathrm{b}^\eta(x) \to (\eta - 1)/2$. Note that this step requires a bit of care, as $\mathrm{b}^\eta(x) = (\eta - 1)/2$ only holds for $T = 0$ if $x > 0$. To properly carry out this limit, one should already use $T = 0$ prior to the fourth line in Eq. (G.27), before going to the continuum limit, as all frequencies ω_1 in this step are indeed larger than zero. The final expression then reads

$$\begin{aligned} W_{T=0}\bullet &\overset{(G.30)}{=} \frac{1}{2\pi\mathrm{i}} \int_{-\infty}^{\infty} d\omega\ \Gamma \sum_{\eta,q} \eta \cdot [q + \delta_{q-}(1-\eta)] \cdot B^-_{\bar\eta} \int_0^\infty d\Delta t\, e^{-\mathrm{i}\Delta t(L-\eta\omega-\mathrm{i}\epsilon)} B^q_\eta \bullet \\ &= \frac{\Gamma}{2} \sum_{\eta,q} \eta \cdot [q + \delta_{q-}(1-\eta)] \cdot B^-_{\bar\eta} B^q_\eta \bullet = \frac{\Gamma}{2} \sum_\eta \left[\eta \cdot B^-_{\bar\eta} B^+_\eta - B^-_{\bar\eta} B^-_\eta\right] \bullet \\ &\underset{(G.9)}{\overset{(G.6)}{=}} -\frac{\Gamma}{\sqrt{2}} \left[B^-_+ (b_- \bullet) - B^-_- (\bullet b_+)\right] \underset{(G.2)}{\overset{(G.6)}{=}} -\frac{\Gamma}{\hbar} \left[\frac{1}{2} L^+_N - \zeta\right] \bullet, \end{aligned} \tag{G.33}$$

having introduced the boson number anti-commutator and the incoherent boson number lowering superoperator

$$L^+_N \bullet = [N \bullet + \bullet N]\ ,\ N = b^\dagger b \quad , \quad \zeta \bullet = b \bullet b^\dagger. \tag{G.34}$$

We stress that when the two superoperators in Eq. (G.33) are written in the conventional, second quantized form (G.34), the master equation kernel (G.33) corresponds exactly to the zero temperature dissipator obtained in the usual quantum optics fashion, see, e.g., Refs. [206, 207].

References

[1] M. A. Reed, J. N. Randall, R. J. Aggarwal, R. J. Matyi, T. M. Moore, and A. E. Wetsel, "Observation of discrete electronic states in a zero-dimensional semiconductor nanostructure", Phys. Rev. Lett. **60**, 535–537 (1988) (cit. on pp. 1, 3).

[2] J. Alsmeier, E. Batke, and J. P. Kotthaus, "Voltage-tunable quantum dots on silicon", Phys. Rev. B **41**, 1699–1702 (1990) (cit. on pp. 1, 3).

[3] A. Lorke, J. P. Kotthaus, and K. Ploog, "Coupling of quantum dots on GaAs", Phys. Rev. Lett. **64**, 2559–2562 (1990) (cit. on pp. 1, 3).

[4] P. Guéret, N. Blanc, R. Germann, and H. Rothuizen, "Confinement and single-electron tunneling in Schottky-gated, laterally squeezed double-barrier quantum-well heterostructures", Phys. Rev. Lett. **68**, 1896–1899 (1992) (cit. on pp. 1, 3).

[5] B. Meurer, D. Heitmann, and K. Ploog, "Single-electron charging of quantum-dot atoms", Phys. Rev. Lett. **68**, 1371–1374 (1992) (cit. on pp. 1, 3).

[6] M. Razavy, *Quantum Theory of Tunneling* (World Scientific Publishing Company, Jan. 2003) (cit. on p. 1).

[7] T. A. Fulton and G. J. Dolan, "Observation of single-electron charging effects in small tunnel junctions", Phys. Rev. Lett. **59**, 109–112 (1987) (cit. on pp. 3, 5).

[8] J. H. F. Scott-Thomas, S. B. Field, M. A. Kastner, H. I. Smith, and D. A. Antoniadis, "Conductance Oscillations Periodic in the Density of a One-Dimensional Electron Gas", Phys. Rev. Lett. **62**, 583–586 (1989) (cit. on pp. 3, 5).

[9] U. Meirav, M. A. Kastner, and S. J. Wind, "Single-electron charging and periodic conductance resonances in GaAs nanostructures", Phys. Rev. Lett. **65**, 771–774 (1990) (cit. on pp. 3, 5).

[10] A. T. Johnson, L. P. Kouwenhoven, W. de Jong, N. C. van der Vaart, C. J. P. M. Harmans, and C. T. Foxon, "Zero-dimensional states and single electron charging in quantum dots", Phys. Rev. Lett. **69**, 1592–1595 (1992) (cit. on pp. 3, 5).

[11] E. B. Foxman, P. L. McEuen, U. Meirav, N. S. Wingreen, Y. Meir, P. A. Belk, N. R. Belk, M. A. Kastner, and S. J. Wind, "Effects of quantum levels on transport through a Coulomb island", Phys. Rev. B **47**, 10020–10023 (1993) (cit. on pp. 3, 5).

[12] J. Weis, R. J. Haug, K. v. Klitzing, and K. Ploog, "Competing channels in single-electron tunneling through a quantum dot", Phys. Rev. Lett. **71**, 4019–4022 (1993) (cit. on pp. 3, 5).

[13] M. A. Kastner, "The single electron transistor and artificial atoms", Ann. Phys. **9**, 885–894 (2000) (cit. on pp. 3, 5).

[14] M. Büttiker, A. Prêtre, and H. Thomas, "Dynamic conductance and the scattering matrix of small conductors", Phys. Rev. Lett. **70**, 4114–4117 (1993) (cit. on p. 3).

[15] M. Büttiker, H. Thomas, and A. Prêtre, "Mesoscopic capacitors", Phys. Lett. A **180**, 364–369 (1993) (cit. on p. 3).

[16] A. Prêtre, H. Thomas, and M. Büttiker, "Dynamic admittance of mesoscopic conductors: Discrete-potential model", Phys. Rev. B **54**, 8130–8143 (1996) (cit. on p. 3).

[17] J. Gabelli, G. Fève, J.-M. Berroir, B. Plaçais, A. Cavanna, B. Etienne, Y. Jin, and D. C. Glattli, "Violation of Kirchhoff's Laws for a Coherent RC Circuit", Science **313**, 499–502 (2006) (cit. on pp. 3, 4, 6, 7).

[18] G. Fève, A. Mahé, J.-M. Berroir, T. Kontos, B. Plaçais, D. C. Glattli, A. Cavanna, B. Etienne, and Y. Jin, "An On-Demand Coherent Single-Electron Source", Science **316**, 1169–1172 (2007) (cit. on pp. 3, 6–8, 77).

[19] A. Mahé, F. D. Parmentier, E. Bocquillon, J.-M. Berroir, D. C. Glattli, T. Kontos, B. Plaçais, G. Fève, A. Cavanna, and Y. Jin, "Current correlations of an on-demand single-electron emitter", Phys. Rev. B **82**, 201309 (2010) (cit. on pp. 3, 6, 8).

[20] S. P. Giblin, S. J. Wright, J. D. Fletcher, M. Kataoka, M. Pepper, T. J. B. M. Janssen, D. A. Ritchie, C. A. Nicoll, D. Anderson, and G. A. C. Jones, "An accurate high-speed single-electron quantum dot pump", New J. Phys. **12**, 073013 (2010) (cit. on pp. 3, 6, 77, 80, 81).

[21] S. P. Giblin, M. Kataoka, J. D. Fletcher, P. See, T. J. B. M. Janssen, J. P. Griffiths, G. A. C. Jones, I. Farrer, and D. A. Ritchie, "Towards a quantum representation of the ampere using single electron pumps", Nat. Commun. **3**, 930 (2012) (cit. on pp. 3, 6, 19).

[22] J. D. Fletcher, P. See, H. Howe, M. Pepper, S. P. Giblin, J. P. Griffiths, G. A. C. Jones, I. Farrer, D. A. Ritchie, T. J. B. M. Janssen, and M. Kataoka, "Clock-Controlled Emission of Single-Electron Wave Packets in a Solid-State Circuit", Phys. Rev. Lett. **111**, 216807 (2013) (cit. on pp. 3, 10, 11, 19, 20, 77, 80, 87).

[23] A. Rossi, T. Tanttu, K. Y. Tan, I. Iisakka, R. Zhao, K. W. Chan, G. C. Tettamanzi, S. Rogge, A. S. Dzurak, and M. Möttönen, "An Accurate Single-Electron Pump Based on a Highly Tunable Silicon Quantum Dot", Nano Lett. **14**, 3405–3411 (2014) (cit. on pp. 3, 6).

[24] N. Ubbelohde, F. Hohls, V. Kashcheyevs, T. Wagner, L. Fricke, B. Kästner, K. Pierz, H. W. Schumacher, and R. J. Haug, "Partitioning of on-demand electron pairs", Nat. Nanotechnol. **10**, 46–49 (2014) (cit. on pp. 3, 6, 11, 19, 77, 79).

[25] B. Kaestner and V. Kashcheyevs, "Non-adiabatic quantized charge pumping with tunable-barrier quantum dots: a review of current progress", Rep. Prog. Phys. **78**, 103901 (2015) (cit. on pp. 3, 6, 80, 81).

[26] L. Schreiber and T. Leonhardt, *Lehrstuhl für Experimentalphysik und II. Physikalisches Institut, RWTH Aachen*, (2014) `https://www.rwth-aachen.de/cms/Quantuminfo/Forschung/Institut-fuer-Quantentechnologie/~eyea/Bluhm-SiGe/?lidx=1` (visited on 01/05/2016) (cit. on p. 4).

[27] M. T. Björk, C. Thelander, A. E. Hansen, L. E. Jensen, M. W. Larsson, L. R. Wallenberg, and L. Samuelson, "Few-Electron Quantum Dots in Nanowires", Nano Lett. **4**, 1621–1625 (2004) (cit. on pp. 3, 6, 9).

[28] J. Splettstoesser, M. Governale, J. König, and M. Büttiker, "Charge and spin dynamics in interacting quantum dots", Phys. Rev. B **81**, 165318 (2010) (cit. on pp. 5, 8, 33, 34, 77, 79, 85).

[29] P. W. Anderson, "Localized Magnetic States in Metals", Phys. Rev. **124**, 41–53 (1961) (cit. on pp. 5, 22, 83).

[30] G. Rosselló, R. López, and J. S. Lim, "Time-dependent heat flow in interacting quantum conductors", Phys. Rev. B **92**, 115402 (2015) (cit. on p. 6).

[31] N. Dittmann, J. Splettstoesser, and N. Helbig, "Nonadiabatic Dynamics in Single-Electron Tunneling Devices with Time-Dependent Density-Functional Theory", Phys. Rev. Lett. **120**, 157701 (2018) (cit. on pp. 6, 44).

[32] D. E. Nikonov and I. A. Young, "Overview of Beyond-CMOS Devices and a Uniform Methodology for Their Benchmarking", Proc. IEEE **101**, 2498–2533 (2013) (cit. on p. 6).

[33] D. Loss and D. P. DiVincenzo, "Quantum computation with quantum dots", Phys. Rev. A **57**, 120–126 (1998) (cit. on p. 6).

[34] J. M. Elzerman, R. Hanson, L. H. Willems van Beveren, B. Witkamp, L. M. K. Vandersypen, and L. P. Kouwenhoven, "Single-shot read-out of an individual electron spin in a quantum dot", Nature **430**, 431 (2004) (cit. on pp. 6, 8, 79).

[35] J. R. Petta, A. C. Johnson, J. M. Taylor, E. A. Laird, A. Yacoby, M. D. Lukin, C. M. Marcus, M. P. Hanson, and A. C. Gossard, "Coherent Manipulation of Coupled Electron Spins in Semiconductor Quantum Dots", Science **309**, 2180–2184 (2005) (cit. on p. 6).

[36] E. Bocquillon, V. Freulon, J.-M. Berroir, P. Degiovanni, B. Plaçais, A. Cavanna, Y. Jin, and G. Fève, "Coherence and Indistinguishability of Single Electrons Emitted by Independent Sources", Science **339**, 1054–1057 (2013) (cit. on p. 6).

[37] C. Bäuerle, D. C. Glattli, T. Meunier, F. Portier, P. Roche, P. Roulleau, S. Takada, and X. Waintal, "Coherent control of single electrons: a review of current progress", Rep. Prog. Phys. **81**, 056503 (2018) (cit. on p. 6).

[38] L. J. Geerligs, V. F. Anderegg, P. A. M. Holweg, J. E. Mooij, H. Pothier, D. Esteve, C. Urbina, and M. H. Devoret, "Frequency-locked turnstile device for single electrons", Phys. Rev. Lett. **64**, 2691–2694 (1990) (cit. on p. 6).

[39] H. Pothier, P. Lafarge, C. Urbina, D. Esteve, and M. H. Devoret, "Single-Electron Pump Based on Charging Effects", EPL **17**, 249 (1992) (cit. on p. 6).

[40] L. P. Kouwenhoven, A. T. Johnson, N. C. van der Vaart, C. J. P. M. Harmans, and C. T. Foxon, "Quantized current in a quantum-dot turnstile using oscillating tunnel barriers", Phys. Rev. Lett. **67**, 1626–1629 (1991) (cit. on p. 6).

[41] A. Fujiwara, N. M. Zimmerman, Y. Ono, and Y. Takahashi, "Current quantization due to single-electron transfer in Si-wire charge-coupled devices", Appl. Phys. Lett. **84**, 1323–1325 (2004) (cit. on pp. 6, 80).

[42] M. D. Blumenthal, B. Kaestner, L. Li, S. Giblin, T. J. B. M. Janssen, M. Pepper, D. Anderson, G. Jones, and D. A. Ritchie, "Gigahertz quantized charge pumping", Nat. Phys. **3**, 343 (2007) (cit. on p. 6).

[43] J. P. Pekola, O.-P. Saira, V. F. Maisi, A. Kemppinen, M. Möttönen, Y. A. Pashkin, and D. V. Averin, "Single-electron current sources: Toward a refined definition of the ampere", Rev. Mod. Phys. **85**, 1421–1472 (2013) (cit. on pp. 6, 8, 80).

[44] D. B. Newell, F. Cabiati, J. Fischer, K. Fujii, S. G. Karshenboim, H. S. Margolis, E. de Mirandés, P. J. Mohr, F. Nez, K. Pachucki, T. J. Quinn, B. N. Taylor, M. Wang, B. M. Wood, and Z. Zhang, "The CODATA 2017 values of h , e , k , and N A for the revision of the SI", Metrologia **55**, L13 (2018) (cit. on p. 6).

[45] R. Kosloff, "Quantum Thermodynamics: A Dynamical Viewpoint", Entropy **15**, 2100–2128 (2013) (cit. on p. 6).

[46] J. P. Pekola, "Towards quantum thermodynamics in electronic circuits", Nat. Phys. **11**, 118 (2015) (cit. on p. 6).

[47] J. Goold, M. Huber, A. Riera, L. del Rio, and P. Skrzypczyk, "The role of quantum information in thermodynamics—a topical review", J. Phys. A: Math. Theor. **49**, 143001 (2016) (cit. on p. 6).

[48] J. Millen and A. Xuereb, "Perspective on quantum thermodynamics", New J. Phys. **18**, 011002 (2016) (cit. on pp. 6, 11).

[49] S. Vinjanampathy and J. Anders, "Quantum thermodynamics", Contemp. Phys. **57**, 545–579 (2016) (cit. on p. 6).

[50] R. Alicki and R. Kosloff, "Introduction to Quantum Thermodynamics: History and Prospects", arXiv (2018), eprint: 1801.08314 (cit. on p. 6).

[51] M. Esposito, R. Kawai, K. Lindenberg, and C. Van den Broeck, "Finite-time thermodynamics for a single-level quantum dot", EPL **89**, 20003 (2010) (cit. on pp. 6, 9, 11).

[52] M. Esposito, R. Kawai, K. Lindenberg, and C. Van den Broeck, "Quantum-dot Carnot engine at maximum power", Phys. Rev. E **81**, 041106 (2010) (cit. on pp. 6, 9).

[53] J. S. Lim, R. López, and D. Sánchez, "Dynamic thermoelectric and heat transport in mesoscopic capacitors", Phys. Rev. B **88**, 201304 (2013) (cit. on pp. 6, 9).

[54] S. Juergens, F. Haupt, M. Moskalets, and J. Splettstoesser, "Thermoelectric performance of a driven double quantum dot", Phys. Rev. B **87**, 245423 (2013) (cit. on pp. 6, 9, 10, 19, 44, 83).

[55] M. F. Ludovico, J. S. Lim, M. Moskalets, L. Arrachea, and D. Sánchez, "Dynamical energy transfer in ac-driven quantum systems", Phys. Rev. B **89**, 161306 (2014) (cit. on pp. 6, 9).

[56] M. F. Ludovico, M. Moskalets, D. Sánchez, and L. Arrachea, "Dynamics of energy transport and entropy production in ac-driven quantum electron systems", Phys. Rev. B **94**, 035436 (2016) (cit. on pp. 6, 9).

[57] A. Bruch, M. Thomas, S. Viola Kusminskiy, F. von Oppen, and A. Nitzan, "Quantum thermodynamics of the driven resonant level model", Phys. Rev. B **93**, 115318 (2016) (cit. on pp. 6, 9).

[58] A.-M. Daré and P. Lombardo, "Time-dependent thermoelectric transport for nanoscale thermal machines", Phys. Rev. B **93**, 035303 (2016) (cit. on pp. 6, 9).

[59] M. F. Ludovico, L. Arrachea, M. Moskalets, and D. Sánchez, "Periodic Energy Transport and Entropy Production in Quantum Electronics", Entropy **18**, 419 (2016) (cit. on pp. 6, 9).

[60] A. Crépieux, F. Šimkovic, B. Cambon, and F. Michelini, "Enhanced thermopower under a time-dependent gate voltage", Phys. Rev. B **83**, 153417 (2011) (cit. on pp. 6, 9).

[61] H. Zhou, J. Thingna, P. Hänggi, J.-S. Wang, and B. Li, "Boosting thermoelectric efficiency using time-dependent control", Sci. Rep. **5**, 14870 (2015) (cit. on pp. 6, 9).

[62] M. F. Ludovico, F. Battista, F. von Oppen, and L. Arrachea, "Adiabatic response and quantum thermoelectrics for ac-driven quantum systems", Phys. Rev. B **93**, 075136 (2016) (cit. on pp. 6, 9).

[63] M. Field, C. G. Smith, M. Pepper, D. A. Ritchie, J. E. F. Frost, G. A. C. Jones, and D. G. Hasko, "Measurements of Coulomb blockade with a noninvasive voltage probe", Phys. Rev. Lett. **70**, 1311–1314 (1993) (cit. on pp. 6, 8).

[64] M. Grifoni and P. Hänggi, "Driven quantum tunneling", Phys. Rep. **304**, 229–354 (1998) (cit. on pp. 6, 8, 43, 80).

[65] R. J. Schoelkopf, P. Wahlgren, A. A. Kozhevnikov, P. Delsing, and D. E. Prober, "The Radio-Frequency Single-Electron Transistor (RF-SET): A Fast and Ultrasensitive Electrometer", Science **280**, 1238–1242 (1998) (cit. on pp. 6, 8, 79).

[66] W. Lu, Z. Ji, L. Pfeiffer, K. W. West, and A. J. Rimberg, "Real-time detection of electron tunnelling in a quantum dot", Nature **423**, 422 (2003) (cit. on pp. 6, 8, 79).

[67] T. Fujisawa, T. Hayashi, Y. Hirayama, H. D. Cheong, and Y. H. Jeong, "Electron counting of single-electron tunneling current", Appl. Phys. Lett. **84**, 2343–2345 (2004) (cit. on pp. 6, 8, 79).

[68] B. Kaestner, V. Kashcheyevs, S. Amakawa, M. D. Blumenthal, L. Li, T. J. B. M. Janssen, G. Hein, K. Pierz, T. Weimann, U. Siegner, and H. W. Schumacher, "Single-parameter nonadiabatic quantized charge pumping", Phys. Rev. B **77**, 153301 (2008) (cit. on pp. 6, 77, 80, 81).

[69] S. Gustavsson, R. Leturcq, M. Studer, I. Shorubalko, T. Ihn, K. Ensslin, D. C. Driscoll, and A. C. Gossard, "Electron counting in quantum dots", Surf. Sci. Rep. **64**, 191–232 (2009) (cit. on pp. 6, 8).

[70] C. Barthel, M. Kjærgaard, J. Medford, M. Stopa, C. M. Marcus, M. P. Hanson, and A. C. Gossard, "Fast sensing of double-dot charge arrangement and spin state with a radio-frequency sensor quantum dot", Phys. Rev. B **81**, 161308 (2010) (cit. on pp. 6, 8, 79).

[71] J. Güttinger, J. Seif, C. Stampfer, A. Capelli, K. Ensslin, and T. Ihn, "Time-resolved charge detection in graphene quantum dots", Phys. Rev. B **83**, 165445 (2011) (cit. on pp. 6, 8).

[72] E. Bocquillon, F. D. Parmentier, C. Grenier, J.-M. Berroir, P. Degiovanni, D. C. Glattli, B. Plaçais, A. Cavanna, Y. Jin, and G. Fève, "Electron Quantum Optics: Partitioning Electrons One by One", Phys. Rev. Lett. **108**, 196803 (2012) (cit. on pp. 6, 8).

[73] F. Battista, "Single particle sources and quantum heat fluctuations", Contemp. Phys. **55**, 286–301 (2014) (cit. on p. 6).

[74] M. Kataoka, J. D. Fletcher, and N. Johnson, "Time-resolved single-electron wave-packet detection", Phys. Status solidi B **254**, 1600547 (2017) (cit. on pp. 6, 10, 11, 20, 80, 87).

[75] J. J. Sakurai and J. J. Napolitano, *Modern Quantum Mechanics (2nd Edition)* (Pearson, July 2010) (cit. on pp. 8, 35).

[76] L. D. Contreras-Pulido, J. Splettstoesser, M. Governale, J. König, and M. Büttiker, "Time scales in the dynamics of an interacting quantum dot", Phys. Rev. B **85**, 075301 (2012) (cit. on pp. 8, 33, 50, 77, 79, 85).

[77] H.-P. Breuer and F. Petruccione, *The Theory of Open Quantum Systems* (Oxford University Press, 2002) (cit. on pp. 8, 25, 43).

[78] H. Schoeller, "A perturbative nonequilibrium renormalization group method for dissipative quantum mechanics", Eur. Phys. J. Spec. Top. **168**, 179–266 (2009) (cit. on pp. 8, 43).

[79] C. Karrasch, S. Andergassen, M. Pletyukhov, D. Schuricht, L. Borda, V. Meden, and H. Schoeller, "Non-equilibrium current and relaxation dynamics of a charge-fluctuating quantum dot", EPL **90**, 30003 (2010) (cit. on pp. 8, 43).

[80] S. Andergassen, M. Pletyukhov, D. Schuricht, H. Schoeller, and L. Borda, "Renormalization group analysis of the interacting resonant-level model at finite bias: Generic analytic study of static properties and quench dynamics", Phys. Rev. B **83**, 205103 (2011) (cit. on pp. 8, 43).

[81] Á. Rivas, S. F. Huelga, and M. B. Plenio, "Quantum non-Markovianity: characterization, quantification and detection", Rep. Prog. Phys. **77**, 094001 (2014) (cit. on pp. 8, 43, 62).

[82] H.-P. Breuer, E.-M. Laine, J. Piilo, and B. Vacchini, "Colloquium: Non-Markovian dynamics in open quantum systems", Rev. Mod. Phys. **88**, 021002 (2016) (cit. on pp. 8, 43, 62).

[83] O. Kashuba and H. Schoeller, "Transient dynamics of open quantum systems", Phys. Rev. B **87**, 201402 (2013) (cit. on pp. 8, 43).

[84] O. Kashuba, D. M. Kennes, M. Pletyukhov, V. Meden, and H. Schoeller, "Quench dynamics of a dissipative quantum system: A renormalization group study", Phys. Rev. B **88**, 165133 (2013) (cit. on pp. 8, 43).

[85] D. M. Kennes, O. Kashuba, M. Pletyukhov, H. Schoeller, and V. Meden, "Oscillatory Dynamics and Non-Markovian Memory in Dissipative Quantum Systems", Phys. Rev. Lett. **110**, 100405 (2013) (cit. on pp. 8, 43).

[86] S. Das and G. S. Agarwal, "Decoherence effects in interacting qubits under the influence of various environments", J. Phys. B: At. Mol. Opt. Phys. **42**, 205502 (2009) (cit. on p. 8).

[87] E. Ferraro, M. Scala, R. Migliore, and A. Napoli, "Non-Markovian dissipative dynamics of two coupled qubits in independent reservoirs: Comparison between exact solutions and master-equation approaches", Phys. Rev. A **80**, 042112 (2009) (cit. on p. 8).

[88] L. Aolita, F. de Melo, and L. Davidovich, "Open-system dynamics of entanglement:a key issues review", Rep. Prog. Phys. **78**, 042001 (2015) (cit. on p. 8).

[89] R.-P. Riwar, J. Splettstoesser, and J. König, "Zero-frequency noise in adiabatically driven interacting quantum systems", Phys. Rev. B **87**, 195407 (2013) (cit. on p. 8).

[90] T. J. Suzuki and T. Kato, "Effects of Coulomb interaction on photon-assisted current noise through a quantum dot", Phys. Rev. B **91**, 165302 (2015) (cit. on p. 8).

[91] R. S. Whitney, R. Sánchez, and J. Splettstoesser, "Quantum thermodynamics of nanoscale thermoelectrics and electronic devices", arXiv (2018), eprint: `1805.04297` (cit. on pp. 9, 10).

[92] L. Onsager, "Reciprocal Relations in Irreversible Processes. I.", Phys. Rev. **37**, 405–426 (1931) (cit. on pp. 10, 14).

[93] H. B. Callen, *Thermodynamics and an Introduction to Thermostatistics* (Wiley, Sept. 1985) (cit. on pp. 10, 13).

[94] F. Giazotto, T. T. Heikkilä, A. Luukanen, A. M. Savin, and J. P. Pekola, "Opportunities for mesoscopics in thermometry and refrigeration: Physics and applications", Rev. Mod. Phys. **78**, 217–274 (2006) (cit. on p. 10).

[95] R. Scheibner, M. König, D. Reuter, A. D. Wieck, C. Gould, H. Buhmann, and L. W. Molenkamp, "Quantum dot as thermal rectifier", New J. Phys. **10**, 083016 (2008) (cit. on p. 10).

[96] Y. Dubi and M. Di Ventra, "Colloquium: Heat flow and thermoelectricity in atomic and molecular junctions", Rev. Mod. Phys. **83**, 131–155 (2011) (cit. on p. 10).

[97] R. Sánchez and M. Büttiker, "Optimal energy quanta to current conversion", Phys. Rev. B **83**, 085428 (2011) (cit. on pp. 10, 12, 14, 15, 20, 73, 83).

[98] A. Levy, R. Alicki, and R. Kosloff, "Quantum refrigerators and the third law of thermodynamics", Phys. Rev. E **85**, 061126 (2012) (cit. on p. 10).

[99] C. Lotze, M. Corso, K. J. Franke, F. von Oppen, and J. I. Pascual, "Driving a Macroscopic Oscillator with the Stochastic Motion of a Hydrogen Molecule", Science **338**, 779–782 (2012) (cit. on p. 10).

[100] O. Abah, J. Roßnagel, G. Jacob, S. Deffner, F. Schmidt-Kaler, K. Singer, and E. Lutz, "Single-Ion Heat Engine at Maximum Power", Phys. Rev. Lett. **109**, 203006 (2012) (cit. on p. 10).

[101] J.-P. Brantut, C. Grenier, J. Meineke, D. Stadler, S. Krinner, C. Kollath, T. Esslinger, and A. Georges, "A Thermoelectric Heat Engine with Ultracold Atoms", Science **342**, 713–715 (2013) (cit. on p. 10).

[102] D. Sánchez and R. López, "Scattering Theory of Nonlinear Thermoelectric Transport", Phys. Rev. Lett. **110**, 026804 (2013) (cit. on pp. 10, 14).

[103] B. Sothmann, R. Sánchez, and A. N. Jordan, "Thermoelectric energy harvesting with quantum dots", Nanotechnology **26**, 032001 (2015) (cit. on pp. 10, 12, 14).

[104] H. Thierschmann, R. Sánchez, B. Sothmann, F. Arnold, C. Heyn, W. Hansen, H. Buhmann, and L. W. Molenkamp, "Three-terminal energy harvester with coupled quantum dots", Nat. Nanotechnol. **10**, 854–858 (2015) (cit. on pp. 10, 12, 14, 15, 20, 73, 84, 87).

[105] H. Thierschmann, R. Sánchez, B. Sothmann, H. Buhmann, and L. W. Molenkamp, "Thermoelectrics with Coulomb-coupled quantum dots", C.R. Phys. **17**, 1109–1122 (2016) (cit. on pp. 10, 12, 14, 20, 73, 84, 87).

[106] G. Benenti, G. Casati, K. Saito, and R. S. Whitney, "Fundamental aspects of steady-state conversion of heat to work at the nanoscale", Phys. Rep. **694**, 1–124 (2017) (cit. on pp. 10, 14).

[107] R. Sánchez, H. Thierschmann, and L. W. Molenkamp, "Single-electron thermal devices coupled to a mesoscopic gate", New J. Phys. **19**, 113040 (2017) (cit. on pp. 10, 12, 14, 20, 73, 84, 87).

[108] A. Marcos-Vicioso, C. López-Jurado, M. Ruiz-Garcia, and R. Sánchez, "Thermal rectification with interacting electronic channels: Exploiting degeneracy, quantum superpositions, and interference", Phys. Rev. B **98**, 035414 (2018) (cit. on pp. 10, 73).

[109] S. Gasparinetti, K. L. Viisanen, O.-P. Saira, T. Faivre, M. Arzeo, M. Meschke, and J. P. Pekola, "Fast Electron Thermometry for Ultrasensitive Calorimetric Detection", Phys. Rev. Appl. **3**, 014007 (2015) (cit. on pp. 11, 80).

[110] J. Schulenborg, *Time-dependent relaxation of charge and energy in electronic nanosystems*, Licentiate thesis, Feb. 2016 (cit. on pp. 11, 23, 29, 30, 35, 36, 43, 46, 47, 49, 51, 74, 94, 114).

[111] M. Esposito, M. A. Ochoa, and M. Galperin, "Quantum Thermodynamics: A Nonequilibrium Green's Function Approach", Phys. Rev. Lett. **114**, 080602 (2015) (cit. on p. 11).

[112] M. Esposito, M. A. Ochoa, and M. Galperin, "Nature of heat in strongly coupled open quantum systems", Phys. Rev. B **92**, 235440 (2015) (cit. on p. 11).

[113] U. Seifert, "First and Second Law of Thermodynamics at Strong Coupling", Phys. Rev. Lett. **116**, 020601 (2016) (cit. on p. 11).

[114] R. Uzdin, A. Levy, and R. Kosloff, "Quantum Heat Machines Equivalence, Work Extraction beyond Markovianity, and Strong Coupling via Heat Exchangers", Entropy **18**, 124 (2016) (cit. on p. 11).

[115] P. Strasberg, G. Schaller, T. Brandes, and M. Esposito, "Quantum and Information Thermodynamics: A Unifying Framework Based on Repeated Interactions", Phys. Rev. X **7**, 021003 (2017) (cit. on p. 11).

[116] P. Strasberg, G. Schaller, T. L. Schmidt, and M. Esposito, "Fermionic reaction coordinates and their application to an autonomous Maxwell demon in the strong-coupling regime", Phys. Rev. B **97**, 205405 (2018) (cit. on p. 11).

[117] P. Streda, "Quantised thermopower of a channel in the ballistic regime", J. Phys.: Condens. Matter **1**, 1025 (1989) (cit. on p. 12).

[118] C. W. J. Beenakker and A. A. M. Staring, "Theory of the thermopower of a quantum dot", Phys. Rev. B **46**, 9667 (1992) (cit. on pp. 12, 13, 57, 82, 84, 86).

[119] A. A. M. Staring, L. W. Molenkamp, B. W. Alphenaar, H. van Houten, O. J. A. Buyk, M. A. A. Mabesoone, C. W. J. Beenakker, and C. T. Foxon, "Coulomb-Blockade Oscillations in the Thermopower of a Quantum Dot", EPL **22**, 57 (1993) (cit. on pp. 12–14, 56, 82, 86).

[120] L. D. Hicks and M. S. Dresselhaus, "Effect of quantum-well structures on the thermoelectric figure of merit", Phys. Rev. B **47**, 12727–12731 (1993) (cit. on pp. 12, 13).

[121] L. D. Hicks and M. S. Dresselhaus, "Thermoelectric figure of merit of a one-dimensional conductor", Phys. Rev. B **47**, 16631–16634 (1993) (cit. on pp. 12, 13).

[122] G. D. Mahan and J. O. Sofo, "The best thermoelectric", Proc. Natl. Acad. Sci. U.S.A. **93**, 7436–7439 (1996) (cit. on pp. 12, 13).

[123] B. Sothmann, R. Sánchez, A. N. Jordan, and M. Büttiker, "Rectification of thermal fluctuations in a chaotic cavity heat engine", Phys. Rev. B **85**, 205301 (2012) (cit. on p. 12).

[124] B. Muralidharan and M. Grifoni, "Performance analysis of an interacting quantum dot thermoelectric setup", Phys. Rev. B **85**, 155423 (2012) (cit. on pp. 12, 14).

[125] J. Kern and M. Grifoni, "Transport across an Anderson quantum dot in the intermediate coupling regime", Eur. Phys. J. B **86**, 384 (2013) (cit. on pp. 12, 14).

[126] A. N. Jordan, B. Sothmann, R. Sánchez, and M. Büttiker, "Powerful and efficient energy harvester with resonant-tunneling quantum dots", Phys. Rev. B **87**, 075312 (2013) (cit. on p. 12).

[127] B. Roche, P. Roulleau, T. Jullien, Y. Jompol, I. Farrer, D. A. Ritchie, and D. C. Glattli, "Harvesting dissipated energy with a mesoscopic ratchet", Nat. Commun. **6**, 6738 (2015) (cit. on pp. 12, 20).

[128] F. Hartmann, P. Pfeffer, S. Höfling, M. Kamp, and L. Worschech, "Voltage Fluctuation to Current Converter with Coulomb-Coupled Quantum Dots", Phys. Rev. Lett. **114**, 146805 (2015) (cit. on pp. 12, 20).

[129] S. B. Riffat and X. Ma, "Thermoelectrics: a review of present and potential applications", Appl. Therm. Eng. **23**, 913–935 (2003) (cit. on p. 12).

[130] L. E. Bell, "Cooling, Heating, Generating Power, and Recovering Waste Heat with Thermoelectric Systems", Science **321**, 1457–1461 (2008) (cit. on p. 12).

[131] S. E. Jo, M. K. Kim, M. S. Kim, and Y. J. Kim, "Flexible thermoelectric generator for human body heat energy harvesting", Electron. Lett. **48**, 1015–1017 (2012) (cit. on p. 12).

[132] V. Leonov, "Thermoelectric Energy Harvesting of Human Body Heat for Wearable Sensors", IEEE Sens. J. **13**, 2284–2291 (2013) (cit. on p. 12).

[133] S. J. Kim, J. H. We, and B. J. Cho, "A wearable thermoelectric generator fabricated on a glass fabric", Energy Environ. Sci. **7**, 1959–1965 (2014) (cit. on p. 12).

[134] T. W. Kerlin and M. Johnson, *Practical Thermocouple Thermometry, Second Edition* (International Society of Automation, July 2012) (cit. on p. 12).

[135] D. Zhao and G. Tan, "A review of thermoelectric cooling: Materials, modeling and applications", Appl. Therm. Eng. **66**, 15–24 (2014) (cit. on p. 12).

[136] G. D. Mahan and H. B. Lyon, "Thermoelectric devices using semiconductor quantum wells", J. Appl. Phys. **76**, 1899–1901 (1994) (cit. on pp. 12, 13).

[137] C. W. J. Beenakker, "Theory of Coulomb-blockade oscillations in the conductance of a quantum dot", Phys. Rev. B **44**, 1646 (1991) (cit. on pp. 13, 39, 40, 82, 84).

[138] A. S. Dzurak, C. G. Smith, M. Pepper, D. A. Ritchie, J. E. F. Frost, G. A. C. Jones, and D. G. Hasko, "Observation of Coulomb blockade oscillations in the thermopower of a quantum dot", Solid State Commun. **87**, 1145–1149 (1993) (cit. on pp. 13, 56, 82, 86).

[139] A. S. Dzurak, C. G. Smith, C. H. W. Barnes, M. Pepper, L. Martín-Moreno, C. T. Liang, D. A. Ritchie, and G. A. C. Jones, "Thermoelectric signature of the excitation spectrum of a quantum dot", Phys. Rev. B **55**, R10197 (1997) (cit. on pp. 13, 56, 82, 86).

[140] D. Andrieux, P. Gaspard, T. Monnai, and S. Tasaki, "The fluctuation theorem for currents in open quantum systems", New J. Phys. **11**, 043014 (2009) (cit. on p. 14).

[141] R. López and D. Sánchez, "Nonlinear heat transport in mesoscopic conductors: Rectification, Peltier effect, and Wiedemann-Franz law", Phys. Rev. B **88**, 045129 (2013) (cit. on p. 14).

[142] J. Meair and P. Jacquod, "Scattering theory of nonlinear thermoelectricity in quantum coherent conductors", J. Phys.: Condens. Matter **25**, 082201 (2013) (cit. on p. 14).

[143] S. F. Svensson, E. A. Hoffmann, N. Nakpathomkun, P. M. Wu, H. Q. Xu, H. A. Nilsson, D. Sánchez, V. Kashcheyevs, and H. Linke, "Nonlinear thermovoltage and thermocurrent in quantum dots", New J. Phys. **15**, 105011 (2013) (cit. on p. 14).

[144] R. S. Whitney, "Nonlinear thermoelectricity in point contacts at pinch off: A catastrophe aids cooling", Phys. Rev. B **88**, 064302 (2013) (cit. on p. 14).

[145] R. S. Whitney, "Thermodynamic and quantum bounds on nonlinear dc thermoelectric transport", Phys. Rev. B **87**, 115404 (2013) (cit. on p. 14).

[146] M. A. Sierra and D. Sánchez, "Strongly nonlinear thermovoltage and heat dissipation in interacting quantum dots", Phys. Rev. B **90**, 115313 (2014) (cit. on p. 14).

[147] P. A. Erdman, F. Mazza, R. Bosisio, G. Benenti, R. Fazio, and F. Taddei, "Thermoelectric properties of an interacting quantum dot based heat engine", Phys. Rev. B **95**, 245432 (2017) (cit. on pp. 14, 39, 40, 57, 84).

[148] D. Andrieux and P. Gaspard, "Fluctuation theorem and Onsager reciprocity relations", J. Chem. Phys. **121**, 6167–6174 (2004) (cit. on pp. 14, 41).

[149] P. Strasberg, G. Schaller, T. Brandes, and M. Esposito, "Thermodynamics of a Physical Model Implementing a Maxwell Demon", Phys. Rev. Lett. **110**, 040601 (2013) (cit. on pp. 16, 83).

[150] J. V. Koski, A. Kutvonen, I. M. Khaymovich, T. Ala-Nissila, and J. P. Pekola, "On-Chip Maxwell's Demon as an Information-Powered Refrigerator", Phys. Rev. Lett. **115**, 260602 (2015) (cit. on pp. 16, 83, 84).

[151] K. Kaasbjerg and A.-P. Jauho, "Correlated Coulomb Drag in Capacitively Coupled Quantum-Dot Structures", Phys. Rev. Lett. **116**, 196801 (2016) (cit. on p. 16).

[152] A. J. Keller, J. S. Lim, D. Sánchez, R. López, S. Amasha, J. A. Katine, H. Shtrikman, and D. Goldhaber-Gordon, "Cotunneling Drag Effect in Coulomb-Coupled Quantum Dots", Phys. Rev. Lett. **117**, 066602 (2016) (cit. on p. 16).

[153] A. Hamo, A. Benyamini, I. Shapir, I. Khivrich, J. Waissman, K. Kaasbjerg, Y. Oreg, F. von Oppen, and S. Ilani, "Electron attraction mediated by Coulomb repulsion", Nature **535**, 395–400 (2016) (cit. on pp. 16, 44, 82).

[154] F. Haupt, M. Leijnse, H. L. Calvo, L. Classen, J. Splettstoesser, and M. R. Wegewijs, "Heat, molecular vibrations, and adiabatic driving in non-equilibrium transport through interacting quantum dots", Phys. Status solidi B **250**, 2315–2329 (2013) (cit. on pp. 19, 44).

[155] E. Cota, R. Aguado, and G. Platero, "ac-Driven Double Quantum Dots as Spin Pumps and Spin Filters", Phys. Rev. Lett. **94**, 107202 (2005) (cit. on p. 19).

[156] R.-P. Riwar and J. Splettstoesser, "Charge and spin pumping through a double quantum dot", Phys. Rev. B **82**, 205308 (2010) (cit. on pp. 19, 20).

[157] N. Dittmann, J. Splettstoesser, and F. Giazotto, "Clocked single-spin source based on a spin-split superconductor", New J. Phys. **18**, 083019 (2016) (cit. on p. 19).

[158] G. C. Wick, A. S. Wightman, and E. P. Wigner, "The Intrinsic Parity of Elementary Particles", Phys. Rev. **88**, 101–105 (1952) (cit. on pp. 19, 61, 116).

[159] Y. Aharonov and L. Susskind, "Charge Superselection Rule", Phys. Rev. **155**, 1428–1431 (1967) (cit. on pp. 19, 61, 116).

[160] R. F. Streater and A. S. Wightman, *PCT, Spin and Statistics, and All That* (Princeton University Press, Dec. 2000) (cit. on pp. 19, 61, 116).

[161] V. N. Golovach, X. Jehl, M. Houzet, M. Pierre, B. Roche, M. Sanquer, and L. I. Glazman, "Single-dopant resonance in a single-electron transistor", Phys. Rev. B **83**, 075401 (2011) (cit. on p. 20).

[162] G. Rosselló, R. López, and R. Sánchez, "Dynamical Coulomb blockade of thermal transport", Phys. Rev. B **95**, 235404 (2017) (cit. on p. 20).

[163] V. N. Golovach and D. Loss, "Transport through a double quantum dot in the sequential tunneling and cotunneling regimes", Phys. Rev. B **69**, 245327 (2004) (cit. on p. 20).

[164] H. Schoeller and G. Schön, "Mesoscopic quantum transport: Resonant tunneling in the presence of a strong Coulomb interaction", Phys. Rev. B **50**, 18436–18452 (1994) (cit. on pp. 23, 26, 94).

[165] J. König, J. Schmid, H. Schoeller, and G. Schön, "Resonant tunneling through ultrasmall quantum dots: Zero-bias anomalies, magnetic-field dependence, and boson-assisted transport", Phys. Rev. B **54**, 16820–16837 (1996) (cit. on pp. 23, 26, 94).

[166] R. B. Saptsov and M. R. Wegewijs, "Fermionic superoperators for zero-temperature nonlinear transport: Real-time perturbation theory and renormalization group for Anderson quantum dots", Phys. Rev. B **86**, 235432 (2012) (cit. on pp. 23, 25, 27, 29, 50, 79, 85, 94, 117, 118, 121, 122).

[167] R. B. Saptsov and M. R. Wegewijs, "Time-dependent quantum transport: Causal superfermions, exact fermion-parity protected decay modes, and Pauli exclusion principle for mixed quantum states", Phys. Rev. B **90**, 045407 (2014) (cit. on pp. 23, 25, 26, 29, 50, 62, 85, 94, 117, 118, 121, 122).

[168] R. K. Wangsness and F. Bloch, "The Dynamical Theory of Nuclear Induction", Phys. Rev. **89**, 728–739 (1953) (cit. on p. 26).

[169] C. Timm, "Tunneling through molecules and quantum dots: Master-equation approaches", Phys. Rev. B **77**, 195416 (2008) (cit. on p. 26).

[170] C. Karlewski and M. Marthaler, "Time-local master equation connecting the Born and Markov approximations", Phys. Rev. B **90**, 104302 (2014) (cit. on p. 26).

[171] S. Koller, M. Grifoni, M. Leijnse, and M. R. Wegewijs, "Density-operator approaches to transport through interacting quantum dots: Simplifications in fourth-order perturbation theory", Phys. Rev. B **82**, 235307 (2010) (cit. on p. 28).

[172] J. N. Pedersen and A. Wacker, "Tunneling through nanosystems: Combining broadening with many-particle states", Phys. Rev. B **72**, 195330 (2005) (cit. on p. 28).

[173] J. N. Pedersen, B. Lassen, A. Wacker, and M. H. Hettler, "Coherent transport through an interacting double quantum dot: Beyond sequential tunneling", Phys. Rev. B **75**, 235314 (2007) (cit. on p. 28).

[174] N. M. Gergs, C. B. M. Hörig, M. R. Wegewijs, and D. Schuricht, "Charge fluctuations in nonlinear heat transport", Phys. Rev. B **91**, 201107 (2015) (cit. on p. 28).

[175] N. M. Gergs, *Transport and topological states in strongly correlated nanostructures*, PhD thesis, Sept. 2017 (cit. on p. 28).

[176] M.-D. Choi, "Completely positive linear maps on complex matrices", Linear Algebra Appl. **10**, 285–290 (1975) (cit. on p. 31).

[177] R. Serfozo, *Basics of Applied Stochastic Processes* (Springer, Berlin, Heidelberg, 2009) (cit. on pp. 35, 36).

[178] J. Schnakenberg, "Network theory of microscopic and macroscopic behavior of master equation systems", Rev. Mod. Phys. **48**, 571–585 (1976) (cit. on pp. 35, 36).

[179] K. Pearson, "The Problem of the Random Walk", Nature **72**, 294 (1905) (cit. on p. 35).

[180] S. Chandrasekhar, "Stochastic Problems in Physics and Astronomy", Rev. Mod. Phys. **15**, 1–89 (1943) (cit. on p. 35).

[181] C. Timm, "Random transition-rate matrices for the master equation", Phys. Rev. E **80**, 021140 (2009) (cit. on p. 36).

[182] M. Kac, "On the notion of recurrence in discrete stochastic processes", Bull. Amer. Math. Soc. **53**, 1002–1010 (1947) (cit. on pp. 36, 65).

[183] A. Kolmogoroff, "Zur Theorie der Markoffschen Ketten", Math. Ann. **112**, 155–160 (1936) (cit. on p. 38).

[184] H. Barakov, *Spin- and pseudospin relaxation in quantum dot set-ups*, Master thesis, June 2017 (cit. on pp. 40, 66).

[185] A. Ben-Israel and T. N. E. Greville, *Generalized Inverses* (Springer, New York, NY, 2003) (cit. on p. 40).

[186] J. J. Hunter, "Generalized inverses of Markovian kernels in terms of properties of the Markov chain", Linear Algebra Appl. **447**, 38–55 (2014) (cit. on p. 40).

[187] J. Splettstoesser, M. Governale, J. König, and R. Fazio, "Adiabatic pumping through a quantum dot with coulomb interactions: A perturbation expansion in the tunnel coupling", Phys. Rev. B **74**, 085305 (2006) (cit. on pp. 43, 80).

[188] F. Cavaliere, M. Governale, and J. König, "Nonadiabatic Pumping through Interacting Quantum Dots", Phys. Rev. Lett. **103**, 136801 (2009) (cit. on pp. 43, 44, 81).

[189] K. Burke, J. Werschnik, and E. K. U. Gross, "Time-dependent density functional theory: Past, present, and future", J. Chem. Phys. **123**, 062206 (2005) (cit. on p. 44).

[190] M. A. L. Marques, C. A. Ullrich, F. Nogueira, A. Rubio, K. Burke, and E. K. U. Gross, *Time-Dependent Density Functional Theory* (Springer Science & Business Media, Aug. 2006) (cit. on p. 44).

[191] J. Vanherck, *Time-dependent particle and energy currents through interacting quantum dots, Master Thesis*, 2016 (cit. on pp. 44, 81, 86).

[192] T. Pluecker, M. R. Wegewijs, and J. Splettstoesser, "Gauge freedom in observables and Landsberg's nonadiabatic geometric phase: Pumping spectroscopy of interacting open quantum systems", Phys. Rev. B **95**, 155431 (2017) (cit. on pp. 44, 80).

[193] T. Baquet, *Time-dependent particle and energy currents through interacting quantum dots, Master Thesis*, 2018 (cit. on pp. 44, 81).

[194] B. A. Placke, T. Pluecker, J. Splettstoesser, and M. R. Wegewijs, "Attractive and driven interactions in quantum dots: Mechanisms for geometric pumping", Phys. Rev. B **98**, 085307 (2018) (cit. on pp. 44, 81).

[195] G. E. D. K. Prawiroatmodjo, M. Leijnse, F. Trier, Y. Chen, D. V. Christensen, M. von Soosten, N. Pryds, and T. S. Jespersen, "Transport and excitations in a negative-U quantum dot at the LaAlO3/SrTiO3 interface", Nat. Commun. **8**, 395 (2017) (cit. on pp. 44, 82).

[196] *Jordan normal form - Wikipedia*, [Online; accessed 31. Jul. 2018], July 2018 (cit. on pp. 49, 95).

[197] P. W. Anderson, "Model for the Electronic Structure of Amorphous Semiconductors", Phys. Rev. Lett. **34**, 953–955 (1975) (cit. on pp. 55, 82).

[198] A. Taraphder and P. Coleman, "Heavy-fermion behavior in a negative-U Anderson model", Phys. Rev. Lett. **66**, 2814–2817 (1991) (cit. on pp. 55, 66, 75, 82, 86).

[199] K. A. Matveev, "Thermopower in quantum dots", in *Statistical and Dynamical Aspects of Mesoscopic Systems*, edited by D. Reguera, G. Platero, L. L. Bonilla, and J. M. Rubi (Springer, 1999) Chap. 1, pp. 3–15 (cit. on p. 56).

[200] X. Zianni, "Coulomb oscillations in the electron thermal conductance of a dot in the linear regime", Phys. Rev. B **75**, 045344 (2007) (cit. on p. 57).

[201] M. Leijnse and K. Flensberg, "Introduction to topological superconductivity and Majorana fermions", Semicond. Sci. Technol. **27**, 124003 (2012) (cit. on p. 62).

[202] C. W. J. Beenakker, "Search for Majorana Fermions in Superconductors", Annu. Rev. Condens. Matter Phys. **4**, 113–136 (2013) (cit. on p. 62).

[203] D. Aasen, M. Hell, R. V. Mishmash, A. Higginbotham, J. Danon, M. Leijnse, T. S. Jespersen, J. A. Folk, C. M. Marcus, K. Flensberg, and J. Alicea, "Milestones Toward Majorana-Based Quantum Computing", Phys. Rev. X **6**, 031016 (2016) (cit. on p. 62).

[204] Y. Kayanuma, "Direct solution of the eigenvalue problem of the damping superoperator for a boson field", Phys. Lett. A **76**, 211–212 (1980) (cit. on pp. 62, 117).

[205] U. Harbola and S. Mukamel, "Superoperator nonequilibrium Green's function theory of many-body systems; applications to charge transfer and transport in open junctions", Phys. Rep. **465**, 191–222 (2008) (cit. on pp. 62, 117).

[206] H. J. Carmichael, *Statistical Methods in Quantum Optics 1* (Springer-Verlag Berlin Heidelberg, 1999) (cit. on pp. 62, 123).

[207] C. Gardiner and P. Zoller, *Quantum Noise* (Springer-Verlag Berlin Heidelberg, 2004) (cit. on pp. 62, 123).

[208] R. J. Glauber, "Coherent and Incoherent States of the Radiation Field", Phys. Rev. **131**, 2766–2788 (1963) (cit. on p. 62).

[209] A. Kossakowski, A. Frigerio, V. Gorini, and M. Verri, "Quantum detailed balance and KMS condition", Commun. Math. Phys. **57**, 97–110 (1977) (cit. on pp. 65, 114).

[210] Á. M. Alhambra and M. P. Woods, "Dynamical maps, quantum detailed balance, and the Petz recovery map", Phys. Rev. A **96**, 022118 (2017) (cit. on p. 65).

[211] P. Sinkovicz, T. Kiss, and J. K. Asbóth, "Generalized Kac lemma for recurrence time in iterated open quantum systems", Phys. Rev. A **93**, 050101 (2016) (cit. on p. 65).

[212] G. Iche and A. Zawadowski, "Partial cancellation in the electron-hole and electron-electron correlation in the symmetric anderson model", Solid State Commun. **10**, 1001–1004 (1972) (cit. on pp. 66, 75, 86).

[213] J. Koch, E. Sela, Y. Oreg, and F. von Oppen, "Nonequilibrium charge-Kondo transport through negative-U molecules", Phys. Rev. B **75**, 195402 (2007) (cit. on pp. 66, 75, 86).

[214] J. König and J. Martinek, "Interaction-Driven Spin Precession in Quantum-Dot Spin Valves", Phys. Rev. Lett. **90**, 166602 (2003) (cit. on p. 66).

[215] M. Braun, J. König, and J. Martinek, "Theory of transport through quantum-dot spin valves in the weak-coupling regime", Phys. Rev. B **70**, 195345 (2004) (cit. on pp. 66, 67).

[216] S. Braig and P. W. Brouwer, "Rate equations for Coulomb blockade with ferromagnetic leads", Phys. Rev. B **71**, 195324 (2005) (cit. on p. 66).

[217] J. R. Hauptmann, J. Paaske, and P. E. Lindelof, "Electric-field-controlled spin reversal in a quantum dot with ferromagnetic contacts", Nat. Phys. **4**, 373 (2008) (cit. on p. 66).

[218] J. Splettstoesser, M. Governale, and J. König, "Adiabatic charge and spin pumping through quantum dots with ferromagnetic leads", Phys. Rev. B **77**, 195320 (2008) (cit. on pp. 66, 67).

[219] B. Muralidharan and M. Grifoni, "Thermoelectric spin accumulation and long-time spin precession in a noncollinear quantum dot spin valve", Phys. Rev. B **88**, 045402 (2013) (cit. on p. 66).

[220] B. Sothmann, "Electronic waiting-time distribution of a quantum-dot spin valve", Phys. Rev. B **90**, 155315 (2014) (cit. on p. 66).

[221] M. Hell, B. Sothmann, M. Leijnse, M. R. Wegewijs, and J. König, "Spin resonance without spin splitting", Phys. Rev. B **91**, 195404 (2015) (cit. on p. 66).

[222] M. Moskalets, "High-temperature fusion of a multielectron leviton", Phys. Rev. B **97**, 155411 (2018) (cit. on p. 77).

[223] A. Beckel, A. Kurzmann, M. Geller, A. Ludwig, A. D. Wieck, J. König, and A. Lorke, "Asymmetry of charge relaxation times in quantum dots: The influence of degeneracy", EPL **106**, 47002 (2014) (cit. on p. 77).

[224] J. Bylander, T. Duty, and P. Delsing, "Current measurement by real-time counting of single electrons", Nature **434**, 361 (2005) (cit. on p. 79).

[225] M. Hell, M. R. Wegewijs, and D. P. DiVincenzo, "Qubit quantum-dot sensors: Noise cancellation by coherent backaction, initial slips, and elliptical precession", Phys. Rev. B **93**, 045418 (2016) (cit. on p. 79).

[226] M. Switkes, C. M. Marcus, K. Campman, and A. C. Gossard, "An Adiabatic Quantum Electron Pump", Science **283**, 1905–1908 (1999) (cit. on p. 80).

[227] B. Roche, R.-P. Riwar, B. Voisin, E. Dupont-Ferrier, R. Wacquez, M. Vinet, M. Sanquer, J. Splettstoesser, and X. Jehl, "A two-atom electron pump", Nat. Commun. **4**, 1581 (2013) (cit. on p. 80).

[228] P. W. Brouwer, "Scattering approach to parametric pumping", Phys. Rev. B **58**, R10135–R10138 (1998) (cit. on p. 80).

[229] V. Kashcheyevs and B. Kaestner, "Universal Decay Cascade Model for Dynamic Quantum Dot Initialization", Phys. Rev. Lett. **104**, 186805 (2010) (cit. on p. 81).

[230] R. Landauer, “Irreversibility and Heat Generation in the Computing Process”, IBM J. Res. Dev. **5**, 183–191 (1961) (cit. on p. 83).

[231] C. H. Bennett, “Notes on Landauer’s principle, reversible computation, and Maxwell’s Demon”, Stud. Hist. Philos. Sci. Part B Stud. Hist. Philos. Mod. Phys. **34**, 501–510 (2003) (cit. on p. 83).